ZooKeys 1060: 1–16 (2021)
doi: 10.3897/zookeys.1060.70427
https://zookeys.pensoft.net

RESEARCH ARTICLE

A peer-reviewed open-access journal
ZooKeys
Launched to accelerate biodiversity research

Three new species, and new distributional data, of *Haltichella* (Hymenoptera, Chalcididae) from China

Zi-Tong Wang[1], Cheng-De Li[1]

1 *School of Forestry, Northeast Forestry University, Harbin, 150040, China*

Corresponding author: Cheng-De Li (lichengde0608@sina.com)

Academic editor: Kees van Achterberg | Received 21 June 2021 | Accepted 20 August 2021 | Published 15 September 2021

http://zoobank.org/9B08E7E5-3FB7-4E8F-A8DF-DB158313C696

Citation: Wang Z-T, Li C-D (2021) Three new species, and new distributional data, of *Haltichella* (Hymenoptera, Chalcididae) from China. ZooKeys 1060: 1–16. https://doi.org/10.3897/zookeys.1060.70427

Abstract

Five species of *Haltichella* (Hymenoptera, Chalcididae) from China are reviewed, including three new species, *H. bimaculata* Wang & Li, **sp. nov.**, *H. bomiana* Wang & Li, **sp. nov.**, *H. strigata* Wang & Li, **sp. nov.** *Haltichella clavicornis* (Ashmead) is newly recorded from China and *H. nipponensis* Habu is newly recorded from Heilongjiang, Shanxi, Shandong, Xizang, Guangdong and Yunnan Provinces in China. A key to the Chinese species of the *Haltichella* is provided.

Keywords

Chalcidoidea, chalcid wasps, Haltichellini, Haltichellinae, identification key, taxonomy

Introduction

The genus *Haltichella* Spinola, 1811 (Chalcididae, Haltichellinae, Haltichellini) currently contains 35 valid species worldwide (Noyes 2019), but only four species were recorded from China (Walker 1862; Narendran 1989). Members of the genus possess a cosmopolitan distribution and are primarily parasitoids of Lepidoptera (Bucculatricidae, Gelechiidae, Momphidae, Notodontidae, Oecophoridae, Pyralidae, Tortricidae) and Hymenoptera (Braconidae, Ichneumonidae) (Narendran and van Achterberg 2016; Noyes 2019). Here we review five species of the genus *Haltichella* from China, including three new species, and a new report of *H. clavicornis* Habu for China. Distributional records of *H. nipponensis* and a key to species of *Haltichella* occurring in China are also provided.

Materials and methods

Specimens were collected by using sweep nets, yellow pan traps and Malaise traps, and glued to triangle cards. Photographs were taken with a digital CCD camera attached to an AOSVI Hk830 microscope. Relative measurements and total body lengths were measured using an eye-piece reticle in the ocular of the microscope. All the specimens examined were deposited in the insect collections at Northeast Forestry University (NEFU), Harbin, China. In addition, literature used to identify this genus mainly include the keys and original descriptions of Narendran (1989), Narendran and van Achterberg (2016), Roy and Farooqi (1984). Terminology follows that of the Hymenoptera Anatomy Consortium (2021). The following abbreviations are used for the repositories:

IARI Indian Agricultural Research Institute, New Delhi, India;
NEFU Northeast Forestry University, Harbin, China;
NIAS National Institute of Agricultural Sciences, Tokyo, Japan;
USNM United States National Museum of Natural History, Washington D.C., USA.

The following abbreviations are used in the text:

Fu1–7 funiculars 1–7;
OOL oculo-ocellar distance, minimum distance between a posterior ocellus and eye;
POL postocellar distance, the distance between both posterior ocelli;
Gt1–2 tergites 1–2 of metasoma;
YPT yellow pan trap.

Results

Key to Chinese species of *Haltichella Spinola*

1 Apex of mesoscutellum not emarginate and without any distinct tooth **2**
– Apex of mesoscutellum emarginate forming two distinct teeth (Figs 1H, 2I) **3**
2 Forewing with two blackish bands, marginal vein 0.25× as long as submarginal vein; metasoma fusiform, a little longer but not narrower than mesosoma ..... ***H. sulcator* Walker**
– Forewing without blackish bands, marginal vein half as long as submarginal vein; metasoma elongate-oval, a little narrower but hardly longer than mesosoma ..... ***H. finator* Walker**
3 Metasoma with more than two basal carinae on Gt1 (Figs 5B, 6D) or with some longitudinal striae between two carinae (Fig. 3H) **4**
– Metasoma with only two basal carinae on Gt1 ..... **5**

4 Mesoscutellum with a median longitudinal fovea; apex of mesoscutellum with two diverging and short teeth (Fig. 4E); eye without obvious setae (Fig. 4B, 5D) ..... ***H. clavicornis* (Ashmead)**

– Mesoscutellum without a median longitudinal fovea; apex of mesoscutellum with two diverging and longer teeth (Fig. 3I); eye with dense and long setae (Fig. 3D)..... ***H. strigata* Wang & Li, sp. nov.**

5 Forewing with two brown patches (Fig. 1E); scrobe reaching anterior ocellus....**6**

– Forewing at most with one patch; scrobe not reaching anterior ocellus (Figs 2B, 4B) **7**

6 Postmarginal vein absent (Fig. 1E); submedian carinae not obvious and median area of propodeum irregularly rugose (Fig. 1F); mesoscutellum as long as broad ..... ***H. bimaculata* Wang & Li, sp. nov.**

– Postmarginal vein present and shorter than stigmal vein (Fig. 7C); submedian carinae distinct and parallel (Fig. 7F); mesoscutellum longer than broad (Fig. 7I) ..... ***H. nipponensis* Habu**

7 First tooth of metafemural comb of teeth prominent; postmarginal vein longer than marginal vein ..... ***H. variicolor* Masi**

– First tooth of metafemural comb of teeth not prominent (Fig. 2G); postmarginal vein about 2/3 the length of marginal vein (Fig. 2E) .... ***H. bomiana* Wang & Li, sp. nov.**

***Haltichella bimaculata* Wang & Li, sp. nov.**

http://zoobank.org/9EAF85B7-E3C5-4A2C-AF4F-B31E6DE62ECF

Figure 1

Type material. ***Holotype***, ♀ (NEFU), China, Henan Province, Xinyang City, 17–18.V.2012, YPT, Guo-Hao Zu, Jiang Liu. ***Paratypes*** (NEFU): 1 ♀, China: Yunnan Province, Huanglianshan Nature Reserve, 27–28.VII.2018, YPT, Jun Wu, Ming-Rui Li.

Diagnosis. Body black (Fig. 1A), scape to Fu3 yellowish brown, Fu4–7 and club dark brown (Fig. 1C), fore wing cinereous with two brown patches (Fig. 1E); scape (Fig. 1C) approximately half as long as remaining antennomeres combined, pedicel 1.5× as long as Fu1, Fu1–7 gradually increases in breadth and Fu4–7 gradually decreases in length distad; mesoscutellum (Fig. 1H) as long as broad, apex with two teeth, distance between outer margins of the two teeth about 1.4× as long as individual length of teeth; propodeum (Fig. 1F) with irregularly rugose in middle area; postmarginal vein (Fig. 1E) absent, marginal vein 3× as long as stigmal vein; metasoma oval; Gt1 occupying 0.7× length of metasoma (Fig. 1H).

Description. Female (holotype). Body length 2.9 mm, mostly black (Fig. 1A), with dense punctures and white pubescence; antenna (Fig. 1C) with scape to Fu3 yellowish brown, Fu4–7 and club dark brown; eye and ocelli silvery gray (Fig. 1D); tegula testaceous; fore and mid legs yellowish brown; metacoxa black with apical reddish brown, metatrochanter yellowish brown, metafemur black with base yellowish brown to reddish brown,

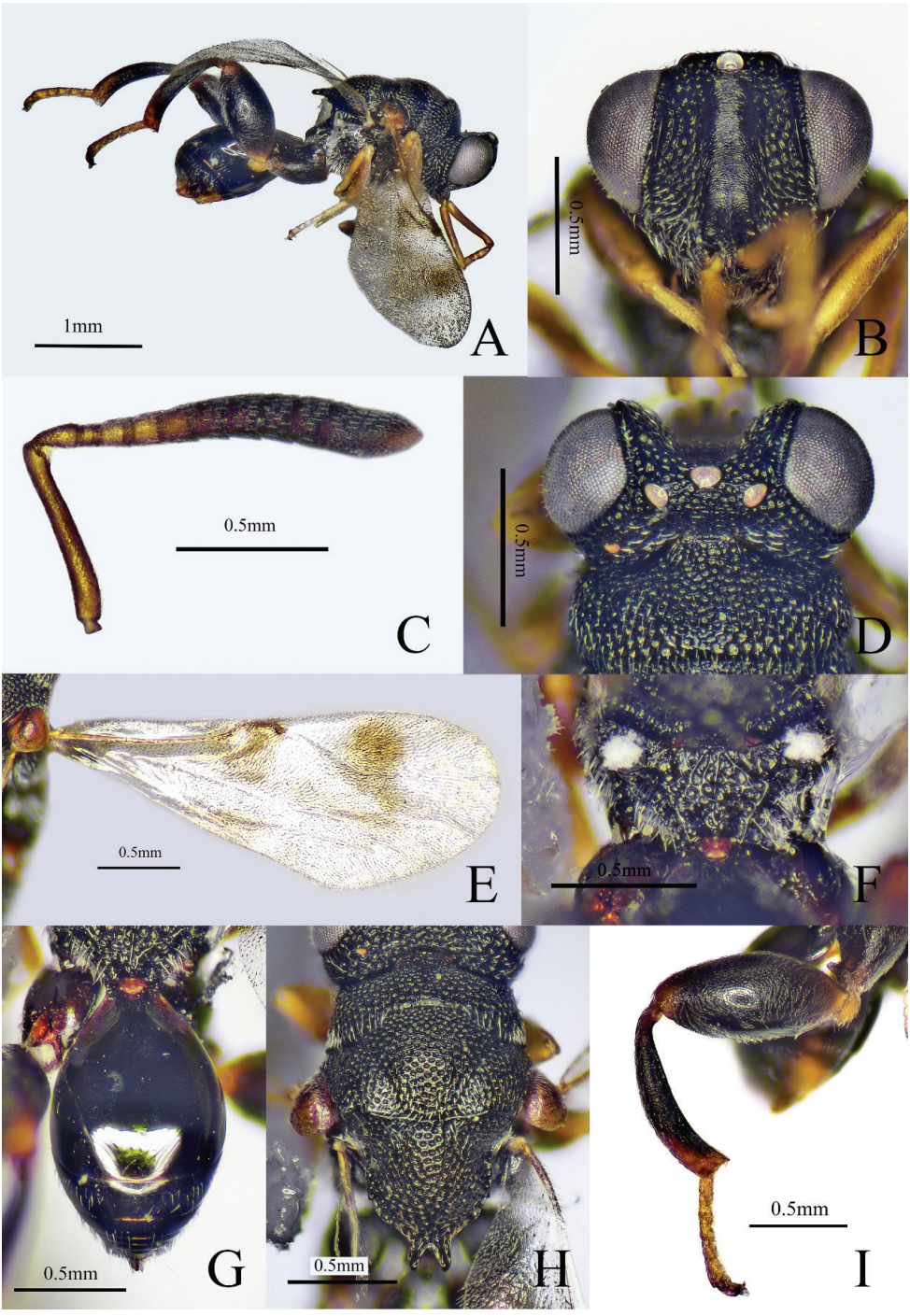

Figure 1. *Halticella bimaculata* sp. nov. (holotype female) **A** habitus, lateral view **B** head, front view **C** antenna **D** head and part of mesosoma, dorsal view **E** forewing **F** propodeum **G** metasoma **H** head and mesosoma, dorsal view **I** hind leg.

apex reddish brown, metatibia black with base slightly reddish brown, apex yellowish brown, metatarsus yellowish brown; fore wing (Fig. 1E) cinereous with two brown patches, one adjoining marginal vein and another near posterior margin of wing, venation brown.

Head (Fig. 1B, D), with coarsely rugose punctures, except in scrobal area, 1.2× as wide as long in frontal view; scrobe reaching anterior ocellus, finely striate; preorbital carinae distinct; POL 4.3× as long as OOL; antenna (Fig. 1C) clavate; scape approximately a half of remaining antennomeres combined; pedicel triangular, longer than broad; anellus quadrate, looks like a funicular segment; Fu1–2 subquadrate, Fu1 shorter than pedicel, 0.9× as broad as long; Fu3–7 broader than long; Fu1–7 gradually increases in breadth and Fu4–7 gradually decreases in length distad, Fu7 1.5× as broad as long; club coniform, 2× as long as maximum width, 3× as long as and about as broad as the preceding segment.

Mesosoma (Fig. 1H), punctures on mesoscutum and mesoscutellum smaller than on head; mesoscutellum as long as broad, apex with two teeth, distance between outer margins of the two teeth about 1.4× as long as individual length of teeth; outer margins of the two teeth approximately parallel, inner margins of the two teeth meet at an acute angle; propodeum (Fig. 1F) irregularly rugose in middle area. Forewing (Fig. 1E) 2.5× as long as broad; submarginal vein 4.5× as long as marginal vein, marginal vein 3× as long as stigmal vein, postmarginal vein absent. Metacoxa with coxal tooth on baso-dorsal side; metafemur (Fig. 1I) 2.2× as long as broad, with a row of comb of teeth but without forming any lobes.

Metasoma (Fig. 1G) oval, 1.6× as long as broad in dorsal view, surface smooth; Gt1 longest, occupying 0.7× length of metasoma, with two short carinae at base; Gt2–6 with sparse microsculptured and white pubescence on lateral sides.

Male. Unknown.

Hosts. Unknown.

Distribution. China (Hennan, Yunnan).

Etymology. Latin: *bi* = two; *macula* = stain, blemish; and refers to the two brown patches on the forewing.

Comments. *Haltichella bimaculata* sp. nov. is similar to *H. nipponensis* Habu, 1960 in having similar body colouration and shape of the antenna and similar shape of the metafemur, but can be separated from the latter by the following characters. *Haltichella bimaculata* has the postmarginal vein of the forewing absent (vs present and shorter than the stigmal vein in *H. nipponensis*); median area of the propodeum irregularly rugose and the submedian carinae not obvious (vs less sculptured and the carinae distinct and parallel); the mesoscutellum as long as broad (vs longer than broad).

Haltichella bomiana Wang & Li, sp. nov.

http://zoobank.org/676C10E6-E55A-42E3-8C39-8273B21BC3A8
Figure 2

Type material. ***Holotype***, ♂ (NEFU), China, Xizang Province, Bomi County, Shuangyu Village, 8.VIII.2017, sweeping, Hui-Lin Han. ***Paratypes*** (NEFU): 2 ♂, same data as holotype.

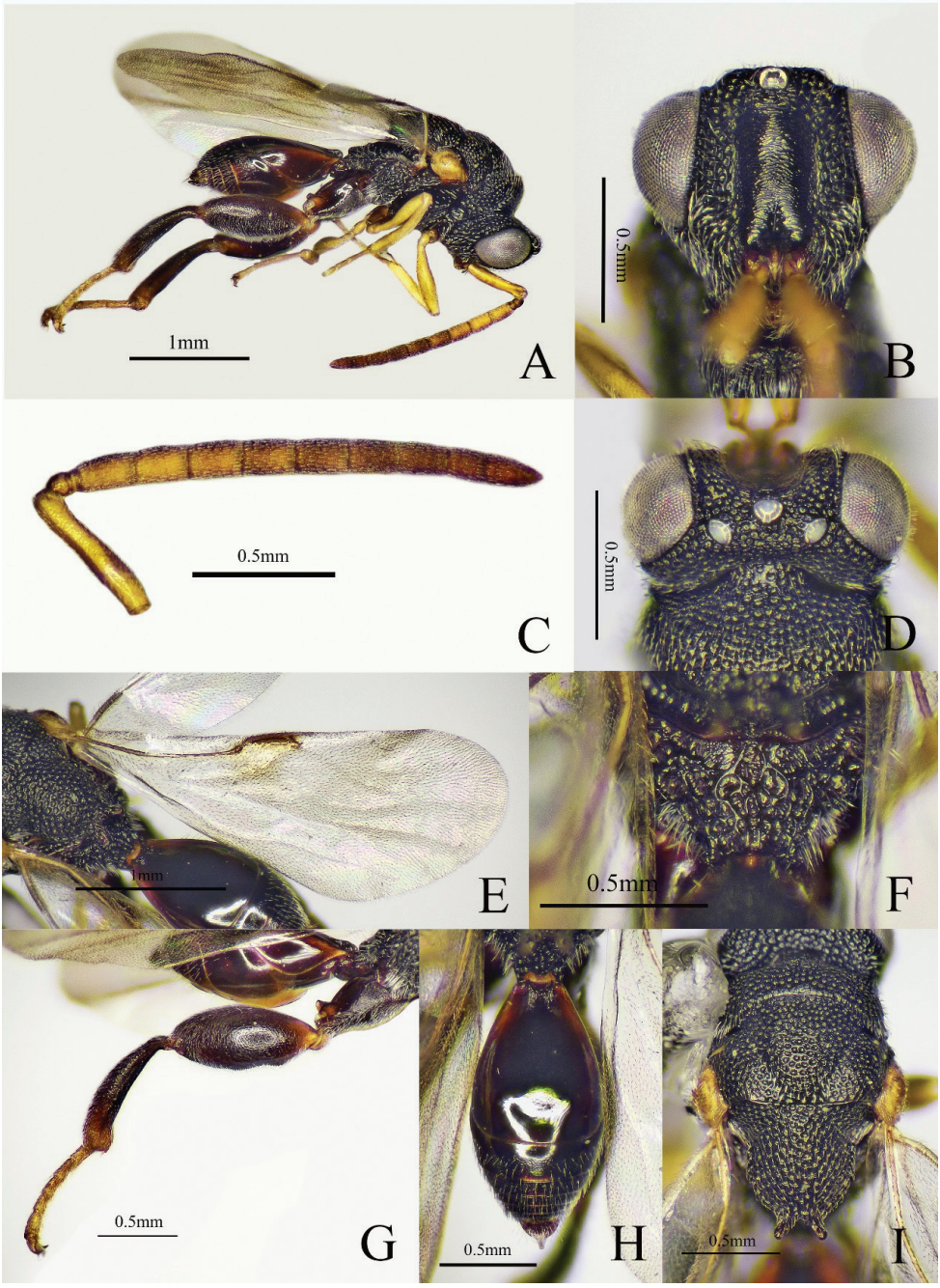

Figure 2. *Halticella bomiana* sp. nov. (holotype male) **A** habitus, lateral view **B** head, front view **C** antenna **D** head and part of mesosoma, dorsal view **E** forewing **F** propodeum **G** hind leg **H** metasoma **I** mesosoma, dorsal view.

Diagnosis. Body black (Fig. 2A), antenna with scape yellowish brown and flagellum yellowish brown to brown; fore and mid legs yellowish brown; scrobe not reaching anterior ocellus (Fig. 2B); antenna (Fig. 2C) slender, scape longer than pedicel to Fu2 combined; all the funicular segments longer than broad; mesoscutellum apically with two diverging teeth (Fig. 2I); submedian carinae of propodeum indicated, distinct on posterior half (Fig. 2F); fore wing (Fig. 2E) largely hyaline with small brown patch adjoining marginal vein; postmarginal vein slightly longer than stigmal vein; metasoma (Fig. 2H) fusiform, Gt1 occupying 0.6× length of metasoma, Gt2 with the basal half smooth and distal half with microsculptured and white pubescence.

Description. Male (holotype). Body length 2.9 mm, mostly black (Fig. 2A), head and mesosoma with dense punctures and white pubescence; antenna with scape yellowish brown and flagellum yellowish brown to brown; eye and ocelli silvery gray (Fig. 2D); tegula yellowish brown; fore and mid legs yellowish brown; metacoxa black, metatrochanter yellowish brown, metafemur black with base yellowish brown to reddish brown, metatibia black with apex yellowish brown, metatarsus yellowish brown; fore wing largely hyaline with small brown patch adjoining marginal vein and venation brownish.

Head (Fig. 2B, D) with coarsely rugose punctures, 1.2× as wide as long in frontal view; scrobe slightly wider, not reaching anterior ocellus, finely striate; preorbital carinae distinct; POL 5× as long as OOL; antenna (Fig. 2C) slender; scape longer than pedicel to Fu2 combined; pedicel small; anellus short and transverse; Fu1 longest, 1.7× as long as broad; Fu2–7 approximately equal in length, all the funicular segments longer than broad; club 2-segmented and slender, 3.2× as long as maximum width, 2× as long as and as broad as the preceding segment.

Mesosoma (Fig. 2I) with dense punctures and white pubescence; apex of mesoscutellum with two diverging teeth, inner margins of the two teeth at a right angle; submedian carinae of propodeum (Fig. 2F) indicated, distinct on posterior half. Fore wing hyaline (Fig. 2E), forewing 2.6× as long as broad; submarginal vein 4× as long as marginal vein, marginal vein 1.6× as long as postmarginal vein, postmarginal vein slightly longer than stigmal vein. Metafemur and metatibia with long and white pubescence (Fig. 2G); metacoxa with coxal tooth on baso-dorsal side; metafemur 2.3× as long as broad, with a row of comb of teeth.

Metasoma (Fig. 2H) fusiform, 2× as long as broad in dorsal view; Gt1 dorsum smooth and shiny, occupying 0.6× length of metasoma, with two longitudinal carinae at base; Gt2 with basal half smooth and distal half with microsculptured and white pubescence; dorsal surface of Gt2–6 with sparse microsculptured and white pubescence.

Female. Unknown.

Hosts. Unknown.

Distribution. China (Xizang).

Etymology. The specific name is derived from the name of the collection locality of the holotype.

Comments. The new species is similar to *H. variicolor* Masi, 1929 in having similar colouration and shape of the antenna and similar shape of the scrobe, but can be separated

from the latter by the following characters. The new species has the marginal vein 1.6× as long as the postmarginal vein (vs postmarginal vein longer than marginal vein in *H. variicolor*) and metafemur without prominent first tooth (vs first tooth present and prominent).

The new species is characterized by two diverging teeth of the mesoscutellum, a unique propodeum and the scrobe not reaching the anterior ocellus. A female holotype would be preferable but we failed to collect female specimens. However, most likely the female will share at least part of the differences listed for the male holotype.

Haltichella strigata Wang & Li, sp. nov.

http://zoobank.org/A1242FA3-10BA-4CD1-BACA-7EDBEB6AE821
Figure 3

Type material. ***Holotype***, ♂ (NEFU), China, Heilongjiang Province, Harbin City, Maoershan Town, 19.VII.2014, sweeping, Hai-Feng Bai. ***Paratypes*** (NEFU): 1 ♂, China: Heilongjiang Province, Yichun City, Liangshui National Nature Reserve, 11.VII.2013, sweeping, Hui Geng, Yang Peng, Si-Zhu Liu, Guo-Hao Zu; 1 ♂, China: Heilongjiang Province, Yichun City, Liangshui National Nature Reserve, 1.VIII.2015, sweeping, Xing-Yue Jin, Si-Zhu Liu, Xin-Yu Zhang; 1 ♂, China: Heilongjiang Province, Yichun City, Fenglin National Nature Reserve, 15.VII.2011, sweeping, Jun-Chao Wang.

Diagnosis. Body mostly black (Fig. 3A), antenna with scape yellowish brown, funicle yellowish brown to brown and club yellowish brown; fore and mid legs yellowish brown, metafemur reddish brown; eye (Fig. 3D) with dense and long setae; scape shorter than pedicel to Fu2 combined; Fu1 longest; all the funicular segments longer than broad; postmarginal vein shorter than marginal vein and 3.5× as long as stigmal vein (Fig. 3E); Gt1 with two longitudinal carinae at base, between them with some longitudinal striae (Fig. 3H).

Description. Male (holotype). Body length 2.9 mm, mostly black (Fig. 3A). Head and mesosoma with dense punctures and white pubescence; antenna (Fig. 3C) with scape yellowish brown, funicle yellowish brown to brown and club yellowish brown; eye silvery gray and ocelli brownish (Fig. 3D); tegula yellowish brown; fore and mid legs yellowish brown; hind leg mostly reddish brown except yellowish brown tarsus, distal apex of tibia yellowish brown; fore wing hyaline, venation brownish.

Head (Fig. 3B, D) with long, white pubescence, 1.2× as wide as long in frontal view; eye with long, white setae; scrobe not reaching anterior ocellus, finely striate; preorbital carinae distinct and not reaching behind anterior ocellus; POL 5× as long as OOL; antenna (Fig. 3C) with scape shorter than pedicel to Fu2 combined; pedicel small; Fu1 longest, 1.7× as long as broad; all the funicular segments longer than broad; Fu2–7 subequal in length; club 2-segmented, 2.6× as long as maximum width, 1.8× as long as and about as broad as the preceding segment.

Mesosoma (Fig. 3I) with dense punctures and white pubescence, apex of mesoscutellum with two teeth, pubescence on mesoscutellum longer than that on pronotum

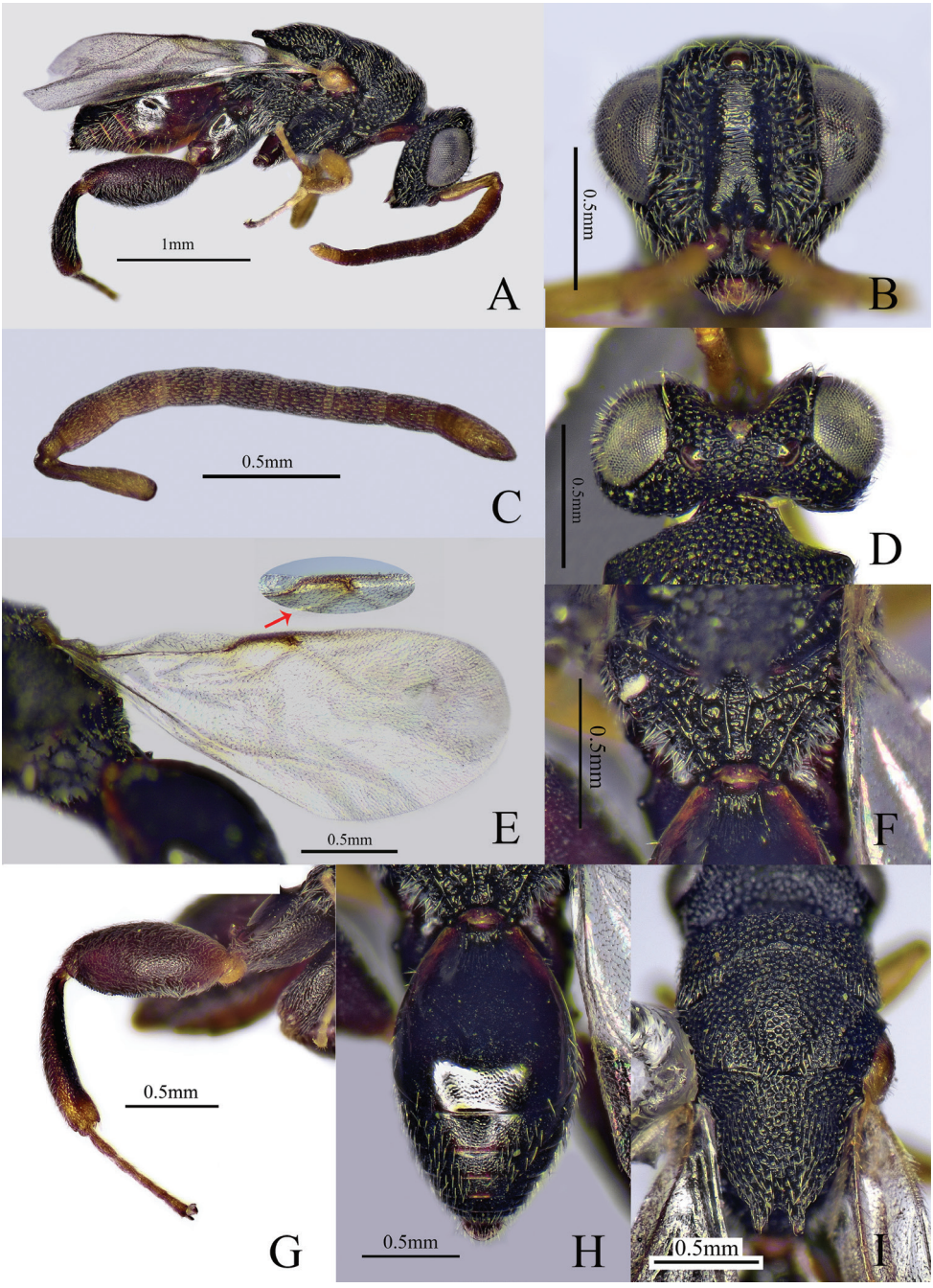

Figure3. *Haltichella strigata* sp. nov. (holotype male) **A** habitus, lateral view **B** head, front view **C** antenna **D** head, dorsal view **E** forewing **F** propodeum **G** hind leg **H** metasoma **I** mesosoma, dorsal view.

and mesoscutum; propodeum (Fig. 3F) with submedian carinae distinct and parallel, between them with some transverse and fine striations. Fore wing hyaline (Fig. 3E), 2.4× as long as broad; postmarginal vein shorter than marginal vein and 3.5× as long as stigmal vein. Metafemur (Fig. 3G) and metatibia with long and white pubescence; metacoxa with coxal tooth on baso-dorsal side; metafemur 2.2× as long as broad, with a row of comb of teeth but without forming any lobes.

Metasoma (Fig. 3H) oblong, 1.6× as long as broad in dorsal view; Gt1 longest, occupying 0.6× length of metasoma with two longitudinal carinae at base, between them with some longitudinal striae, with white pubescence on lateral sides; dorsal surface of Gt2–6 with microsculptured and white pubescence.

Female. Unknown.

Hosts. Unknown.

Distribution. China (Heilongjiang).

Variation. Two paratypes differ from the holotype by having black eyes, but no other significant differences were found in the available material.

Etymology. Latin: *stria* = furrow, line; and refers to the longitudinal striae between two longitudinal carinae of T1.

Comments. *Haltichella strigata* sp. nov. is similar to *H. achterbergi* Narendran, 1989 in having a similar shape of the antenna and the metasoma, but can be separated from the latter by the following combination of characters. The new species has the fore wing hyaline (vs partly infuscated in *H. achterbergi*); Gt1 with some striae between the two longitudinal carinae (vs absent); postmarginal vein shorter than the marginal vein (vs longer); dorsal surface of Gt 2–6 with white pubescence (vs glabrous and polished on the dorsal side medially).

Compared with other species of this genus, the new species differs by having dense and long setae on its eyes (Fig. 3D) and Gt1 with some striae between the two longitudinal carinae. A female holotype would be preferable but we failed to collect female specimens. However, most likely the female will share at least part of the differences listed for the male holotype.

Distribution. New distributional records for China.

Haltichella clavicornis (Ashmead, 1904)

Figures 4–6

Stomatoceras clavicornis Ashmead, 1904: 148; holotype ♂, USNM, Japan, not examined.
Haltichella clavicornis: Habu 1960: 241.
Haltichella macroclava Roy & Farooqi, 1984: 27; holotype ♀, IARI, India, not examined. Synonymised with *Haltichella clavicornis* by Narendran 1989: 152–153.

Material. (NEFU). 1 ♀, **China**: Henan Province, Xinyang City, Wusheling, 7–9. VIII. 2015, YPT, Yan Gao, Hui Geng, Zhi-Guang Wu; 1 ♀ 2 ♂, China: Hainan Province, Haikou City, Haida Base, 27–29.IV.2019, YPT, Yu-Ting Jiang; 1 ♀, id., but

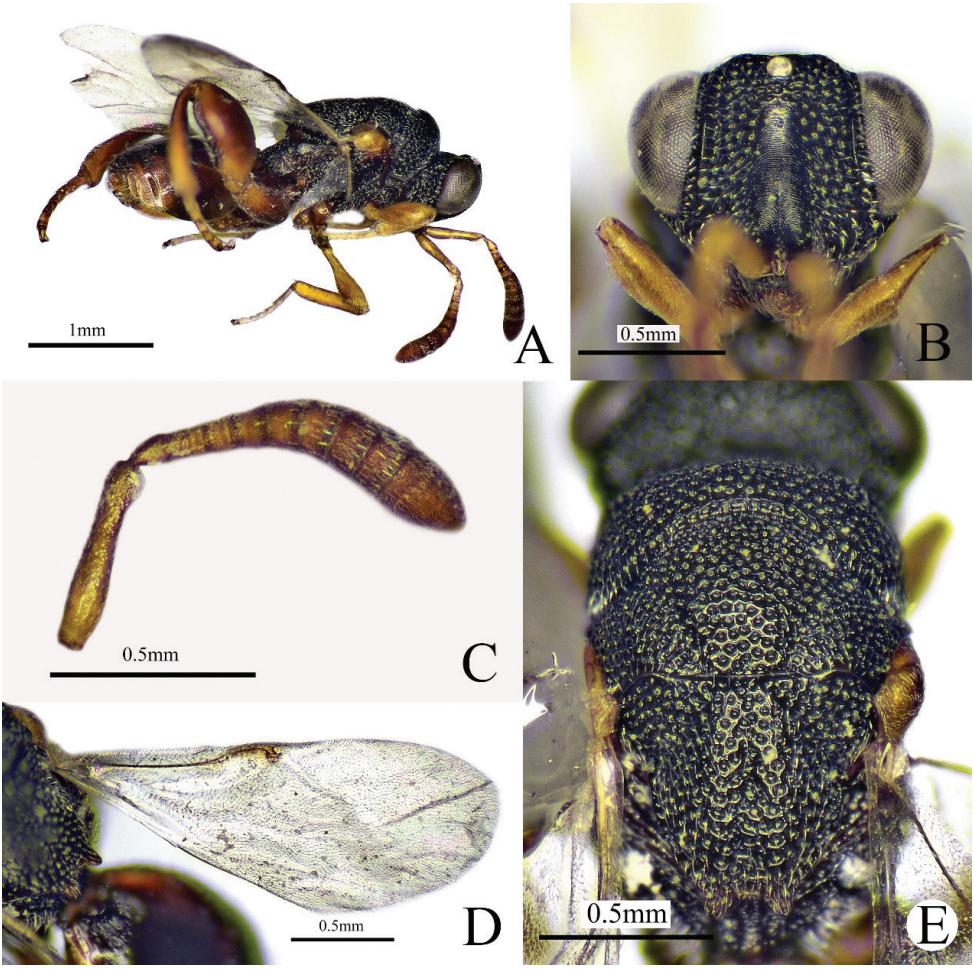

Figure 4. *Halticella clavicornis*, (female) **A** habitus, lateral view **B** head, front view **C** antenna **D** fore-wing **E** mesosoma, dorsal view.

Pinnacle Ridge, 17–19.V.2021, Gang Fu, Ming-Rui Li; 1 ♀, China: Yunnan Province, Yuanjiang County, 26–28.XI.2020, YPT, Jun-Jie Fan, Ming-Rui Li, Gang Fu, Jun Wu; 1 ♀, id., but Mengla Town, Mengla County, 17–18. XI. 2020.

Diagnosis. Female. Body length 2.8–3.1 mm, mostly black (Fig. 4A); antenna with scape and pedicel yellowish brown, flagellum brown to dark brown (Fig. 4C); eye and ocelli silvery gray (Fig. 5D); tegula yellowish brown; fore and mid legs yellowish brown; hind leg (Fig. 5A) and metasoma reddish brown (Fig. 5B); fore wing hyaline (Fig. 4D), venation brownish. Head 1.3× as wide as long in frontal view (Figs 4B, 5D); scrobe not reaching anterior ocellus (Fig. 4B); POL 4.3× as long as OOL; antenna (Fig. 4C) distinctly clavate; pedicel longer than Fu1, flagellum increases in breadth distad; mesoscutellum (Fig. 4E) flat with a median longitudinal fovea; apex of mesoscutellum

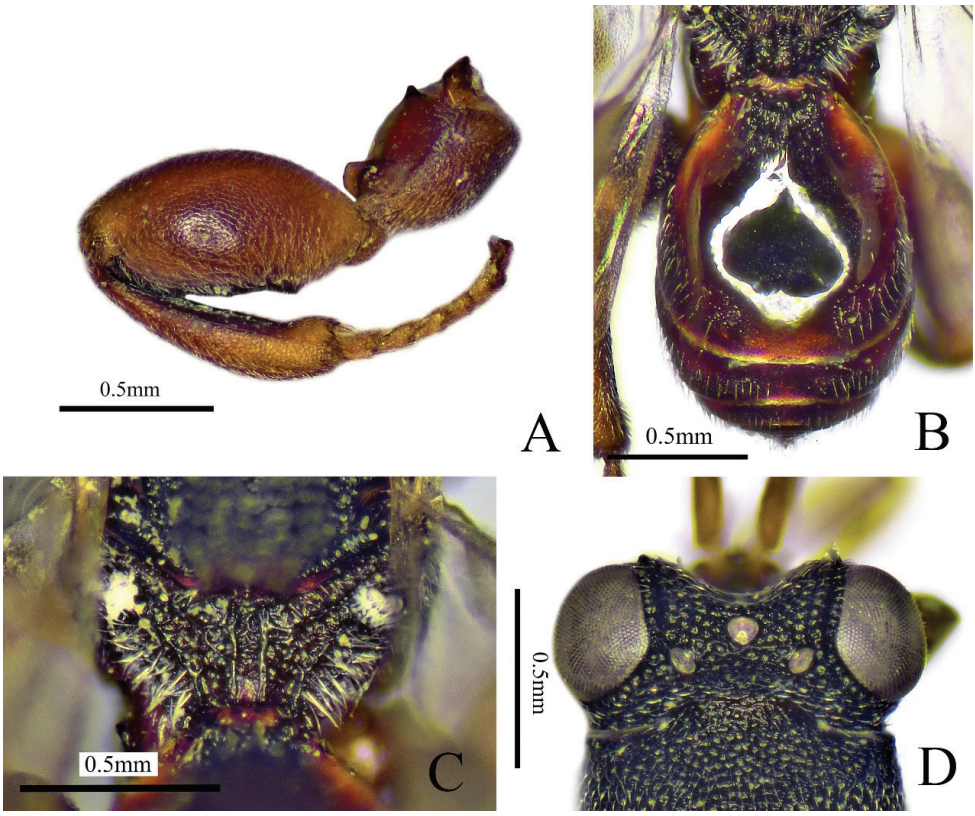

Figure 5. *Halticella clavicornis*, (female) **A** hind leg **B** metasoma **C** propodeum **D** head and mesosoma, dorsal view.

with two short diverging and short teeth; submedian carinae of propodeum parallel (Fig. 5C); postmarginal vein (Fig. 4D) shorter than stigmal vein. Metasoma (Fig. 5B) oval, Gt1 occupying 0.75× length of metasoma, with three longitudinal carinae at base.

Male. Body length 2.8–2.9 mm. Scape and pedicel brown, flagellum brownish black (Fig. 6B); hind leg black except brown tarsus, extreme apex of femur brown, distal apex of tibia brown; metasoma black (Fig. 6A); anellus not obvious; Fu1–7 subquadrate; club 2× as long as and as broad as the preceding segment (Fig. 6B). Gt1 occupying 0.6× length of metasoma (Fig. 6D), distal half of Gt1 with microsculpture. Other features similar to female.

Hosts. Unknown.

Distribution. China (Henan [new record], Hainan [new record], Yunnan [new record]), Japan, Laos, India, Malaysia, Vietnam, Nepal, Philippines (Narendran 1989; Narendran and van Achterberg 2016).

Comments. Our specimens agree well with the original description except for the colour of the antenna and metasoma. This is the first record from Henan, Hainan and Yunnan Provinces, China.

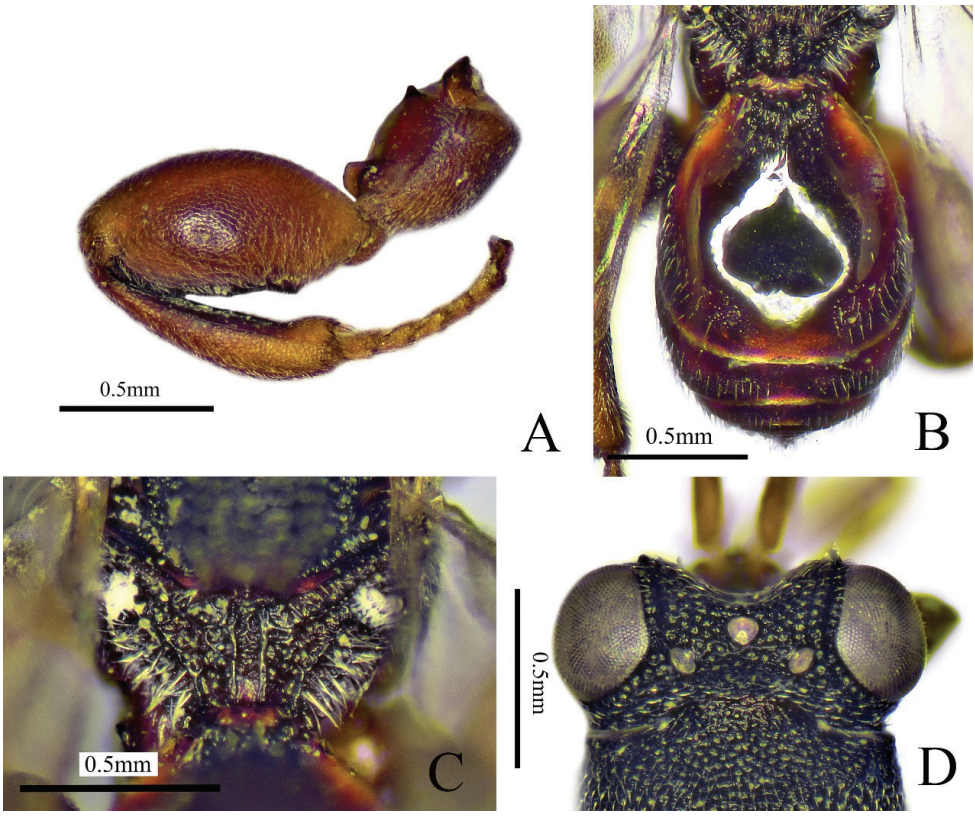

Figure 6. *Halticella clavicornis*, (male) **A** habitus, lateral view **B** antenna **C** forewing **D** metasoma.

Haltichella nipponensis Habu, 1960

Figure 7

Haltichella nipponensis Habu, 1960: 245; holotype ♀, NIAS, Japan, not examined.

Material. (NEFU). 2 ♀, **China:** Xizang Province**,** Chayu County, Gadui Village, 14–16.V.2015, YPT, Ye Chen, Chao Zhang; 1 ♀, id., but Talin Village, 6–13. VII.2017, Malaise trap, Sang Tuo; 3 ♀, China: Xizang Province**,** Linzhi City, Bomi County, Shuangyu Village, 8. VIII. 2017, sweeping, Hui-Lin Han; 1 ♀, China: Yunnan Province, Ruili City, Nanjingli Village, 26–27.IV.2013, YPT, Xiang-Xiang Jin, Guo-Hao Zu, Chao Zhang; 1 ♀; id., but Huanglianshan National Nature Reserve, 27–28.VII.2018, YPT, Jun Wu, Ming-Rui Li; 1 ♀, China: Shanxi Province**.** Ningshan County, Xunyangba Village, 5–6.VIII.2015, YPT, Ye Chen, Chao Zhang; 2 ♀, China, Shandong Province, Qingdao City, Xiaozhushan, 20.V.2014, sweeping, Xiang-Xiang Jin, Guo-Hao Zu, Si-Zhu Liu; 1 ♀, id., but 22–24.V.2014; 1 ♀, China: Heilongjiang Province, Yichun City, Liangshui National Nature Reserve, 30.VI.–2. VII.2018, YPT, Jun Wu, Jun-Jie Fan, Guang-Xin Wang; 1 ♀, id., but 2–3.VII.2018;

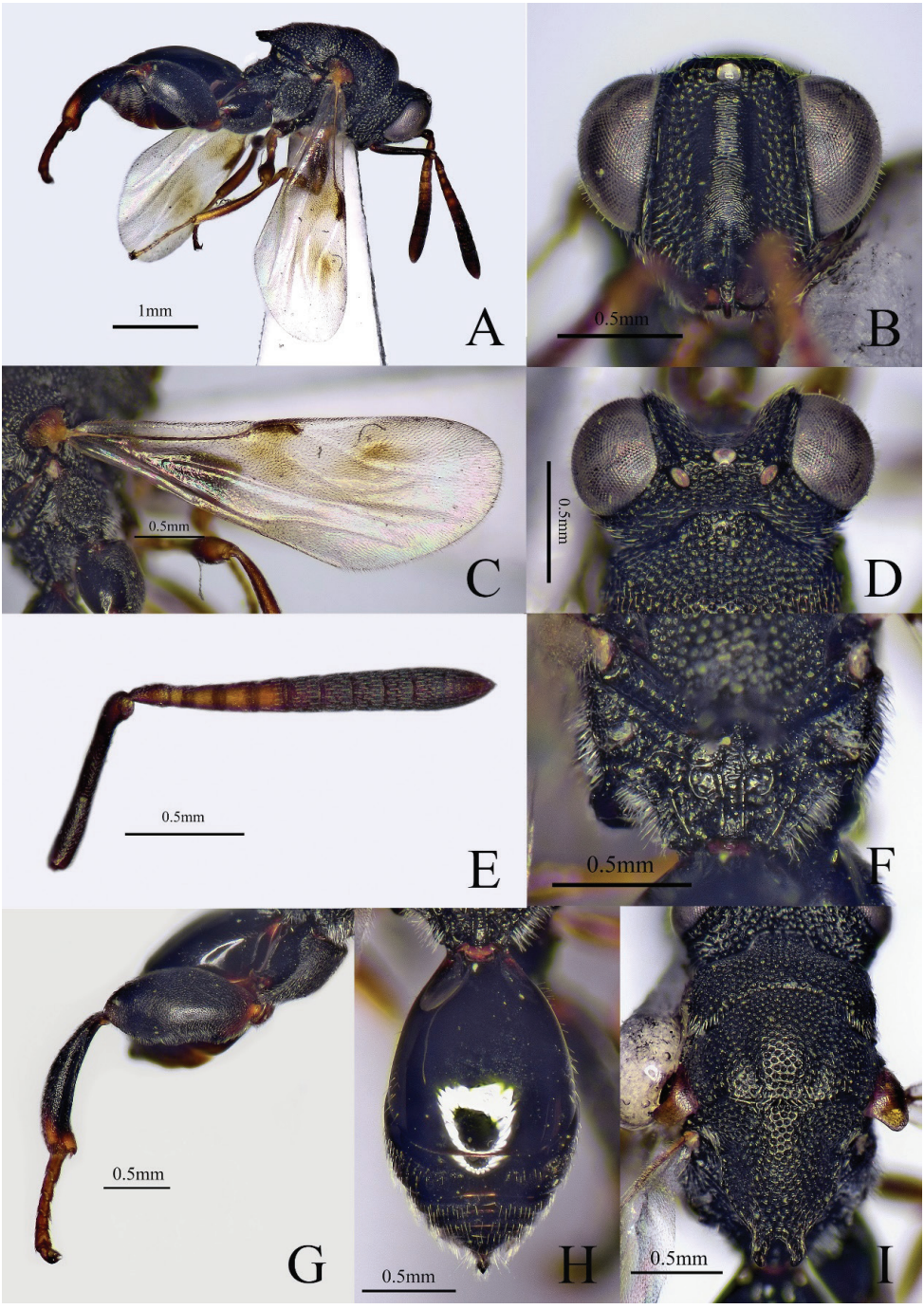

Figure 7. *Halticella nipponensis*, (female) **A** habitus, lateral view **B** head, front view **C** forewing **D** head, dorsal view **E** antenna **F** propodeum **G** hind leg **H** metasoma **I** mesosoma, dorsal view.

1 ♀, China: Guangdong Province, Zhaoqing City, DingHu Mountain, 6–7.V.2019, YPT, Wen-Jian Li, Jun Wu.

Diagnosis. Female. Body length 2.7−4.3 mm, mostly black (Fig. 7A); scape (Fig. 7E) dark brown except brown pedicel to Fu3, eye and ocelli silvery gray (Fig. 7D); tegula brown; fore and mid legs brown, femora slightly darker in middle; hind leg black except yellowish brown tarsus. Head (Fig. 7B, D) 1.1× as wide as long; eye with sparse and short setae; POL 4.9× as long as OOL; scrobe reaching anterior ocellus. Antenna clavate (Fig. 7E), scape a half as long as the remaining antennomeres combined; pedicel longer than Fu1; club coniform, 2× as long as maximum width, 3× as long as and about as broad as the preceding segment; mesoscutellum longer than broad, apex of mesoscutellum (Fig. 7I) with two teeth, distance between outer margins of the two teeth at least 1.5× as long as individual length of teeth. Fore wing largely hyaline (Fig. 7C) with two brown patches; postmarginal vein shorter than stigmal vein; metafemur 2.3× as long as broad (Fig. 7G); metasoma oval (Fig. 7H), 1.6× as long as broad in dorsal view; Gt1 occupying 0.7× length of metasoma.

Hosts. Unknown.

Distribution. China (Heilongjiang [new record], Shanxi [new record], Shandong [new record], Xizang [new record], Yunnan [new record], Guangdong [new record], Taiwan), Japan, India (Narendran 1989), Vietnam (Narendran and van Achterberg 2016).

Comments. Our specimens agree well with the original description except for slight colour differences of the teeth of the mesoscutellum. This is the first record from continental China.

Acknowledgements

Thanks to Prof Hui-Lin Han, Dr Xiang-Xiang Jin, Dr Guo-Hao Zu, Dr Chen Ye, Dr Hui Geng, Dr Si-Zhu Liu, Dr Jun Wu, Dr Ming-Rui Li, Mr Guang-Xin Wang, Mr Hai-Feng Bai, Mr Jun-Chao Wang, Mr Zhi-Guang Wu, Mr Jiang Liu, Mr Tuo Sang, Miss Yang Peng, Miss Xing-Yue Jin, Miss Chao Zhang, Miss Xin-Yu Zhang and Miss Yan Gao for specimen collection.

References

Ashmead WH (1904) Descriptions of new Hymenoptera from Japan. II. Journal of the New York Entomological Society 12(3): 146–165.

Habu A (1960) A revision of the Chalcididae (Hymenoptera) of Japan with description of sixteen new species. Bulletin of National Institute of Agricultural Sciences, Tokyo (C)11: 131–363.

Hymenoptera Anatomy Consortium (2021) Hymenoptera Anatomy Ontology Portal. http://glossary.hymao.org/. [Accessed June 2021]

Masi L (1929) Contributo alla conoscenza dei calcididi orientali della sottofamiglia Chalcidinae. Bollettino del Laboratorio di Entomologia del R.Istituto Superiore Agrario di Bologna 2: e177.

Narendran TC (1989) Oriental Chalcididae (Hymenoptera: Chalcidoidea). Zoological Monograph, Department of Zoology, University of Calicut, Kerala, 441 pp.

Narendran TC, van Achterberg C (2016) Revision of the family Chalcididae (Hymenoptera, Chalcidoidea) from Vietnam, with the description of 13 new species. ZooKeys 576: 1–202. https://doi.org/10.3897/zookeys.576.8177

Noyes JS (2019) Universal Chalcidoidea Database. World Wide Web electronic publication. http://www.nhm.ac.uk/chalcidoids. [Last updated March 2019] [Accessed June 2021]

Roy CS, Farooqi SI (1984) Taxonomy of Indian Haltichellinae (Chalcididae: Hymenoptera) at National Pusa Collection, IARI, New Delhi. Memoirs of the Entomological Society of India 10, 59 pp.

Walker F (1862) Notes on Chalcidites, and characters of undescribed species. Transactions of the Entomological Society of London (3)1: 345–397. https://doi.org/10.1111/j.1365-2311.1862.tb01285.x

ZooKeys 1060: 17–32 (2021)
doi: 10.3897/zookeys.1060.67674
https://zookeys.pensoft.net

DATA PAPER

A peer-reviewed open-access journal
ZooKeys
Launched to accelerate biodiversity research

Three new species of the genus *Araeopteron* Hampson, 1893 (Lepidoptera, Erebidae, Boletobiinae) from the Xizang Autonomous Region, China with an updated list of the world species

Hui Lin Han[1,2], Vladimir S. Kononenko[3]

1 *School of Forestry, Northeast Forestry University, Harbin, 150040, China* **2** *Key Laboratory of Sustainable Forest Ecosystem Management-Ministry of Education, Northeast Forestry University, Harbin, 150040, China* **3** *Laboratory of Entomology, Federal Scientific Center of the East Asia Terrestrial Biodiversity, Far Eastern Branch, Russian Academy of Sciences, Vladivostok-22, 690022, Russia*

Corresponding author: Vladimir S. Kononenko (vsk528217@gmail.com)

Academic editor: Alberto Zilli | Received 20 April 2021 | Accepted 6 August 2021 | Published 15 September 2021

http://zoobank.org/7B214F86-33A7-4A5E-9A04-01D118EDD5A9

Citation: Han HL, Kononenko VS (2021) Three new species of the genus *Araeopteron* Hampson, 1893 (Lepidoptera, Erebidae, Boletobiinae) from the Xizang Autonomous Region, China with an updated list of the world species. ZooKeys 1060: 17–32. https://doi.org/10.3897/zookeys.1060.67674

Abstract

Three new species of the genus *Araeopteron* Hampson, 1893: *A. dawai* **sp. nov.**, *A. medogensis* **sp. nov.** and *A. tibeta* **sp. nov.** are described from Motuo (= Medog) County of the Xizang Autonomous Region (= Tibet), China. The imagines as well as the male genitalia are illustrated. A checklist of the 45 species of the genus *Araeopteron* in the world fauna is presented, including recently and presently described species.

Keywords

Araeopteronini, checklist, moths, new species, Noctuoidea systematics, Tibet

Introduction

The genus *Araeopteron* Hampson, 1893 (type species *A. pictale* Hampson, 1893) belongs to the tribe Araeopteronini, subfamily Boletobiinae, Erebidae. The early authors considered *Araeopteron* in the Eustrotiinae = Erastriinae (Erastrianae

sensu Hampson 1910) or Acontiinae (sensu auctorum) of the Noctuidae (Hampson 1910; Inoue 1958, 1965; Nye 1975; Sugi 1982; Poole 1989; Kononenko 1990, 2003, 2005; Kononenko et al. 1998; Fibiger and Agassiz 2001; Fibiger and Hacker 2001).

Araeopteronini Fibiger, 2005 originally has been designated and used as a subfamily Araeopteroninae of the family Noctuidae (Fibiger and Lafontaine 2005; Lafontaine and Fibiger 2006), but later it was downgraded to tribal status and placed to the subfamily Boletobiinae of the family Erebidae (Holloway 2011; Zahiri et al. 2012; Kononenko 2016; Wu et al. 2020).

The group's distribution is mainly pantropical, but a few species extend into the temperate zone: six species are recorded in Japan, the Russian Far East, and the Korean Peninsula (Inoue 1958, 1965; Kononenko et al. 1998; Kononenko and Han 2007; Fibiger and Kononenko 2008) and one species is recorded in the Near East and southern Europe (Fibiger and Agassiz 2001; Fibiger and Hacker 2001).

The world fauna list of 36 species of *Araeopteron* was published by Fibiger and Kononenko (2008). Subsequently, a review of the Araeopteronini from Borneo followed by a list of species was published by Holloway (2009, 2011). Contributions to the taxonomy of the genus *Araeopteron* was made by Guillermet (2009) and Bippus (2018), designating two new *Araeopteron* species, *A. papaziani* Guillermet, 2009 and *A. legraini* Bippus, 2018 from Réunion Island, western Indian Ocean. The total number of described species of the genus *Araeopteron* in the world fauna (with accounts of the currently described species) now enumerates 45 species.

In China, the genus represented by eight species: *Araeopteron amoena* Inoue, 1958, *A. fragmenta* Inoue, 1965, *A. nebulosa* Inoue, 1965, *A. canescens* (Walker, [1866]), *A. fasciale* (Hampson, 1896), *A. dawai* sp. nov., *A. medogensis* sp. nov., *A. tibeta* sp. nov. distributed from the cool temperate zone to the subtropics.

As a result of intensive collecting and study of the Noctuoidea in remote regions of the Xizang Autonomous Region (= Tibet) in China, three new *Araeopteron* species were found. This article describes and illustrates them in detail.

Materials and methods

The material was collected by UV light in remote parts of the Xizang Autonomous Region, Tibet, China. Standard methods for dissection and preparation of the genitalia slides have been used as described by Kononenko and Han (2007). Specimens were photographed with a Nikon D700 camera; the genitalia slides were photographed with an Olympus photomicroscope with Helicon Focus software, with the images further processed in Adobe Photoshop CS4.

The materials of the present article, including holotypes, are deposited in the collection of Northeast Forestry University, Harbin, China (**NEFU**).

Systematic account

Tribe Araeopteronini Fibiger, 2005

Araeopteroninae Fibiger, 2005, *Esperiana* 11: 25 (in Fibiger and Lafontaine 2005). Type genus *Araeopteron* Hampson, 1893. Lafontaine and Fibiger 2006; Kononenko 2005, 2010; Fibiger and Kononenko 2008; Holloway 2009.

Araeopteronini: Holloway 2011; Zahiri et al. 2012; Kononenko and Pinratana 2013; Kononenko 2016; Wu et al. 2020.

Remarks. The tribe comprises rather uniform and small or very small moths with quadrifine hindwing venation. The most conspicuous autapomorphic character states defining the Araeopteronini are: in external appearance, their small size, and the shape of the wings with a long, narrow, pointed forewing and short, rounded, triangular hindwing; in the male genitalia, the shape of the tegumen, hugely developed paratergal sclerites, the structure of the valve and the articulation of uncus; and in the female genitalia the patch between the ovipositor lobes on the ventral side and the shape of the signum in the corpus bursae (e.g., Fibiger and Hacker 2001; Fibiger and Lafontaine 2005; Fibiger and Kononenko 2008; Holloway 2009).

Araeopteronini is a poorly studied and neglected group of Erebidae moths. At present, the tribe Araeopterinini includes the Old World genus *Araeopteron* with many undescribed species and some other tropical genera belonging to the Boletobiinae (*Hyriodes* Hampson, 1910, *Pseudcraspedia* Hampson, 1889, and *Niaccaba* Walker, 1895) (Holloway 2009, 2011; Kononenko and Pinratana 2013).

Genus *Araeopteron* Hampson, 1893

Figures 1–12

Araeopteron Hampson, 1893, *Illustrations of Typical Specimens of Lepidoptera Heterocera in the Collection of the British Museum* 9: 33, 136. Type species: *Araeopteron pictale* Hampson, 1893 [Sri Lanka].

Synonymy. *Araeopterum* Hampson, 1896, emendation; *Thelxinoa* Turner, 1902; *Essonistis* Meyrick, 1902; *Araeopterella* Fibiger & Hacker, 2001; *Araeoptera* Hampson, 1910, emendation.

References. Inoue 1958, 1965; Nye 1975; Sugi 1982; Poole 1989; Kononenko 1990, 2003, 2005, 2010, 2016; Kononenko et al. 1998; Fibiger and Agassiz 2001; Fibiger and Hacker 2001; Fibiger 2002; Kononenko and Han 2007; Fibiger and Kononenko 2008; Guillermet 2009; Holloway 2009, 2011; Kononenko and Pinratana 2013; Bippus 2018; Wu et al. 2020.

Diagnosis. Small and very small species, wingspan 9–18 mm. Forewing narrow, with oblique outer margin and long fringes; hindwing shorter than forewing, with shallow concavity under apex; wing colour grey or brown-grey, in some species with or-

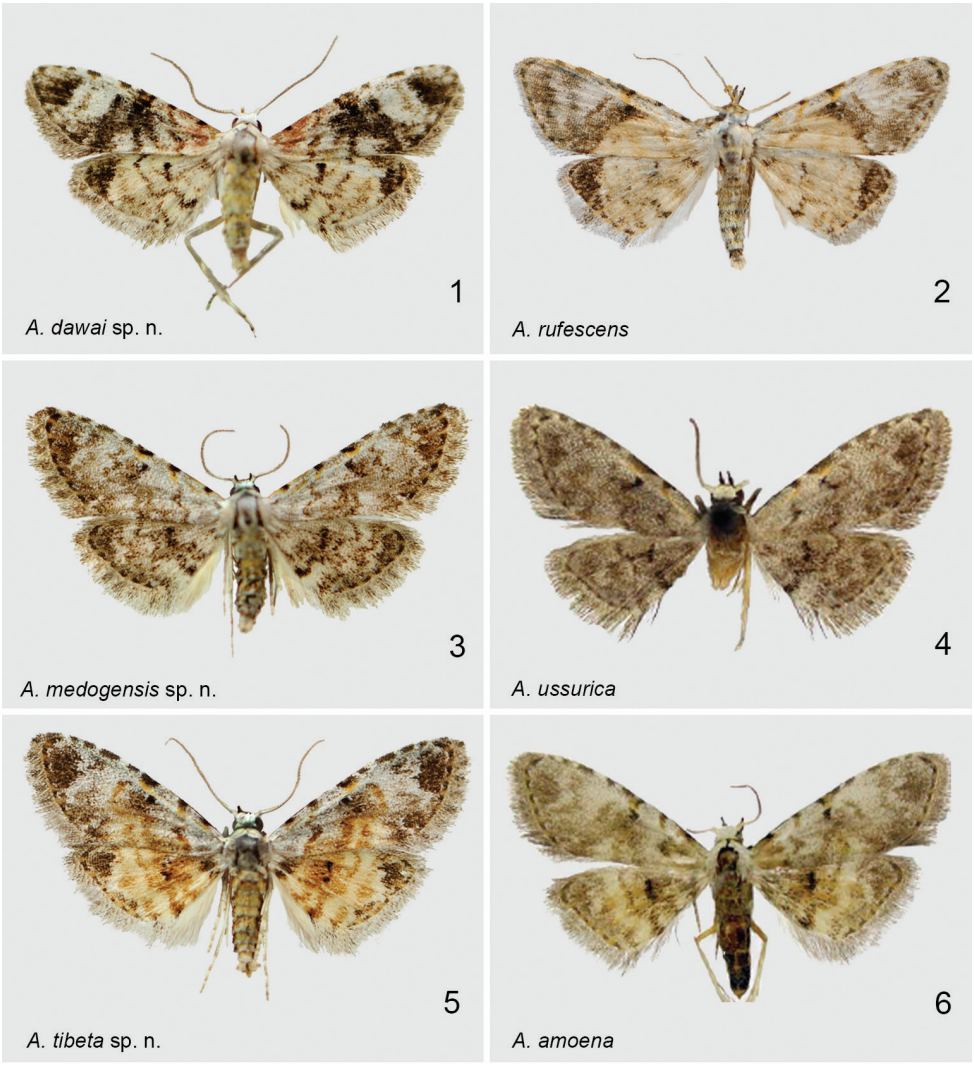

Figures 1–6. Adults of *Araeopteron* spp. **1** *A. dawai* sp. nov. holotype **2** *A. rufescens*. Malaysia, Borneo **3** *A. medogensis* sp. nov. holotype **4** *A. ussurica* (Russia, Primorye, after Fibiger and Kononenko 2008) **5** *A. tibeta* sp. nov. holotype **6** *A. amoena* (Russia, Primorye, after Fibiger and Kononenko 2008).

ange or pale reddish patches, reniform stigma black; frons scaled. In the male genitalia, tegumen short, broad, paratergal sclerites uniting the tegumen and vinculum hugely developed; vinculum short and broad; uncus with long coecum; costa and cucullus membranous; sacculus sclerotised, narrow; apex of sacculus spatulate or club-shaped; uncus thin, rather short, curved. In the female genitalia, a small raised membranous or slightly sclerotised patch or low cone covered with long hair-like setae lies between posterior ends of anal papillae; signum cone-like or hat-like with a rounded top, fringed

basally with spines; sometimes signum as relatively large flat plate. Larva and food specialisation are unknown.

The genus includes 45 described species and many undescribed species distributed mainly in tropical and subtropical regions; a few species extend into the temperate zone.

In China five described species of the genus *Araeopteron* are known (Fibiger and Kononenko 2008), of which two species, *A. canescens* (Walker, [1866]) and *A. fasciale* (Hampson, 1896) have recently been found in southeast China by Wu et al. (2020). Three further new *Araeopteron* species are described below.

***Araeopteron dawai* sp. nov.**

http://zoobank.org/E70C4C1C-18F5-46B0-B103-77E5F0FF8574

Figures 1, 7, 13–15

Type material. ***Holotype*** male, China, Xizang Autonomous Region, Motuo (= Medog) County, 16–17.iv.2018, H.L. Han, genit. prep. no. hhl-4010-1 (NEFU). ***Paratypes.*** 2 ♂♂, same data as holotype, genit. prep. no. hhl-4009-1 (NEFU).

Diagnosis. The new species (Figs 1, 7), externally and in the male genitalia, is similar to *A. rufescens* Hampson, 1910 (Sri Lanka, Malaysia, Borneo; figs 2, 8), but differs by a narrower forewing with sharp apex, bearing a dark triangular patch (in *A. rufescens* apex blunt, without blackish triangular patch; only a weak arched dark band present); the transverse lines are distinct (in *A. rufescens* they are indistinct); the dark apical triangular patch on the hindwing is small (in *A. rufescens* it is broader); the discal spot is distinct and stout (in *A. rufescens* indistinct and slender).

***Male genitalia*:** clasper with medially sclerotised harpe and small thorn-like apical extension (in *A. rufescens* the clasper with small smooth teeth apically); the costa rounded and swollen in the terminal part of the valva (in *A. rufescens* it is swollen and triangular in apical third of valva); the uncus as long as the tegumen (in *A. rufescens* the uncus is ca 1/2 tegumen length); aedeagus slightly curved (in *A. rufescens* it is straight); vesica with a toothed band (in *A. rufescens* it bears more than 20 small thin spines).

Description. Adult (Fig. 1). Wingspan 11.5–12.0 mm. Antennae filiform, head, patagia, and tegulae covered with flat white scales, thorax whitish with grey; abdomen greenish yellow, mixed with white. Forewing pale yellow to pale greyish yellow, mixed with a little orange; apex rather sharp; basal area dark orange, basal line expressed with distinct black costal dot; antemedial line blackish brown, almost black, wavy, oblique; median line double, black, filled with mixed brown with orange inside, smoothly incurved, with pale black and orange patches between lines; postmedial line brownish orange and strongly arched before Cu_2, its other part mixed with black, and incurved to inner margin; subterminal line brownish black at costal margin, other part fused with blackish apical patch; terminal line brown to blackish brown, with black dots at the tops of veins; reniform stigma dark black; apex with large black triangular patch; basal, antemedial, and median areas densely covered with orange; postmedial area pale to greyish white, with blackish brown to brown at inner margin; subterminal area pale

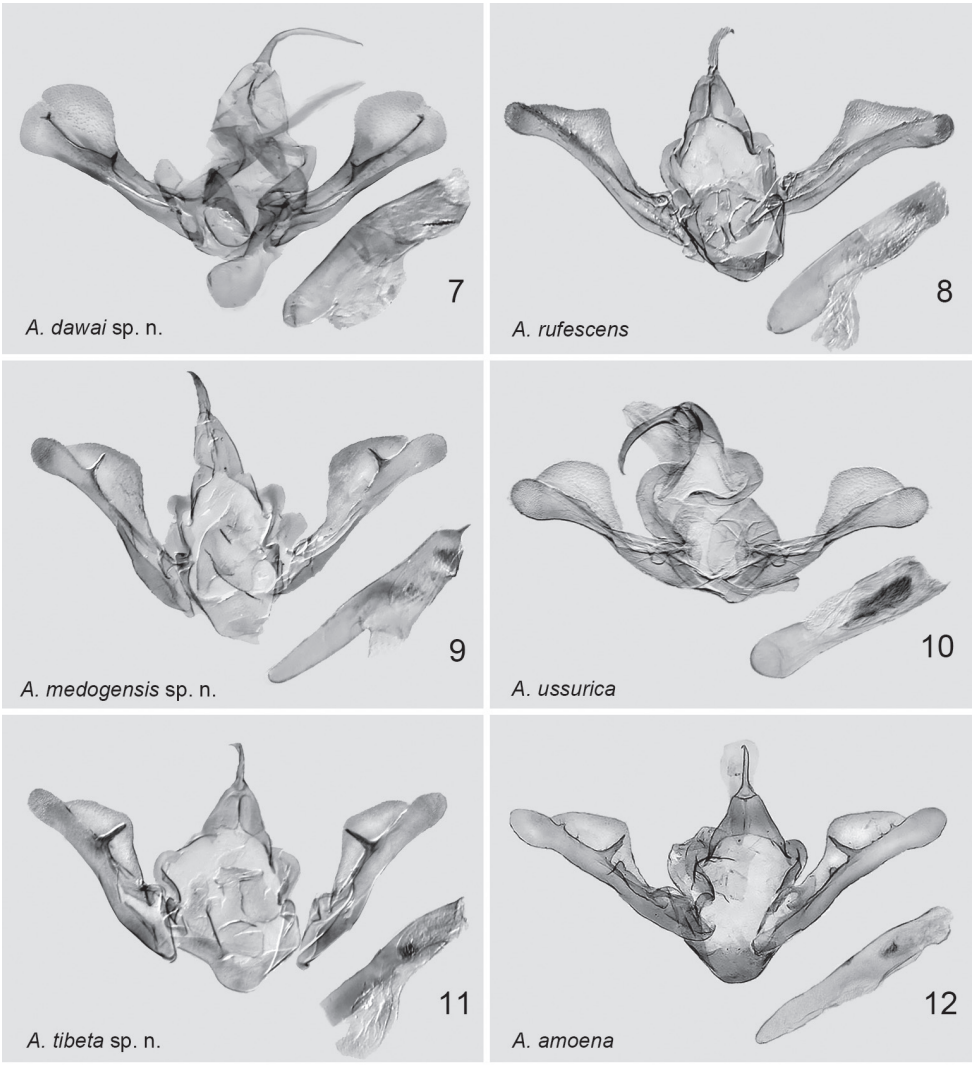

Figures 7–12. Male genitalia of *Araeopteron* spp. **7** *A. dawai* sp. nov. holotype, gen. prep. no. hhl-4010-1 **8** *A. rufescens*, Malaysia, Borneo, gen. prep. no. hhl-4587-1 **9** *A. medogensis* sp. nov. holotype, gen. prep. no. hhl-4022-1 **10** *A. ussurica* (Russia, Primorye, after Fibiger and Kononenko 2008) **11** *A. tibeta* sp. nov. holotype, gen. prep. no. hhl-4026-1 **12** *A. amoena* (Russia, Primorye, after Fibiger and Kononenko 2008).

greyish; fringe grey, mixed with brown; pale and greyish parts of the postmedial and subterminal area forming large patch. Hindwing pale greyish yellow to faint yellow; antemedial line smoky-brown to brownish black, wavy; median line orange, weakly waved; postmedial line brown to brownish black, wavy, incurved posteriorly; subterminal line smoky orange, indistinct; apex sharp with single large black triangular patch; fringe thin and lighter than in forewing; discal spot dark black, formed by two dots.

Male genitalia (Fig. 7). Tegumen triangular, as narrow, strongly arched band; paratergal sclerits hugely developed, flat, curved; vinculum, thick, sclerotised. Saccus U-shaped. Valva racket-shaped, narrower medially, extended and rounded apically; sacculus thin, gradually narrower to 3/4 length of valva, then broadened and rounded apically; clasper fused to sacculus, with pointed triangular ampullae medially and small, hook-like apical extension; costa sclerotised, thick basally, gradually extended and membranous apically; cucullus large with small medial incurving on inner margin. Uncus thin, relatively long (as long as tegumen), smoothly curved medially, sclerotised. Juxta plate-like, large, rounded, slightly sclerotised. Aedeagus short, cylindrical, slightly curved, weakly sclerotised posteriorly; coecum short, ca 1/4 as long as aedeagus; vesica with sclerotised band of teeth.

Female genitalia. Female unknown.

Distribution. (Fig. 13). The species is known only from its type locality: China, Xizang Autonomous Region (Tibet), Motuo (= Medog) County.

Etymology. The species name is dedicated to Mr Wa Da, Chinese entomologist, a famous insect researcher of the fauna in the Xizang Autonomous Region, China.

Bionomics. (Figs 14, 15). The new species was collected in Motuo County, Xizang in April 2018 in the intermediate zone between the subtropical rain forest and broadleaf forest zones, at an altitude 1121 m.

***Araeopteron medogensis* sp. nov.**

http://zoobank.org/E19FDE59-FC6E-4009-B895-B922B4BFBD91

Figures 3, 9, 13–15

Type material. ***Holotype*** male, China, Xizang Autonomous Region, Motuo (= Medog) County, 16–17.iv.2018, H.L. Han, genit. prep. no. hhl-4022-1 (NEFU). ***Paratypes.*** 6 ♂♂, same data as holotype, genit. prep. nos. hhl-4021-1, hhl-4023-1, hhl-4024-1, hhl-4025-1 (NEFU).

Diagnosis. The new species, superficially and by the structure of the male genitalia, is similar to *A. ussurica* Fibiger & Kononenko, 2008 (Figs 4, 10), but can by separated from it by the following characters: the basal line present only as a black dot at the costal margin (in *A. ussurica* the basal line is absent); the transverse lines in the costal margin mixed greyish yellow colour (in *A. ussurica* the transverse lines in the costal margin greenish grey); the terminal area coloured with smoky-brown to black (in *A. ussurica* smoky but the terminal area is grey); the wing ground colour in the new species compared with *A. ussurica* is more whitish (in *A. ussurica* it is darker greyish); the wing pattern of the new species is more distinct with stronger colour contrast, compared with *A. ussurica*, in which the ground colour is pale greyish. In the male genitalia, the paratergal sclerite is moderate in length and slightly rounded (in *A. ussurica* it is huge and strongly rounded); vinculum narrower (in *A. ussurica* it is much broader); saccus U-shaped (in *A. ussurica* it is V-shaped); the harpe is needle-like, placed in the apical part of valva, ca 3/4 length of valva from its basal part (in *A. ussurica* harpe as a small

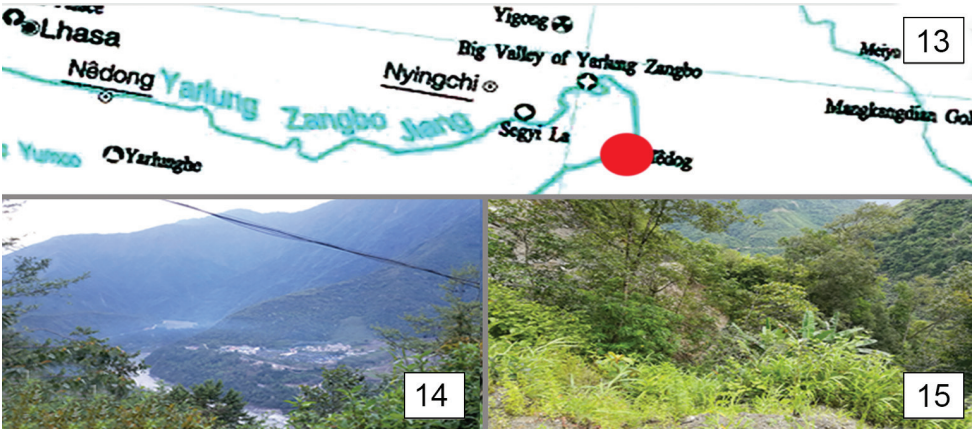

Figures 13–15. The map (**13**) and habitat (**14, 15**) of Araeopteron spp. in the Xizang Autonomous Region, China

bulge 2/3 from basal part of valva); the costa with a smoothly arched bulge in apical 1/2 of valva (in *A. ussurica* the costa with round bulge); the uncus short, as long as 1/2 of tegumen, slightly curved apically vs. 2X longer than tegumen, hooked apically uncus in *A. ussurica*; the aedeagus is narrow and long vs. short and broad in *A. ussurica*; the carina with spines (in *A. ussurica* the carina without spines); the vesica with two sclerotised cornute patches (in *A. ussurica* the vesica with a large cornute band formed by numerous thin, small spines).

Description. Adult (Fig. 3). Wingspan 11.0–12.5 mm. Antennae filiform. Head, patagia, tegulae, and thorax covered with white scales; abdomen greyish white, mixed with orange. Forewing pale greyish yellow, mixed with brown; forewing apex blunt, rounded; basal line present as a black dot at costal margin, its other part distinct, grey with small yellow scales; antemedial line oblique, thin, wavy, brown with yellow at costal area; median line double, indistinct, thin, wavy, smoky-brown between double lines, and as distinct black dot at costal margin; postmedial line broad, brown, rising to M_3, slightly curved, then bending and going obliquely to inner wing margin; subterminal line as brownish green dots at costal margin, its other part fused to brownish apical patch; terminal line pale brown to brownish green, with black dots on vein; reniform stigma dark, black, formed by two diffused dots; terminal area pale brown to brownish green; fringe grey, mixed with brown, in basal part with yellow. Hindwing pale greyish with white, slightly darker than forewing; antemedial line smoky-brown, indistinct; median line blackish brown, indistinct, weakly waved; postmedial line slender, brown to brownish black, wavy, sharp at Cu_1 area; subterminal line smoky-brown, slightly mixed with black, wavy, indistinct; terminal line and fringes same as on forewing; discal spot prominent, dark brown, slightly diffused.

Male genitalia (Fig. 9). Tegumen triangular, narrow dorsally. Paratergal sclerits thin, broaded apically. Vinculum thick, sclerotised, U-shaped, flat, and broader pos-

teriorly. Saccus U-shaped, weakly sclerotised. Valva constricted basally; sacculus thin, sclerotised, gradually narrower medially, then gradually broader and rounded apically, exceed cucullus; clasper fused to sacculus, with pointed and tapered harpe in its apical third; costa slightly sclerotised, with minute grains, thin basally, gradually arched and swollen apically. Uncus relatively short and solid, ca 1/3 length of tegumen, slightly curved, sclerotised. Juxta large, plate-like, with bulb at centre, and broad outer frame. Aedeagus long, cylindrical, slightly curved, carina with short spines, slightly sclerotised; coecum as long as 1/2 length of aedeagus; vesica with weakly sclerotised grainy band and plate.

Female genitalia. Female unknown.

Distribution. (Fig. 13). The species is known only from its type locality: China, Xizang Autonomous Region (Tibet), Motuo (= Medog) County.

Etymology. The species name refers to the Tibetan name of the type locality Medog in Tibet, China.

Bionomics. (Figs 14, 15). The new species has been collected in Motuo County of Xizang in April in the intermediate zone between subtropical rain forest and broad-leaf forest zones, at an altitude 1121 m.

***Araeopteron tibeta* sp. nov.**

http://zoobank.org/2E7076ED-9044-42E5-9FA9-46BB2FA9FA76

Figures 5, 11, 13–15

Material examined. *Holotype*: male, China, Xizang Autonomous Region, Motuo (= Medog) County, 16–17.iv.2018, H.L. Han, genit. prep. no. hhl-4026-1 (NEFU). ***Paratype*:** 1 male with same data (NEFU).

Diagnosis. The new species is similar to *A. amoena* (Figs 6, 12, 13–15) by the external appearance and the male genitalia but differs by the more colourful and distinct wing pattern with greyish orange medial part of the forewing and orange for most of the hindwing (in *A. amoena* the wing pattern and colouration is less distinct and less colourful, with a greyish orange patch in the middle of the hindwing); the forewing basal line in *A. tibeta* presents as a black dot on the costal margin and continues as a very thin line (in *A. amoena* only the small black dot at the costal margin is expressed); blackish apical patch distinct (in *A. amoena* it is indistinct); transverse lines of the forewing distinct (in *A. amoena* they are indistinct); reniform stigma streak-like, formed with two dots (in *A. amoena* it presents as a small dot); the hindwing with black triangular apical patch (in *A. amoena* the triangular apical patch is diffused; fringe paler than in *A. amoena*). In the male genitalia, clasper with spine-like harpe, without three small tooth-like extensions present in *A. amoena*; the smoothly arched bulge of costa is rather straight posteriorly, slightly constricted anteriorly (in *A. amoena* it is smooth and slightly curved posteriorly).

Description. Adult (Fig. 5). Wingspan 11.5–12.0 mm. Antennae filiform. Head, patagia, and tegulae covered with white scales; thorax greyish white, with two medial patches of blackish scales. Abdomen greenish brown, mixed with orange. Forewing pale greyish white; apex rather sharp; basal line present only as a black dot at costal margin, its other part diffused, slender; antemedial line brown, wavy, oblique, with brownish yellow patch at costal area; median line double, reddish brown, diffused, wavy, greyish brown between lines, and as distinct blackish dot at costal margin; postmedial line brown, indistinct, wavy, with fracture at costal region; subterminal line only as brown dot at costal margin, in other part fused to apical greyish brown patch; terminal line pale brown to greenish brown, with black dot at vein; reniform stigma dark black, formed by two fused dots; terminal area blackish brown to dark brownish, forms ovoid patch at wing apex; medial part of wing greyish orange brown colouration; fringe grey, mixed with blackish brown, yellow basally. Hindwing greyish orange-yellow; antemedial line blackish brown, broad and distinct; median line reddish brown, indistinct; postmedial line thin, reddish brown, slightly waved, with blackish inner border; subterminal line reddish brown, slightly waved; terminal area, terminal line, and fringe same colour as on forewing; discal spot dark black, formed with two dots.

Male genitalia (Fig. 11). Tegumen triangular posteriorly, thick, curved, broad anteriorly. Paratergal sclerits large, but smaller than in related *A. amoena*. Vinculum thick, sclerotised, flat, U-shaped, broad band-like posteriorly. Saccus U-shaped, membranous. Valva constricted at 1/3 from base; sacculus thick, sclerotised, gradually constricted to broad medial part, rounded apically, and exceeding cucullus; clasper fused to sacculus, with pointed, sclerotised tapered harpe, placed ca 3/5 length from base of valva; costa slightly sclerotised, minutely granulated, thin basally, gradually arched and extended to swollen, membranous middle part. Uncus short, as long as 1/2 of tegumen, thin, slightly curved apically. Juxta large, plate-like sclerotisation posteriorly. Aedeagus long, cylindrical, slightly curved, weakly sclerotised, carina with very short spines; coecum as long as ca 1/2 aedeagus; vesica with weakly sclerotised patch of minute spines medially.

Female genitalia. Female unknown.

Distribution. (Fig. 13). The species is known only from its type locality: China, Xizang Autonomous Region (Tibet), Motuo (= Medog) County.

Etymology. The species name refers to Tibet.

Bionomics. (Figs 14, 15). The new species has been collected in Motuo County of Xizang in April in the intermediate zone between subtropical rain forest and broad-leaf forest zones, at an altitude of 1121 m.

Checklist of the genus *Araeopteron* Hampson, 1893 of the world

Araeopteron acidalica (Hampson, 1910), "Catalogue of the Lepidoptera Phalaenae in the British Museum" 10: 22, fig. 9 (*Araeoptera*). Type locality: Jamaica, Moneagaue.

Araeopteron adeni Fibiger & Hacker, 2001, "Esperiana" 8: 578, Pl. 28: 8. Type locality: Yemen, Prov. Abyan, 50 km NE Aden, 7 km NNW Zinjibar, 50 m.

Araeopteron alboniger Fibiger & Hacker, 2001, "Esperiana" 8: 581, Pl. 28: 14, 15. Type locality: Yemen, Prov. Ibb, Lower Wadi Duur, village Azuhirya, 1300 m.

Araeopteron amoena Inoue, 1958, "Tinea" 4: 230, fig. 2. Type locality: Japan, Kangawa Pref., Chigasaki.

Araeopteron aulombardi Fibiger & Hacker, 2001, "Esperiana" 8: 580, Pl. 28: 12, 13. Type locality: Yemen, Prov. Ibb, Wadi Merhab, village Lajajil, 1600 m.

Araeopteron betie (Dyar, 1914), "Procceedings of the United States National Museum" 47: 184 (*Araeoptera*). Type locality: Panama, Trinidad.

Araeopteron canescens (Walker, 1866), "Illustrations of Typical Specimens of Lepidoptera Heterocera in the Collection of the British Museum" 34: 1318 (?*Isopteryx*). Type locality: Australia, Queensland, Moreton Bay.

= *favillalis* (Walker, [1866]), "Illustrations of Typical specimens of Lepidoptera Heterocera in the Collection of the British Museum" 34: 1319 (?*Isopteryx*). Type locality: Australia, Queensland, Moreton Bay.

Araeopteron dawai Han & Kononenko, sp. nov., "ZooKeys" (present publication). Type locality: China, Xizang Autonomous Region, Motuo County.

Araeopteron diehli Fibiger, 2002, "Heterocera Sumatrana" 12.3: 129. Type locality: Sumatra, S Medan, Dolok Merengir (*Simarsopa*) 170 m.

Araeopteron ecphaea (Hampson, 1914), "Annals and Magazine of Natural History" (8)13: 167 (*Araeoptera*). Type locality: Nigeria, Faro.

Araeopteron elam (Schaus, 1911), "Annals and Magazine of Natural History" (8)8: 108 (*Acidaliodes*). Type locality: Costa Rica, Juan Vinas.

Araeopteron epiphracta (Turner, 1902), "Proceedings of the Linnaean Society of New South Wales" 27: 132 (*Thelxinoa*). Type locality: Australia, Queensland, Brisbane.

Araeopteron fasciale (Hampson, 1896), "The Fauna of British India, Including Ceylon and Burma. Moths" 4: 543 (*Araeopterum*). Type locality: Sri Lanka.

Araeopteron flaccida Inoue, 1958, "Tinea" 4: 229, Pl. 32: 1. Type locality: Japan, Kanagawa Pref., Chigasaki.

Araeopteron fragmenta Inoue, 1965, "Tinea" 7: 81, Pl. 15: 5A, 5B. Type locality: Japan, Kanagawa Pref., Fujisawa.

Araeopteron goniophora Hampson, 1907, "Journal of the Bombay Natural History Society" 17: 670. Type locality: Sri Lanka, Nawalpitiya.

Araeopteron griseata Hampson, 1907, "Journal of the Bombay Natural History Society" 17: 670. Type locality: Sri Lanka.

Araeopteron imbecilla (Turner, 1933), "Transactions and Proceedings of the Royal Society of South Australia" 57: 161 (*Araeoptera*). Type locality: Australia, North Queensland, Babinda.

Araeopteron koreana Fibiger & Kononenko 2008, "Zootaxa" 1891: 50, Figs 11, 18. Type locality: South Korea, Pyounchang GW, Moonsen-ri.

Araeopteron kurokoi Inoue, 1958, "Tinea" 4: 230. Type locality: Japan, Fukoka Pref., Hikosan Mt.

Araeopteron legraini Bippus, 2018; "Phelsuma" 26: 23; Type locality: Réunion, La Possession, 400 m.

Araeopteron leucoplaga (Hampson, 1910), "Catalogue of the Lepidoptera Phalaenae in the British Museum" 10: 29, Pl. 149: 19 (*Araeoptera*). Type locality: Borneo, Pulo Laut.

Araeopteron makikoae Fibiger & Kononenko 2008, "Zootaxa" 1891: 49, Figs 7, 8, 16, 24, 29. Type locality: Russia, Primorye terr., Gornotaezhnoe.

Araeopteron medogensis Han & Kononenko, sp. nov., "ZooKeys" (present publication). Type locality: China, Xizang Autonomous Region, Motuo County.

Araeopteron micraeola (Meyrick, 1902, April), "Transactions of the Entomological Society of London" 35: 36 (*Essonistis*). Type locality: Australia, Queensland, Brisbane.

= *calliscia* Turner, 1902 (*Thelxinoa*), "Proceedings of the Linnaean Society of New South Wales". Type locality: Australia, Queensland, Brisbane.

Araeopteron microclyta (Turner, 1920), "Transactions and Proceedings of the Royal Society of South Australia" 44: 161 (*Araeoptera*). Type locality: Australia, North Queensland, Kuranda.

Araeopteron minimale Freyer, 1912, "Transactions of the Linnaean Society of London (Zool.)" 15(1): 11. Type locality: Seychelles, Mahe.

Araeopteron nebulosa Inoue, 1965, "Tinea" 7: 82, pl, 15: 4A, 4B. Type locality: Japan, Shizouka Pref., Odaru Spa.

Araeopteron nivalis Hampson, 1907, "Journal of the Bombay Natural History Society" 17: 671. Type locality: Sri Lanka, Paradeniya.

Araeopteron obliquifascia (Joanis, 1910), "Bulletin de la Société Entomologique de France" 1910: 201 (*Araeoptera*). Type locality: Mauritius, Curepipa.

Araeopteron papaziani Guillermet, 2009; "L'Entomologiste" 65 (3): 121; Type locality: Réunion, Les Avirons 250 m.

Araeopteron pictale Hampson, 1893, "Illustrations of Typical Specimens of Lepidoptera Heterocera in the Collection of the British Museum" 9: 33, 137, Pl. 168: 19. Type locality: Sri Lanka, Pundaloya.

Araeopteron pleurotypa (Turner, 1902), "Proceedings of the Linnaean Society of New South Wales" 27: 133 (*Thelxinoa*). Type locality: Australia, Queensland, Cairns, Townsville.

Araeopteron poliobapta (Turner, 1925), "Transactions and Proceedings of the Royal Society of South Australia" 44: 39 (*Araeoptera*). Type locality: Australia, Queensland, Montville.

Araeopteron poliophaea (Hampson, 1910), "Catalogue of the Lepidoptera Phalaenae in the British Museum" 10: 29, Pl. 149: 20 (*Araeoptera*). Type locality: Sri Lanka, Maskeliya.

Araeopteron proleuca Hampson, 1907, "Journal of the Bombay Natural History Society" 17: 671. Type locality: India, Sri Lanka.

Araeopteron rufescens (Hampson, 1910), "Catalogue of the Lepidoptera Phalaenae in the British Museum" 10: 27, Pl. 149: 17 (*Araeoptera*). Type locality: Sri Lanka, Kegalle.

Araeopteron schreieri Fibiger & Hacker, 2001, "Esperiana" 8: 579, Pl. 28: 10, 11. Type locality: Yemen, 36, Prov. Al Hudaydah, Jabal Burra, 25 km SE Bajil, 600 m.

Araeopteron sterrhaoides (Fibiger & Hacker, 2001), "Esperiana" 8: 582: Pl. 28: 16, 17 (*Araeopterella*). Type locality: Yemen, Prov. Sanaa, Jabal Raymah, 25 km E Al Mansuriyah, Wadi Bullbull, 2 km SE Khansa, 700 m.

Araeopteron tibeta Han & Kononenko, sp. nov., "ZooKeys" (present publication). Type locality: China, Xizang Autonomous Region, Motuo County.

Araeopteron vilhelmina (Dyar, 1916), "Proceedings of the United States National Museum" 51: 18 (*Araeoptera*). Type locality: Mexico, Tabasco, Teapa.

Araeopteron xanthopis Hampson, 1907, "Journal of the Bombay Natural History Society" 17: 672. Type locality: Sri Lanka, Haldamulla.

Araeopteron yemeni Fibiger & Hacker, 2001, "Esperiana" 8: 577, Pl. 8: 4. Type locality: Yemen, Prov. Sanaa, Jabal Raymah, 25 km E Al Mansuriyah, Wadi Bullbull, 2 km SE Khansa, 700 m.

Acknowledgements

The present study was supported by the National Nature Science Foundation of China, No. 31872261, 31572294 and 31272355, and the Fundamental Research Funds for the Central Universities (No. 2572019CP11). We are grateful to Mr Wa Da and Mr Yongqiang Xu for their help and support during field work in the Motuo region during 2018.

References

Bippus M (2018) New Erebidae from the Mascarene island and about some Madagascar Lepidoptera (Lepidoptera: Erebidae). Phelsuma 26: 10–43. https://islandbiodiversity.com/Phelsuma27d.pdf

Fibiger M, Hacker H (2001) The *Araeopteron* genus-group in Yemen, with description of one new genus and 6 new species (Lepidoptera, Noctuidae). Esperiana 8: 575–584.

Fibiger M, Agassiz D (2001) *Araeopteron ecphaea*, a small noctuid moth in the West Palaearctic (Noctuidae: Acontiinae). Nota Lepidopterologica 24(1/2): 29–35.

Fibiger M (2002) A new Araeopteron species, *A. diehli* sp. nov. from northern Sumatra (Lepidoptera, Noctuidae). Heterocera Sumatrana 12(3): 129–132.

Fibiger M, Lafontaine DL (2005) A review of the higher classification of the Noctuoidea (Lepidoptera) with special references to the Holarctic fauna. Esperiana 11: 7–92.

Fibiger M, Kononenko VS (2008) A revision of the subfamily Araeopteroninae Fibiger, 2005 in the Russian Far East and neighbouring countries with a description of four new species (Lepidoptera, Noctuidae). Zootaxa 1891: 39–54. https://doi.org/10.11646/zootaxa.1891.1.4

Fibiger M, Ronkay L, Yela J, Zilli A (2010) Rivulinae-Eutelinae and Supplement vols 1–11. Noctuidae Europaea. 12. Entomological Press, Sorø, 452 pp.

Guillermet C (2009) Contributionàc l'étude des Hétérocères de l'île La Réunion: trios nouveaux Tineidae et un nouveau Noctuidae (Lepidoptera Heterocera). L'Entomologiste 65(3): 117–123.

Hampson GF (1893) The Macrolepidoptera Heterocera of Ceylon. Illustrations of Typical Specimens of Lepidoptera Heterocera in the Collection of the British Museum. Taylor and Francis, London 9: 1–182. [+ 20 pl.]

Hampson GF (1896) The Fauna of British India, Including Ceylon and Burma. Moths 4. Taylor and Francis, London, 549 pp.

Hampson GF (1910) Catalogue of the Lepidoptera Phalaenae in the British Museum. Taylor and Francis, London 10: [i–xix,] 829 pp.

Holloway JD (2009) The Moths of Borneo, part 13, Family Noctuidae, subfamilies Pantheinae, Bagisarinae, Acontiinae Aediinae, Eustrotiinae, Bryophilinae, Araeoperoninae, Aventiinae, Eublemminae. Malayan Nature Journal 62(1–2): 1–240.

Holloway JD (2011) The Moths of Borneo. Part 2. Phautidae, Himantopteridae, Zygaenidae. Complete Checklist, Checklist notes, Historical appendix, Index. Malayan Nature Journal 63(1–2): 1–545.

Inoue H (1958) Three new species of the genus Araeopteron (Lepidoptera, Noctuidae) from Japan. Tinea 4(1): 229–233.

Inoue H (1965) Two new species of Araeopteron (Lepidoptera, Noctuidae) from Japan with notes on the known species. Tinea 7(1): 81–83.

Kononenko VS (1990) Synonymic check list of the Noctuidae (Lepidoptera) of the Primorye Territory, the Far East of U.S.S.R. Tinea 13, Suppl. 1, 40 pp.

Kononenko VS (2003) Introduction; Subfamilies Euteliinae, Acontiinae, Acronictinae, Pantheinae, Agaristinae, Amphipyrinae, Cuculliinae, Hadeninae, Noctuinae and Heliothinae. In: Lehr PA (Ed.) Keys for Identification of the Insects of the Far East of Russia vol. 5, Trichoptera and Lepidoptera. Part 4. Vladivostok, Dal'nauka, 1–34, 215–217, 237–603 [in Russian].

Kononenko VS (2005) An annotated check list of the Noctuidae (s. l.) (Lepidoptera, Noctuoidea: Nolidae. Erebidae. Micronoctuidae, Noctuidae) of the Asian part of Russia and the Ural region. – Noctuidae Sibiricae vol. 1. Entomological Press, Sorø, 243 pp.

Kononenko VS (2010) Micronoctuidae, Noctuidae: Rivulinae – Agaristinae (Lepidoptera). – Noctuidae Sibiricae vol. 2. Entomological Press, Sorø, 475 pp.

Kononenko VS, Han HL (2007) Atlas genitalia of the Noctuidae in Korea (Lepidoptera). In: Park KT (Ed.) Insects of Korea, Series 11]. Korea National Arboretum & Center for Insect Systematics, Pocheon, 464 pp.

Kononenko VS, Pinratana A (2013) Moth of Thailand. Vol. 3. Part 2. Noctuoidea. An illustrated Catalogue of Erebidae, Nolidae, Euteliidae and Noctuidae (Insecta, Lepidoptera) in Thailand. Brothers of St. Gabriel, Bangkok, 625 pp.

Kononenko VS, Ahn SB, Ronkay L (1998) Illustrated catalog of Noctuidae in Korea (Lepidoptera). In: K. T. Park (Ed.) Insects of Korea, [Series 3] Korea Research Institute of Bioscience and Biotechnology & Center for Insect Systematics, Daejeon, 509 pp.

Kononenko VS (2016) Erebidae. In: Leley AS (Ed.) Annotated catalogue of the insects of Russian Far East. Volume II. Lepidoptera. Dalnauka, Vladivostok, 812 pp. [in Russian]

Lafontaine JD, Fibiger M (2006) Revised higher classification of the Noctuoidea. Canadian Entomologist 138: 610–635. https://doi.org/10.4039/n06-012

Meyrick BA (1902) Lepidoptera from the Chatham Islands. Transactions of the Entomological Society of London 35: 273–279. https://doi.org/10.1111/j.1365-2311.1902.tb02389.x

Nye IWB (1975) Noctuoidea (Part): Noctuidae, Agaristidae and Nolidae. The generic names of moths of the World. Vol. 1. British Museum (Natural History), London, 568 pp. [1 frontispiece] https://doi.org/10.5962/bhl.title.119777

Poole RW (1989) Noctuidae. Lepidopterorum Catalogues (New Series). Fascicle 118. EJ Brill. Leiden, pt. 1: v–xii +1–500; pt. 2: 501–1013; pt. 3: 1014–1314.

Sugi S (1982) Noctuidae (except Herminiinae). In: Inoue H, Sugi S, Kuroko H, Moriuti S & Kawabe A (Eds) 1: 669–913, 2: 334–405, pls. 37, 164–223, 229, 278, 355–280. Kodansha, Tokyo. [in Japanese with English synopsis]

Turner AJ (1902) New genera and species of Lepidoptera belonging to the family Noctuidae. Proceedings of the Linnean Society of New South Wales 27: 77–136.

Walker F (1866) List of the Specimens of Lepidopterous Insects in the Collection of the British Museum, vol. 34. Edward Newman, London, 1121–1533.

Wu J, Zhao TT, Han HL (2020) Two new records species of the Tribe Araeopteronini (Erebidae: Boletobiinae) from China. Journal of Northeast Forestry University 48(5): 144–147.

Zahiri R, Holloway JD, Kitching IJ, Lafontaine JD, Mutanen M, Wahlberg N (2012) Molecular phylogenetics of Erebidae (Lepidoptera, Noctuoidea). Systematic Entomology 37(1): 102–124. https://doi.org/10.1111/j.1365-3113.2011.00607.x

ZooKeys 1060: 33–84 (2021)
doi: 10.3897/zookeys.1060.63307
https://zookeys.pensoft.net

RESEARCH ARTICLE

A peer-reviewed open-access journal
ZooKeys
Launched to accelerate biodiversity research

Rossellid glass sponges (Porifera, Hexactinellida) from New Zealand waters, with description of one new genus and six new species

Henry M. Reiswig[1,†], Martin Dohrmann[2], Michelle Kelly[3], Sadie Mills[4], Peter J. Schupp[5,6], Gert Wörheide[2,7,8]

1 *Biology Department, University of Victoria, Victoria, British Columbia, Canada* **2** *Department of Earth and Environmental Sciences, Palaeontology and Geobiology, Ludwig-Maximilians-Universität München, München, Germany* **3** *Coasts and Oceans National Centre, National Institute of Water and Atmospheric Research, Auckland, New Zealand* **4** *NIWA Invertebrate Collection, National Institute of Water and Atmospheric Research, Wellington, New Zealand* **5** *ICBM Terramare, University of Oldenburg, Wilhelmshaven, Germany* **6** *Helmholtz Institute for Functional Marine Biodiversity at the University of Oldenburg (HIFMB), Oldenburg, Germany* **7** *SNSB – Bayerische Staatssammlung für Paläontologie und Geologie, München, Germany* **8** *GeoBio-Center, Ludwig-Maximilians-Universität, München, Germany*

Corresponding author: Martin Dohrmann (m.dohrmann@lrz.uni-muenchen.de)

Academic editor: Pavel Stoev | Received 18 January 2021 | Accepted 4 August 2021 | Published 17 September 2021

http://zoobank.org/9CF1AD75-9AD3-4890-A7B3-59BEDA505C0D

Citation: Reiswig HM, Dohrmann M, Kelly M, Mills S, Schupp PJ, Wörheide G (2021) Rossellid glass sponges (Porifera, Hexactinellida) from New Zealand waters, with description of one new genus and six new species. ZooKeys 1060: 33–84. https://doi.org/10.3897/zookeys.1060.63307

Abstract

New Zealand's surrounding deep waters have become known as a diversity hotspot for glass sponges (Porifera: Hexactinellida) in recent years, and description and collection efforts are continuing. Here we report on eight rossellids (Hexasterophora: Lyssacinosida: Rossellidae) collected during the 2017 RV Sonne cruise SO254 by ROV Kiel 6000 as part of Project PoribacNewZ of the University of Oldenburg, Germany. The material includes six species new to science, two of which are assigned to a so far undescribed genus; we further re-describe two previously known species. The known extant rossellid diversity from the New Zealand region is thus almost doubled, from nine species in five genera to 17 species in eight genera. The specimens described here are only a small fraction of hexactinellids collected on cruise SO254. Unfortunately, the first author passed away while working on this collection, only being able to complete the nine descriptions reported here. The paper concludes with an obituary to him, the world-leading expert on glass sponge taxonomy who will be greatly missed.

† Deceased

Keywords
Bathydorus, *Caulophacus*, Hexasterophora, Lyssacinosida, *Nubes* gen. nov., ROV Kiel 6000, RV Sonne, *Scyphidium*

Introduction

The deep sea of the New Zealand region has only recently been recognised as a hotspot of glass sponge diversity, with two major monographs treating the dictyonal and euplectellid hexactinellids (Reiswig and Kelly 2011, 2018). However, the family Rossellidae Schulze, 1885 (order Lyssacinosida Zittel, 1877), has not been extensively treated thus far. In a literature review of the sponge fauna of New Zealand, Dawson (1993) listed three species of rossellid glass sponges in New Zealand waters: *Aulochone cylindrica* Schulze, 1886 [now accepted as *Crateromorpha* (*Aulochone*) *cylindrica*], *Rossella ijimai* Dendy, 1924, and *Symplectella rowi* Dendy, 1924 (see also Dohrmann 2016). *Symplectella rowi*, and to a lesser extent, *Rossella ijimai*, are now fairly well known because they occur in relatively shallow water in many parts of the New Zealand Exclusive Economic Zone, and they have distinctive morphologies that are easily identifiable from images captured in situ by deep-water imaging systems.

The endemic genus *Symplectella* Dendy, 1924 and only known species, *S. rowi*, was first collected from the Terra Nova Expedition Station 96, 7 miles (11.5 km) east of North Cape on the eastern tip of the North Island, at a depth of 70 fathoms (128 m). It is now known to be relatively common around New Zealand, from the type locality south along the East Coast to the Bay of Plenty, East Cape. In the South Island, the distribution extends from southeast of Cook Strait and Kaikoura Coast out onto the Chatham Rise and deep into the subantarctic New Zealand region. *Symplectella rowi* is less common on the West Coast of both Islands, but this is not an unusual distribution pattern for New Zealand Porifera and may reflect the lighter collection effort on that coastline. The species is, however, quite common in Fiordland (Battershill et al. 2010), where it is found in deep SCUBA-diving depths (up to ~ 30 m), along with other attractions such as endemic black and red corals, hydrozoan sea fans, and sea pens that also occur in shallow depths and are impressive tourist attractions. Recently, several important regional populations have come to light in the North Island: off Rakitu Island, Great Barrier Island, Hauraki Gulf (Lee et al. 2015; Kelly 2016); off Mimiwhangata, Northland (Kerr and Doak, pers. comm.); and in the North Taranaki Bight (Jones et al. 2018).

Rossella ijimai was collected from the same Terra Nova Expedition station as *S. rowi*, ~ 12 km east of North Cape, at 128 m. It is now known from the continental shelf around Northland on both the west and east coasts, and on the Chatham Rise. *Rossella ijimai* and *S. rowi* often co-occur and so the important North Island regional populations of the more abundant *S. rowi* include the odd specimen of *R. ijimai*. Of special interest is the North Taranaki Bight population, discovered only in 2018, where the two species co-occur in relatively high numbers. Recent NIWA and Department of Conservation ROV surveys around Fiordland revealed the first, albeit unconfirmed record of *R. ijimai* (Page and Handley, pers. comm.).

In the 2009 inventory of New Zealand biodiversity, Kelly et al. (2009) listed the following species, confirmed in a later draft manuscript on Rossellidae under preparation by HMR and MK. These include *Caulophacus hadalis* Lévi, 1964, now accepted as *Caulophacus* (*Caulophacus*) *hadalis* (not included in Dawson 1993), *Crateromorpha cylindrica* (Schulze, 1886), now accepted as *Crateromorpha* (*Aulochone*) *cylindrica*, and *Caulophacus schulzei* Wilson, 1904, now accepted as *Caulophacus* (*C.*) *schulzei*. Several species were also included and confirmed for New Zealand in Kelly et al. (2009), from a draft 1980 manuscript under preparation by HMR: *Crateromorpha* (*Aulochone*) *haliprum* Tabachnick & Lévi, 2004; *Crateromorpha* (*Caledochone*) *caledoniensis* Tabachnick & Lévi in Tabachnick (2002); *Caulophacus* (*Caulodiscus*) *onychohexactinus* Tabachnick & Lévi, 2004; *Sympagella clavipinula* Tabachnick & Lévi, 2004. These species are beyond the scope of this work and will be dealt with later. Kelly et al. (2015) confirmed the presence of *Caulophacus* (*C.*) *hadalis and Crateromorpha* (*A.*) *cylindrica* in their Kermadec Islands review.

In 2013, several well-preserved body fossils of a new species, *Rossella cylindrica* Buckeridge & Kelly, 2013 (in Buckeridge et al. 2013), from the late Palaeocene-early Eocene Red Bluff Tuff of Chatham Island, were confirmed by HMR. Both *R. antarctica* Carter, 1872 and *R. racovitzae* Topsent, 1901 were stated to be present on the Chatham Rise, but this remains unconfirmed. Various Rossellidae species were also represented in the Oamaru Diatomite (Eocene) as hexactins, pentactins, and stauractins, illustrated in Hinde and Holmes (1892), but microfossil spicules were not recorded in the Tutuiri Greensand (Kelly and Buckeridge 2005), despite the relatively high proportion of hexactinellid taxa in the fauna. Specimens compared to *Rossella racovitzae/R. antarctica* on the Chatham Rise by Buckeridge et al. (2013) and Campbell Plateau (Chin and Kelly, pers. comm.) form a small, squat, open-mouthed barrel with a restricted base, and have a characteristic veil of hypodermal pentactins protruding beyond the surface of the sponge wall. This latter character is highly reminiscent of the new species described herein, *Nubes tubulata* gen. nov., sp. nov. and *Scyphidium variospinosum* sp. nov., the type localities of which are just north of Chatham Rise.

The 2017 German RV Sonne (cruise SO254) expedition to New Zealand afforded an important collection of ~ 100 new hexactinellid specimens and corresponding seafloor images, collected as part of Project PoribacNewZ of the Institute for Chemistry and Biology of the Marine Environment (ICBM), Carl von Ossietzky University of Oldenburg, using the GEOMAR Helmholtz Centre for Ocean Research Kiel Remotely Operated Vehicle (ROV) Kiel 6000 (Schupp et al. 2017). Preparation of a manuscript combining morphological descriptions and molecular systematics of these glass sponges was underway when we were devastated by the untimely death of Henry Reiswig in July 2020. The objective of this work is to provide the descriptions of specimens completed prior to Henry's passing. This work includes the establishment of a new endemic genus, *Nubes* gen. nov., with two new species; a new species of *Bathydorus* Schulze, 1886; redescription of *Scyphidium australiense* Tabachnick, Janussen & Menschenina, 2008, and description of a new species of *Scyphidium* Schulze, 1900; redescription of *Caulophacus* (*Caulophacus*) *discohexaster* Tabachnick & Lévi, 2004, and description of two new species of *Caulophacus* (*Caulophacus*) Schulze, 1886.

Materials and methods

Sample collection

Specimens, seafloor images, and videos were collected as part of Project PoribacNewZ of the Institute for Chemistry and Biology of the Marine Environment (**ICBM**), Carl von Ossietzky University of Oldenburg, on the new German RV Sonne (cruise SO254), using the GEOMAR Helmholtz Centre for Ocean Research Kiel ROV Kiel 6000 (Schupp et al. 2017). With the exception of NIWA 126016, which was collected in International Waters to the east of Norfolk Island and the Three Kings Ridge, all other specimens were collected from the New Zealand Exclusive Economic Zone (**EEZ**); collection sites and general distribution of the species are shown in Fig. 1.

Sample preparation

Subsamples were taken on board, stored in appropriate preservatives for morphological and molecular work, and shipped to the Ludwig-Maximilians-Universität (**LMU**) Munich. Specimens reported here, together with a much larger collection, the remainder of which will be reported on elsewhere, were first subjected to a molecular phylogenetic study (results not shown) based on a mitochondrial 16S ribosomal DNA fragment (cf. Dohrmann et al. 2008) for initial assessment of their relationships. This then allowed selection of interesting specimens for further study, some of which we describe below. Preliminary morphological identifications of these specimens were made by MD by analysing spicule content with light microscopy of temporary bleach digestions of tissue pieces. Sample preparation for formal identification and description of taxa new to science (as well as re-descriptions of known species where appropriate) were then performed by HMR using methods described in Reiswig and Kelly (2011, 2018).

Registration of type and general material

Primary and secondary type materials of new species and additional material are deposited in the Invertebrate Collection (**NIC**) at the National Institute of Water and Atmospheric Research (**NIWA**), Greta Point, Wellington, using the prefix NIWA – . Registration numbers are cited in the text. Taxonomic authority is restricted to Reiswig, Dohrmann & Kelly.

Abbreviations

EEZ Exclusive Economic Zone;
GEOMAR Research Center for Marine Geosciences, Helmholtz Centre for Ocean Research Kiel, Germany;

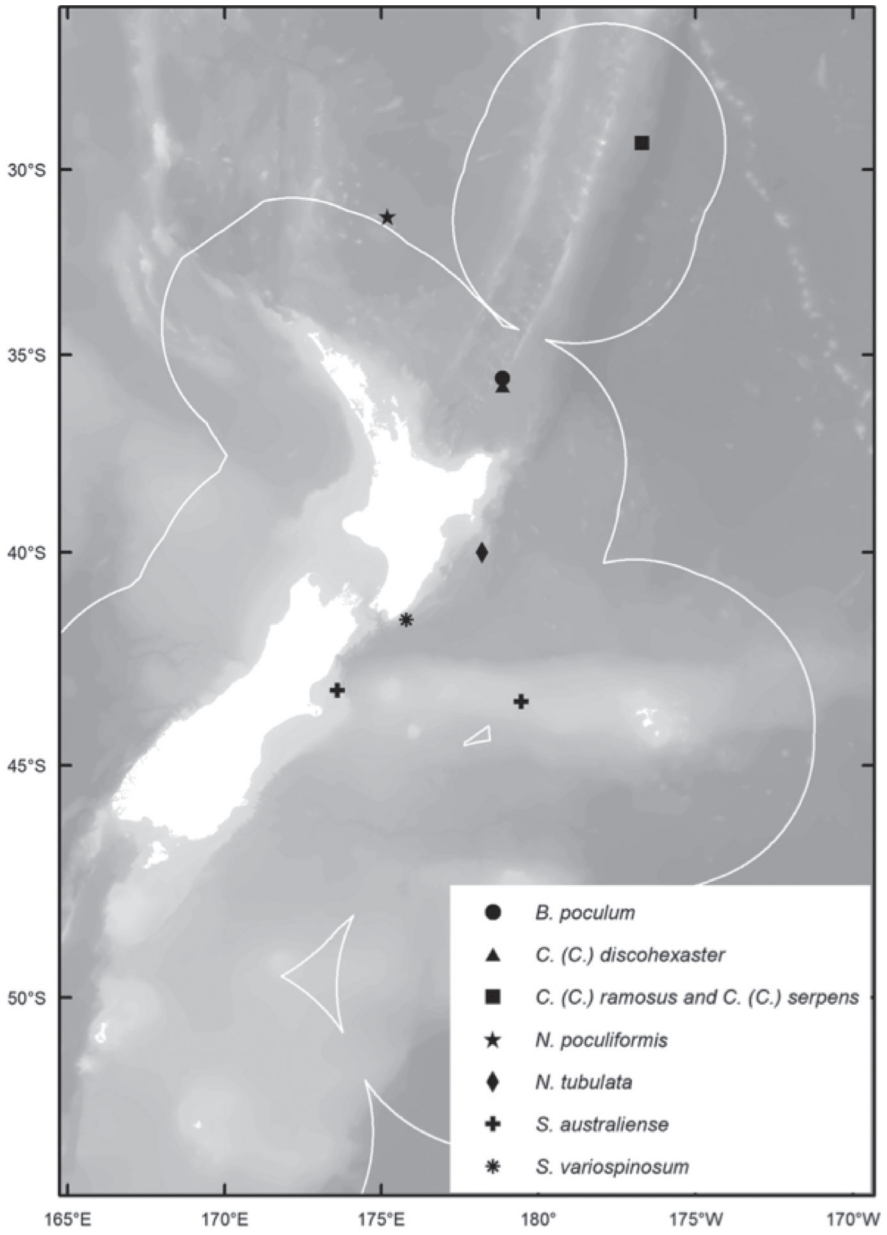

Figure 1. Study area showing the distribution of newly described rossellid sponges in the New Zealand EEZ and in international waters.

ICBM Institute for Chemistry and Biology of the Marine Environment, Carl von Ossietzky University of Oldenburg;
LM light microscopy;
NIC–NIWA Invertebrate Collection, NIWA, Wellington, New Zealand;

NIWA National Institute of Water and Atmospheric Research, Wellington, New Zealand;
SEM scanning electron microscopy.

Systematics

PORIFERA Grant, 1836
HEXACTINELLIDA Schmidt, 1870
HEXASTEROPHORA Schulze, 1886
LYSSACINOSIDA Zittel, 1877
ROSSELLIDAE Schulze, 1885
ROSSELLINAE Schulze, 1885

***Bathydorus* Schulze, 1886**

Bathydorus poculum Reiswig, Dohrmann & Kelly, sp. nov.

***Nubes* Reiswig, Dohrmann & Kelly, gen. nov.**

Nubes tubulata Reiswig, Dohrmann & Kelly, sp. nov.
Nubes poculiformis Reiswig, Dohrmann & Kelly, sp. nov.

***Scyphidium* Schulze, 1900**

Scyphidium australiense Tabachnick, Janussen & Menschenina, 2008
Scyphidium variospinosum Reiswig, Dohrmann & Kelly, sp. nov.

LANUGINELLINAE Gray, 1872

***Caulophacus* (*Caulophacus*) Schulze, 1886**

Caulophacus (*Caulophacus*) *discohexaster* Tabachnick & Lévi, 2004
Caulophacus (*Caulophacus*) *serpens* Reiswig, Dohrmann & Kelly, sp. nov.
Caulophacus (*Caulophacus*) *ramosus* Reiswig, Dohrmann & Kelly, sp. nov.

Rossellidae Schulze, 1885

Diagnosis. The body is usually cup-like basiphytose or lophophytose; in the pedunculate forms the body can be mushroom-like. Prostalia lateralia, when present, are formed

with diactins or outwardly protruding hypodermal pentactins; prostalia basalia, when present, are outwardly protruding hypodermal pentactins which are usually specialised (anchorate). Choanosomal skeleton consists of diactins, sometimes together with less frequent hexactins. Hypodermal pentactins often present, usually they protrude from the dermal surface serving as prostalia. Hypoatrial pentactins are rarely found or absent in some taxa. Dermalia are combinations of various spicules usually pentactins; stauractins and diactins, rarely hexactins. Atrialia are usually hexactins but other holactinoidal spicules can be also found there. Microscleres are various: holactinoidal, asterous and asters; they usually have discoidal or oxyoidal terminations but sometimes floricoidal, onychoidal, or sigmoidal ones (after Tabachnick 2002).

Rossellinae Schulze, 1885

Diagnosis. As for family.

Remarks. This subfamily is clearly not monophyletic (Dohrmann et al. 2017) and retained here for historical reasons only.

Bathydorus Schulze, 1886

Diagnosis. Rossellinae with tubular, saccular, or plate-like gross morphology. Basiphytous or lophophytous, thin-walled. Dermalia are combinations of spicules from hexactins to diactins. Regular pentactins make up a hypodermal layer. Choanosomal skeleton composed of diactins, sometimes with hexactins. Atrialia are hexactins or stauractins. Microscleres are combinations of oxyoidal hexasters, hemihexasters, and hexactins; lacking pappocomes (from Kahn et al. 2013).

Type species. *Bathydorus fimbriatus* Schulze, 1886

Bathydorus poculum Reiswig, Dohrmann & Kelly, sp. nov.

http://zoobank.org/1E8B4837-7A12-4A08-91B6-5A8E63CC79F2
Figs 2, 3; Table 1

Material examined. ***Holotype*** NIWA 126338, RV Sonne Stn SO254/85ROV19_BIOBOX17, Southern Kermadec Ridge, 35.612°S, 178.852°E, 1150 m, 24 Feb 2017.

Distribution. Known only from the type locality, the Southern Kermadec Ridge, north of New Zealand (Fig. 2A).

Habitat. Attached to hard substratum at 1149 m (Fig. 2B).

Description. Morphology of the holotype is a thick-walled funnel attached to rock substratum by a wide basal disc (Fig. 2B). Both dermal and atrial surfaces have a very dense, bushy, cover of prostal diactins (Fig. 2C, E, F). The single terminal osculum is the widest body part and the margin is abruptly sharpened; it has no marginalia (Fig. 2D).

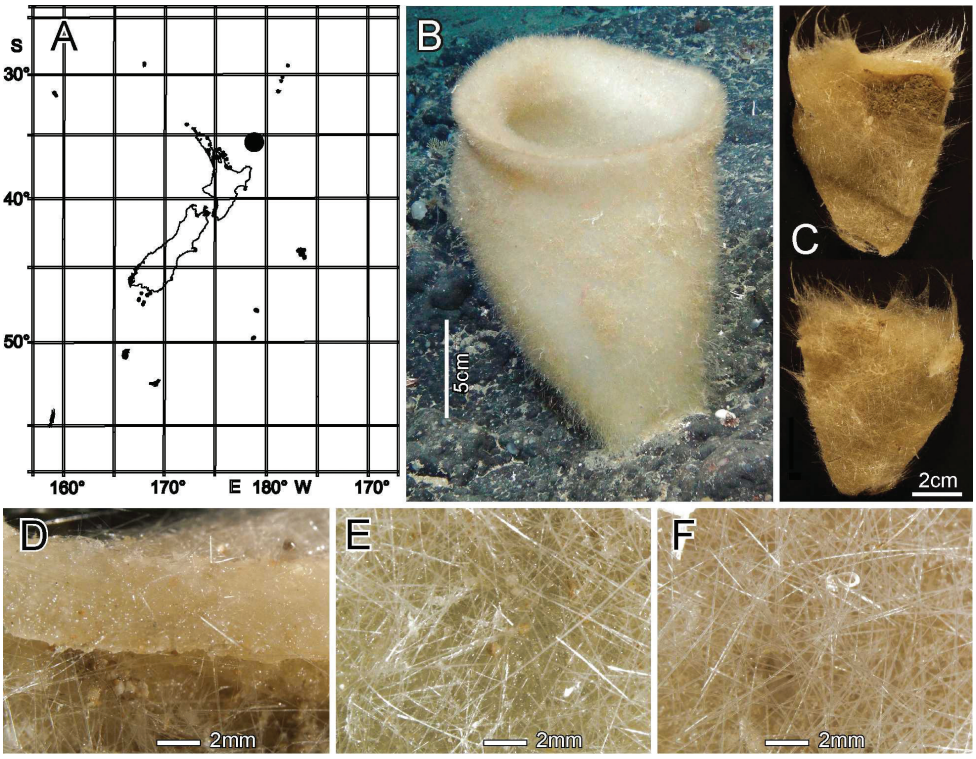

Figure 2. *Bathydorus poculum* sp. nov., holotype NIWA 126338, distribution, skeleton, and morphology **A** distribution in New Zealand waters **B** holotype in situ (scale bar approximate) **C** dermal (upper) and atrial (lower) sides of the preserved main part of the collected fragment **D** magnified area of the oscular margin, showing the atrial surface curving out over the dermal surface **E** dermal surface with dense prostal diactins **F** atrial surface with similarly dense prostal diactins. Image **B** captured by ROV Team GEOMAR, ROV Kiel 6000 onboard RV Sonne (voyage SO254), courtesy of Project PoribacNewZ, GEOMAR, and ICBM.

Dimensions of the holotype are ~ 17.2 cm high and 12.8 cm wide; the measurements are only approximate as only one of the two laser points could be certainly found on the in-situ images. Wall thickness is 10.7 cm, excluding the 1–2.5 cm thick prostal cover layers on each side. Texture is soft, compressible, and resilient, neither hard nor fragile. Surfaces of both the inner and outer walls are hairy to the naked eye, and when inspected at low magnification of a dissecting microscope, both are covered with a bushy layer of prostal diactins. Colour in life is pale beige, and pale brown when preserved in ethanol.

Skeleton. Choanosomal skeleton consists of a loose network of thin choanosomal diactins amongst the thicker proximal ends of prostal diactins, and proximal rays of hypodermal pentactins. No choanosomal hexactins are present. There is no evidence of fusion between any spicules. Microscleres are scattered evenly throughout the choanosome. Ectosomal skeleton of the dermal side consists of abundant prostal diactins passing through the distal tangential parts of hypodermal pentactins and dermalia, which are mostly stauractins (62% of 126 assessed), pentactins (29%) and hexactins (10%).

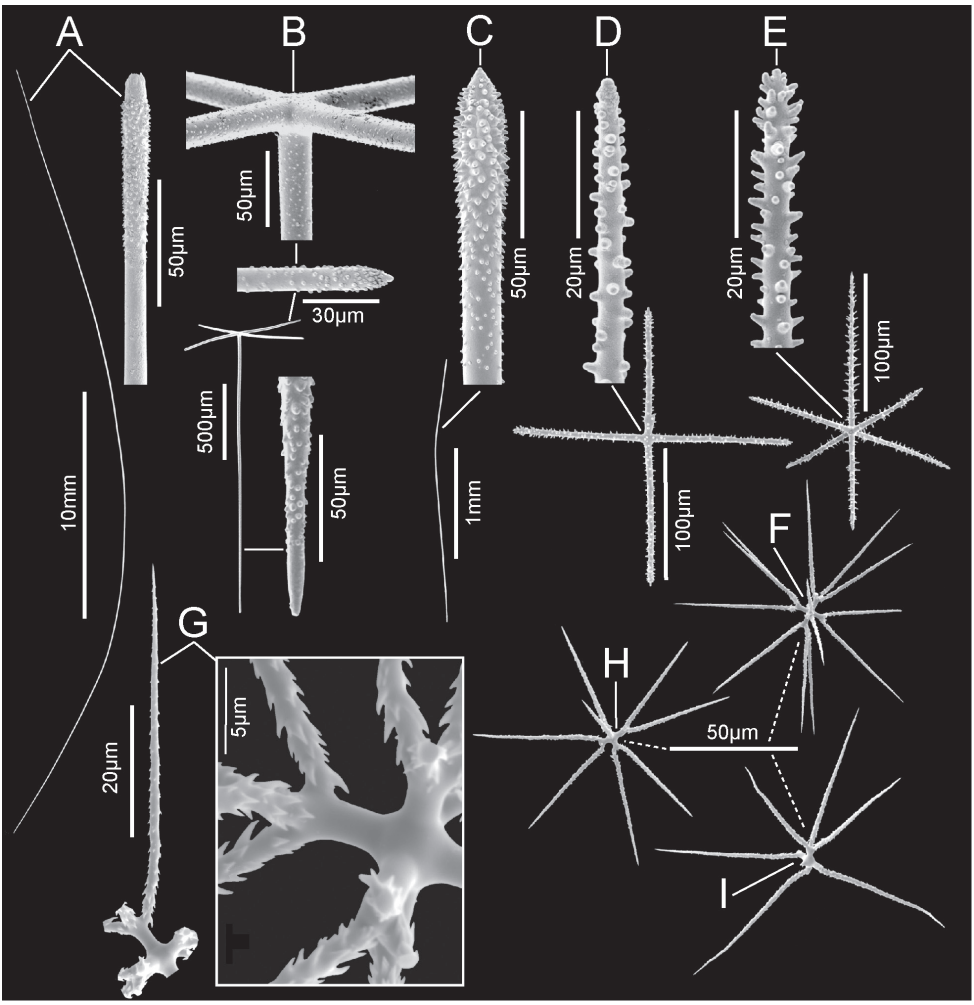

Figure 3. *Bathydorus poculum* sp. nov., holotype NIWA 126338 spicules **A** prostal diactin, whole and enlarged end **B** hypodermal pentactin, whole and enlarged spicule centre, tangential and proximal ray ends **C** choanosomal diactin, whole and enlarged end **D** stauractine dermalium, whole and enlarged ray end **E** pinular hexactine atrialium, whole and enlarged ray end **F** oxyhexaster **G** enlarged whole primary and secondary ray (left) and centre of spicule showing smooth primary and ornamentation of spines on secondary rays (right) **H** hemioxyhexaster **I** hemioxystauraster.

The atrial ectosome lacks hypoatrial pentactins but has atrialia in the form of hexactins (89% of 126 assessed), pentactins (8%), stauractins, and triactins (1.5% each). Microscleres are present as in the choanosome.

Spicules. Megascleres (Fig. 3; Table 1) are prostal diactins, hypodermal pentactins, choanosomal diactins, dermalia mostly as stauractins, and atrialia mostly as hexactins. Prostal diactins (Fig. 3A) are long bow-shaped spicules, smooth except for patches of subterminal spines; the smooth tips are rounded or parabolic; the spicule centre is

Table 1. Spicule dimensions (μm) of *Bathydorus poculum* sp. nov., from holotype NIWA 126338.

Parameter	mean	s.d.	range	no.
Dermal prostal diactin				
length (mm)	26.8	11.7	11.0–63.4	48
width	65.6	14.1	16.1–92.6	63
Hypodermal pentactin				
tangential ray length	476	110	218–995	60
tangential ray width	15.3	3.0	8.4–23.2	62
proximal ray length (mm)	1.6	0.6	0.7–4.2	62
proximal ray width	16.5	3.6	9.1–25.8	60
Choanosomal diactin				
length (mm)	16.8	11.1	1.4–31.5	8
width	12.8	7.3	7.1–38.4	47
Dermalia, stauractin				
ray length	98.5	18.0	66.7–139.0	29
ray width	5.0	0.8	3.4–7.7	32
Atrialia, pinular hexactin				50
pinular ray length	150.0	17.4	107.7–181.1	21
pinular ray width	3.8	0.8	2.4–5.2	21
tangential ray length	92.8	10.6	73.1–110.5	21
tangential ray width	3.6	0.6	2.7–4.6	21
proximal ray length	79.4	13.2	62.6–108.0	16
proximal ray width	3.7	0.6	2.7–5.0	20
Atrialia, non-pinular hexactin				
ray length	89.2	9.5	73.6–106.2	21
ray width	3.4	0.7	2.3–4.6	21
Oxy- and hemioxyhexaster				
diameter	109.0	21.8	66.2–164.3	30
primary ray length	4.6	0.9	2.9–7.3	30
secondary ray length	50.4	11.1	26.9–74.5	30
Oxyhexactin				
diameter	119.5	22.2	81.6–157.0	8
ray width	1.5	0.3	1.2–1.9	8

not swollen. Hypodermal pentactins (Fig. 3B) are regular and crucial in form with very long proximal rays, averaging 3.4 × tangential ray length, and fine spines evenly scattered over the entire surface. All five rays have subterminal patches of larger spines and smooth round tips. Choanosomal diactins (Fig. 3C) are straight, bent or more commonly sinuous in shape. Most are broken so few intact spicules are measurable for length. They are smooth except for subterminal inflated rough patches; the tip is smooth and abruptly tapered to a point. The spicule centre is moderately swollen. Dermalia (Fig. 3D) are mainly crucial stauractins completely covered with short, rounded knobs or spines; rays are tapered to a round tip. Atrialia (Fig. 3E) are mostly hexactins ca. half of which are pinular with one ray longer than the others. Like dermalia, these are entirely covered with short, rounded knobs or spines but longer than those of the dermalia; ray tips are rounded.

Microscleres (Fig. 3; Table 1) are all oxyhexasters and their variants with hemioxyhexasters being the most common. Oxyhexasters (Fig. 3F, G) have short smooth primary rays and long straight secondary rays; the secondary rays are entirely ornamented with reclined spines that increase in size from the ray tip to its proximal end. Secondary

rays on each primary ray vary from 2–5. Hemioxyhexasters (Fig. 3H) are similar to oxyhexasters but at least one of the six primary rays bear only a single secondary ray. Other rare variants include oxyhexactins, oxypentasters, and oxystaurasters (Fig. 3I).

Etymology. Named for the beaker-shaped morphology of this species (*poculum*, beaker; Latin).

Remarks. This New Zealand specimen, NIWA 126338, is entirely consistent with the diagnosis of *Bathydorus* and is assigned there. Each of the known species of the genus differ from this specimen in the following characters: *Bathydorus echinus* Koltun, 1967 has prostal pentactins in addition to diactins, and dermalia as mainly pentactins; *B. fimbriatus* Schulze, 1886 has prostalia including pentactins as marginalia only, and no pinular atrialia; *B. laevis laevis* Schulze, 1886 has no prostalia lateralia and no pinular atrialia; *B. laevis pseudospinosus* Tabachnick & Menshenina, 2013 has some large choanosomal or prostal hexactins and smaller oxyhexasters to only 100 μm diameter; *B. laninger* Kahn, Geller, Reiswig & Smith Jr., 2013 has a flat body form and no prostalia on the atrial (upper) surface; *B. servatus* Topsent, 1927 has no prostal diactins, and dermalia as stauractins and diactins; *B. spinosissimus* Lendenfeld, 1915 has choanosomal hexactins, and oxyhexasters with longer primary rays (4–12 μm); in the original description of *B. spinosus* Schulze, 1886, there is no mention of hypodermal pentactins; although Tabachnick and Menshenina (2013) include these, they fail to certify that they are present in the holotype; this species also has wavy secondary rays on the oxyhexasters; *B. uncifer* Schulze, 1899 has smooth dermal and atrial surfaces, and dermalia as mainly pentactins and stauractins. These differences are sufficient to conclude that the new form is a new species, here designated as *Bathydorus poculum* sp. nov.

Nubes Reiswig, Dohrmann & Kelly, gen. nov.

http://zoobank.org/032AA823-2695-4E82-888D-0051A86BC438

Diagnosis. Rossellinae with basiphytous, saccular, thick-walled body, unstalked or with a short stalk. Hypodermalia are large, raised, paratropal or orthotropal pentactins with strongly curved or straight tangential rays, smooth except for rough tips, forming a cloud or veil around the thick-walled body. Prostal diactins are marginalia only. Choanosomal spicules are diactins and sometimes large hexactins with curved rays, smooth except for rough tips. Dermalia are mainly stauractins and pentactins. Atrialia are mainly hexactins and sometimes pentactins. Microscleres are oxyhexasters, hemioxyhexasters, and anisodiscohexasters.

Etymology. Named for the cloud of large hypodermal pentactins that veils the body of these sponges (*nubes*, cloud; Latin).

Type species. *Nubes tubulata* sp. nov.

Remarks. This new genus diagnosis differs from those of most other anisodiscohexaster-bearing genera or subgenera in the following ways: from *Anoxycalyx* Kirkpatrick, 1907 in not having anchorate hypodermalia, and having pleural hypodermalia raised, having marginalia; in not including pappocomes and discohexasters other than

anisodiscohexasters (strobiloidal discohexasters) as microscleres. It differs from that of *Crateromorpha* (*Crateromorpha*) Gray in Carter, 1872 in body form, having marginal diactins, and having main atrialia as hexactins. It differs from that of *Rossella* Carter, 1872 in having most atrialia as hexactins instead of stauractins, and no calycocomes. However, it does not differ from the present diagnosis of *Vazella* Gray, 1870 (Tabachnick 2002) in any way, but below we offer a modified diagnosis of that genus to separate the two groups.

Nubes tubulata Reiswig, Dohrmann & Kelly, sp. nov.

http://zoobank.org/352141EE-D1CC-4A5A-94F5-F52B731D5C73
Figs 4, 5; Table 2

Material examined. ***Holotype*** NIWA 126159, RV Sonne Stn SO254/36ROV10_BIOBOX7, Seamount No. 986, off Hawkes Bay shelf, 39.990°S, 178.214°E, 782.8 m, 09 Feb 2017. ***Paratype*** NIWA 126160, RV Sonne Stn SO254/36ROV10_BIOBOX10, Seamount No. 986, off Hawkes Bay shelf, 39.989°S, 178.214°E, 767 m, 09 Feb 2017.

Distribution. Known only from the type locality, Seamount 986 off Hawkes Bay shelf, east of North Island, New Zealand (Fig. 4A).

Habitat. Attached to hard substratum; depth 767–783 m (Fig. 4B).

Description. Morphology of the holotype and paratype a thick-walled, tubular sponge, attached to hard substratum by a narrow base (Fig. 4B). A round osculum of moderate size is terminal and opens into a deep atrial cavity. The margin is sharp and there are indications of sparse diactin marginalia in deck images, but we have been unable to verify them in the material at hand. The dermal surface has a dense covering of raised, prostal, hypodermal pentactins (Fig. 4C, D, I) projecting up to 1 cm from the surface proper. There is indication in some of the deck images of long diactins projecting sparsely up to 6 cm from the dermal surface, especially basally, but these may be choanosomal diactins pulled out during collection; we have not found such large diactins in the material we had for examination. Dimensions of the holotype are ~ 13.3 cm high, 7.0 cm wide, and 10.8 (9.2–13.3) (n = 9) mm in body wall thickness; the osculum is 2.2 cm in diameter in situ. The paratype is 19.5 cm high, 13.4 cm wide, and body wall is 7.4 (5.5–9.3) (n = 11) mm in thickness. The osculum is 4.2 cm in diameter in situ. Texture is soft, compressible, and resilient, neither hard nor fragile. Surface of the dermal side is covered by a thick layer of projecting hypodermal pentactins (Fig. 4E). The dermal lattice is torn apart, and dermalia reside in preserved specimens as attached flakes on the hypodermalia (Fig. 4G). The atrial layer retains the atrial lattice covering smaller apertures (Fig. 4F, H); no large megascleres project into the atrium. Colour in life is transparent white, preserved in ethanol is medium brown (Fig. 4C).

Skeleton. Choanosomal skeleton consists of a loose, vacuolar network of thin choanosomal diactins, large choanosomal hexactins, and the thicker proximal rays of the hypodermal pentactins. There is no evidence of fusion between any spicules. Microscleres

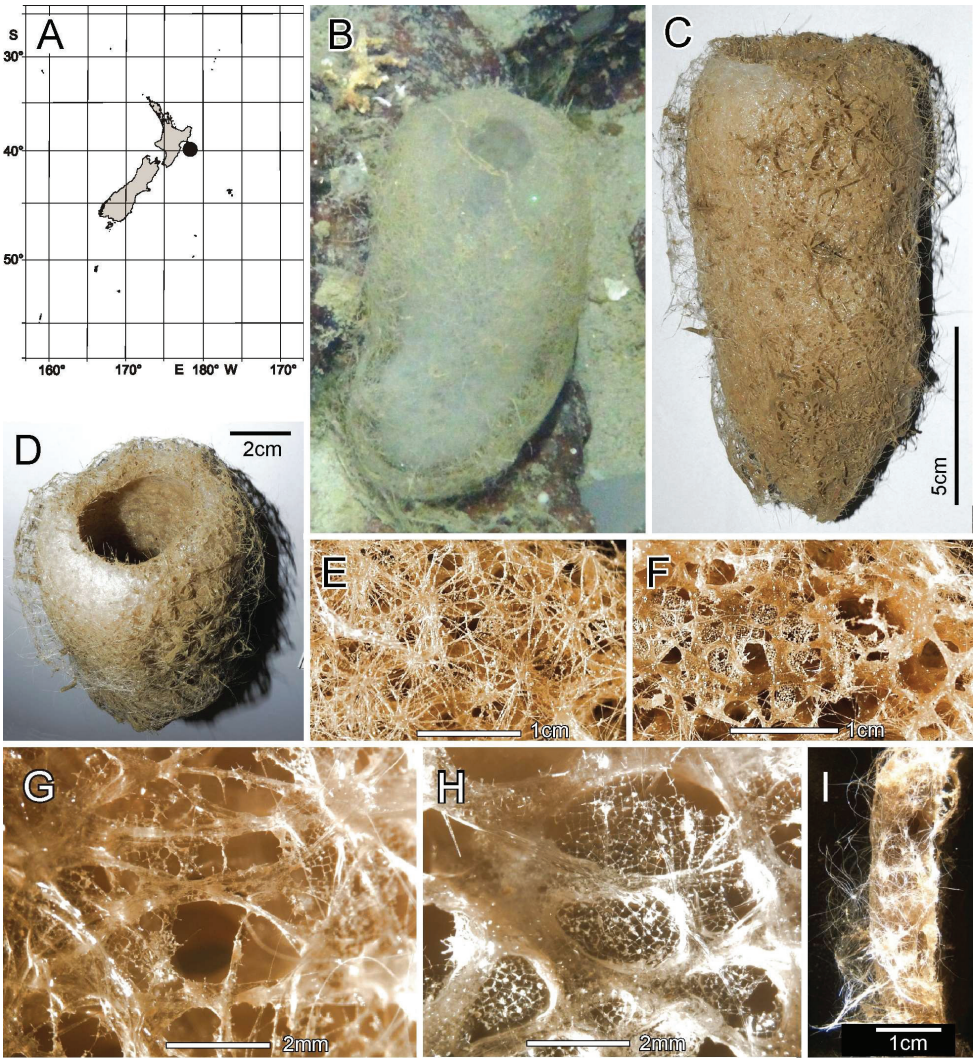

Figure 4. *Nubes tubulata* gen. nov., sp. nov., holotype NIWA 126159, distribution, skeleton and morphology **A** Distribution in New Zealand waters **B** holotype in situ **C** holotype, deck image **D** holotype, deck image showing moderate-sized osculum and veil of hypodermal pentactins (deck images by PJS) **E** dermal surface with dense veil of prostal hypodermal pentactins **F** atrial surface without a hypodermal veil **G** closer view of dermal surface with disrupted lattice **H** closer view of atrial surface with intact lattice over exhalant apertures **I** section of body wall, dermal surface on left side. Image **B** captured by ROV Team GEOMAR, ROV Kiel 6000 onboard RV Sonne (voyage SO254), courtesy of Project PoribacNewZ, GEOMAR, and ICBM.

are scattered evenly throughout the choanosome. Ectosomal skeleton of the dermal side consists of abundant prostal pentactins supporting a delicate lattice of hexactine, pentactine, and stauractine dermalia. The atrial ectosome lacks hypoatrial pentactins but has bands of diactins that support the atrial lattice of hexactins, providing greater support than available to the dermal lattice. Microscleres are present as in the choanosome.

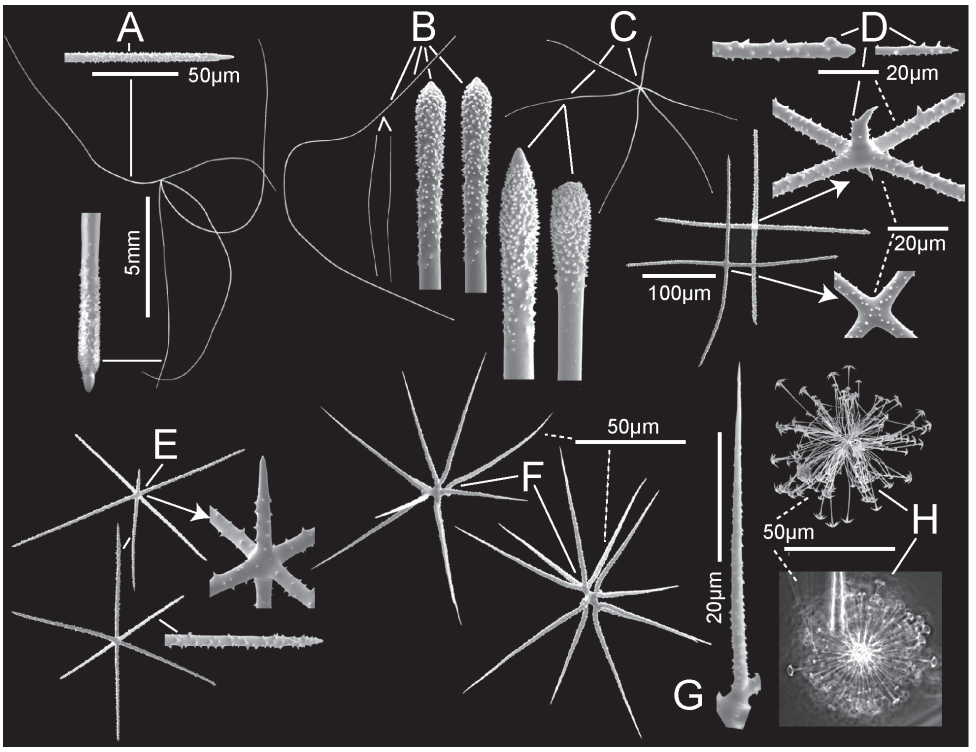

Figure 5. *Nubes tubulata* gen. nov., sp. nov., holotype NIWA 126159, spicules **A** whole prostal hypodermal pentactin and enlarged ray ends **B** whole curved and straight choanosomal diactins with two enlarged ends; scales of whole spicules and parts in **B** and **C** as in **A**; **C** whole choanosomal hexactin with two enlarged ray ends **D** two dermalia, a subhexactin, and a stauractin, with enlarged ray ends and centres **E** two atrialia, a pinular subhexactin, and a regular hexactin with enlarged centrum of the pinular subhexactin and a ray end; scales of whole spicules and parts as in **D**; **F** two oxyhexasters **G** enlarged terminal ray of an oxyhexaster **H** anisodiscohexasters, from SEM preparation (above) and LM preparation (below).

Spicules. Megascleres (Fig. 5; Table 2) are prostal hypodermal pentactins, choanosomal diactins, choanosomal hexactins, dermalia, and atrialia. Prostal hypodermal pentactins (Fig. 5A) are mostly large, raised paratropal forms (90% of 68 scored) with long, very curved tangential rays, but some regular, crucial forms occur (10%) in smaller forms especially near the margin. Tangential rays are 1.7 × the shorter, straighter proximal rays. The spicules are smooth except for the rough sharp tips. Choanosomal diactins (Fig. 5B) are straight or strongly curved, usually with undetectable central swellings; they are smooth except for the rough, slightly inflated tips. Choanosomal hexactins (Fig. 5C) are large forms with strongly curved or nearly straight, nearly equal length rays, which are otherwise similar to those of the hypodermalia. Dermalia (Fig. 5D) are entirely spined and consist of stauractins (31% of 387 scored) and similar forms with reduced fifth ray (subpentactins) or both fifth and sixth rays in one axis (subhexactins) (64%) with a few (1–2%) as tauactins, diactins and paratetractins. It

Table 2. Spicule dimensions (μm) of *Nubes tubulata* gen. nov., sp. nov. from holotype 126159.

Parameter	mean	s.d.	range	no.
Prostal hypodermal pentactin, lateral body				
tangential ray length (mm)	14.4	1.7	10.5–17.9	36
tangential ray width	42.5	3.3	36.8–50.4	35
proximal ray length (mm)	8.4	1.3	5.3–10.7	26
proximal ray width	46.6	5.0	36.8–59.4	28
Prostal hypodermal pentactin, margin				
tangential ray length (mm)	2.0	1.4	0.6–7.4	32
tangential ray width	20.2	7.0	6.5–39.6	31
proximal ray length (mm)	2.8	1.7	0.8–6.0	25
proximal ray width	21.9	7.1	7.3–43.0	30
Choanosomal diactin				
length (mm)	9.1	5.1	1.6–21.3	35
width	16.4	9.1	4.2–47.0	35
Choanosomal hexactin				
ray length (mm)	5.9	1.9	2.5–10.9	46
ray width	39.0	8.9	21.0–60.7	45
Dermalia stauractin				
ray length	132	17	91–174	36
ray width	5.7	0.8	4.5–7.3	20
Dermalia subpentactin/hexactin				
ray length	142	17	107–180	36
ray width	5.4	0.8	4.2–7.1	20
Atrialia subhexactin short pinular				
ray length	21	5	13–40	26
tangential ray length	176	25	130–230	28
proximal ray length	130	22	93–184	26
tangential ray width	5.8	0.9	4.1–7.8	26
Atrialia, non-pinular hexactin				
ray length	171	17	139–220	27
ray width	5.8	1.1	3.8–8.0	26
Oxy- and hemioxyhexaster				
diameter	130.5	14.1	90.2–165.7	32
primary ray length	5.3	1.1	3.7–8.9	32
secondary ray length	60.2	6.2	47.3–77.1	32
Anisodiscohexaster				
diameter	70.9	7.3	47.5–81.7	35
primary ray length	5.5	0.9	4.0–7.5	35
longest secondary ray length	30.3	3.9	19.4–36.0	35

was not possible to differentiate the subpentactins and subhexactins either wet in dishes or mounted spicule microscope slides. Tips are either rounded or more often sharp. Atrialia (Fig. 5E) are entirely spined and mostly subhexactins (71% of 125 scored) with one ray reduced or hexactins (26%) with all rays of nearly equal length; a few (1–2%) are stauractins and tauactins. Ray tips are sharp-pointed.

Microscleres (Fig. 5; Table 2) are oxyhexasters and their variants, with hemioxyhexasters being the most common, and anisodiscohexasters. Oxyhexasters and hemioxyhexasters (Fig. 5F, G) have very short smooth primary rays and long straight secondary rays entirely ornamented with small, reclined spines. Secondary rays on each primary ray vary from 1–4. Anisodiscohexasters (Fig. 5H) are spherical with stellate discs with 4–6 marginal claws on the ends of terminal rays. Primary rays are smooth

and end in strobiloid discs with a short central projecting knob. Each primary strobilum supports 30–40 terminal rays with undulating, probably helically coiled, finely rough shafts of unequal lengths. Terminal discs vary in diameter with shaft length, the longer shafts carrying the larger discs, e.g., a series 1.7, 2.5, 3.1, 3.4, 3.6, 5.4, 6.9 μm diameter for shafts 15.0, 20.5, 23.5, 27.3, 32.0. 33.4, 37.1 μm in length. These spicules look very different in LM (lower image) and SEM (upper image) due to collapse of the rays during drying for SEM and support of them by balsam in LM.

Etymology. Named for the tubular morphology of the sponge (*tubulata*, tubular; Latin).

Remarks. The characters of these two New Zealand specimens are inconsistent with the present diagnoses of all Rossellinae genera except *Vitrollula* Ijima, 1898. They differ, however, from those of *V. fertilis* Ijima, 1898, the only species in the genus, in characters not used as diagnostic. These are that *V. fertilis* has a smooth surface without raised hypodermalia, but the two new specimens have a bristly surface with raised hypodermalia, and that the discohexasters of *V. fertilis* are isodiscohexasters while those of the new species are anisodiscohexasters. In view of these differences, we opt not to include the new species in *Vitrollula* nor to change the diagnosis of that genus at this time. We choose to erect a new genus in Rossellinae with characters of this and the following second species described below, and designate this species as *Nubes tubulata* gen. nov., sp. nov.

Nubes poculiformis Reiswig, Dohrmann & Kelly, sp. nov.

http://zoobank.org/2EBDD0FB-6EB9-498A-8749-595C64824C23
Figs 6, 7; Table 3

Material examined. ***Holotype*** NIWA 126016, RV Sonne Stn SO254/08ROV02_BIOBOX10, Seamount No. 114 in International Waters to the east of Three Kings Ridge and Norfolk Island, 31.301°S, 175.197°E, 1285 m, 31 Jan 2017.

Distribution. Known only from the type locality, Seamount No. 114, in International Waters to the east of Three Kings Ridge and Norfolk Island (Fig. 6A).

Habitat. Attached to hard substratum; depth 1285 m (Fig. 6B).

Description. Morphology of the holotype body is a thick-walled tubular sponge, attached to hard substratum, by a moderately long, narrow stalk (Fig. 6B, C). A moderately sized, round osculum is terminal and opens into a deep atrial cavity. The margin is blunt, bordered by a band of diactine marginalia (Fig. 6D, F). The dermal surface has a dense covering of raised, prostal, hypodermal pentactins (Fig. 6D, E), projecting up to 7 mm from the surface proper. Some of the deck images indicate long diactins projecting sparsely, up to 14 mm, from the dermal surface, but these may be foreign in origin; we have not found such large diactins in the material available for examination. Dimensions of the holotype are ~ 6 cm in total length, including the stalk of 1.8 cm length (Fig. 6G), and 3.5 cm in width; the maximum body wall thickness is 13.9 mm. The osculum is 12.3 by 16.9 mm diameter in situ. Texture is soft, compressible, and resilient, neither hard nor fragile. Surface of the dermal side

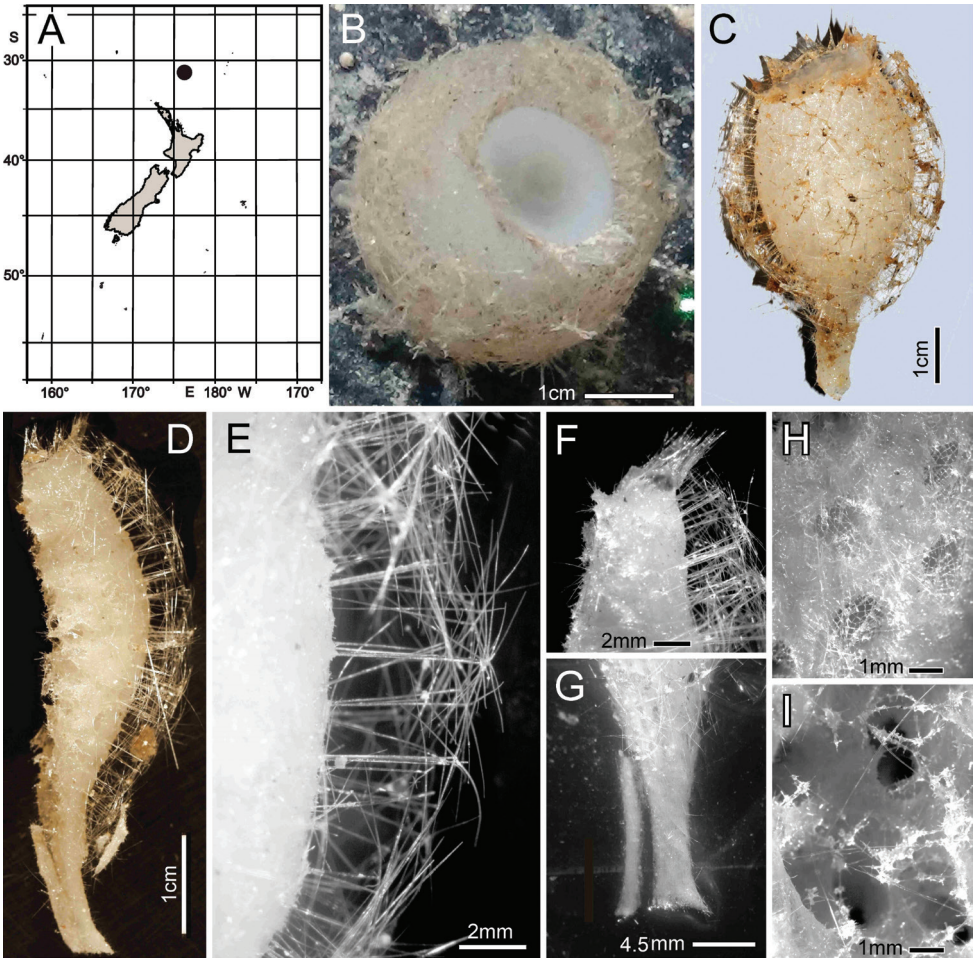

Figure 6. *Nubes poculiformis* gen. nov., sp. nov., holotype NIWA 126016, distribution, skeleton and morphology **A** distribution in New Zealand waters **B** holotype in situ **C** holotype, deck image (by PJS); **D** longitudinal section of holotype, showing hypodermal pentactin veil **E** closer view of hypodermal pentactin veil **F** edge of osculum with tuft of marginalia **G** close view of stalk subdivided for spicule preparation of smaller sample **H** dermal surface with intact lattice of dermalia over inhalant canals **I** atrial surface with disrupted lattice of atrialia. Image **B** captured by ROV Team GEOMAR, ROV Kiel 6000 onboard RV Sonne (voyage SO254), courtesy of Project PoribacNewZ, GEOMAR, and ICBM.

below the layer of projecting hypodermal pentactins is supported by an intact tight lattice of dermalia (Fig. 6H). The atrial surface (Fig. 6I), in contrast, is torn apart by removal from supporting fluids and the atrial lattice remains only as dismembered patches attached to underlying diactins. Colour in life is pale brown as is the specimen preserved in ethanol.

Skeleton. Choanosomal skeleton consists of a loose, vacuolar network of thin choanosomal diactins, large choanosomal hexactins and the thicker proximal rays of the hy-

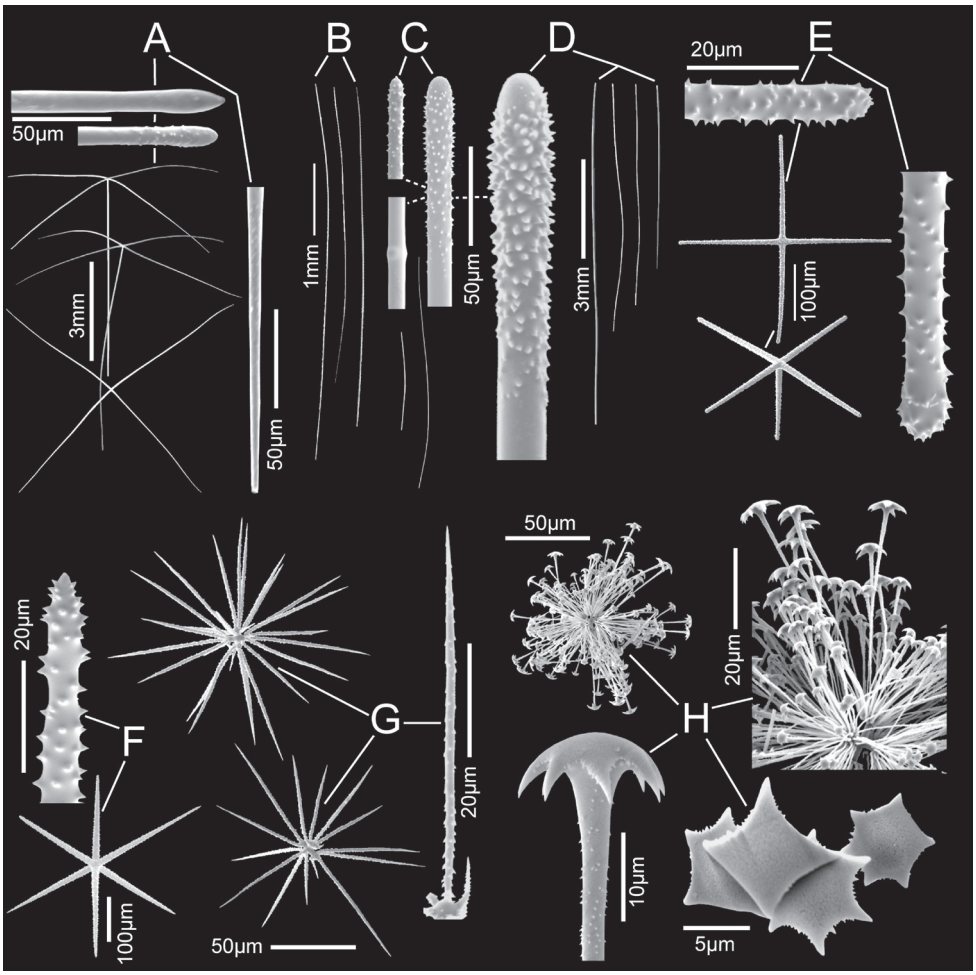

Figure 7. *Nubes poculiformis* gen. nov., sp. nov., holotype NIWA 126016, spicules **A** three prostal hypodermal pentactins, the lower one in plane of tangential rays, with enlarged ray ends **B** whole marginal diactins (ray ends unavailable) **C** two whole choanosomal hexactins with two enlarged ray ends and one centrum. Scale of whole spicules as in **C**; **D** four whole stalk diactins and enlarged end **E** dermalia, stauractin and pentactin with enlarged ray ends **F** atrialium and enlarged ray end **G** two oxyhexasters and enlarged terminal ray **H** whole anisodiscohexaster; an enlarged section showing disc diameter increasing in longer terminal rays; an enlarged side view of a terminal ray and end views of terminal ray discs.

podermal pentactins. There is no evidence of fusion between any spicules. Microscleres are scattered evenly throughout the choanosome. Ectosomal skeleton of the dermal side consists of abundant prostal pentactins providing good support for the sturdy lattice of stauractine (60.0% of 315 assessed), pentactine (38.4%), and rare hexactine (1.64%) dermalia. The atrial ectosome lacks hypoatrial pentactins but has bands of diactins that provide poor support for the atrial lattice of mainly hexactins (86.4% of 118 assessed), pentactins (7.5%), and stauractins (5.1%). Microscleres are present as in the choanosome.

Table 3. Spicule dimensions (μm) of *Nubes poculiformis* gen. nov., sp. nov. from holotype 126016.

Parameter	mean	s.d.	range	no.
Prostal hypodermal pentactin				
tangential ray length (mm)	3.9	0.8	1.9–5.2	73
tangential ray width	51.1	5.4	36.4–59.3	60
proximal ray length (mm)	6.5	1.1	3.3–8.0	69
proximal ray width	51.0	4.5	39.7–58.7	59
Marginal diactin				
length (mm)	4.5	0.7	2.8–6.0	58
width (mm)	18.0	3.3	12.3–27.5	64
Choanosomal diactin				
length (mm)	2.5	1.4	0.6–4.9	52
width (mm)	11.8	2.3	7.5–19.2	52
Stalk diactin				
length (mm)	7.4	2.1	2.5–11.5	25
width (mm)	14.7	4.9	8.1–29.6	25
Dermalia stauractin ray				
length	200	24	130–243	51
width	11.5	1.7	7.3–14.6	51
Dermalia pentactin tangential ray				
length	185	19	146–223	62
width	11.3	1.5	6.3–15.5	63
Dermalia pentactin proximal ray				
length	155	20	119–190	21
width	11.0	1.6	7.8–14.5	23
Atrialia hexactin				
ray length	227	25	176–283	50
ray width	13.9	2.2	9.2–20.0	50
Oxyhexaster				
diameter	137	11	103–165	51
primary ray length	5.7	1.1	3.5–7.8	51
secondary ray length	62.6	4.9	46.7–72.9	51
Anisodiscohexaster				
diameter	148	34	87–201	54
primary ray length	9.0	1.4	6.0–12.6	54
longest secondary ray length	66.4	16.2	32.9–89.5	54

Spicules. Megascleres (Fig. 7; Table 3) are prostal hypodermal pentactins, marginal diactins, choanosomal diactins of the body, choanosomal diactins of the stalk, dermalia and atrialia. Prostal hypodermal pentactins (Fig. 7A) are large, raised orthotropal forms with long straight tangential rays. Tangential rays are ca. one half the length of the longer straight proximal rays. The spicules are smooth except for the rough sharp or round tips. Marginalia (Fig. 7B) are long, slightly curved diactins; no intact tips were found in SEM surveys but an exhaustive survey with LM indicates tips taper to nearly invisible thinness and are quite distinct from the thick roughened tips of choanosomal diactins. Choanosomal diactins (Fig. 7C) are straight or slightly curved with undetectable central swellings; they are smooth except for the rough, slightly inflated tips. Stalk diactins (Fig. 7D) are longer and thicker than the choanosomal diactins, but otherwise similar. Dermalia (Fig. 7E) are mainly entirely rough stauractins and pentactins with rounded ray tips. Atrialia (Fig. 7F) are entirely rough hexactins with equal length rays and more acute ray tips.

Microscleres (Fig. 7; Table 3) are oxyhexasters, hemioxyhexasters, and anisodiscohexasters. Oxyhexasters (Fig. 7G) and hemioxyhexasters have very short, sparsely spined or smooth, thick primary rays, ending in swollen hemispheres; 1–7, usually 3–4, rough, straight, terminal rays tapering to pointed tips emanate from the margins and occasionally from the centre of the hemisphere. Short to very short spur-like terminal rays are common. Anisodiscohexasters (Fig. 7H) have smooth primary rays ending in ovoid strobila. Each strobilum supports ca. 20–30 rough, curved terminal rays that end in discs with 4–7 marginal discs. The tuft of terminal rays from each primary ray varies in length of rays, and with ray length the diameter of terminal discs, in a pattern that is not yet clear, but the whole spicule resembles a radially symmetrical starburst.

Etymology. Named for the goblet shape of the sponge (*poculiformis*, goblet-shaped; Latin).

Remarks. This species differs from *Nubes tubulata* sp. nov. in having a short stalk and orthotropal hypodermal pentactins, but is otherwise similar enough to include it in the genus *Nubes* as its second species, *Nubes poculiformis* sp. nov.

Vazella Gray, 1870

Diagnosis. Body is saccular, basiphytous. Choanosomal skeleton is composed of diactins. Hypodermal pentactins are raised, thorned paratropal pentactins. Prostalia basalia and marginalia are monaxons (diactins). Dermalia are stauractins and pentactins. Atrialia are mainly hexactins. Discoid microscleres are microisodiscohexasters and microanisodiscohexasters; oxyoid microscleres are combinations of hexactins, hexasters, and hemihexasters (modified from Tabachnick 2002).

Remarks. This modified diagnosis allows separation of the present genus, *Nubes* gen. nov., from *Vazella* on the basis of lack of thorned hypodermalia and presence of discoid microscleres that are not anisodiscohexasters in the former. Furthermore, molecular phylogenetic results do not support a close relationship of the two genera (MD, unpubl. results).

Scyphidium Schulze, 1900

Diagnosis. Body is saccular, basiphytous, sometimes rhizophytous. Choanosomal skeleton is composed of diactins. Hypodermal spicules, if present, are pentactins. Prostalia, if present, are hypodermal pentactins and/or diactins. Dermalia are stauractins and/or pentactins in various combinations. Atrialia are mainly hexactins. Microscleres are discohexasters and oxyhexasters often with hemioxyhexasters and oxyhexactins; with two or three types of discohexasters, none as calycocomes. Among the larger is a spherical form with a restricted number of secondary rays (emended from Tabachnick 2002).

Remarks. The genus diagnosis is emended of necessity, to accept *S. australiense* Tabachnick, Janussen & Menschenina, 2008 and *S. variospinosum* sp. nov., described below.

Type species. *Scyphidium septentrionale* Schulze, 1900.

Scyphidium australiense Tabachnick, Janussen & Menschenina, 2008

Figs 8, 9; Table 4

Note. From the ending of its name, *Scyphidium* is a neuter noun, and thus *S. australiensis* (as originally named by Tabachnick et al. 2008) should be *S. australiense*. This is borne out by the names of conspecifics that are also adjectives (e.g., *S. chilense*, *S. septentrionale*, *S. tuberculatum*) (J. Rosser, pers. comm.). We hereby make that change and use the corrected name throughout this work.

Type and locality (not examined). Holotype – NIWA 155561, RV Sonne Stn SO17/80 (NZOI Stn Z3951B), Chatham Rise, 43.553°S, 179.457°E, 409 m, 10 Apr 1981 [Originally cited in Tabachnick et al. (2008) as WAM (p14), RV Soela Stn SO 17–80, 43°33.10'–33.05'S, 179°27.25'–27.08'E, depth unknown].

Material examined. NIWA 126237, RV Sonne, Stn SO254/77ROV14_ BIOBOX02, Pegasus Canyon slope, off Christchurch shelf, 43.2927361°S, 173.6066742°E, 853 m, 20 Feb 2017.

Distribution. Chatham Rise and Pegasus Canyon slope, off Christchurch shelf Christchurch shelf, New Zealand (Fig. 8A).

Habitat. Attached to hard substratum; depth 409–853 m.

Description. Body form is a heavy-looking, thick-walled, club-shaped, pendant sponge with a narrow basal attachment, widening gradually to a hemispherical rounded terminal end (Fig. 8B, C) where a large osculum is centrally located. The osculum opens into a deep atrial cavity (Fig. 8D). The margin is sharp-edged with indication of sparse marginalia that do not differ from prostal diactins of the lower body. The external surface of the upper body is fairly smooth, without prostalia, but the lower half is conspicuously conulose with long prostal diactins projecting in small groups from conules (Fig. 8E). We did not have access to the basal attachment so we cannot comment on the basidictyonalia. Dimensions of the specimen are 27.6 cm in height, 11.7 cm in maximum width, 5.7–10.9 cm in diameters of the osculum, 10.0 mm in maximum wall thickness, 8.3 mm in length of projecting part of prostal diactins. Texture is firm but compressible and resilient, neither soft nor fragile. Surface of the dermal side is covered by an intact lattice of dermalia (Fig. 8G) consisting mostly of pentactins (98% of 302 assayed), and a few stauractins and diactins (1% each). The upper body surface is fairly smooth, but the lower body is covered with conspicuous conules up to 3.2 mm high, from which prostal diactins project in small groups of one to four. One large pentactin was found but it was broken and assumed to be foreign. The atrial surface is covered by a felt-like layer of disarranged atrialia (Fig. 8H)

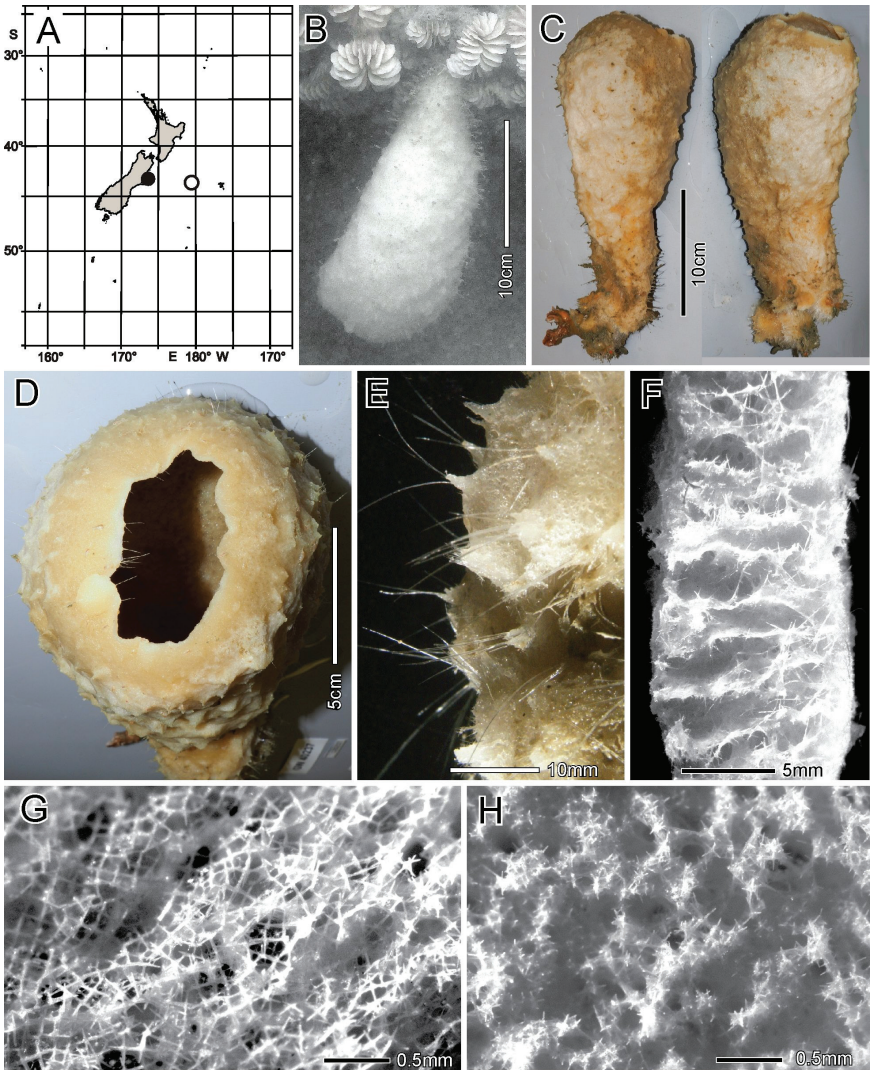

Figure 8. *Scyphidium australiense* Tabachnick, Janussen & Menschenina, 2008, NIWA 126237, distribution, skeleton and morphology **A** distribution in New Zealand waters, holotype as open circle, new specimen as filled circle **B** new specimen in situ (scale bar is approximate) **C** deck image (two sides, image by PJS) **D** osculum, deck image (by PJS) **E** preserved conulose outer surface of the lower body with prostal diactins **F** preserved wall section of the mid-body without conules **G** preserved dermal surface with intact pentactin lattice **H** preserved atrial surface with hexactins displaced from the atrial lattice. Image **B** captured by ROV Team GEOMAR, ROV Kiel 6000 onboard RV Sonne (voyage SO254), courtesy of Project PoribacNewZ, GEOMAR, and ICBM.

composed of hexactins (57% of 168 assayed), pentactins (20%), paratetractins (8%), diactins (6%), stauractins (5%), and triactins (3%). Colour in life is very pale brown, preserved in ethanol is medium brown.

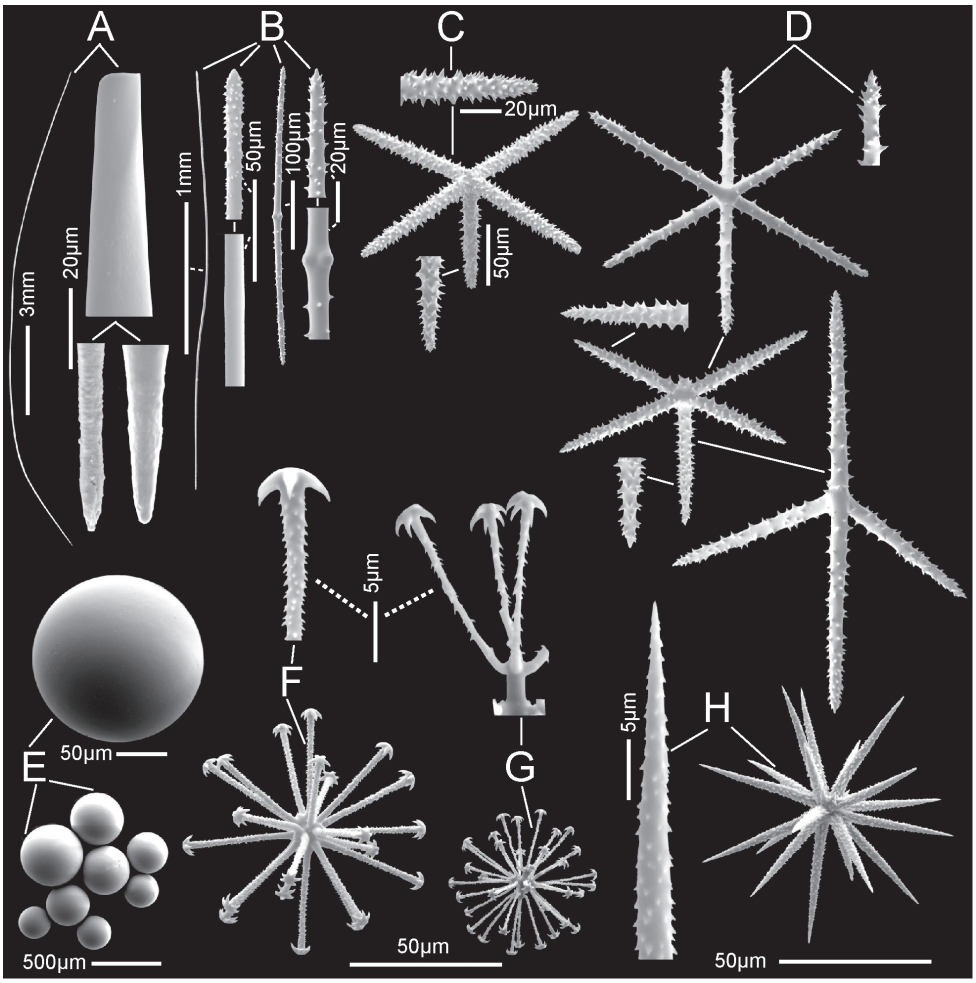

Figure 9. *Scyphidium australiense* Tabachnick, Janussen & Menschenina, 2008, NIWA 126237, spicules **A** prostal diactin, whole and enlarged ends, one broken distal end and two intact proximal ends **B** choanosomal diactins, whole long and short versions at different scales plus enlarged tips and central swellings **C** dermalium: pentactin, whole and enlarged tips **D** atrialia, hexactin, whole and enlarged tip, pentactin, whole with enlarged tips, and paratetractin, whole; scales are the same as those for dermalium **E** spheres as small group of whole ones and one enlarged **F** discohexaster 1, whole and enlarged terminal ray end **G** discohexaster 2, whole and enlarged part of one ray tuft **H** oxyhexaster, whole and enlarged terminal ray end. Scales are the same for all whole microscleres and their enlarged parts.

Skeleton. Choanosomal skeleton consists of a tight series of macroscopic partitions of inhalant and exhalant channels running perpendicular to the body surfaces (Fig. 8F). They consist of networks of choanosomal diactins and microscleres and in the lower body the proximal ends of the prostal diactins. A few small patches of fused choanosomal diactins occur but these are too rare to provide significant support to the body. Ectosomal skeleton of the dermal side consists of the robust lattice of

Table 4. Spicule dimensions (μm) of *Scyphidium australiense* Tabachnick, Janussen & Menschenina, 2008 from holotype NIWA 126237.

Parameter	mean	s.d.	range	no.
Prostal diactin				
length (mm)	10.9	3.9	5.7–18.3	31
width	83.9	27.7	37.8–172.3	46
Choanosomal diactin				
length (mm)	2.0	1.3	0.4–4.4	38
width	13.1	3.6	6.1–21.7	50
Dermalia pentactin				
tangential ray length	145	17	106–186	31
ray width	15.3	1.8	11.0–18.4	31
proximal ray length	119	19	57–165	31
ray width	14.4	1.8	12.0–18.2	31
Atrialia hexactin				
ray length	206	80	88–359	40
ray width	14.3	3.4	7.7–24.5	40
Sphere				
diameter	189	77	90–388	54
Discohexaster 1				
diameter	69.8	10.2	50.0–91.2	32
primary ray length	4.8	0.7	3.4–6.8	32
secondary ray length	30.3	5.4	20.6–42.8	32
Discohexaster 2				
diameter	50.2	10.0	33.4–79.4	68
primary ray length	4.8	0.9	2.7–7.0	68
secondary ray length	20.3	4.9	11.7–34.6	68
Oxyhexaster				
diameter	86.2	10.6	63.5–111.3	59
primary ray length	5.6	1.2	3.2–9.0	59
secondary ray length	37.3	5.5	23.8–49.8	59

pentactine dermalia and in the lower body the projecting prostal diactins. The atrial ectosomal skeleton consists of the felt-like lattice of atrialia and the supporting layer of hypoatrial diactins.

Spicules. Megascleres (Fig. 9; Table 4) are prostal diactins, choanosomal diactins, dermalia, and atrialia. Prostal diactins (Fig. 9A) are large, curved, and smooth spicules with rounded proximal tips either smooth or bearing very low suggestions of obsolete spines. They have neither an axial cross nor central swellings. Distal tips are invariably broken off. Choanosomal diactins (Fig. 9B) come in three distinct forms. The larger ones over 2 mm long are straight or slightly curved or sinuous and are smooth except for the patches of spines at the rounded or abruptly pointed tips. Those between 1 and 2 mm long have sharp tips and longer spines on the tip patches. The shortest, less than 1 mm long, are entirely spined with sharp tips and often with a central tyle or four knobs. Dermalia (Fig. 9C) are thick stubby pentactins, entirely profusely spined without a knob of a sixth ray. Atralia (Fig. 9D) are highly diverse; the most common hexactins have thinner and less densely spined rays than the dermalia. Pentactin atrialia are very similar to the dermal pentactins but have a knob in place of the sixth ray. Paratropal atrialia have rays similar to the hexactine atrialia. Spheres (Fig. 9E) are common and here considered megascleres.

Microscleres (Fig. 9; Table 4) are two types of discohexasters and one type of oxyhexaster and its variants, rare hemioxyhexasters and oxyhexactins. Discohexasters 1 (Fig. 9F) are spherical with very short smooth primary rays, each supporting 3.5 (2–5) thick secondary rays ornamented with reclined spines. Terminal discs invariably have six stout marginal teeth. Discohexasters 2 (Fig. 9G) are smaller spherical forms with each smooth primary ray supporting 6.3 (5–8) thinner terminal rays; the terminal discs also invariably have 6 marginal teeth. Oxyhexasters (Fig. 9H) are stout spherical forms with each short smooth primary ray supporting 3.2 (3–5) fully developed secondary rays ornamented with dense reclined spines and ending in sharp tips. Each oxyhexaster also has 2–12 poorly developed secondary rays only a few micrometres in length. Only one hemioxyhexaster and three oxyhexactins, all of a similar size and ray characters as the oxyhexaster, were discovered in microsclere surveys.

Remarks. The characters of this new specimen agree with those in the original description of *S. australiense* by Tabachnick et al. (2008) except for the absence of prostal diactins and sphere megascleres in the latter, and absence of the rare discohexactins in the former. Absence of prostal diactins in the holotype is likely attributable to it being a distal fragment where we also found no prostalia in the new specimen. Spheres appear to be spicules of erratic occurrence in hexactinellids and are unlikely to be of phylogenetic significance. Absence of discohexactins in the new specimen is not considered an important difference. Sizes and shapes of the common microscleres are similar enough in both specimens to conclude that they are from specimens of the same species. It is somewhat surprising that the authors of this species assigned it to the genus *Scyphidium* without altering the generic diagnosis to encompass it; we have done so here.

Prior to the discovery of a second specimen of *S. australiense* here, there was considerable doubt as to the true type locality of the holotype described by Tabachnick et al. (2008). This work focused on hexactinellid sponges "sampled mainly off the Australian West Coast", and the holotype was named "after the type locality of this species", i.e., Australia. However, the latitude and longitude for RV Soela Stn SO 17–80 (43°33.10'–33.05'S, 179°27.25'–27.08'E) placed the type locality as on the north central Chatham Rise on the east coast of New Zealand. The Western Australian Museum (WAM) has confirmed that the RV Soela carried out fieldwork off western and northern Australia, and that the material covered in Tabachnick et al. (2008) was sent to the MNHN to be worked on taxonomically. Unfortunately, WAM has no details for "RV Soela Stn SO 17–80" (Jane Fromont, Western Australian Museum, pers. comm.), but interestingly, the specimen reported here, NIWA 126237, is also from Chatham Rise (Pegasus Canyon Slope, off Christchurch Shelf), intensifying the mystery surrounding the type locality of this species. Investigation of pre-2004 electronic records at NIC revealed that the specimen listed from station "RV Soela Stn SO 17–80", given in Tabachnick et al. (2008), was more likely to have been collected on the RV Sonne Cruise SO-17 on the Chatham Rise phosphorite deposits east of New Zealand (Von Rad 1984), because the NZOI Stn Z3951B from that cruise, a large grab with Porifera listed in the Remarks col-

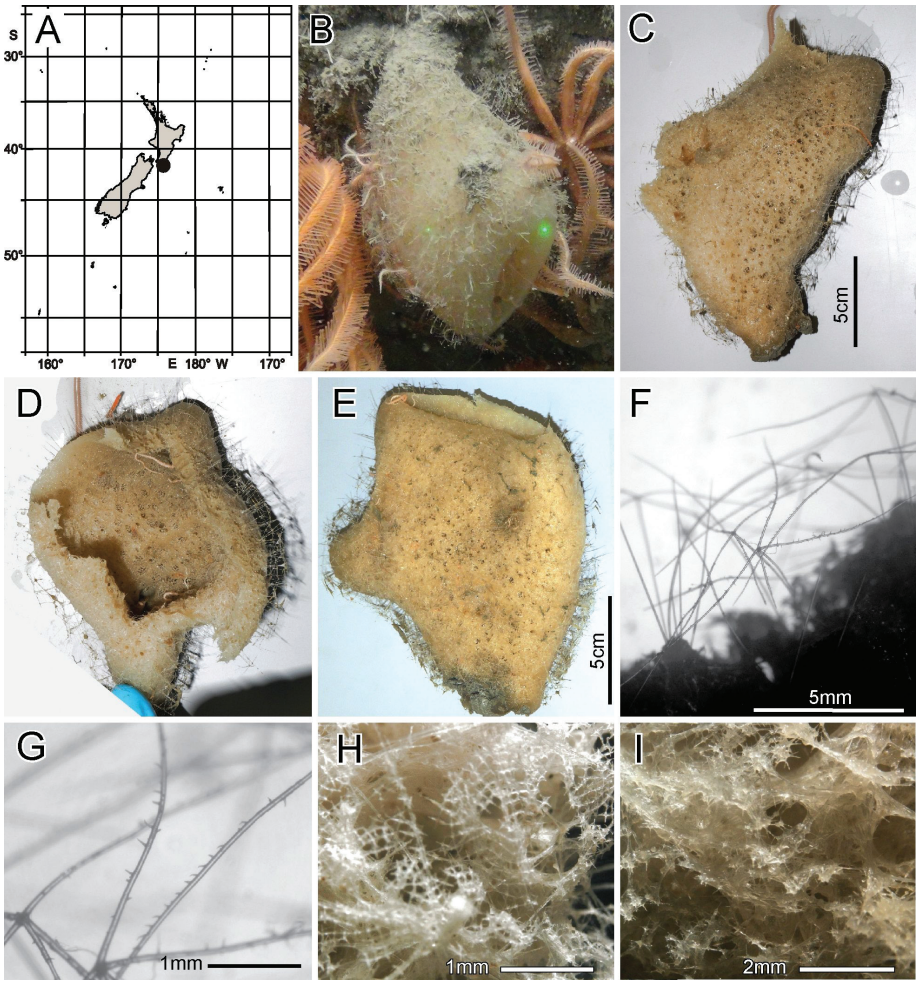

Figure 10. *Scyphidium variospinosum* sp. nov.: **A** distribution in New Zealand waters, location of both holotype NIWA 126279 and paratype NIWA 126274 on Wairarapa Slope **B** holotype NIWA 126279 in situ (green laser spots are 6.24 cm apart) **C** holotype, deck image, torn open on the left side. Note the distinct pentactin veil around body **D** holotype, superior end, deck image, where torn wall is obvious, and osculum is partly intact on the upper left side. Scale bar unavailable **E** paratype, NIWA 126274 (deck images by PJS) **F** close view of the prostal pentactins forming the veil of the holotype **G** Closer view of the thorns on the prostal pentactin tangential rays **H** dermal surface of preserved holotype with partly damaged lattice of dermalia **I** atrial surface of the preserved holotype with no lattice evident. Image **B** captured by ROV Team GEOMAR, ROV Kiel 6000 onboard RV Sonne (voyage SO254), courtesy of Project PoribacNewZ, GEOMAR, and ICBM.

umn, has identical coordinates and similar station numbers. We are still unsure as to how the specimen reached Tabachnick's attention at the MNHN, and indeed, the whereabouts of the holotype, but we know that errors were made in translation of the station data from the specimen labels to this publication, and it is possible that

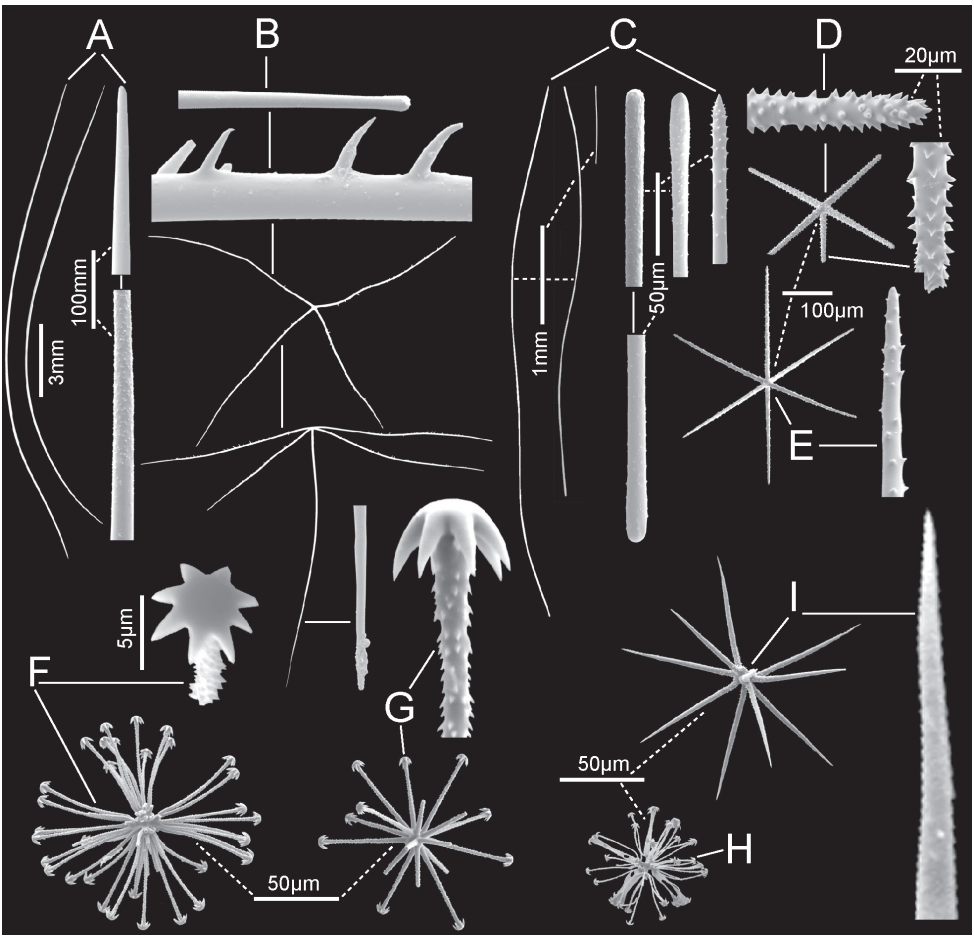

Figure 11. *Scyphidium variospinosum* sp. nov., holotype NIWA 126279, spicules **A** prostal diactins, two whole and enlarged end and near-end segment **B** prostal pentactins, two whole spicules, inside and end views and parts including a tangential ray end (top), a thorned part and a proximal end (lower). Scale bars of whole and parts are same as in **A C** choanosomal diactins, three whole long and short versions plus enlarged tips **D** one pentactine dermalium and enlarged tangential and proximal ray tips **E** one hexactine atrialium and enlarged ray end **F** discohexaster 1 and enlarged terminal ray end **G** discohexaster 2 with enlarged terminal ray end **H** discohexaster 3 **I** hemioxyhexaster with enlarged terminal ray end. All microscleres and their enlarged parts are at same scale bars.

the authors assumed that the RV Sonne representation of "Stn SO17/80" was just another RV Soela Stn, represented as SO 17–80 in the publication. The MNHN was temporarily closed for most of 2020 and the early months of 2021 due to measures of the French government to prevent the spread of COVID-19 (novel coronavirus disease), so the repatriation of this specimen was not able to be completed at time of publication.

Table 5. Spicule dimensions (μm) of *Scyphidium variospinosum* sp. nov. from holotype NIWA 126279.

Parameter	mean	s.d.	range	no.
Prostal diactin				
length (mm)	15.8	3.9	8.3–22.9	22
width	76.0	18.5	34.0–104.6	30
Prostal pentactin				
tangential ray length (mm)	6.4	1.4	1.0–9.1	36
tangential ray width	77.6	11.3	38.4–94.5	32
proximal ray length (mm)	9.1	1.5	3.8–10.9	31
proximal ray width	91.8	12.0	54.6–109.4	32
Choanosomal diactin				
length (mm)	2.5	1.4	0.4–5.5	32
width	9.5	2.5	5.6–14.4	40
Dermalia pentactin				
tangential ray length	188	21	140–238	53
tangential ray width	14.6	2.2	11.0–18.6	47
proximal ray length	143	21	79–188	45
proximal ray width	14.0	1.9	8.3–18.2	47
Atrialia hexactin				
ray length	275	40	181–384	47
ray width	10.1	1.7	6.2–12.9	49
Discohexaster 1				
diameter	116	19	67–142	33
primary ray length	8.4	1.1	6.2–10.5	33
secondary ray length	49.7	9.3	27.2–61.2	33
Discohexaster 2				
diameter	113	11	94–136	33
primary ray length	5.6	1.7	2.4–10.0	29
secondary ray length	51.7	4.8	43.4–60.7	29
Discohexaster 3				
diameter	75	15	44–94	22
primary ray length	7.1	1.7	3.8–12.1	22
secondary ray length	30.7	7.5	10.4–39.5	22
Oxyhexaster 1				
diameter	126	21	76–179	79
primary ray length	4.3	1.1	2.2–9.3	79
secondary ray length	58.8	10.3	32.0–85.3	79
Oxyhexaster 2				
diameter	74	25	31–116	23
primary ray length	5.9	1.1	4.3–8.0	23
secondary ray length	30.5	11.7	12.4–51.5	23
Oxyhexactin diameter	138		119–149	4

***Scyphidium variospinosum* Reiswig, Dohrmann & Kelly, sp. nov.**
http://zoobank.org/6CB20C98-6A3E-41E3-B8A3-C9410668207D
Figs 10, 11; Table 5

Material examined. ***Holotype*** NIWA 126279, RV Sonne Stn SO254/78ROV15_BIOBOX3–5, Wairarapa Slope, 41.619°S, 175.788°E, 1630.5 m, 21 Feb 2017. ***Paratype*** NIWA 126274, RV Sonne Stn SO254/78ROV15_BIOBOX1, Wairarapa Slope, 41.619°S, 175.788°E, 1675.1 m, 21 Feb 2017.

Distribution. Known only from two locations on the Wairarapa Slope, New Zealand (Fig. 10A).

Habitat. Attached to hard substratum; depth 1631–1675 m (Fig. 10B).

Description. Morphology of the holotype and paratype is a thick-walled, club-shaped sponge with a narrow basal attachment, widening gradually to a hemispherical rounded terminal end where a large osculum is centrally located (Fig. 10B–E). The osculum opens into a deep atrial cavity. The margin is sharp-edged with indication of sparse marginalia that do not differ from prostal diactins of the general body wall. The external surface of the entire body is clean and conulose, with prostal diactins and hypodermal pentactins emanating from conules in small groups of 1–10. Dimensions of the holotype and paratype are, respectively, length 16.5 and 15.8 cm, width 9.5 and, excluding the lateral bulge, 9.5 cm, diameter of the osculum 6.4 and 6.6 cm, wall thickness 11.1 and 10.0 mm. Texture is soft, compressible, and resilient, but not fragile. Surface of the dermal side is conulose and bears a layer of prostal diactins projecting 12.5 (6.5–19.3) (n = 9) mm above the dermal surface, intermingled with a veil of prostal, hypodermal, thorned, paratropal pentactins (Fig. 10F, G) projecting 8.6 (7.2–10.0) (n = 9) mm above the surface. On the surface below is a lattice of overlapping dermalia of mostly pentactins (94% and 82% of 160 and 101 assessed) (Fig. 10H). The atrial surface bears a poorly preserved atrial lattice of mostly hexactins (94.7% and 94% of 133 and 131 assessed) (Fig. 10I) forming a cover over the exhalant apertures. Colour in life and preserved is very pale brown.

Skeleton. Choanosomal skeleton is composed of choanosomal diactins without detectable macroscopic or microscopic organisation. No evidence of spicule fusion was noted in either specimen. Microscleres are scattered throughout the choanosome. Ectosomal skeleton of the dermal side consists of the prostal diactins and projecting veil of thorned pentactins. The dermal surface is covered by a robust lattice of mostly pentactine dermalia. The atrial ectosome consists of the felt-like disorganised lattice of mostly hexactine atrialia and the supporting layer of hypoatrial diactins.

Spicules. Megascleres (Fig. 11; Table 5) are prostal diactins, prostal hypodermal pentactins, choanosomal diactins, dermalia, and atrialia. Prostal diactins (Fig. 11A) are large, curved, and smooth spicules with rough subterminal patches and round tips. They have neither axial crosses nor central swellings. Prostal hypodermal pentactins (Fig. 11B) are large spicules with proximal rays ~ 1.4 times the length of tangential rays; the tangential rays are mainly paratropal, occasionally orthotropal. Both tangential and proximal rays have smooth rounded tips, but only tangential rays bear large thorns on the middle halves of the rays. Choanosomal diactins (Fig. 11C) occur in two distinct forms. Large ones > 2 mm in length are straight, slightly curved or sinuous, and are smooth except for rough subterminal areas; tips are rounded or abruptly pointed. Small forms < 2 mm in length are entirely spined, have sharp tips and often four central knobs or a single tyle. Dermalia (Fig. 11D) are thick stubby pentactins, entirely and profusely spined without a knob of a sixth ray. Atralia (Fig. 11D) are most commonly hexactins, with rays longer, thinner, and less profusely spined than those of dermalia.

Microscleres (Fig. 11; Table 5) are three types of discohexasters and two types of oxyhexasters and their variants, rare hemioxyhexasters and oxyhexactins. The centrum in all categories tends to be varyingly swollen to the extent that the spicules approach asteroid forms. The oxyhexasters are extremely difficult to separate into types due to presence

of intermediates. Discohexasters 1 (Fig. 11F) are semi-stellate with very short smooth primary rays, each supporting 4–8 gently curved secondary rays ornamented with reclined spines; terminal discs invariably have eight stout marginal teeth. Discohexasters 2 (Fig. 11G) are very slightly smaller spherical forms with each smooth primary ray supporting 2–4 straight thick terminal rays ornamented with reclined spines; the terminal discs have 5–9 marginal teeth. Discohexasters 3 (Fig. 11H) are small semi-stellate forms like discohexasters 1, with very short, smooth primary rays, each supporting 7–11 thin, curved, rough secondary rays, each ending in a terminal disc with 4–9 marginal teeth. Oxyhexasters 1, including hemioxyhexasters (Fig. 11H), are stout spherical forms with each short smooth primary ray supporting 1–3 secondary rays ornamented with dense reclined spines and ending in sharp tips. Oxyhexasters 2 (no SEM image available) are forms with very thin secondary rays and often broken; they have diverse characters but are not considered immature forms of oxyhexasters 1. The centres are very small or swollen to globular form and the distal ends of the primary rays are either very thin or globular, each primary end supports two or three thin secondary rays that appear totally smooth. We are not confident in recognising this as a spicule category since the only practical character in defining it is the thinness of the secondary rays and size. Oxyhexactins (no SEM available) are rare: only four have been verified in spicule surveys. They have characteristics of oxyhexasters 1 in the stoutness and ornamentation of their rays.

Etymology. Named for the large, irregularly thorned hypodermal pentactins, that project from the body of this species (*variospinosum*, with irregular thorns; Latin).

Remarks. The characters of these new specimens agree with the revised diagnosis of *Scyphidium* (see above) but differ from those of all eight recognised species of that genus. None has raised, thorned, hypodermal pentactins as prostalia. Only three species, *S. tuberculatum* (Okada, 1932), *S. jamatai* Tabachnick, 1991, and *S. australiense* Tabachnick, Janussen & Menschenina, 2008 (see above) have dermalia as mostly pentactins and atrialia as mostly hexactins, in agreement with the two new specimens. The sizes of the discohexasters are considerably smaller in all three than those in the new forms described here. On the basis of these and other differences, we are confident that the two new specimens described here represent a new species, here designated as *Scyphidium variospinosum* sp. nov.

Lanuginellinae Gray, 1872

Diagnosis. Basiphytous, rarely lophophytous, often pedunculate, Rossellidae; dermalia hexactins, pentactins, stauractins, or diactins supported by large hypodermal pentactins; choanosomal spicules diactins, often supplemented by significant amount of hexactins; atrialia pentactins or hexactins often supported by large hypoatrial pentactins; dermal and atrial hexactins and pentactins frequently pinular; prostalia, if present, pentactins or diactins; microscleres include strobiloplumicomes, which may be absent in some species, oxy-, onycho-, or disco-tipped forms (hexasters, hemihexasters, hexactins); microdiscohexasters absent (after Dohrmann et al. 2017).

Caulophacus Schulze, 1886

Diagnosis. Body is fungus-like or cup-like, basiphytose with long stalk. Choanosomal spicules are diactins and hexactins. Dermalia are pinular hexactins and/or pentactins. Atrialia are pinular hexactins and/or pentactins. Hypodermalia and hypoatrialia are pentactins. Microscleres are spicules of hexactinous or hexasterous forms with discoidal, onychoidal, and oxyoidal termination (emended from Janussen et al. 2004).

Type species. *Caulophacus* (*Caulophacus*) *elegans* Schulze, 1886.

Caulophacus (*Caulophacus*) Schulze, 1886

Diagnosis. Body is mushroom-shaped or cup-like, basiphytous with long stalk. Choanosomal spicules are diactins and hexactins. Dermalia and atrialia are pinular hexactins and/or pinular pentactins. Hypodermalia and hypoatrialia are pentactins. Microscleres are represented chiefly by spicules with discoidal terminations. They usually can be divided into two categories. The first are spicules with thick rays covered with dense spines: usually discohexactins but also discohexasters, hemidiscohexasters, and rarely discasters. The second are discohexasters with thin, smooth, or rough secondary rays usually in the form of lophodiscohexasters but sometimes calycocomes and spherical discohexasters are present among them (emended from Tabachnick 2002).

Remarks. The subgenus *Caulophacus* is likely paraphyletic (Dohrmann 2019; MD, unpubl. results) and retained here for historical reasons only. Diagnoses of genus *Caulophacus* and subgenus *Caulophacus* are emended to include the new species *Caulophacus* (*Caulophacus*) *serpens* sp. nov. (described below) with mostly pinular pentactins as both dermalia and atrialia.

Type species. *Caulophacus* (*Caulophacus*) *elegans* Schulze, 1886.

Caulophacus (*Caulophacus*) *discohexaster* Tabachnick & Lévi, 2004

Figs 12, 13; Table 6

Type and locality (not examined). Holotype – MNHN HCL519, Norfolk Ridge, HALIPRO 2, Zoneco Stn BT 062, 24.71°S, 168.648°E, 720–1048 m.

Material examined. NIWA 126342, RV Sonne Stn SO254/85ROV19_BIOBOX6, Southern Kermadec Ridge, 35.609°S, 178.854°E, 1163.6 m, 24 Feb 2016; NIWA 126343, RV Sonne Stn SO254/85ROV19_BIOBOX17, Southern Kermadec Ridge, 35.612°S, 178.852°E, 1149.8 m, 24 Feb 2017.

Distribution. Known from the type locality, Norfolk Ridge near New Caledonia, and southern Kermadec Ridge, ~ 223 km N of East Cape, North Island, New Zealand.

Habitat. Attached to hard substratum; depth 720 to 1348 m (New Zealand locations, Fig. 12A).

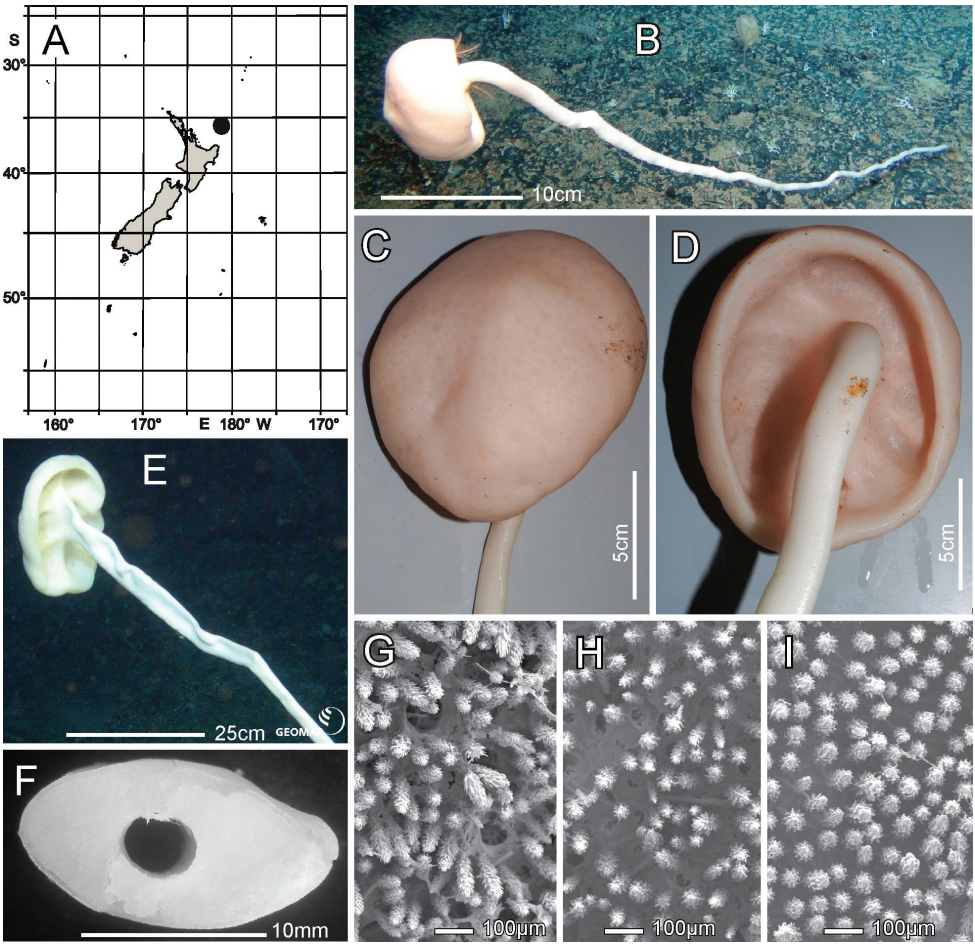

Figure 12. *Caulophacus* (*Caulophacus*) *discohexaster* Tabachnick & Lévi, 2004, NIWA 126342, 126343, distribution, skeleton, and morphology **A** distribution in New Zealand waters **B** smaller specimen, NIWA 126342 in situ **C** smaller specimen atrial surface on-deck image **D** smaller specimen dermal surface and stalk connection (deck images by PJS) **E** larger specimen, NIWA 126343 in situ **F** section of the stalk of the smaller specimen **G–I** SEM images of surfaces of smaller specimen; dermal **G** atrial **H** and stalk **I** at same magnification. Images **B** and **E** captured by ROV Team GEOMAR, ROV Kiel 6000 onboard RV Sonne (voyage SO254), courtesy of Project PoribacNewZ, GEOMAR and ICBM.

Description. This description refers to New Zealand specimens only. Body forms a solitary mushroom cap-shaped upper body on a long, kinked, somewhat crooked, flattened, hollow stalk (Fig. 12B, E). Surfaces of the upper body are smooth (Fig. 12C, D) with a slight blunt eminence on the outer atrial face opposite the stalk insertion, but there is no indication of an osculum. The upper dermal surface lacks any visual indication of a lattice. The lower dermal surface of the specimen is divided by ridges into six depressions not seen in the smaller specimen. The stalks of both are flattened and that of the smaller bears a cylindrical central canal (Fig. 12F). SEM views of the

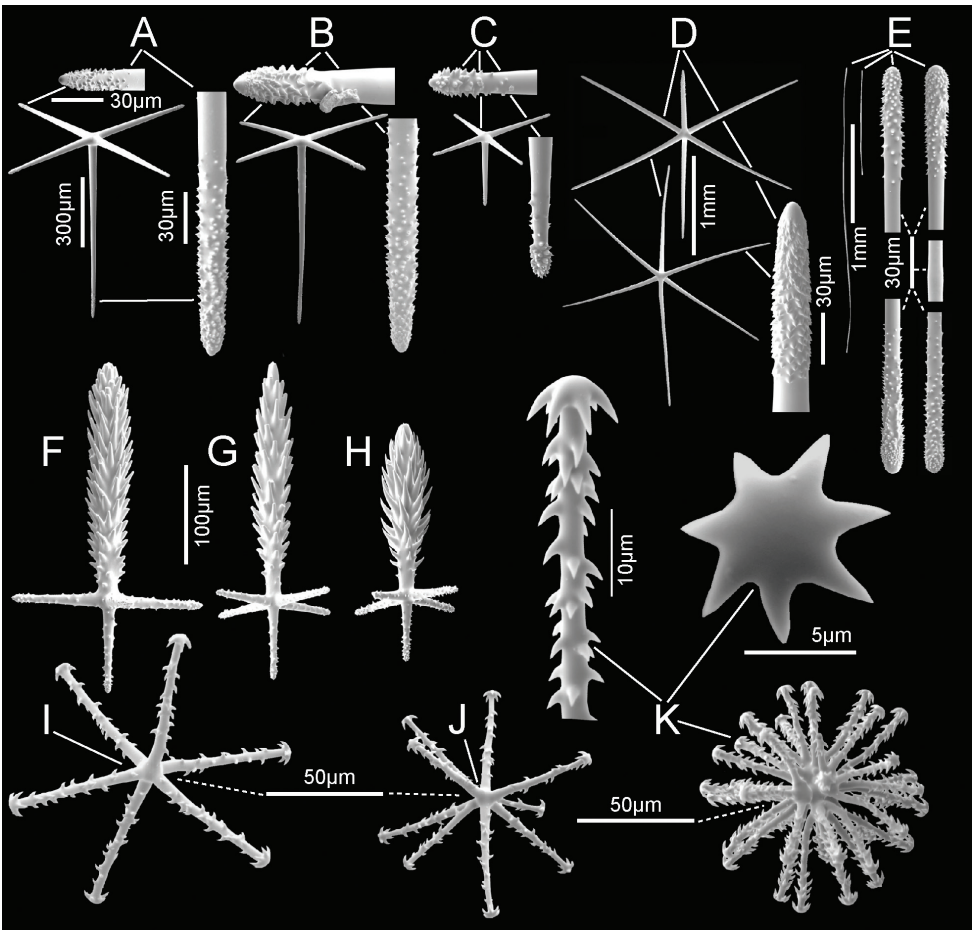

Figure 13. *Caulophacus* (*Caulophacus*) *discohexaster* Tabachnick & Lévi, 2004, NIWA 126342, spicules: **A** hypodermal body pentactin; whole and enlarged tangential and proximal ray ends **B** hypoatrial body pentactin; whole and enlarged tangential and proximal ray ends **C** hypodermal stalk pentactin; whole and enlarged tangential and proximal ray ends **D** choanosomal hexactins; two whole and enlarged ray end **E** choanosomal diactins; two whole and four enlarged ends and one central swelling **F** dermal body pinular hexactin **G** atrial body pinular hexactin **H** stalk dermal pinular hexactin **I** discohexactin **J** hemidiscohexaster **K** discohexaster and magnified terminal ray and terminal disc. Scale bars in **A** apply to **B** and **C**; scale bar is the same for **F–H, I–K**.

dried surfaces show pores in the dermal body surface membrane (Fig. 12G), apparently contracted pores in the atrial body surface involving the atrial pinules (Fig. 12H), and no indication of pores on the dermal stalk surface (Fig. 12I). Dimensions of the smaller specimen upper body is ~ 12.5 × 10.6 cm in diameter; stalk is 15.9 × 9.0 mm in diameter and stalk canal is 4.1 × 3.3 mm in diameter. Length of the stalk could not be approximated. The larger specimen upper body is 25.0 × 15.9 cm in diameter while the flattened stalk is 5.9 cm wide. Measurable ostia of the smaller specimen

Table 6. Spicule dimensions (μm) of *Caulophacus* (*Caulophacus*) *discohexaster* Tabachnick & Lévi, 2004, NIWA 126342.

Parameter	mean	s.d.	range	no.
Hypodermal body pentactin				
tangential ray length	484	83	235–637	76
tangential ray width	33.9	5.3	13.0–43.4	79
proximal ray length	602	214	256–967	56
proximal ray width	38.5	5.9	18.0–52.0	72
Hypoatrial body pentactin				
tangential ray length	495	81	318–668	61
tangential ray width	31.3	5.2	18.3–41.3	62
proximal ray length (mm)	804	173	213–1088	57
proximal ray width	35.8	6.3	6.8–50.5	60
Hypodermal stalk pentactin				
tangential ray length (mm)	289	46	174–415	100
tangential ray width	22.7	3.5	14.0–32.0	64
proximal ray length (mm)	296	32	205–355	43
proximal ray width	25.4	3.8	14.7–33.3	50
Choanosomal hexactin ray				
length (mm)	1.1	0.5	0.5–2.1	53
width	48.4	13.7	17.6–78.5	53
Choanosomal diactin				
length (mm)	1.6	0.5	0.7–2.9	52
width	7.7	2.1	4.6–13.3	52
Body dermal pinular hexactin				
pinular ray length	200	28	158–241	52
basal ray width	16.6	2.2	11.3–21.4	51
maximum ray width	49.7	6.2	36.6–70.6	52
tangential ray length	84.0	18.5	51.8–115.1	52
ray width	12.5	2.0	8.6–17.1	52
proximal ray length	80.9	14.1	47.7–111.5	50
ray width	12.4	2.3	8.8–17.3	52
Body atrial pinular hexactin				
pinular ray length	242	17	180–264	51
basal ray width	14.7	1.6	11.3–17.9	51
maximum ray width	49.9	5.7	37.0–61.4	51
tangential ray length	71.2	9.5	53.2–100.0	51
ray width	10.7	1.6	7.514.3	51
proximal ray length	71.2	8.1	39.9–88.5	51
ray width	10.4	1.6	7.6–14.9	51
Stalk dermal pinular hexactin				
pinular ray length	170	15	131–198	51
basal ray width	16.2	1.9	11.2–20.6	51
maximum ray width	54.8	5.8	43.9–69.2	51
tangential ray length	59.1	8.4	7.5–15.8	51
ray width	12.0	1.9	7.5–15.8	51
proximal ray length	63.8	6.5	47.9–88.7	48
ray width	11.4	1.6	8.4–14.6	51
Discohexactin				
diameter	131	21	75–163	51
ray width	4.7	1.1	2.5–7.6	51
Hemidiscohexaster				
diameter	119	14	90–150	52
primary ray length	7.3	1.3	4.0–10.0	51
secondary ray length	52.7	7.2	34.4–69.9	52
Discohexaster				
diameter	108	18	55–143	52
primary ray length	7.0	1.7	3.1–10.7	51
secondary ray length	47.4	7.8	22.4–60.3	52

Table 7. Comparison of the key morphological characters that differentiate the 24 species of *Caulophacus* (*Caulophacus*) from each other and from New Zealand specimens of *Caulophacus* (*Caulophacus*) *discohexaster* Tabachnick & Lévi, 2004) (NIWA 126342 and NIWA 126343).

taxa	location	**body shape** differs radically	**dermal pinule** differs visually in shape	**atrial pinule** differs visually in shape	**stalk pinule** differs visually in shape	**dermal pinule**, 2 or more forms	**dermal, atrial or stalk pinules** mostly pentactins	**dermal, atrial or stalk pinules** exclusively pentactins	**dermal pinule** ray is much shorter	**atrial pinule** ray is much shorter	**dermal and atrial pinules**, basal rays of nearly smooth	**choanosomal hexactins**, some or all are centrally spined	**hypodermal pentactins**, some or all are centrally spined	**hypodermal pentactins** are very small	**hypodermal pentactins** of stalk, atrial pinules are mostly pentactins	**hypodermal pentactins** of stalk, some or all are centrally spined	**hypoatrial pentactins** tangential rays, some or all centrally spined	**hypoatrial pentactins** very small	**microsclere** hemidiscohexasters absent	**microsclere** discohexasters absent	**microsclere** discohexactins absent	**microsclere** discohexasters include thin-rayed forms	**microsclere** discohexasters in two or more forms	**microsclere** oxy-tipped forms present
abyssalis	Argentine Basin		x			x						x	x						x					
adakensis	Aleutian Islands											x	x				x							
agassizi	Gulf of Maine/Bay of Fundy		x	x			x					x	x				x		x					
antarcticus	East Antarctic Wilkes Land		x	x			x							x				x		x				
arcticus	Greenland and Arctic Ocean		x	x					x				x		x		x					x		
basispinosus	Indian Ocean						x					x	x				x		x	x				x
chilense	Central Chile	x										x	x				x					x		x
cyanae	Mexican Tropical Pacific		x	x			x						x						x				x	x
discohexactinus	Antarctica						x						x						x			x	x	
discohexaster	New Caledonia		x																					
elegans	North Pacific		x	x							x		x											
galatheae	Indian Ocean								x				x						x	x				x
hadalis	Southern Kermadec Ridge		x				x									x			x					
instabilis	South Orkney Islands				x								x						x					
latus	Crozet Islands		x	x					x				x									x		x
oviformis	East Antarctica	x	x	x							x	x							x		x			
palmeri	Drake Passage									x									x		x			
pipetta	East Antarctica	x	x	x							x		x									x	x	
ramosus	Kermadec Trench							x							x									
schulzei	Panama Bight, Pacific Ocean				x						x		x				x					x	x	
serpens	Kermadec Trench						x																	
scotiae	Weddell Sea, Antarctica		x	x									x									x	x	
variens	Western Pacific Ocean		x	x								x							x			x	x	
wilsoni	Eastern Pacific Ocean	x	x	x									x						x			x		

*Taxonomic authorities have been excluded from this column but are available from van Soest et al. (2021)

Table 8. Spicule dimensions (μm) of *Caulophacus* (*Caulophacus*) *serpens* sp. nov., NIWA 126084.

Parameter	mean	s.d.	range	no.
Hypodermal body pentactin				
tangential ray length	398	187	192–1385	43
tangential ray width	13.5	2.7	8.2–19.6	41
proximal ray length	482	207	210–865	30
Hypoatrial body pentactin				
tangential ray length	360	72	206–689	46
tangential ray width	14.7	3.0	8.0–20.1	47
proximal ray length	670	96	450–898	46
Hypodermal stalk pentactin				
tangential ray length	205	64	117–460	51
tangential ray width	10.8	2.2	7.2–19.0	50
proximal ray length	305	129	140–789	49
Choanosomal hexactin ray				
length	555	75	286–718	53
width	10.3	2.2	5.5–14.2	58
Choanosomal diactin				
length (mm)	1.31	0.35	0.63–2.22	50
width	7.1	1.4	4.9–11.4	50
Body dermal pinular pentactin				
pinular ray length	218	28	164–273	29
basal ray width	8.4	1.6	6.0–14.6	44
maximum ray width	21.3	3.0	14.7–29.1	60
tangential ray length	95.5	12.5	72.2–117.8	30
ray width	7.0	1.0	4.8–9.3	53
Body dermal pinular hextactin				
pinular ray length	169	14	156–184	3
pinular ray basal width	7.7	0.9	6.2–8.8	7
pinular ray maximum width	25.2	4.2	21.7–30.6	4
tangential ray length	93.5	15.0	84.5–110.8	3
tangential ray width	6.5	1.0	4.8–7.7	7
proximal ray length	77.1	13.1	63.8–90.0	3
proximal ray width	6.8	0.6	6.2–7.7	4
Body atrial pinular pentactin				
pinular ray length	362	51	263–440	30
pinular ray basal width	8.2	1.2	5.0–10.2	55
pinular ray maximum width	17.9	3.1	11.8–27.0	44
tangential ray length	123	16	98–167	44
tangential ray width	7.2	1.2	4.2–9.8	59
Stalk dermal pinular pentactin				
pinular ray length	283	22	242–326	30
pinular ray basal width	8.6	1.5	6.0–13.7	50
pinular ray maximum width	32.3	6.3	18.2–47.9	50
tangential ray length	102	14	65–133	34
tangential ray width	7.0	1.1	4.5–9.3	57
Discohexactin				
diameter	185	18	142–225	58
ray width	4.6	0.7	2.9–6.8	58
Thick-ray discohexaster				
diameter	94	32	48–139	9
primary ray length	7.5	1.4	5.0–9.4	9
secondary ray length	39.8	15.8	18.0–60.7	9
Thin-ray discohexaster				
diameter	46.1	4.5	34.0–58.0	59
primary ray length	7.6	1.2	4.4–11.4	59
secondary ray length	15.4	2.0	8.8–21.3	59

(Fig. 12G) are 70 and 99 μm in diameter. Texture of the body is firm but compressible; the stalk is hard. Surface of all parts are smooth, consisting of tight palisades of pinular rays of dermalia and atralia supported on hypodermal and hypoatrial pentactins. There are no projecting prostalia. Colour in life is pale pinkish brown as are the specimens preserved in ethanol.

Skeleton. Choanosomal skeleton of the body consists of a tight network of choanosomal hexactins and diactins. There is no evidence of fusion between any spicules within the body. Microscleres are scattered evenly throughout the choanosome. The stalk internal skeleton is composed of large diactins oriented longitudinally and fused by synapticula. Ectosomal skeleton of the dermal and atrial sides consists of tightly packed pinular hexactins and very few pinular pentactins (1.6% of 623 assessed). These are supported on, respectively, hypodermal and hypoatrial pentactins which are never raised above the surfaces. Microscleres are present as in the choanosome.

Spicules. Megascleres (Fig. 13; Table 6) are hypodermal pentactins, choanosomal hexactins and diactins, and pinular hexactins and a few pentactins. Hypodermal pentactins of the body (Fig. 13A) are regular and usually smooth except for spined ray ends; 8% have indistinct spines on the proximal part of the proximal ray. The proximal rays are longer, averaging 1.24 × the length of tangential rays. Hypoatrial pentactins of the body (Fig. 13B) are regular and spined on both ray-ends and 61% of them on the proximal part of the proximal rays. The proximal ray is longer, averaging 1.62 × the length of tangential rays. Hypodermal pentactins of the stalk (Fig. 13C) are regular in shape but significantly smaller than those of the body; they are spined only on ray ends. Tangential and proximal rays are approximately equal in length. Choanosomal hexactins (Fig. 13D) are restricted to the body; rays are smooth, and spines are restricted to the ray ends except where the ray is exceptionally short. These hexactins occur in two forms, one with a short spiny ray (upper figure) and the other with all rays approximately equal in length (lower figure). Choanosomal diactins (Fig. 13E) are straight or slightly curved and are smooth except for ends on which they have small but detectable central swellings. Dermal pinular hexactins of the body (Fig. 13F) have bushy, nearly cylindrical pinular rays with a short, thick, rounded apical tip. Tangential and proximal rays are entirely spined and approximately similar in size and shape. Very rarely, these and pinules of other body surfaces are pentactine with only a round nub in place of the proximal ray. Atrial pinular hexactins of the body (Fig. 13G) have pinular rays that taper in length of scales at both ray ends, resulting in fusiform shape. The pinular ray has a thick and rounded tip. Tangential and proximal rays are entirely spined and similar in size and shape. Stalk pinular hexactins (Fig. 12H) have a pinular ray that is squat and slightly wider than those of the body spicules. Scale lengths taper basally and apically and again the apex of the pinule is a blunt, thick cap. Tangential and proximal rays are entirely spined and similar in size and shape.

Microscleres (Fig. 13; Table 6) are discohexactins (43% of 221 assessed), hemidiscohexactins (54.7%), and discohexasters (2.3%); all are thick-rayed forms. Discohexactins (Fig. 13I) have rays ornamented with large, reclined spines and a terminal disc

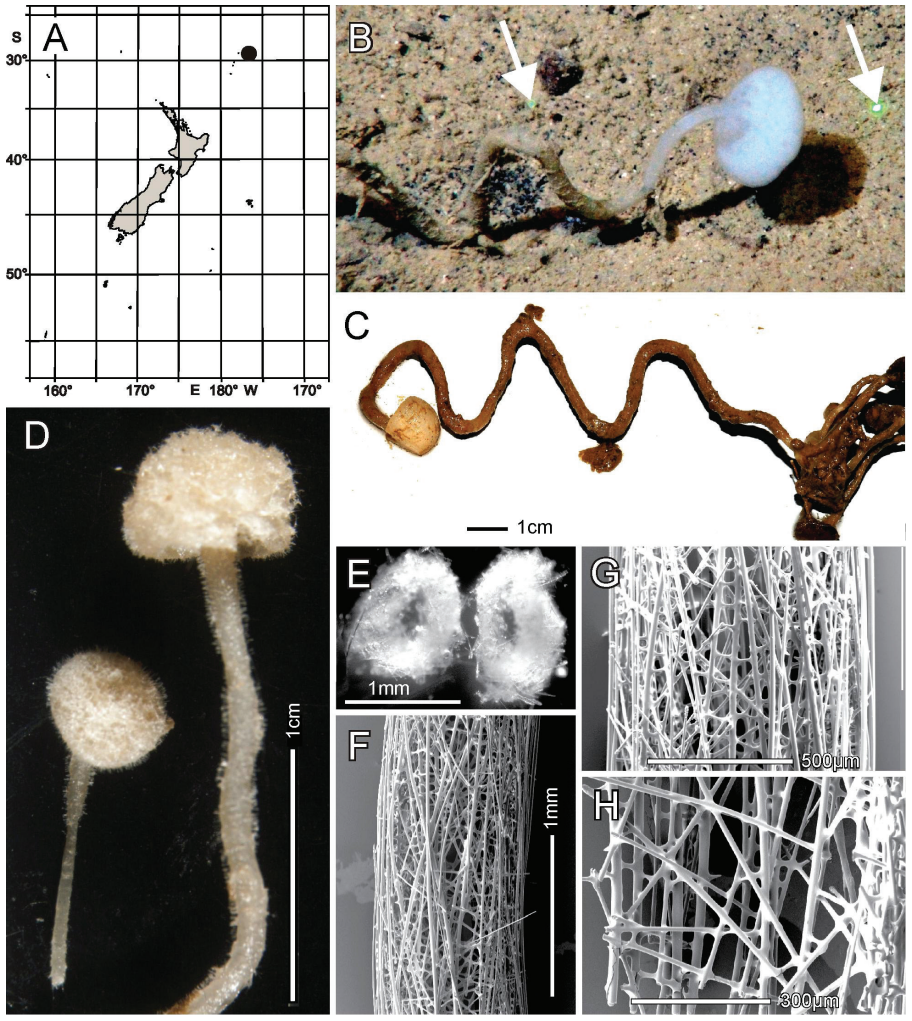

Figure 14. *Caulophacus* (*Caulophacus*) *serpens* sp. nov., NIWA 126084, distribution, skeleton, and morphology **A** distribution in New Zealand waters, collection location of holotype on the Kermadec Trench slope **B** in situ image of the largest specimen body and the irregular undulating stalk associated with it. The laser spots indicated by the arrows are 6.24 cm apart **C** deck image of the same with smaller specimens in the stalk tangle at right (image by PJS) **D** two smaller bodies and their stalks, previously attached to the main mass, used for spicule analysis **E** cross sections of the uncleaned stalk of the larger specimen in **D**; **F** Acid-cleaned part of the stalk of the same (SEM) **G** closer view of the outer stalk surface showing most fused diactins oriented nearly parallel to the stalk axis (SEM) **H** close view of the internal stalk surface showing most superficial spicules oriented at large angles to the stalk axis (SEM). Image **B** captured by ROV Team GEOMAR, ROV Kiel 6000 onboard RV Sonne (voyage SO254), courtesy of Project PoribacNewZ, GEOMAR, and ICBM.

with 5 (4–7) marginal teeth. Hemidiscohexasters (Fig. 13J) are similar with at least one ray being branched and at least one ray being unbranched; the total number of rays is 9.4 (7–13). Terminal discs are similar to discohexactins. Discohexasters (Fig. 13K)

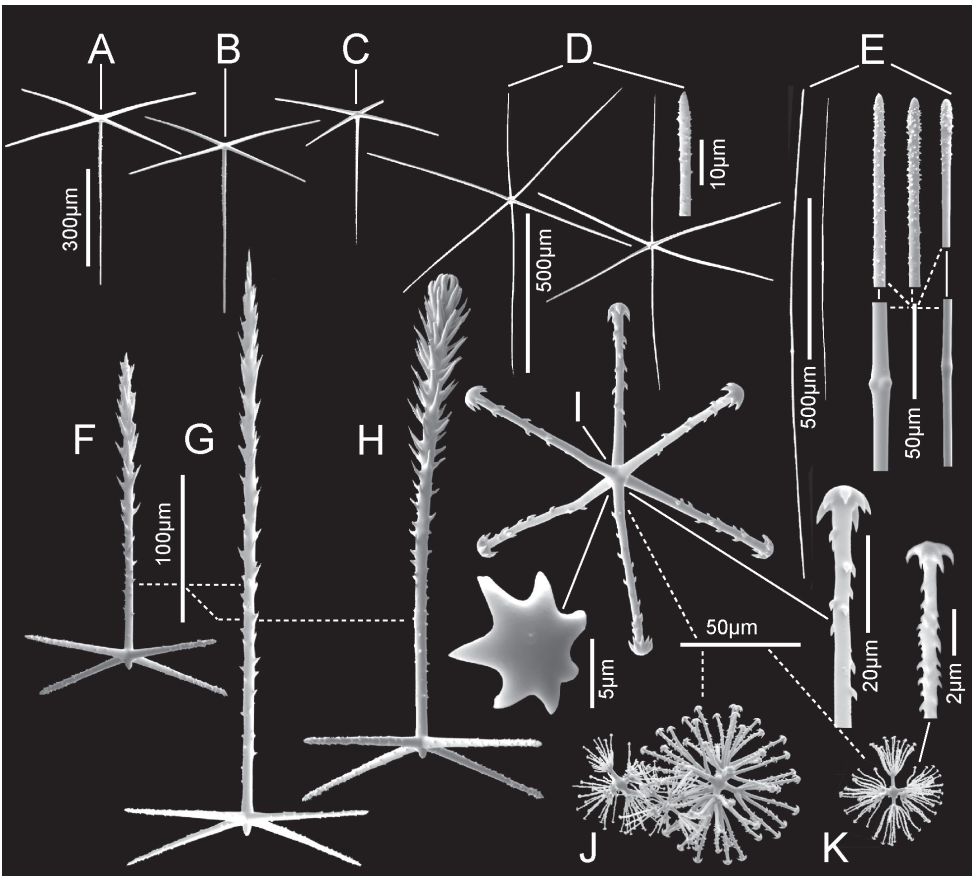

Figure 15. *Caulophacus* (*Caulophacus*) *serpens* sp. nov., NIWA 126084, spicules **A** hypodermal body pentactin **B** hypoatrial body pentactin **C** hypodermal stalk pentactin **D** two whole choanosomal hexactins and an enlarged ray end **E** two whole choanosomal diactins and enlarged ends and central swellings; **F** dermal body pinular pentactin **G** atrial body pinular pentactin **H** stalk dermal pinular pentactin **I** discohexactin with enlarged terminal ray and facial view of end disc **J** large thick-rayed discohexaster with two smaller thin-rayed discohexasters entangled **K** thin-rayed discohexaster and magnified terminal ray. Scale bar in **A** applies to **B–E** scale bar in **F** applies to **G** and **H** whole microscleres are at the same scale.

have all primary rays branched varying from 2–6 terminal rays on each primary ray. Terminal discs have 3–8 marginal teeth.

Remarks. The morphological characters of the two New Zealand specimens place them clearly in subgenus *Caulophacus* (*Caulophacus*), of which there are 22 recognised species. Table 7 compares the key morphological characters that differentiate them from each other and from the New Zealand specimens, NIWA 126342 and NIWA 126343. We admit that some of these differences are subjective and the list is not exhaustive. Table 7 shows only a single species, *C.* (*C.*) *discohexaster*, that has a single morphological difference from the specimens described here, i.e., the visual impression of the dermal pinule (Tabachnick and Lévi 2004: 51, fig. 24A). Measurement of the

Table 9. Spicule dimensions (μm) of *Caulophacus* (*Caulophacus*) *ramosus* sp. nov., NIWA 126085.

Parameter	mean	s.d.	range	no.
Hypodermal body pentactin				
tangential ray length	417	107		42
tangential ray width	19.7	4.0		44
proximal ray length	526	187		35
Hypoatrial body pentactin				
tangential ray length	438	73		53
tangential ray width	21.2	2.7		54
proximal ray length	617	129		52
Hypodermal stalk pentactin				
tangential ray length	203	37		46
tangential ray width	10.8	2.5		49
proximal ray length	337	187		25
Choanosomal hexactin				
short ray length	497	70		14
long ray width	847	143		16
ray width	24.3	3.0		16
Choanosomal diactin				
length (mm)	1.7	0.7		44
width	8.6	2.3		44
Body dermal pinular pentactin				
pinular ray length	504	133		8
pinular ray basal width	9.2	2.1		29
pinular ray maximum width	11.2	3.0		29
tangential ray length	118	22		20
tangential ray width	7.4	1.7		30
Body atrial pinular pentactin				
pinular ray length	630	127		41
pinular ray basal width	9.2	1.6		40
pinular ray maximum width	11.7	1.8		41
tangential ray length	122	20		35
tangential ray width	7.6	1.5		40
Stalk dermal pinular pentactin				
pinular ray length	530	125		30
pinular ray basal width	11.4	4.9		30
pinular ray maximum width	16.4	7.0		30
tangential ray length	132	33		23
tangential ray width	8.8	3.9		30
Discohexactin				
diameter	263	30		52
ray width (from SEM only)	6.7	0.9		5
Thin-ray stellate discohexaster				
diameter	154	24		50
primary ray length	50.9	7.5		50
secondary ray length	26.2	7.8		50

dermal pinule in that figure shows that the figured pinular ray is too wide (84 μm) to fit within the data given for the pinular ray of the dermal hexactin given there (106–220 μm/30–46 μm). Removing this illustration error from the list results in no differences between the New Zealand specimens and the type material described by Tabachnick and Lévi (2004) from New Caledonia; therefore, we assign the specimens to that species.

***Caulophacus* (*Caulophacus*) *serpens* Reiswig, Dohrmann & Kelly, sp. nov.**
http://zoobank.org/BF258FB6-7C4B-4A90-95B9-5E8BF02B8B5A
Figs 14, 15; Table 8

Material examined. ***Holotype*** NIWA 126084, RV Sonne Stn SO254/22ROV06_BIOBOX6, Kermadec Trench slope, 29.266°S, 176.702°W, 4816 m, 04 Feb 2017.

Distribution. Known only from the type locality, the Kermadec Trench slope, north of New Zealand (Fig. 14A).

Habitat. Attached to large pieces of rubble lying on a sediment plain at 4816 m.

Description. Morphology of the holotype a rhizome-like, hard, hollow, thin stem that creeps across the sediment seabed, attaching to rubble here and there, in places forming a tangled mass, from which arises the main mushroom-shaped body on a zigzag stem (Fig. 14B, C), and two tiny, mushroom-shaped bodies (Fig. 14D). Overall dimension of the holotype, spreading across the seabed, is 64 cm. Dimension of the larger body (Fig. 14B) is 22.2 mm in diameter and 11.2 mm in height; its associated stalk is 3.6 (2–6–4.3) (n = 12) mm in diameter. The associated stalk measures 3.3 (2.7–4.0) (n = 29) mm in diameter, the length, measured in conformation from the body to the stalk tangle, is 167 mm. The smaller bodies (Fig. 14D) are 7.2 × 5.4 and 5.2 × 4.3 mm in diameter and height, respectively; the stalk of the larger one is 1.1 (1.0–1.3) (n = 12) mm in diameter. The piece of thick stalk received from NIWA is 72 mm long and 3.0 (2.8–3.3) (n = 12) mm in diameter, approximately the same gauge as the convoluted stalk shown in the in situ and deck images. Surfaces of the body are a bit lumpy and fuzzy (Fig. 14D); that of the thin attached stalks is also fuzzy. There are no projecting prostal spicules. Colour of the body in life is white, and the stem pale brown; when preserved in ethanol it is very pale brown, almost white.

Skeleton. Choanosomal skeleton of the body is a network of diactins and hexactins. There is no evidence of fusion between any spicules within the body. Spicule fusion is restricted to the choanosomal diactins of the hollow stalks where the diactins are joined by synapticula and points of spot contacts between spicules. Microscleres are scattered evenly throughout the choanosome. Ectosomal skeleton of the dermal and atrial sides of the body and living stalks consists of tightly packed pinular pentactins and very few pinular hexactins (1.3% of 374 assessed). These are supported on, respectively, hypodermal and hypoatrial pentactins which are never raised above the surfaces. Microscleres are present as in the choanosome.

Spicules. Megascleres (Fig. 15; Table 8) are hypodermal and hypoatrial pentactins, choanosomal hexactins and diactins, and pinular pentactins and a few pinular hexactins. Hypodermal pentactins of the body (Fig. 15A) are regular and usually smooth except for spined ray ends; 31% have macrospines on the central part of the proximal ray. The proximal rays are longer, averaging 1.21 × the length of tangential rays. Hypoatrial pentactins of the body (Fig. 15B) are regular and spined on both tangential and proximal ray ends; macrospines are present on the central part of most (60%) proximal rays but all tangential rays lack macrospines. The proximal ray is longer, on average 1.86 × the length

of tangential rays. Hypodermal pentactins of the stalk (Fig. 15C) are regular in shape but significantly smaller than those of the body; they are spined on ray ends but macrospines are uncommon (12%) on the central part of only the proximal rays. Proximal rays are generally longer, on average 1.49 × tangential ray length. Choanosomal hexactins (Fig. 15D) are restricted to the body; rays are smooth, and spines are restricted to the ray ends. Macrospines are never found in the central part of these spicules. Choanosomal diactins (Fig. 15E) are straight or slightly curved and are smooth except for ends; they have small but detectable central swellings. Dermal pinular pentactins of the body (Fig. 15F) have narrow pinular rays topped with a short, sharp apical spine. Their basal rays are entirely spined and end in abruptly pointed tips. Approximately 10% of the dermal pinules are hexactine forms. Atrial pinular pentactins of the body (Fig. 15G) have narrow pinular rays like the dermal pinules but with a longer pinular ray (on average 2.1 ×) and longer apical spine; basal rays are like those of the dermal pinules. Stalk pinular hexactins (Fig. 15H) have a pinular ray that is narrow in its basal half but curves to one side and swells in width apically, assuming an overt club-shape. It has no atrial spine since the apex is enfolded by the apical scales. Basal rays are like those of the dermal and atrial pinules.

Microscleres (Fig. 15; Table 8) are discohexactins, thick-ray discohexasters and thin-ray discohexasters. Discohexactins (Fig. 15I) are the most abundant microscleres; they have rays ornamented with large, reclined spines and a terminal disc with 5–8 marginal teeth. Thick-ray discohexasters (Fig. 15J) are the least abundant microsclere; they are spherical, have 6–9 thorned terminal rays on each smooth primary ray, and terminal discs have 4–8 marginal teeth. Thin-ray discohexasters (Fig. 15J, K) are among the most numerous microscleres, but comparing their abundance with discohexactins is not possible since detection of the two spicule types requires different microscope arrangements. They are semi-stellate with each smooth primary ray supporting 16 (8–28) (n = 16) thorned terminal rays ending in discs with 3–7 marginal teeth.

Etymology. Named for the rhizome-like stem that may form tangled, convoluted stems from which the main bodies arise, the whole creeping along the substrate (*serpens*, creeping; Latin).

Remarks. The morphological character of all microscleres being discoid, places this species in the subgenus *Caulophacus* (*Caulophacus*). In comparing them to the 22 recognised species of this subgenus (Table 7), it is apparent that there are no forms known with both dermal and atrial spicules as mainly pinular pentactins. It is thus clear that the form described here is the holotype of a new species named *Caulophacus* (*Caulophacus*) *serpens* sp. nov.

Caulophacus (*Caulophacus*) *ramosus* Reiswig, Dohrmann & Kelly, sp. nov.

http://zoobank.org/C3DFB4B3-84C0-4794-A26F-84CB58A9F7E3
Figs 16, 17; Table 9

Material examined. ***Holotype*** NIWA 126085, RV Sonne Stn SO254/22ROV06_BIOBOX4, Kermadec Trench slope, 29.266°S, 176.702°W, 4819 m, 04 Feb 2017.

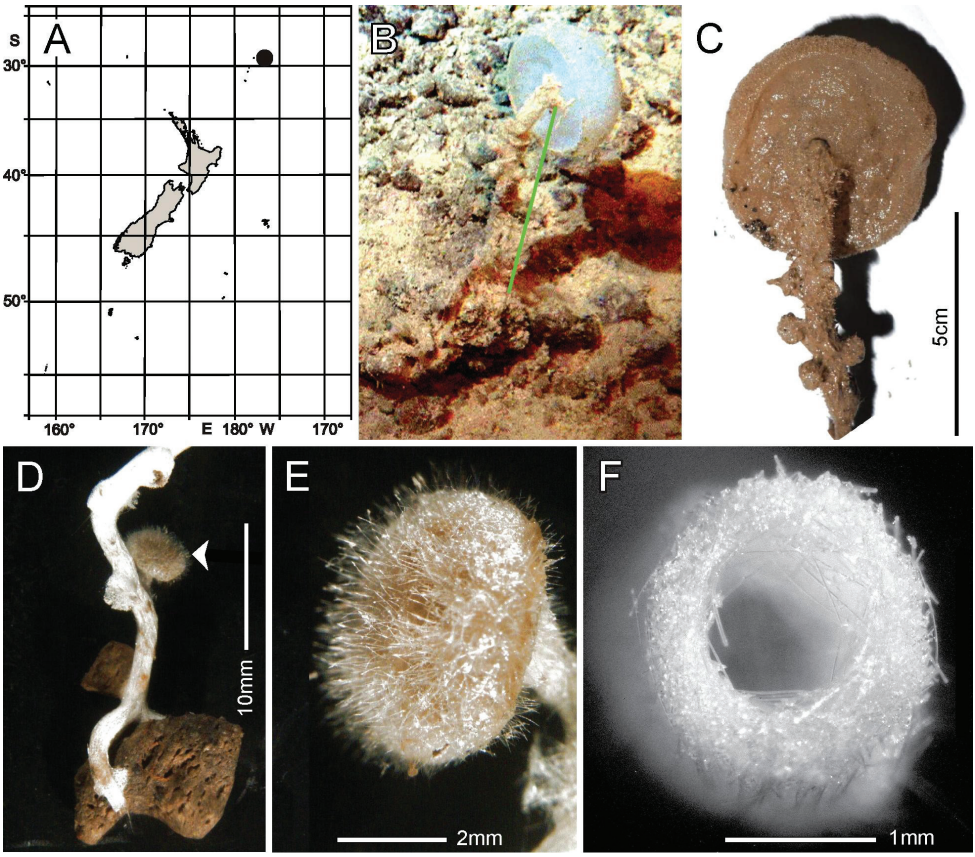

Figure 16. *Caulophacus* (*Caulophacus*) *ramosus* sp. nov., NIWA 126085, distribution, skeleton, and morphology **A** map of collection location on Kermadec Trench slope **B** in-situ image of the largest body; the irregular undulating stalk associated with it is largely hidden in accumulated sediment. The green line is 6.24 cm long copied from between laser spots elsewhere in the image **C** deck image of the large body, which was unavailable for taxonomic description since used for other analyses (image by PJS) **D** a smaller body (arrowhead) attached presumably to the same stalk but lower in the sinuous section with multiple branching attachments to small cobbles **E** The same body enlarged to show the plush of long atrial pinular pentactins **F** cross section of the larger contort white stalk and its central canal. Image **B** captured by ROV Team GEOMAR, ROV Kiel 6000 onboard RV Sonne (voyage SO254), courtesy of Project PoribacNewZ, GEOMAR, and ICBM.

Distribution. Known only from the type locality, the Kermadec Trench slope, north of New Zealand (Fig. 16A).

Habitat. Attached to hard substratum; depth 4819 m.

Description. Morphology of the holotype is a compound mass of a thin, convoluted stalk-part, with at least one small mushroom-shaped body branching from it (Fig. 16D, E), and a longer, thicker, upright stalk-part bearing a larger terminal mushroom-shaped body (Fig. 16B, C). The larger upright stalk has six lateral knobs just below the larger body on its stalk (Fig. 16C) whose nature and function are unknown, possibly sites for attachment to a hard substratum, or are new buds. The lower convo-

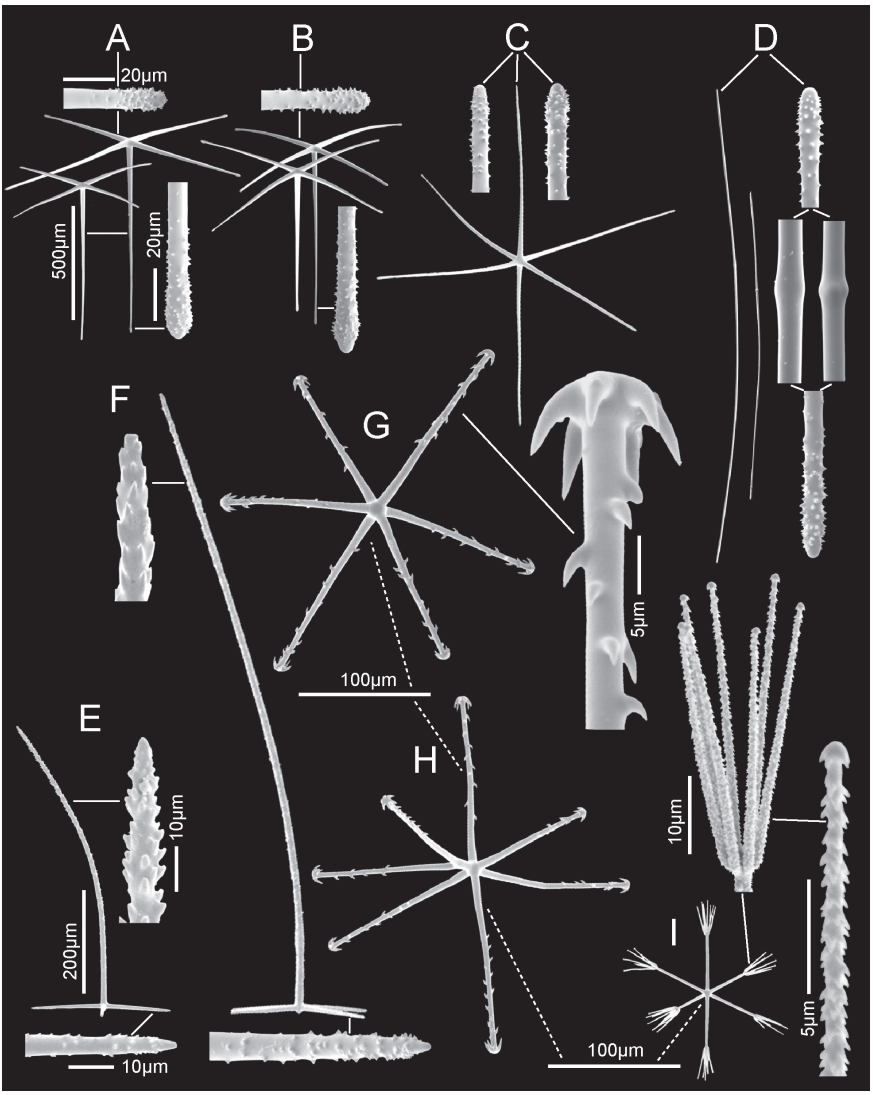

Figure 17. *Caulophacus* (*Caulophacus*) *ramosus* sp. nov., NIWA 126085, spicules **A** two whole hypodermal body pentactins and enlarged ray tips **B** two whole hypoatrial body pentactins and enlarged ray ends **C** a choanosomal hexactin and two enlarged ray tips **D** t wo whole choanosomal diactins and enlarged ends and central swellings **E** dermal body pinular pentactin and enlarged ray ends **F** atrial body pinular pentactin and enlarged ray ends **G** discohexactin and enlarged ray end **H** hemidiscohexaster **I** thin-rayed stellate discohexaster with enlarged secondary ray tuft and a secondary ray. Scale bars in **A** apply to **B–D** scales in **E** apply to **F** whole microscleres are at the same scale.

luted stalk part branches into many attachment points, at least eight within a 27 mm length (Fig. 16D). The smaller of the two bodies attached to this stalk system has a felt-like cover of long pinular pentactins on the outer surface (Fig. 16E); we have had no opportunity to examine the larger body. The stalk in all parts is hollow (Fig. 16F). Overall dimension of the larger body in the in-situ image is 45.5 mm in diameter

with the stalk having a diameter of 5.9 mm at a point 5 mm below the attachment. The smaller specimen is 5.3 mm in diameter and 3.6 mm in height. Stalk diameter varies from 1.0 mm at the short branch joining the small specimen to the convoluted stalk which is mostly ca 1.8 mm thick. The connection of the convoluted part of the stalk to the thicker upright stalk part was not available for assessment. Surfaces of the small body are covered by a villous plush of long pinular pentactins, but there are no special prostalia present. The lower convoluted stalk surfaces appear devoid of any visible surface spicules, but spicule preparations of this apparently "barren" stalk still show that typical stalk spicules are present. Thus, spicules obtained from stalks may derive from other locations on the specimen and should be considered as possibly from other original sources. Surfaces of the upper straight stalk and the terminal larger body are known only from fresh seawater-wet lab photos; they are covered by a thick spiny layer of brown tissue (Fig. 16C). Colour of the body in life is translucent white; when preserved in ethanol it is pale brown.

Skeleton. Choanosomal skeleton of the body is a network of diactins and hexactins. There is no evidence of fusion between any spicules within the body. Spicule fusion is restricted to the choanosomal diactins of the hollow stalks where the diactins are joined by fusion at spot contacts and by relatively long synapticula forming ladders. Microscleres are scattered evenly throughout the choanosome. Ectosomal skeleton of the dermal and atrial sides of the body consists of tightly packed pinular pentactins; no pinular hexactins are present. These are supported on, respectively, hypodermal and hypoatrial pentactins, which are never raised above the surfaces. Microscleres are present as in the choanosome.

Spicules. Megascleres (Fig. 17; Table 9) are hypodermal and hypoatrial pentactins, choanosomal hexactins and diactins, and pinular pentactins. Hypodermal pentactins of the body (Fig. 17A) are regular and smooth except for spined ray ends. The proximal rays are longer, averaging 1.26 × the length of tangential rays. Hypoatrial pentactins of the body (Fig. 17B) are also regular and smooth except for spined areas on both tangential and proximal ray ends. The proximal ray is longer, averaging 1.41 × the length of tangential rays. Hypodermal pentactins of the stalk (not figured) are regular in shape but significantly smaller than those of the body. Choanosomal hexactins (Fig. 17C) are restricted to the body; rays are smooth and spines are present only on ray ends. Macrospines are never found in the central part of these spicules. Choanosomal diactins (Fig. 17D) are straight or slightly curved and are smooth except for the ends; they have small but detectable central swellings. Dermal pinular pentactins of the body (Fig. 17E) have narrow pinular rays topped with a short, blunt apical spine. Their basal rays are entirely spined and end in abruptly rounded tips. Atrial pinular pentactins of the body (Fig. 17F) have narrow pinular rays like the dermal pinules, but with a longer pinular ray (on average 1.25 ×); however, presence of an apical spine was not determined since all of these examined in SEM had broken tips. Basal rays are like those of the dermal pinules. Stalk pinular pentactins (not figured) are morphologically similar to the dermal body pentactins.

Microscleres (Fig. 17; Table 9) are thick-rayed discohexactins and rare hemidiscohexasters and thin-rayed stellate discohexasters. Discohexactins (Fig. 17G) are the most abundant microscleres; they have rays ornamented with large, reclined spines and a terminal disc with 5–8 marginal teeth. Rare hemidiscohexasters (Fig. 17H) are

similar to the discohexactins. Thin-rayed stellate discohexasters (Fig. 17I) have long, smooth primary rays supporting a narrow shorter brush of 3–9 straight, rough, terminal rays ending in small discs.

Etymology. Named for the lower, convoluted stalk part, which branches into many attachment points (*ramosus*, branching; Latin).

Remarks. The morphological character of all microscleres being discoid, places this species in the subgenus *Caulophacus* (*Caulophacus*). In comparing it to the 22 recognised species of this subgenus (Table 7), it is apparent that there are no forms known with all pinules, both dermal and atrial, as exclusively pentactins. It is very like the previous described new species, *C.* (*Caulophacus*) *serpens* sp. nov. in its mainly, but not exclusively, pinular pentactins, and in the body form with a significant portion of the stalk convoluted, attached by many attachment sites and compound bearing several bodies. The two differ, however, in pinule morphology and types of microscleres. Also, molecular data (MD, unpubl. results) suggest a closer relationship of this specimen to *C.* (*Caulophacus*) *arcticus*, *C.* (*Caulodiscus*) *valdiviae*, and *C.* (*Oxydiscus*) *weddelli* than to *C.* (*C.*) *serpens* sp. nov. Since it cannot be assigned to any of the former species on the basis of morphology, it is thus clear that the form described here represents the holotype of a new species named *Caulophacus* (*Caulophacus*) *ramosus* sp. nov.

Conclusions

ith the material described herein, the known diversity of rossellids from the surrounding waters of New Zealand has almost doubled, from previously known nine species in five genera to 17 species in eight genera, including six species and one genus new to science:

Bathydorus poculum Reiswig, Dohrmann & Kelly, sp. nov.
Caulophacus (*Caulodiscus*) *onychohexactinus* Tabachnick & Lévi, 2004
Caulophacus (*Caulophacus*) *discohexaster* Tabachnick & Lévi, 2004
Caulophacus (*Caulophacus*) *hadalis* Lévi, 1964
Caulophacus (*Caulophacus*) *ramosus* Reiswig, Dohrmann & Kelly, sp. nov.
Caulophacus (*Caulophacus*) *schulzei* Wilson, 1904
Caulophacus (*Caulophacus*) *serpens* Reiswig, Dohrmann & Kelly, sp. nov.
Crateromorpha (*Aulochone*) *cylindrica* (Schulze, 1886)
Crateromorpha (*Aulochone*) *haliprum* Tabachnick & Lévi, 2004
Crateromorpha (*Caledochone*) *caledoniensis* Tabachnick & Lévi in Tabachnick (2002)
Nubes poculiformis Reiswig, Dohrmann & Kelly, gen. nov., sp. nov.
Nubes tubulata Reiswig, Dohrmann & Kelly, gen. nov., sp. nov.
Rossella ijimai Dendy, 1924
Scyphidium australiense Tabachnick, Janussen & Menschenina, 2008
Scyphidium variospinosum Reiswig, Dohrmann & Kelly, sp. nov.

Figure 18. Dr Henry Michael Reiswig (8 July 1936–4 July 2020) of Saanichton, British Columbia, Canada **A** henry at work examining a dictyonal glass sponge. Image provided by Heidi Gartner, Invertebrate Collection Manager and Researcher at the Royal British Columbia Museum, with permission **B** henry and Dr Manuel Maldonado, Sponge Ecobiology and Biotechnology Group, Department of Marine Ecology, Centro de Estudios Avanzados de Blanes (CEAB), onboard the Canadian Coast Guard Ship Vector in the Strait of Georgia, Vancouver, using the ROV Ropos to work on the hexactinellid reef (October 2007) **C** Henry with Dr Kim Conway, the geologist who discovered the Canadian hexactinellid reef, ibid; **D** Henry demonstrating sponge taxonomy techniques in a workshop at the 10th World Sponge Conference, Galway, 25–30 June 2017. Images reproduced with permission.

Sympagella clavipinula Tabachnick & Lévi, 2004
Symplectella rowi Dendy, 1924

Descriptions of two further new rossellids (Lanuginellinae) from RV Sonne cruise SO254 could not be completed by HMR and will be reported elsewhere, together with numerous other hexactinellid specimens collected on that cruise.

Obituary

Dr Henry Michael Reiswig of Saanichton, British Columbia, Canada (born 8 July 1936 in St. Paul, Minnesota, USA), died on 4 July 2020 at the age of 83, in his garage laboratory, doing what he loved most: science (Fig. 18). Henry was a marine biologist and globally renowned expert on the glass sponges (Hexactinellida), contributing enormously to knowledge of sponges in general.

Henry began his career at the University of California, Berkeley and completed a PhD at Yale University, after which he served as Professor of Biology at McGill University and Redpath Museum, Montreal, from 1972, until he officially retired in 2001. Those who knew him well chuckled at his 'retirement': in 2020 he was still hard at work describing the glass sponge fauna of New Zealand with his Kiwi and German friends. After formal retirement, he took up 'post-retirement' offices at the University of Victoria and the Royal British Columbia Museum in Victoria, B.C., ever busier and juggling numerous projects with colleagues and students all over the world.

Henry leaves an enormous legacy: his beloved wife, Ann, who died in February 2019 and their three wonderful daughters, Jennifer, Penelope, and Amy; more than 100 publications including journal articles, book chapters, and conference presentations; several sponge species and a sponge-derived secondary metabolite named after him, and hundreds of research colleagues and students who loved and respected him.

Henry also leaves a huge legacy at the National Institute of Water and Atmospheric Research (NIWA), New Zealand. He first began his work on New Zealand glass sponges in the 1980s as a visiting scientist at NIWA. Dr Dennis P. Gordon, now emeritus at NIWA, and then editor of the NIWA Biodiversity Memoir series, encouraged Michelle's involvement and working with Henry, helping him make progress on this dauntingly huge project: to identify and name more than 329 glass sponges that had been collected by the original New Zealand Oceanographic Institute. With a sense of trepidation, Michelle began to work closely with Henry, ably assisted by the NIWA Invertebrate Collection manager, Sadie Mills. The current collection now includes more than 2000 glass sponges, most examined by Henry. Together we were able to get two major NIWA Biodiversity Memoirs, on the dictyonal and euplectellid glass sponges, over the line, and were in the process of describing the last two big groups, the Rossellidae and Amphidiscophora, when the shocking news arrived.

How do we go on? Well, continue in his name we do. Henry was utterly dedicated to his work and had a formidable intellect; for all his profound knowledge, he was also slightly 'weird' and wonderful, and there was nothing more fun than sitting with Henry, after a conference lecture, enjoying a cool beer in the sunshine. In the words of his official family obituary, he was, "a rascal, a scholar, a deeply moral man, and is profoundly and deeply missed."

Acknowledgements

Specimens were supplied by the NIWA Invertebrate Collection (NIC). We are also grateful to John Rosser MA LTCL for his assistance with suggestions for new species names and for advising on the correct form of the new taxon names. We gratefully acknowledge Brent Gowen, University of Victoria, Philip Lambert, Kelly Sendall, Heidi Gartner, and Moretta Frederick, Royal British Columbia Museum, for technical assistance. Collections were made onboard the new German RV Sonne (voyage SO254). Specimens and numerous deck images were provided by PJS. Underwater images and videos were carried out with the ROV KIEL 6000 from the GEOMAR Helmholtz Centre for Ocean Research, Kiel. We greatly acknowledge the crew and scientific party of RV Sonne cruise SO254, as well as the ROV Kiel 6000 team for their valuable support at sea. We also thank Sven Rohde, Tessa Clemens, and the entire benthic invertebrate team of the RV Sonne Cruise SO254 for their assistance in sample collection, processing, and cataloguing. Sample collection was carried out under the "Application for consent to conduct marine scientific research in areas under national jurisdiction of New Zealand (dated 7.6.2016)." PJS acknowledges funding by the Federal Ministry of Education and Research (BMBF) for the cruise SO254, grant 03G0254A, PORIBACNEWZ. GW acknowledges funding by LMU Munich's Institutional Strategy LMU excellent within the framework of the German Excellence Initiative. NIWA voyage participation was funded through MBIE SSIF 'Enhancing Collections' project. This work was made possible by financial support from the University of Victoria and the Royal British Columbia Museum to HMR. This research was funded by NIWA under Coasts and Oceans Research Programme 2 Marine Biological Resources: Discovery and definition of the marine biota of New Zealand (2017/2018 to 2020/2021a SCIs). We thank Dorte Janussen and an anonymous reviewer for suggestions to improve the manuscript.

References

Battershill CN, Bergquist PR, Cook SdC (2010) Phylum Porifera. In: Cook SdC (Ed.) New Zealand Coastal Marine Invertebrates 1. Canterbury University Press, Christchurch, 58–135. https://www.canterbury.ac.nz/engage/cup/catalogue/books/new-zealand-coastal-marine-invertebrates-volume-one.html

Buckeridge JS, Kelly M, Janussen D, Reiswig HM (2013) New Palaeogene sponges from the Red Bluff Tuff, Chatham Island, New Zealand. New Zealand Journal of Geology and Geophysics 56: 171–185. https://dx.doi.org/10.1080/00288306.2013.808235

Carter HJ (1872) On two new Sponges from the Antarctic Sea, and on a new species of *Tethya* from Shetland; together with observations on the reproduction of sponges commencing from zygosis of the sponge animal. Annals and Magazine of Natural History Series 4, 9: 409–435. https://doi.org/10.1080/00222937208696612

Dawson EW (1993) The Marine Fauna of New Zealand: Index to the Fauna: 2 Porifera. New Zealand Oceanographic Institute Memoir 100: 1–98.

Dendy A (1924) Porifera. Part I. Non-Antarctic sponges. Natural History Report. British Antarctic (Terra Nova) Expedition, 1910 (Zoology) 6: 269–392.

Dohrmann M (2016) *Symplectella rowi* (Porifera: Hexactinellida: Lyssacinosida) is a rossellid, not a euplectellid. Journal of the Marine Biological Association of the United Kingdom 96: 291–295. https://dx.doi.org/10.1017/S0025315414001805

Dohrmann M, Janussen D, Reitner J, Collins AG, Wörheide G (2008) Phylogeny and evolution of glass sponges (Porifera, Hexactinellida). Systematic Biology 57: 388–405. https://dx.doi.org/10.1080/10635150802161088

Dohrmann M, Kelley C, Kelly M, Pisera A, Hooper JNA, Reiswig HM (2017) An integrative systematic framework helps to reconstruct skeletal evolution of glass sponges (Porifera, Hexactinellida). Frontiers in Zoology 14: e18. https://doi.org/10.1186/s12983-017-0191-3

Grant RE (1836) Animal Kingdom. In: Todd RB (Ed.) The Cyclopaedia of Anatomy and Physiology. Volume 1. Sherwood, Gilbert, and Piper, London, 107–118. https://doi.org/10.5962/bhl.title.106668

Gray JE (1870) Notes on anchoring sponges (in a letter to Mr. Moore). Annals and Magazine of Natural History Series 4, 6: 309–312. https://doi.org/10.1080/00222937008696253

Gray JE (1872) Notes on the classification of the sponges. Annals and Magazine of Natural History Series 4, 9: 442–461. https://doi.org/10.1080/00222937208696616

Hinde GJ, Holmes WM (1892) On the sponge-remains in the Lower Tertiary Strata near Oamaru, Otago, New Zealand. Journal of the Linnean Society. Zoology 24: 177–262. https://doi.org/10.1111/j.1096-3642.1892.tb02480.x

Ijima I (1898) The genera and species of Rossellidae. Annotationes Zoologicae Japonenses 2: 41–55. https://www.biodiversitylibrary.org/item/151945-page/5/mode/1up

Janussen D, Tabachnick KR, Tendal OS (2004) Deep-sea Hexactinellida (Porifera) of the Weddell Sea. Deep-Sea Research Part II 51: 1857–1882. https://dx.doi.org/10.1016/j.dsr2.2004.07.018

Jones EG, Morrison MA, Davey N, Mills S, Pallentin A, George S, Kelly M, Tuck I (2018) Biogenic habitats on New Zealand's continental shelf. Part II: National field survey and analysis. New Zealand Aquatic Environment and Biodiversity Report No. 202.

Kahn AS, Geller JB, Reiswig HM, Smith Jr KL (2013) *Bathydorus laniger* and *Docosaccus maculatus* (Lyssacinosida; Hexactinellida): Two new species of glass sponge from the abyssal eastern North Pacific Ocean. Zootaxa 3646: 386–400. https://doi.org/10.11646/zootaxa.3646.4.4

Kelly M (2016) Window on the past. In: Armitage D (Ed.) True Tales of Great Barrier Island. Great Barrier Island History Research Group Inc., Whangarei, New Zealand.

Kelly M, Buckeridge JS (2005) An early Paleogene sponge fauna, Chatham Island, New Zealand. New Zealand Journal of Marine and Freshwater Research 39: 899–914. https://doi.org/10.1080/00288330.2005.9517361

Kelly M, Edwards AR, Wilkinson MR, Alvarez B, Cook SdC, Bergquist PR, Buckeridge JS, Campbell H, Reiswig HM, Valentine C, Vacelet J (2009) Phylum Porifera. Sponges. In: Gordon DP (Ed.) New Zealand Inventory of Biodiversity Volume 1. Kingdom Animalia: Radiata, Lophotrochozoa, and Deuterostomia. Canterbury University Press, Christchurch, 23–46.

Kelly M, Amirapu S, Mills S, Page M, Reiswig H (2015) Kermadec Islands sponge biodiversity: A review and description of a new species, *Suberea meandrina* sp. nov. (Demospongiae, Verongiida, Aplysinellidae). Bulletin of the Auckland Museum 20: 311–324. https://www.

aucklandmuseum.com/getmedia/e3b64a6c-f46e-4e58-9296-e3ae72a871b4/bulletin-vol20-kermadec-biodiscovery-expedition-12-kelly-etal

Kirkpatrick R (1907) Porifera Hexactinellida. National Antarctic Expedition (S.S. 'Discovery') 1901–1904. Natural History: 1–25. http://www.marbef.org/data/aphia.php?p=sourcedetails&id=7728

Koltun VM (1967) Glass, or hexactinellid sponges of the Northern and far-Eastern seas of the USSR (Class Hyalospongiae). [In Russian]. Opredeliteli po faune SSR, izdavaemye Zoologicheskim muzeem Akademii nauk 94: 1–124.

Lendenfeld R von (1915) Reports on the scientific results of the expedition to the eastern tropical Pacific, in charge of Alexander Agassiz, by the U.S. Fish Commission Steamer 'Albatros', from October 1904 to March 1905, Lieut. Commander L.M. Garrett, U.S.N.M. commanding, and of other expeditions of the 'Albatros', 1891–1899. XXIX. The sponges. 3 Hexactinellida. Memoirs of the Museum of Comparative Zoology of Harvard College 42: 1–397.

Lee STM, Kelly M, Langlois TJ, Costello MJ (2015) Baseline seabed habitat and biotope mapping for a proposed Marine Reserve. PeerJ 3: e1446. https://doi.org/10.7717/peerj.1446

Lévi C (1964) Spongiaires des zones bathyale, abyssale et hadale. Galathea Report. Scientific Results of The Danish Deep-Sea Expedition Round the World, 1950–52, 7: 63–112.

Okada Y (1932) Report on the hexactinellid sponges collected by the United States Fisheries steamer 'Albatros' in the northwestern Pacific during the summer of 1906. Proceedings of the United States National Museum 81: 1–118. https://doi.org/10.5479/si.00963801.81-2935.1

Reiswig HM, Kelly M (2011) The Marine Fauna of New Zealand: Hexastophoran glass sponges of New Zealand (Porifera: Hexactinellida: Hexasterophora): Orders Hexactinosida, Aulocalycoida and Lychniscosida. NIWA Biodiversity Memoirs 124: 1–176. https://docs.niwa.co.nz/library/public/Memoir124_TheMarineFaunaofNewZealand_HexastophoranGlasssponges.pdf

Reiswig HM, Kelly M (2018) The marine fauna of New Zealand. Euplectellid glass sponges (Hexactinellida, Lyssacinosida, Euplectellidae). NIWA Biodiversity Memoirs 130: 1–170. https://docs.niwa.co.nz/library/public/Memoir130_TheMarineFaunaofNewZealand_Euplectellidsponges-2018.pdf

Schmidt O (1870) Grundzüge einer Spongien-Fauna des atlantischen Gebietes. Wilhelm Engelmann, Leipzig), 88 pp.

Schulze FE (1885) The Hexactinellida. In: Tizard TH, Moseley HM, Buchanan JY, Murray J (Eds) Report on the Scientific Results of the Voyage of H.M.S. 'Challenger', 1873–1876. Narrative 1(1): 437–451.

Schulze FE (1886) Über den Bau und das System der Hexactinelliden. Abhandlungen der Königlichen Akademie der Wissenschaften zu Berlin (Physikalisch-Mathematische Classe) 1886: 1–97. https://play.google.com/books/reader?id=R0vPAAAAMAAJ&hl=de&pg=GBS.PP1

Schulze FE (1899) Amerikanische Hexactinelliden nach dem Materiale der Albatross- Expedition. G. Fischer, Jena, 129 pp. https://doi.org/10.5962/bhl.title.85189

Schulze FE (1900) Hexactinelliden des Indischen Oceanes. III. Theil. Abhandlungen der Preussischen Akademie der Wissenschaften Berlin 1900: 1–46.

Schupp PJ, Rohde S, Versluis D, Petersen L-E, Clemens T, Conrad KP, Mills S, Kelly M (2017) Section 7.14. Investigations on the biodiversity of benthic sponge and inverte-

brate communities and their associated microbiome. In: Simon M (Ed.) Functional diversity of bacterial communities and the metabolome in the water column, sediment and in sponges in the southwest Pacific around New Zealand. RV SONNE SO254 Cruise Report, 57–59. https://www.portal-forschungsschiffe.de/lw_resource/datapool/_items/item_337/03g0254a_20170427_fahrtbericht.pdf

Tabachnick KR (1991) Hexactinellid sponges from the Japanese Sea with the description of a new species of *Scyphidium*. Zoologichesky Journal 70: 129–131.

Tabachnick KR (2002) Family Rossellidae Schulze, 1885. In: Hooper JNA, van Soest RWM (Eds) Systema Porifera: A Guide to the Classification of Sponges, Plenum, New York, 1441–1505. https://doi.org/10.1007/978-1-4615-0747-5_148

Tabachnick KR, Lévi C (2004) Lyssacinosida du Pacifique sud-ouest (Porifera: Hexactinellida). In: Marshall B, Richer de Forges B (Eds) Tropical Deep-Sea Benthos. Vol 23. Mémoires du Muséum national d'Histoire naturelle 191: 11–71.

Tabachnick KR, Janussen D, Menschenina LL (2008) New Australian Hexactinellida (Porifera) with a revision of *Euplectella aspergillum*. Zootaxa 1866: 7–68. https://doi.org/10.11646/zootaxa.1866.1.3

Tabachnick KR, Menshenina LL (2013) New data on glass sponges (Porifera, Hexactinellida) of the northern Mid-Atlantic Ridge. Part 2. Aphrocallistidae, Euretidae, Euplectellidae and Rossellidae (with descriptions of two new species of *Sympagella*). Marine Biology Research 9: 469–487. https://dx.doi.org/10.1080/17451000.2012.749996

Topsent E (1901) Spongiaires. Résultats du voyage du S.Y. 'Belgica'en 1897–99 sous le commandement de A. de Gerlache de Gomery. Expédition antarctique belge. Zoologie 4: 1–54. https://www.biodiversitylibrary.org/item/18689-page/5/mode/1up

Topsent E (1927) Diagnoses d'Éponges nouvelles recueillies par le Prince Albert ler de Monaco. Bulletin de l'Institut océanographique Monaco 502: 1–19.

van Soest RWM, Boury-Esnault N, Hooper JNA, Rützler K, de Voogd NJ, Alvarez B, Hajdu E, Pisera AB, Manconi R, Schönberg C, Klautau M, Kelly M, Vacelet J, Dohrmann M, Díaz M-C, Cárdenas P, Carballo JL, Ríos P, Downey R, Morrow CC (2021) World Porifera Database. http://www.marinespecies.org/porifera

Von Rad U (1984) Outline of SONNE Cruise SO-17 on the Chatham Rise Phosphorite Deposits East of New Zealand. In: Von Rad U, Kudrass H-R (Eds) Geologisches Jahrbuch, Reihe D, Heft 65. Bundesanstalt für Geowissenschaften und Rohstoffe und den geologischen Landesämtern in der Bundesrepublik Deutschland, Hannover, 5–23. https://core.ac.uk/download/pdf/11774455.pdf

Wilson HV (1904) Reports on an exploration off the west coasts of Mexico, Cental and South America, and off the Galapagos Islands, in charge of Alexander Agassiz, by the U.S. Fish Commission Steamer *Albatross*, during 1891, Lieut. Commander Z.L. Tanner, U.S.N. commanding. XXX. The sponges. Memoirs of the Museum of Comparative Zoology at Harvard College 30: 1–164. https://www.biodiversitylibrary.org/page/28870460-page/8/mode/1up

Zittel KA (1877) Studien über fossile Spongien. I. Hexactinellidae. Abhandlungen der Königlich Bayerischen Akademie der Wissenschaften, Mathematisch-Physikalische Klasse 13: 1–63. https://publikationen.badw.de/en/003796863

ZooKeys 1060: 85–92 (2021)
doi: 10.3897/zookeys.1060.71934
https://zookeys.pensoft.net

RESEARCH ARTICLE

A peer-reviewed open-access journal
ZooKeys
Launched to accelerate biodiversity research

Bombyciella linzhiensis, a new species from southern Xizang, China (Lepidoptera, Noctuidae, Noctuinae)

Enyong Chen[1], Zhaohui Pan[1], Anton V. Volynkin[2], Aidas Saldaitis[3], Balazs Benedek[4]

1 *Key Laboratory of Forest Ecology in Tibet Plateau (Institute of Plateau Ecology, Tibet Agricultural and Animal Husbandry University), Ministry of Education, Linzhi 860000, China* **2** *Altai State University, Lenina Avenue, 61, RF-656049, Barnaul, Russia* **3** *Nature Research Centre, Akademijos str., 2, LT-08412, Vilnius-21, Lithuania* **4** *H-2045 Törökbálint, Árpád u. 53, Hungary*

Corresponding authors: Zhaohui Pan (panzhaohui2005@163.com), Anton V. Volynkin (monstruncusarctia@gmail.com)

Academic editor: Alberto Zilli | Received 21 July 2021 | Accepted 4 September 2021 | Published 17 September 2021

http://zoobank.org/F5FDB11A-4FF0-482B-8032-E1C7F061D1B9

Citation: Chen E, Pan Z, Volynkin AV, Saldaitis A, Benedek B (2021) *Bombyciella linzhiensis*, a new species from southern Xizang, China (Lepidoptera, Noctuidae, Noctuinae). ZooKeys 1060: 85–92. https://doi.org/10.3897/zookeys.1060.71934

Abstract

A new species of the genus *Bombyciella* Draudt, 1950, *Bombyciella linzhiensis* **sp. nov.**, is described from the Linzhi (Nyingchi) Prefecture in southern Xizang (China), following a diagnostic comparison with *B. talpa* Draudt, 1950 and *B. antra* Saldaitis, Benedek, Behounek & Stüning, 2014. The adults and the male genitalia of the new and related species are illustrated.

Keywords

Male genitalia, morphology, Owlet moth, taxonomy, Xylenina, Xylenini

Introduction

Bombyciella Draudt, 1950 is a noctuid genus distributed in mountain areas in southwestern and northern China. The genus is closely related to the Holarctic *Brachylomia* Hampson, 1906 (Saldaitis et al. 2014) and belongs to the subtribe Xylenina of the tribe Xylenini of the subfamily Noctuinae (Lafontaine and Schmidt 2010; Zahiri et al. 2011). The genus has recently been revised by Saldaitis et al. (2014) and currently comprises two valid species. The male genitalia structures of *Bombyciella* and *Brachylomia* are very similar and display no distinctive apomorphic features. Therefore,

it is possible that these taxa represent one genus, an issue that can be resolved in the future by using molecular methods through a multi-gene phylogenetic analysis covering these and other related genera.

During an entomological survey in the southern Xizang Province of China, a long series of unusual dark-coloured *Bombyciella* specimens was collected by the senior and the second authors. After comparing the male genitalia structures of these specimens with the other two species in the genus, they proved to be diagnostic and the specimens are therefore considered to represent a new species which is here described.

Materials and methods

Abbreviations for private and institutional collections used herein are as follows:

AFM collection of Alessandro Floriani (Milan, Italy);
TAAHU Tibet Agricultural and Animal Husbandry University (Linzhi, China);
WIGJ World Insect Gallery (Joniškis, Lithuania);
ZFMK Zoological Research Museum Alexander Koenig (Zoologisches Forschungsmuseum Alexander Koenig, Bonn, Germany);
ZSM Bavarian State Collection of Zoology (Zoologische Staatssammlung München, Munich, Germany).

Other abbreviations used in the illustrations are:

HT holotype;
LT lectotype;
PT paratype.

The male genitalia terminology follows Fibiger (1997) and Kononenko (2010).

Results

Noctuidae Latreille, 1809
Noctuinae Latreille, 1809
Xylenini Guenée, 1837
Xylenina Guenée, 1837

***Bombyciella linzhiensis* sp. nov.**
http://zoobank.org/08CFBD59-8B98-40C5-91B3-B0EAF8E96C2B
Figs 1–5, 9, 10

Type material. *Holotype*: male (Fig. 1), "Sejila Mountain, Linzhi, Tibet, China, 29°35'36"N, 94°36'4"E, 4160 m a.s.l., 8.IX.2020, Enyong Chen [leg.]" (in Chinese),

unique number: STS-31844, gen. prep. in glycerol by Enyong Chen (coll. TAAHU). ***Paratypes*:** 31 males (Figs 2–5), with the same data as in the holotype, unique numbers: STS-31032, STS-31044, STS-31045, STS-31046, STS-31047, STS-31048, STS-31049, STS-31050, STS-31051, STS-31052, STS-31101, STS-31102, STS-31127, STS-31129, STS-31131, STS-31133, STS-31136, STS-31137, STS-31140, STS-31840, STS-31845, STS-31851, STS-33192, STS-33202, STS-33203, STS-33419, STS-33421, STS-33424, STS-33427, STS-33433, STS-33438, gen. prep. in glycerol by Enyong Chen; 6 males, "Sejila Mountain, Linzhi, Tibet, China, 29°37'2"N, 94°38'32"E, 4500 m a.s.l., 8.IX.2020, Zhaohui Pan [leg.]" (in Chinese), unique numbers: STS-29906, STS-29907, STS-29908, STS-31666, STS-31668, STS-31669, gen. preps. in glycerol by Enyong Chen (colls TAAHU and WIGJ).

Diagnosis. The new species (Figs 1–5) is externally similar to the type species of the genus *Bombyciella*, namely *Bombyciella talpa* Draudt, 1950 (Figs 7, 8), but it can be distinguished by its darker body colouration, the more tapered forewing apex, the more indistinct transverse lines of the forewing and the dark grey hindwing having a distinct discal spot, whereas in *B. talpa* the hindwing is pale brown and the discal spot is absent or faint. *Bombyciella linzhiensis* sp. nov. differs clearly from another congener, *B. antra* Saldaitis, Benedek, Behounek & Stüning, 2014 (Fig. 6), by its significantly smaller size (the forewing length is 26 mm vs 39 mm in *B. antra*), the blackish brown head and thorax (bluish grey in *B. antra*), the blackish brown abdomen (pale brown in *B. antra*), the straight costal margin (slightly convex in *B. antra*), the more convex outer margin of the forewing, the blackish brown or olive brown forewing colouration (it is bluish grey in *B. antra*), and the dark grey hindwing with a distinct discal spot (whereas in *B. antra* the hindwing is pale brown with a grey suffusion and lacks a discal spot but has a diffuse thin transverse line). The male genital capsule of *B. linzhiensis* sp. nov. (Figs 9, 10) is reminiscent of that of *B. talpa* (Fig. 11) but differs by the wider uncus, the considerably smaller, tubercle-like medioventral process of juxta, the more apically rounded valva, the downward pointing and evenly-wide clasper tapered only apically (it is subapically constricted with an upward pointing apex in *B. talpa*), and the thicker and longer costal process. Additionally, the peniculus of the new species is shorter than in *B. talpa* and the saccus is somewhat shorter and narrower. The aedeagus of *B. linzhiensis* sp. nov. is shorter (in relation to the tegumen-vinculum complex) and less sub-proximally curved than in *B. talpa*. The carina of the new species bears a bunch of spines directed ventrally whereas that of *B. talpa* bears a row of laterally directed spikes. The vesica of *B. linzhiensis* sp. nov. is broader than that of *B. talpa* and bears distally a cluster of more robust spike-like cornuti. Compared to that of *B. antra* (Fig. 12), the male genital capsule of *B. linzhiensis* sp. nov. has a more distally elongated and apically obtuse uncus (apically pointed in *B. antra*), a basally wider and less elongated valva having a straight dorsal margin and a well-developed costal process protruding beyond the ventral margin, whereas in *B. antra* the dorsal margin of valva is medially slightly convex and distally somewhat curved dorsally, and the costal process is reduced. The clasper of the new species is thicker and evenly down-curved whereas it is up-curved in *B. antra*. Additionally, the peniculus of the new species is shorter and narrower than that of *B. antra*, the juxta is

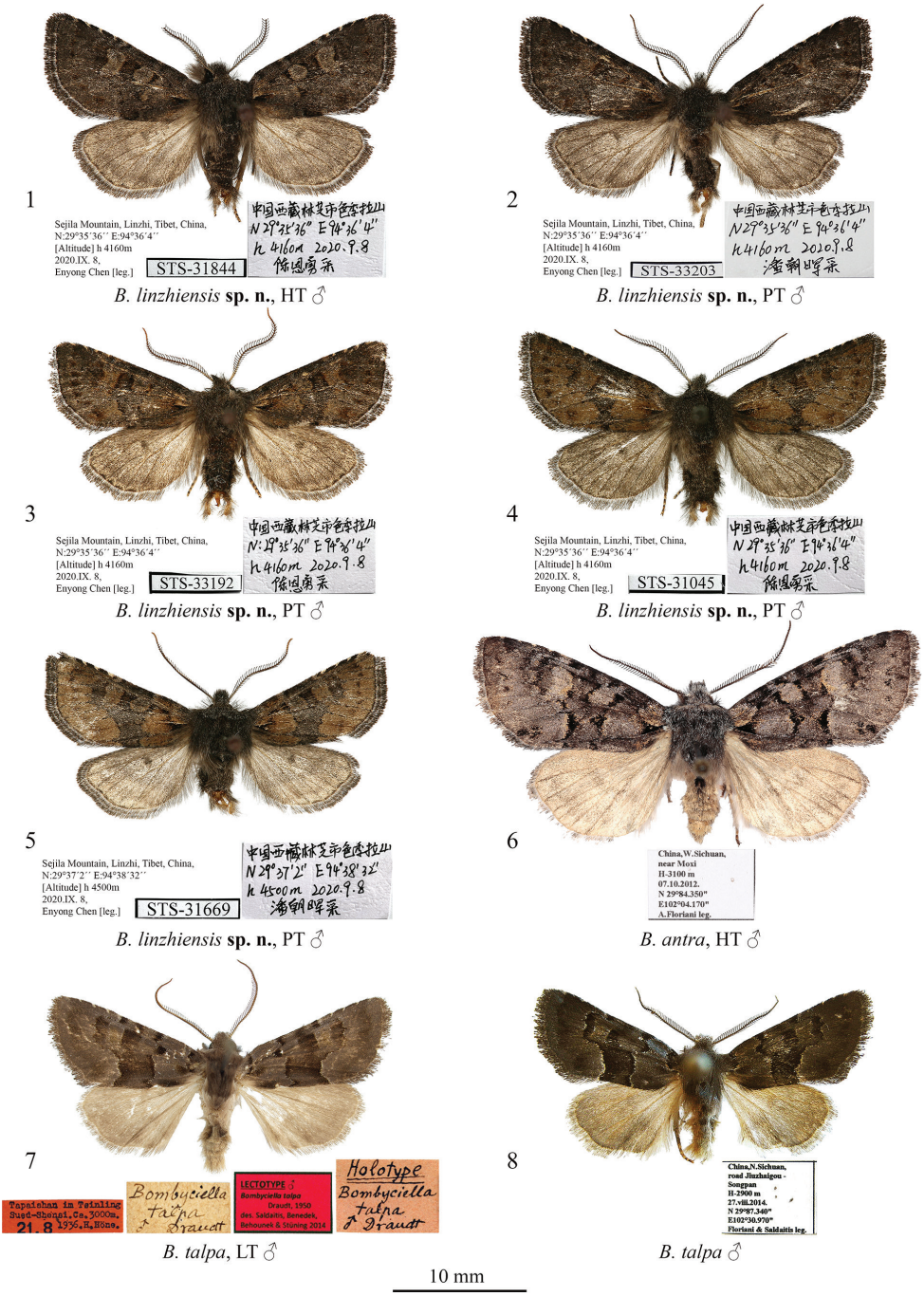

Figures 1–8. *Bombyciella* spp., adults. Depositories of the specimens **1–5** in TAAHU **6** in ZSM **7** in ZFMK (photo by D. Stüning) **8** in AFM.

9

***B. linzhiensis* sp. n., HT**
China, Xizang, Linzhi, gen. prep. by Enyong Chen

10

***B. linzhiensis* sp. n., PT**
China, Xizang, Linzhi, gen. prep. by Enyong Chen

11

***B. talpa*, LT**
China, Shaanxi, Taibai Mt., slide 2269-DS Stüning

12

***B. antra*, HT**
China, W Sichuan, near Moxi, slide BJ2160 Babics

Figures 9–12. *Bombyciella* spp., male genitalia. Depositories of the specimens dissected **9, 10** in TAAHU **11** in ZFMK (photo by D. Stüning) **12** in AFM.

markedly longer and the saccus is narrower and somewhat longer. In the aedeagus of *B. linzhiensis* sp. nov., the carina bears a bunch of spines whereas it is plate-like without spines in *B. antra*. The vesica of the new species is somewhat shorter and broader (in proportion to the aedeagus size) than in *B. antra* and bears a cluster of markedly shorter cornuti distally.

Description. Male. Forewing length 26–27 mm (holotype: 26 mm). Antenna shortly bipectinate. Head and thorax blackish grey with suffusion of pale grey scales. Forewing triangular with tapered apex and almost straight costa and convex termen. Forewing ground colour varies from blackish brown to olive brown. Subbasal dash short, black. Antemedial line irregularly sinuous, black, indistinct, oblique outwards posteriorly. Postmedial line indistinct, dentate on veins, loop-like curved anteriorly and oblique inwards posteriorly. In olive brown form, medial area intensely suffused with black scales. Orbicular stigma elliptical, from greyish- to olive brown. Reniform stigma wide, slightly dilated anteriorly, from greyish- to olive brown. Subterminal line evenly curved, parallel to termen, brown, interrupted into diffuse spots on veins. Terminal line blackish brown, thin. Costal margin intensely suffused with blackish scales, with three thin and short whitish subapical dashes. Cilia from dark grey to blackish grey. Hindwing dark grey with brown suffusion on veins, thin brown terminal line and comma-like, dark brownish grey discal spot. Hindwing cilia brownish grey. Abdomen blackish brown, with suffusion of pale grey scales along segment edges.

Male genitalia (Figs 9, 10). Tegumen short, with arcuate arms. Penicular lobe small, rounded. Vinculum ca 1.6 times longer than tegumen, with more or less U-shaped saccus. Valva elongated with almost parallel margins medially, distally tapered and apically rounded, with densely setose apex. Sacculus short (ca 1/3 of valva length) and broad (ca 4/5 of valva width). Clasper flattened, smoothly downward pointing, distally tapered and apically rounded. Costal process (= digitus sensu Forbes nec Pierce) elongated, blade-like, apically pointed, directed ventro-distally and protruding beyond the ventral edge of valva. Uncus arrowhead-shaped, dorso-ventrally flattened, apically obtuse, densely setose. Tuba analis narrow and membranous. Juxta pentagonal shield-like, with a small tubercle-like medio-ventral process. Aedeagus elongated and narrow (length to width ratio ca 7.5:1), somewhat dilated proximally and distally, with short (less than 1/5 of aedeagus length) and rounded coecum. Carina triangular plate-like, apically rounded, bearing bunch-like cluster of 6–8 ventrally directed, thin spikes of various lengths. Vesica relatively short (ca 1/2 of aedeagus length), dorsally projected, slightly medially broader than aedeagus, somewhat twisted subbasally and dilated distally with a stripe of few robust spine-like cornuti before the gonopore.

Female. Unknown.

Distribution. The new species is known only from Sejila Mountain in southern Xizang Province of China (Figs 13, 14).

Etymology. The specific epithet refers to the type locality located in the Linzhi (Nyingchi) prefecture of Xizang.

Figure 13. South of the collecting locality on Sejila Mountain, Linzhi, Tibet, China, 29°35'36"N, 94°36'4"E, 4160 m a.s.l., the type locality of *Bombyciella linzhiensis* (photo by Enyong Chen).

Figure 14. North of the collecting locality on Sejila Mountain, Linzhi, Tibet, China, 29°35'36"N, 94°36'4"E, 4160 m a.s.l., the type locality of *Bombyciella linzhiensis* (photo by Enyong Chen).

Acknowledgements

The work of Enyong Chen and Zhaohui Pan was supported by the Natural Science Foundation of Tibet Autonomous Region (Study on species diversity and protection of butterfly resources in Southeast Tibet), the Second Tibetan Plateau Scientific Expedition and Research Program (Grant No. 2019QZKK05010602), the National Natural

Science Foundation of China (Grant No. 31760631), and Tutor innovation project of Forestry Subject of Tibet agricultural and Animal Husbandry University (Species diversity and conservation of Geometridae (Lepidoptera) in southeastern Tibet). Anton Volynkin, Aidas Saldaitis and Balazs Benedek had no funding. We express our sincere thanks to National Forest Ecosystem Observation and Research Station of Nyingchi Tibet, United Key Laboratory of Tibet plateau ecological security, and South-East Tibetan plateau Station for integrated observation and research of alpine environment in Linzhi. We are also indebted to Dr Dieter Stüning (Bonn, Germany) for pictures of the holotype of *B. talpa* provided.

References

Fibiger M (1997) Noctuidae Europaeae. Vol. 3. Noctuinae III. Entomological Press, Sorø, 452 pp.

Draudt M (1950) Beiträge zur Kenntnis der Agrotiden-Fauna Chinas aus den Ausbeuten Dr. H. Höne's. Mitteilungen der Münchner Entomologischen Gesellschaft 40(1): 1–174. [in German]

Hampson GF (1906) Catalogue of the Lepidoptera Phalaenae in the British Museum. Vol. 6. Printed by order of the Trustees, London, 532 pp. [pls 96–107]

Kononenko VS (2010) Noctuidae Sibiricae. Vol. 2. Micronoctuidae, Noctuidae: Rivulinae – Agaristinae (Lepidoptera). Entomological Press, Sorø, 475 pp.

Lafontaine JD, Schmidt BC (2010) Annotated check list of the Noctuoidea (Insecta, Lepidoptera) of North America north of Mexico. ZooKeys 40: 1–239. https://doi.org/10.3897/zookeys.40.414

Saldaitis A, Benedek B, Behounek G, Stüning D (2014) A revision of the genus *Bombyciella* Draudt, 1950, with description of a new species and a new genus (Lepidoptera, Noctuidae: Xyleninae). Zootaxa 3893(4): 551–561. https://doi.org/10.11646/zootaxa.3893.4.4

Zahiri R, Kitching IJ, Lafontaine JD, Mutanen M, Kaila L, Holloway JD, Wahlberg N (2011) A new molecular phylogeny offers hope for a stable family level classification of the Noctuoidea (Lepidoptera). Zoologica Scripta 40(2): 158–173. https://doi.org/10.1111/j.1463-6409.2010.00459.x

ZooKeys 1060: 93–110 (2021)
doi: 10.3897/zookeys.1060.28809
https://zookeys.pensoft.net

RESEARCH ARTICLE

A peer-reviewed open-access journal
ZooKeys
Launched to accelerate biodiversity research

Rare specimen identification in an un-integrated taxonomy: implications of DNA sequences from a Taiwanese *Philine* (Mollusca, Philinidae)

Donald J. Colgan[1], Shane T. Ahyong[1,2], Karine Mardon[3], Ian M. Brereton[3]

1 *Australian Museum Research Institute, 1 William St., Sydney 2010 Australia* **2** *School of Biological, Earth & Environmental Sciences, University of New South Wales, Kensington, NSW 2052, Australia* **3** *Centre for Advanced Imaging/National Imaging Facility, University of Queensland, Brisbane 4072, Australia*

Corresponding author: Donald J. Colgan (don.colgan@austmus.gov.au)

Academic editor: Nathalie Yonow | Received 6 August 2018 | Accepted 24 August 2021 | Published 17 September 2021

http://zoobank.org/350F75C2-66E7-418F-8051-CD78EB3919B4

Citation: Colgan DJ, Ahyong ST, Mardon K, Brereton IM (2021) Rare specimen identification in an un-integrated taxonomy: implications of DNA sequences from a Taiwanese *Philine* (Mollusca, Philinidae). ZooKeys 1060: 93–110. https://doi.org/10.3897/zookeys.1060.28809

Abstract

Many species of the gastropod genus *Philine* have been named from northeastern Asia but scanty descriptions based predominantly on shells make it difficult to determine which are valid. This, plus the sporadic anatomical and genetic information available for many of these species has led to what may be described as an un-integrated taxonomy. In this situation, it is generally preferable to postpone dissection of rare and unusual specimens until relevant diagnostic characters can be established in broader studies. Micro-CT scanning and DNA sequencing were used to examine such a specimen collected recently from deep waters off northeastern Taiwan. Micro-CT examination of the morphology of the internal shell and gizzard plates suggested that, among named species, the sequenced specimen is most similar to *P. otukai*. It cannot, however, be definitively referred to *P. otukai* as that species lacks adequate anatomical description or known DNA sequences. Phylogenetic analyses of newly collected DNA sequences show the specimen to be most closely related to, but distinct from the northern Atlantic Ocean and Mediterranean species, *Philine quadripartita*. The sequences also confirm genetically that five or more species of *Philine* occur in northeast Asia, including at least three subject to considerable taxonomic uncertainty.

Keywords

Gizzard plates, 16S ribosomal RNA, micro-CT scanning, Scaphopoda

Introduction

Accurate delimitation of species of the highly speciose cephalaspidean genus *Philine* Ascanius, 1772 is hampered by the brief original descriptions of many of its named taxa. Many such descriptions were made using only the shell, which has limited diagnostic value, and often these have not been subsequently supplemented by studies of internal anatomy, including morphology of the diagnostically important gizzard plates, or DNA sequences.

The difficulty of delimitation is especially marked in northeastern Asia, as exemplified by the situation in Taiwan from which three named *Philine* species (*P. argentata* Gould, 1859; *P. vitrea* Gould, 1859, and *P. otukai* Habe, 1946) are currently recognised (Lee 1998; Wu 2004; Wu and Lee 2005). We have recently collected a specimen from deep waters off Taiwan that is not readily identifiable owing to the lack of an adequate taxonomic description of comparable species. A fourth species, *Philine kurodai* Habe, 1946, has been recorded in Taiwan but the relevant specimens were supposed to belong to *P. otukai* according to Lee (1998) and Wu (2004). Many other species of *Philine* have been named from nearby regions, and in total, 15 named recent species with medium to large shells have been recorded (Table 1) from the coasts of China, Korea, and Japan (Zhang 2008; Price et al. 2011; Chaban 2014; Chaban and Chernyshev 2014; Chaban et al. 2019; and references in these articles). The anatomical and genetic information available for most of these species is sporadic, resulting in a taxonomy that may be described as un-integrated, with a general lack of diagnostic characters suitable for species discrimination. In this situation, we consider it advisable to minimise destructive sampling of rare specimens until such diagnostic characters can be established from more frequently collected taxa.

We used non-destructive morphological analysis of the collected specimen and DNA sequencing of a small external tissue sample to make initial comparisons with named species. For morphological analysis, we used micro-CT scanning (Shepelenko et al. 2015) which is potentially very useful for studying specimens where dissection would be premature. We focussed on the shape and sculpture of the shell, which is internal in *Philine*, and the three gizzard plates which have been applied to morphological diagnoses of the genus (e.g., Price et al. 2011).

We determined sequences of 16S ribosomal RNA (16S rRNA), histone H3 (H3), and the D1 expansion region of 28S ribosomal RNA (D1 28S rRNA). We then performed phylogenetic analyses of the sequences, including sequences from previous DNA studies of the Philinidae (Krug et al. 2012; Ohnheiser and Malaquias 2013; Gonzales and Gosliner 2014; Oskars et al. 2015; Chaban et al. 2019). We were unable to sequence the cytochrome *c* oxidase subunit I bar-coding region, a difficulty also found by Krug et al. (2012), possibly explaining why there are relatively few GenBank accessions for this gene from *Philine*.

Table 1. *Philine* species from northeastern Asia with medium- or large-sized shells. Localities of identified type specimens are followed by (T). Information categories are abbreviated as: D, DNA sequence; G, gizzard plate morphology, O, other anatomical.

Species	Locality	Information	Status
P. acutangula Adams, 1862	Gulf of Lian-Tung, Hulu-Shan Bay, China [Gulf of Liadong, Hulushan Bay]	No figure or type description	Species inquirendum
P. argentata Gould, 1859	Hokkaido Bay, Japan (T)	G, O: Chaban (2014) D: Chaban et al. (2019)	Synonym of *P. orientalis* (Price et al. 2011); species status maintained by Chaban (2014)
P. coreanica Adams, 1855	Coreen archipelago on mud flats [Korea]	Sowerby (1855) fig. 166 (figured type?)	Species inquirendum: "*P. aperta*" fide Herdman (1906)
P. crenata Adams, 1862	Tsu-Shima, Korea Strait, 46 m		Species inquirendum: "*P. aperta*" fide Herdman (1906)
P. habei Valdés, 2008	Fiji, 17°05'S, 178°55'W, 654–656 m (T)	D: Oskars et al. (2015) G, O: Valdés (2008)	Accepted
P. japonica Lischke, 1872	Jedo (Tokyo Bay), Japan (T)	D: Chaban et al. (2019) O: Larvae: Hamatani (1961) and Tanaka (1958).	*P. orientalis* synonym (Price et al. 2011). Species status maintained by Chaban et al. (2019)
P. kinglipini Tchang, 1934	Bays of Tsangkou and Nukukou	G, O: Tchang (1934)	Accepted. No type designated.
P. kurodai Habe, 1946	Wakayama Prefecture, Japan (T)		Accepted by Chaban (2016)
P. miyadii Habe, 1946			Synonym of *P. scalpta* fide Habe (1950) (= *P. vitrea* (see below)
P. orientalis Adams, 1854	"Eastern seas" (T)	G, O: Price et al. (2011) D: Krug et al. (2012)	Accepted
P. otukai Habe, 1946	Penghu Islands, Taiwan (T)		Accepted
P. paucipapillata Price, Gosliner & Valdés, 2011	Kampote and Prek Romeas, Cambodia (T)	G, O: Price et al. (2011) D: Krug et al. (2012)	
P. scalpta A. Adams, 1862	Tsu-Shima and Korea Strait 50–80 m	D: Chaban et al. (2019)	Synonym of *P vitrea* (Higo et al. 1999). Species status maintained by Chaban and Chernyshev (2014).
P. striatella Tapparone-Canefri,1874	Yokohama, Japan (T)	O (radula): Tapparone-Canefri (1874)	Synonym of *P. japonica* fide Pilsbry (1895), or *P.orientalis* fide Price et al. (2011)
P. vitrea Gould, 1859	Hong Kong (T)		Accepted

Materials and methods

Material

AMS C.559479, off Dasi, Yilan County, north-east Taiwan, 24°54'N, 122°E, 5 xi 2015, coll. S. Ahyong, commercial bottom trawl, 300–400 m depth, fixed and stored in 80% ethanol. The specimen was collected together with other deep-water species including the crustaceans, *Bathynomus doederleini* Ortmann, 1894, *Homola orientalis* Henderson, 1888, and *Metanephrops thomsoni* (Bate, 1888).

Measurements

Digital callipers were used for external measurements, made after preservation. Measurements of the relative sizes of internal structures, such as gizzard plates, were deter-

mined from images using the beta 4.0.3 version of Scion Image (Scion Corporation, Frederick, MD, USA). Sizes of internal structures were estimated by multiplying the ratio of the relative lengths of the relevant structure and the longest shell axis on an image by the length of this axis determined by callipers on the actual specimen.

Micro-CT imaging

Micro-CT scanning was performed directly on the specimen after removal from ethanol storage with a Siemens Inveon micro-CT scanner operated at 80 KV energy, 250 μA intensity with 540 projections per 360° and 2200 ms exposure time. The sample was scanned at a nominal isotropic resolution of 27.8 μm. The data were reconstructed using a Feldkamp conebeam back-projection algorithm provided by an Inveon Acquisition Workstation from Siemens.

DNA methods and molecular phylogenetic analysis

DNA was extracted from a small amount of mantle tissue using the Bioline Isolate II Kit following the manufacturer's instructions. The final centrifugation was performed with 100 μL of the kit's elution buffer. PCR amplifications followed the methods of Colgan and Da Costa (2009) using the following primers:

16S rRNA:	16Sar CGCCTGTTTATCAAAAACAT (Palumbi 1996), 16sbr CCGGTCTGAACTCAGATCACGT (Palumbi 1996)
28S rRNA:	28S D1F ACCCSCTGAAYTTAAGCAT (McArthur and Koop 1999) 28S D1R AACTCTCTCMTTCARAGTTC (Colgan et al. 2003)
H3:	H3NF ATGGCTCGTACCAAGCAGAC (Colgan et al. 2000)
H3NR	ATRTCCTTGGGCATGATTGTTAC (Colgan et al. 2000)

PCR products were checked by electrophoresis on 2% agarose gels run with TAE buffer, including Gel Red (Biotium Inc., Fremont, CA) and visualised with UV-fluorescence. Single-banded products of the appropriate size were purified by Exo-SAP-IT™ (Thermo-Fisher Scientific) and sequenced commercially at Macrogen (Seoul, Korea) with the primers used in the original amplification.

GenBank Accession Numbers for new sequences: MH340050 (D1 28S rRNA), MH340051 (16S rRNA), MH340052 (histone H3).

Phylogenetic analyses were conducted using all *Philine* sequences for each gene available on 20 September 2020. Sequences from *Philinopsis* Pease, 1860 were used to root analyses for the 16S rRNA dataset. The sets of sequences for each gene were aligned with ClustalW (Thompson et al. 1997).

Maximum likelihood analyses (ML) analyses were conducted at the CIPRES Science Gateway (https://www.phylo.org/portal2/home.action, Miller et al. 2010) using the RAxML Blackbox (Stamatakis et al. 2008), assuming no invariable sites, using empirical base frequencies and assessing node support by rapid bootstrap

with the number of replicates determined by the software, according to the MRE-based bootstopping criterion (Pattengale et al. 2010). Analyses of the complete 16S rRNA data were also run on a filtered alignment for which GBlocks (Castresana 2000) was used to remove less well supported sections, allowing gap positions within the final blocks and less strict flanking positions. Analyses were also conducted for a reduced set of 16S rRNA sequences comprising members of a strongly supported clade of taxa allied with *P. aperta*. MEGA 7.0 (Kumar et al. 2016) was used to conduct other analyses including calculation of genetic distances and minimum evolution phylogenetic trees.

Results

Morphology

Animal, external: (Fig. 1) **Colour.** headshield creamy yellow, parapodia paler, foot off-white. Headshield: anterior three-fifths transversely rugose; central anterior to posterior furrow more marked posteriorly; dividing into two short processes posteriorly, overlapping posterior shield very slightly; tapering posteriorly in dorsal view (length 15.6 mm, width at widest 12.2 mm, width at shell 9.00 mm). Parapodial lobes broad, not remarkably thickened. Foot extending slightly posterior to shell. Posterior shield mostly occupied by a thinly covered internal shell. Posterior shield appearing grey-black due to pigmentation of internal organs, maintained after fixation. **Dimensions:** Animal 35.3 mm long (buccal mass everted) and 21.5 mm wide when newly collected (measured from photograph). After fixation: length from front of headshield to tail of foot 34 mm, width 19.8 mm and maximum height 9.3 mm.

Shell: (Fig. 2) fragile, internal, height of body whorl, measured vertically from the posterior end of the aperture to the tip of the (damaged) elevated anterior outer lip: 18.4 mm, width of body whorl 14.2 mm, measured by callipers; spire involute, aperture extremely wide and rounded below, upper margin rising above shell vertex, columellar lip notably reflected, albeit slightly, (Fig. 2A). Frequent irregularly-spaced curved growth lines and spiral ribs, covering most of body whorl (except for bottom quarter). Radial and spiral ribs sometimes intersecting to form weak, irregularly cancellate sculpture (Suppl. material 2: Fig. S1).

Gizzard plates: (Figs 2B–D, 3). One pair of similar plates (12.5 mm in longest dimension) and notably smaller, unpaired plate (9.0 mm in longest dimension), all with outer surface (that facing towards the animal's surface) slightly dimpled. Plates spindle-shaped, each with two large, circular pores in central area markedly depressed inwards. Smallest plate with spindle arms aligned axially; axes of spindle arms of larger plates form an obtuse angle (~ 135°). Spindle arms unequal in length (measured from the midpoint of the line between the two pores in each plate). Ratio of arm lengths: 1.15 for the small plate; 1.18 for paired plates. Posterior arm of all plates more slender than anterior arm.

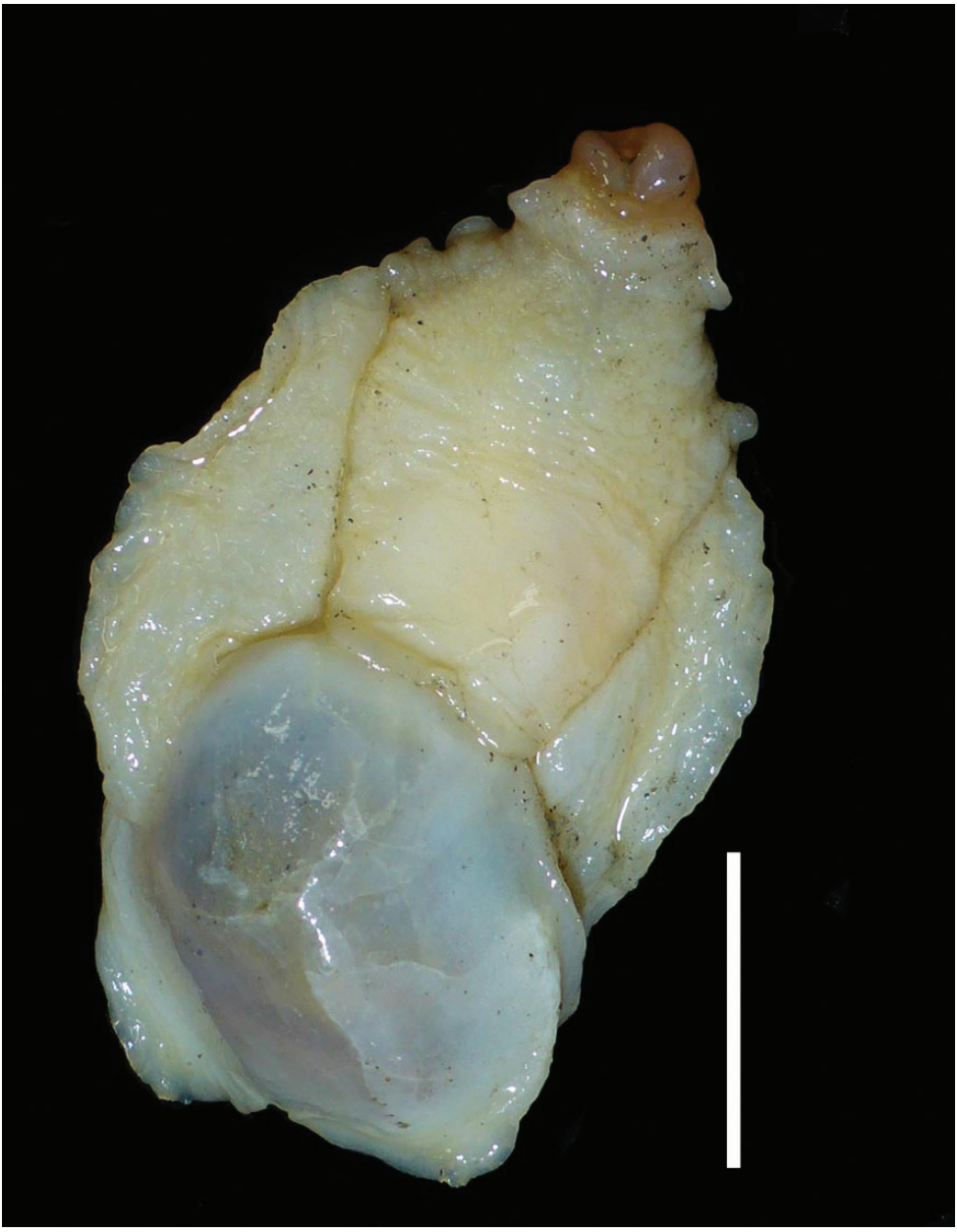

Figure 1. C.559479, freshly caught animal (photograph Shane Ahyong). Scale bar: 10 mm.

Gut contents

The prey of *Philine* are predominantly bivalves (Morton and Chiu 1990) but gastropods are also taken. For example, *P. orientalis* is known to prey on at least 11 species of small

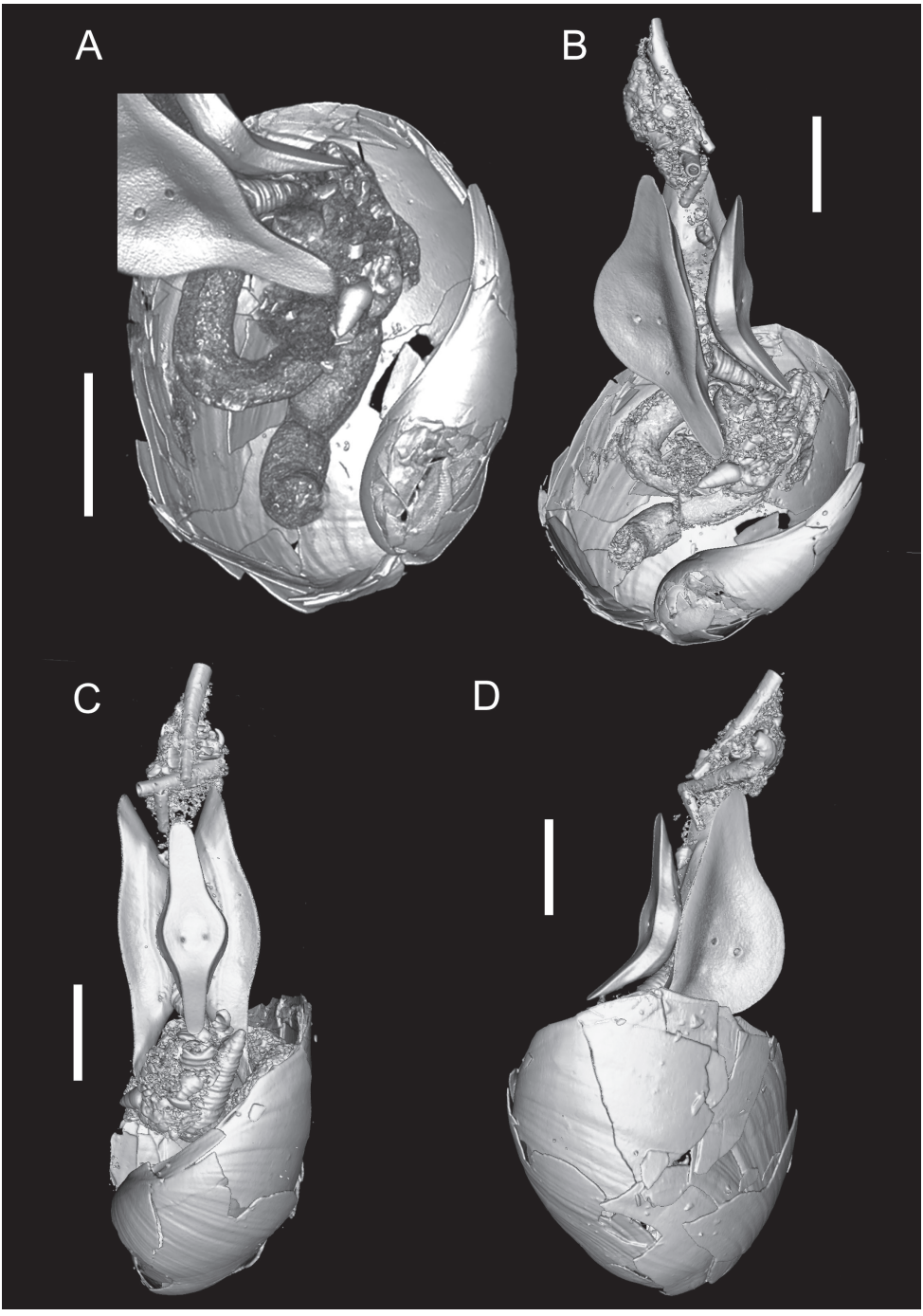

Figure 2. Micro-CT reconstruction images of C.559479 **A** ventral view of the shell **B–D** three perspectives from the reconstruction. Scale bar: 5 mm (**A–D**).

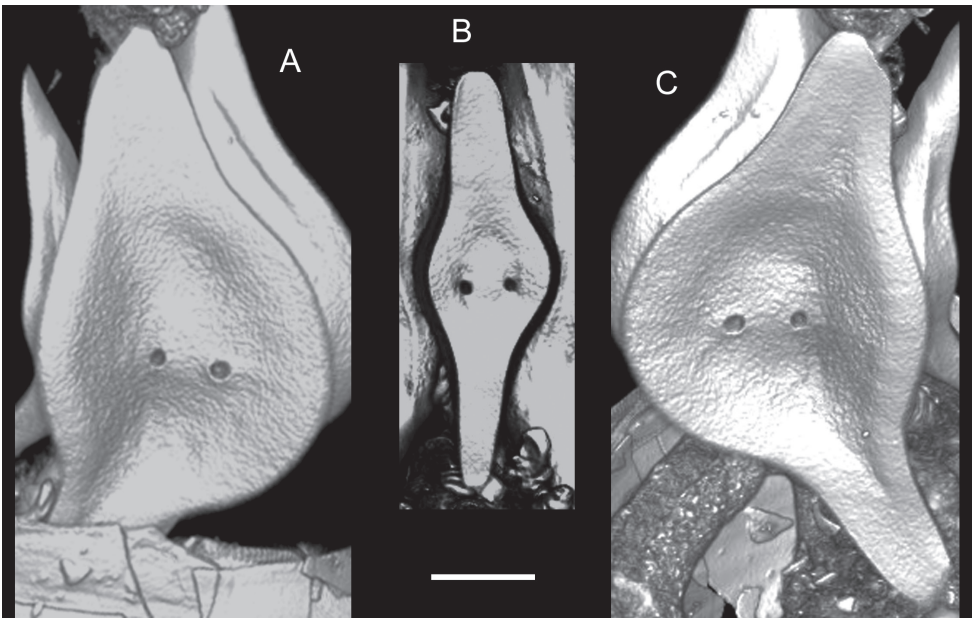

Figure 3. C.559479, outer surface of gizzard plates from the micro-CT reconstruction **A** paired plate, left **B** unpaired plate **C** paired plate, right. Scale bar: 2 mm (**A–C**).

snails (Taylor 1982). The diet of C.559479 included multiple species of micro-gastropods (at least three are observable in Fig. 2B, including the sparsely pustulated micro-gastropod between the gizzard plates) and scaphopods (at the mouth in Fig. 2C and in the Suppl. material 1). We are not aware of previous reports of Philinidae feeding on this class of molluscs.

DNA

The 16S rRNA alignment comprised 444 positions of which 38 were variable but not parsimony-informative and 169 which were parsimony-informative. The optimal tree found in the ML analysis of the alignment had a *ln* likelihood of –3619.22 and there were 650 bootstrap replicates conducted under the MRE criterion. After Gblocks filtering, there were 370 positions in the alignment, of which 30 were variable but not parsimony-informative and 133 were parsimony-informative. ML analysis of these data had a *ln* likelihood of –2831.37 and there were 800 bootstrap replicates conducted under the MRE criterion. The optimal tree found in the ML analysis of the reduced 16S rRNA dataset (Fig. 4) had a *ln* likelihood of –1787.45 and 500 bootstrap replicates were conducted under the MRE criterion. In the optimal trees based on the Gblocks-filtered data and the reduced dataset, the sequence of C.559479 was resolved but without bootstrap support as the sister group of a clade of three sequences apparently, as discussed below, from *Philine quadripartita* Ascanius, 1772. The sequence of C.559479 and the three *P. quadripartita* sequences formed two separate basal lineages

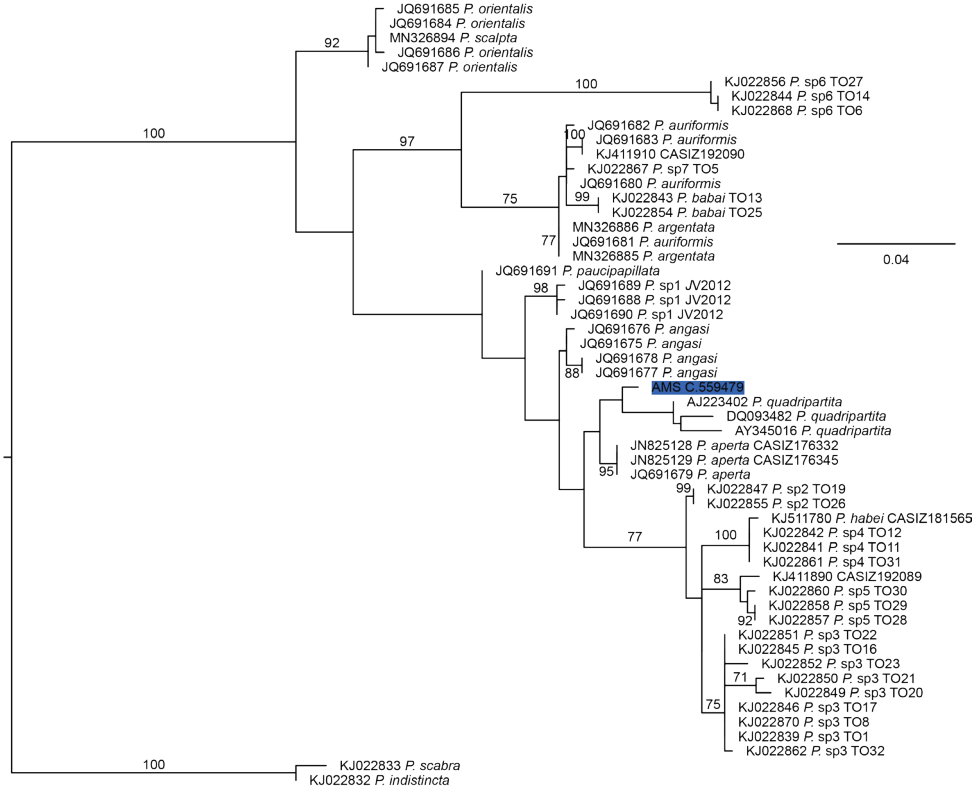

Figure 4. Phylogenetic relationships of C.559479 based on maximum likelihood analysis of the reduced 16S rRNA dataset. More distant outgroups have been removed and the topology rooted on *Philine scabra* + *P. indistincta*. Numbers near nodes refer to bootstrap percentages above 70%. The scale bar indicates 0.05 changes per site. Sequences are identified by accession number and species name or informal designation recorded in GenBank except those labelled *P. quadripartita* for which the species names have been changed for reasons outlined in the text. Accessions with an sp. number designation followed by a space and "TO" with a one or two digit designation refer to sequences from Oskars et al. (2015). Note that this article refers to the undescribed species in alphabetical rather than numerical order so that sp. 4 in GenBank is identified as sp. D in Oskars et al. (2015).

in a large clade that received bootstrap support of 56% in the analysis of the complete 16S rRNA alignment. The K2P distances from C.559479 to the three *P. quadripartita* specimens averaged 0.027 (minimum 0.023).

In all analyses of the 16S rRNA data, MN326885 collected from *P. argentata* by Chaban et al. (2019) and the two *P. auriformis* Suter, 1909 sequences form a clade close to other specimens from the former species. Price et al. (2011) proposed that *P. argentata* is a synonym of *P. orientalis* Adams, 1854. The type specimen of the former has shell dimensions of 6 × 5 mm (Gould 1859) which is much smaller than those of the latter species. *Philine argentata* was maintained as a distinct species by Chaban (2014) owing to differences in gizzard plate morphology, and subsequently by Cha-

ban et al. (2019). The Chaban et al. (2019) sequence of *P. scalpta* A. Adams, 1862 (MN326894) was unexpectedly included with robust bootstrap support in a clade of sequences supposed to be from *P. orientalis* that were collected by Krug et al. (2012).

The 28S rRNA D1 alignment (Suppl. material 2: Fig. S1) comprised 337 bases, 300 of which were constant, 15 parsimony-uninformative and 22 parsimony-informative. The optimal ML topology had a *ln* likelihood of –832.825 based on 1000 bootstrap replicates. The sequence of C.559479 was most similar to the only available sequence of *P. aperta* (Linnaeus, 1767) (K2P distance of 0.003, with the next most similar sequence having a distance of 0.006). The C.559479 and *P. aperta* specimens were not resolved as sister groups in the ML analysis but did have this relationship in minimum evolution topologies (not shown). 28S rDNA D1 sequences were not available from *P. quadripartita*.

The histone H3 alignment (Suppl. material 3: Fig. S2) comprised 365 bases, of which 258 were constant, 23 parsimony-uninformative and 84 parsimony-informative. The optimal ML topology had a *ln* likelihood of –1819.273 based on 500 bootstrap replicates conducted under the MRE criterion. The sequence of C.559479 was included in a large clade (bootstrap support 81%) with sequences from *P. scalpta*, *P. japonica*, and five undescribed species (Oskars et al. 2015) from the Philippines, southwest Pacific, and Taiwan (one specimen: accession KJ022956). The latter specimen was collected from deep water (326–331 m) off northeastern Taiwan (24°48'22.8024"N, 122°07'58.206"E). The most similar sequence to C.559479 was from Panglao in the Philippines (KJ022971, K2P distance 0.012), with the next most similar (K2P distance 0.015) being from *P. aperta* (DQ093508) and the Taiwanese specimen.

Discussion

Morphologically, C.559479 has more apparent affinity with *P. otukai* Habe, 1946, than other Taiwanese species. If the taxa were conspecific, this would represent a very large increase in the depth range of *P. otukai* which is reported to extend only to 100 metres (Lin 2004). The definite identification of C.559479 as *P. otukai* would, however, be premature because of the lack of relevant morphological information for that species. The shell of *P. otukai* is generally larger than that of C.559479, with the type specimen (Otuka 1936: figs 22, 23, as "*P. aperta*") of the former having a length of 24 mm and width of 17 mm (Otuka 1936). Although Lee (1998) gives a minimum of 15 mm (in a range of 15–28 mm) most reports from other regions (e.g., Lin 2004) suggest that the shell is much longer (> 25 mm). The gizzard plates of C.559479 appear similar in shape to those of *P. otukai* illustrated by Lee (1998) depicting the inner surface. However, no pores are visible in the illustrations of the outer surfaces of the plates in Lee (2018).

Specimen C.559479 is readily distinguished from *P. argentata*, which has two slit-like recesses on the outer surfaces of its gizzard plates (Chaban and Chernyshev 2014), that are absent here (Fig. 3). *Philine argentata* and *P. orientalis* were synonymised by (Price et al. 2011). However, they were treated as distinct species by Chaban (2014) so the possibility that C.559479 belongs to *P. orientalis* may be considered. The specimen C.559479 is dis-

tinct externally from *P. orientalis* sensu (Price et al. 2011) in its smaller size and creamy yellow headshield colour (vs. white in the latter species). C.559479 has a large pair of circular pores on all gizzard plates, whereas the pores are small in *P. orientalis* Price et al. (2011).

Specimen C.559479 differs from *P. vitrea* in the small size of the latter (shell dimensions of the type specimen 10 × 8 × 3 mm: Gould 1859). It also differs in the apparently much lower projection of the upper end of the outer lip of *P. vitrea*, allowing for the damaged condition of this shell section in the specimen studied here.

Sufficient information is available to distinguish C.559479 morphologically from only a few other regional species of *Philine*. These include *P. scalpta* in which the gizzard plates are quasi-trapezoidal with elongated pores (Chaban and Chernyshev 2014). The shell of the shallow water *P. kinglipini* Tchang, 1934 differs by the absence of spiral sculpture (Lin 1997: 198). *Philine kinglipini* attains a larger size of ~ 40–42 mm length and 18–19 mm width with shell dimensions of 19–20 mm × 14–14.5 mm (Lin 1997). The gizzard plates of *P. kinglipini* are all dissimilar to each other in size (Tchang 1934), with the second largest being quasi-trapezoidal. Both arms on all three plates of *P. kinglipini* are broad and nearly equal in length.

Philine paucipapillata Price, Gosliner & Valdés, 2011 was described as a new species from the South China Sea. Specimen C.559479 is readily distinguished morphologically from this species in coloration and size (*P. paucipapillata* is uniformly white and ~ 4–5 cm in length). The pores in the gizzard plates of *P. paucipapillata* are minute (Price et al. 2011) in contrast to those of C.559479.

Philine kurodai Habe, 1946, described from Japan, has been reported from Taiwan although the Taiwanese records are now regarded as being based on specimens of *P. otukai* (Lee 1998; Wu 2004). However, although both *P. otukai* and *P. kurodai* were described in Habe (1946) no characters distinguishing them from each other were listed and we have been unable to find any subsequent discussion discriminating these species. Neither *P. kurodai* nor *P. otukai* was mentioned by Price et al. (2011) but both are accepted by Chaban (2016).

Three species from northeastern Asia, *P. acutangula* Adams, 1862, *P. crenata* Adams, 1862, and *P. coreanica* Adams, 1855, have received little recent attention, particularly after Herdman (1906) made the latter two synonyms of "*Philine aperta*" (Table 1). The species all appear to belong to the group of species described by Adams (1855, 1862) categorised by Kurodai and Habe (1954) as "unobvious" and are presently best regarded as species inquirenda. To the best of our knowledge, the locations of their type specimens are unknown.

Analyses including the DNA sequences of C.559479 collected here highlight the taxonomic complexity of *Philine* in northeastern Asia. The available 16S rRNA data from the region represent at least five species. One of these species is represented by the C.559479 sequence from Taiwan. The other species are *P. paucipapillata*, *P. argentata* sensu Chaban et al. (2019), a species uncertainly referred to "*P. orientalis*", *P. japonica* or *P. scalpta* – see below), and an additional species, denoted "species D" by Oskars et al. (2015), which is represented by histone H3 DNA sequences. The latter may have affinity with *Philine habei* Valdés, 2008. The Taiwanese specimen of "species D" lacks 16S rDNA sequences but the other specimens referred to it by Oskars et al. (2015) are found in analyses of this

gene (Fig. 4) in a strongly supported clade with the *P. habei* sequence (KJ511780). This clade clearly excludes C.559479. The gizzard plates of *P. habei* have large elongate pores (Valdés 2008; Price et al. 2011) that appear very different from those of C.559479.

The three sequences of 16S rRNA that were most similar to C.559479 are recorded in GenBank as belonging to *Philine aperta*. However, the true identity of the specimens from which these sequences were derived appears to be *P. quadripartita*, a species from the northern Atlantic Ocean and Mediterranean Sea. The sequences form a distinct lineage separate from the two South African specimens from near the type locality of true *P. aperta*, and were determined from specimens taken within the range of *P. quadripartita*: AY345016 derives from a specimen from south-eastern Spain (Grande et al. 2004); and both AJ223402 (Thollesen 1999) and DQ093482 (Aktipis et al. 2008) are from Sweden.

The "*P. orientalis*" 16S rRNA sequence accession JQ691684) from Japan (Krug et al. (2012) is from a specimen identified as *P. japonica* in the catalogue of the Natural History Museum, London (BMNH:1996409). This is included in a clade with three Californian (non-native range) haplotypes of "*P. orientalis*" sequenced by Krug et al. (2012) and another from a specimen identified by Chaban et al. (2019) as *P. scalpta*, a species that was redescribed by Chaban and Chernyshev (2014) who removed it from the synonymy of *P. vitrea* in which it had been placed by Higo et al. (1999). If *P. japonica* and *P. scalpta* are, as maintained by Chaban et al. (2019), distinct from *P. orientalis*, then sequences truly from the latter species are probably yet to be determined. It is possible that the sequences from the taxon from near Darwin in northern Australia labelled sp. 1 JV 2012 in GenBank (Krug et al. 2012) may belong to *P. orientalis* or a closely related species. The named species to which these sequences are most similar are the Australasian *Philine angasi* (Crosse, 1865, in Crosse and Fischer 1865) and *P. paucipapillata*. Some radular and penial morphology characters distinguish *P. paucipapillata* and *P. orientalis* but they are closely related in the morphologically based phylogeny of Price et al. (2011). In this phylogeny, *P. paucipapillata* is shown as the sister group of the pair composed of *P. orientalis* and *P. angasi*.

Conclusions

The difficulty of identifying the unusual deep water *Philine* specimen studied here emphasises that destructive sampling should be minimised where the taxonomy is unintegrated. We tentatively suggest from examination of the external morphology and micro-CT scanning that it may have affinities with the shallow water *P. otukai* but any certainty is precluded by the lack of a description of that species, especially one detailing the range of variation it might encompass in characters such as the size of the gizzard plate pores. There is no diagnosis of *P. otukai* that would guide specimen dissection for relevant anatomical characters. Considerable further research efforts are required to provide a framework in which such characters could be sought. These include DNA studies of a wider range of regional species of *Philine*, particularly sequences definitely from *P. orientalis*, *P. kurodai*, *P. otukai*, and *P. vitrea*. Detailed morphological investigations are

needed for *P. japonica*, *P. otukai*, *P. kurodai*, and *P. vitrea*. The status of species such as *P. coreanica* may remain unknown but it may possibly be resolved if shell fragments from type material ever become available for macromolecular analysis, especially proteomics.

Acknowledgements

We thank the Australian Museum for funding and Cameron Slatyer for logistical support. We are grateful to Dr W. Rudman, Dr E. Chaban, Dr T. Gosliner, and anonymous reviewers for comments on earlier versions of the manuscript and to the editor, Dr N. Yonow, for very helpful advice. STA gratefully acknowledges support and hospitality of Prof. T.-Y. Chan in Taiwan in 2015. The authors acknowledge the facilities and the scientific and technical assistance of the National Imaging Facility at the Centre for Advanced Imaging, University of Queensland. We thank Professor K.K. Chan for providing the copy of a reference.

References

Adams A (1854) Descriptions of some new species of Lophocercidae and Philinidae, from the Cumingian Collection. Proceedings of the Zoological Society of London 22: 94–95. https://doi.org/10.1111/j.1469-7998.1854.tb07238.x

Adams A (1862) On some new species of Cylichnidae, Bullidae and Philinidae. Annals and Magazine of Natural History, Series 3, 9: 150–161. https://doi.org/10.1080/00222936208681198

Aktipis SW, Giribet G, Lindberg DR, Ponder, WF (2008) Gastropoda: an overview and analysis. In: Ponder WF, Lindberg DR (Eds) Phylogeny and Evolution of the Mollusca. University of California Press, Berkeley, 201–237. https://doi.org/10.1525/california/9780520250925.003.0009

Castresana J (2000) Selection of conserved blocks from multiple alignments for their use in phylogenetic analysis. Molecular Biology and Evolution 17: 540–552. https://doi.org/10.1093/oxfordjournals.molbev.a026334

Chaban EM, Chernyshev AV (2014) Opisthobranch cephalaspidean mollusks (Gastropoda: Opisthobranchia) of Vostok Bay, Sea of Japan. Part 1. The Bulletin of the Russian Far East Malacological Society 18: 41–62. [In Russian]

Chaban EM (2014) Notes on *Yokoyamaia ornatissima* (Yokoyama, 1927) and *Philine argentata* Gould, 1859 (Opisthobranchia: Cephalaspidea: Philinidae) from the Sea of Japan. Abstracts of the Conference Mollusks of the Eastern Asia and Adjacent Seas October 6–8, 2014, Vladivostok, Russia, 7–10.

Chaban EM (2016) Heterobranch mollusks of the orders Acteonoidea and Cephalaspidea (Gastropoda: Heterobranchia) of Vietnam: annotated check-list with illustrations of some species. In: Adrianov AV, Lutaenko KA (Eds) Biodiversity of the western part of the South China Sea. Dalnauka, Vladivostok, 415–448.

Chaban EM, Ekimova IA, Schepetov DM, Kohnert PC, Schroedl M, Chernyshev AV (2019) Euopisthobranch mollusks of the order Cephalaspidea (Gastropoda: Heterobranchia) of

the Kuril-Kamchatka Trench and the adjacent Pacific abyssal plain with descriptions of three new species of the genus *Spiraphiline* (Philinidae). Progress in Oceanography 178: e102185. https://doi.org/10.1016/j.pocean.2019.102185

Colgan DJ, Da Costa P (2009) DNA haplotypes cross species and biogeographic boundaries in estuarine hydrobiid snails of the genus *Tatea*. Marine and Freshwater Research 60: 861–872. https://doi.org/10.1071/MF08200

Colgan DJ, Ponder WF, Eggler PE (2000) Gastropod evolutionary rates and phylogenetic relationships assessed using partial 28S rDNA and histone H3 sequences. Zoologica Scripta 29: 29–63. https://doi.org/10.1046/j.1463-6409.2000.00021.x

Colgan DJ, Ponder WF, Beacham E, Macaranas JM (2003) Molecular phylogenetic studies of Gastropoda based on six gene segments representing coding or non-coding and mitochondrial or nuclear DNA. Molluscan Research 23: 123–148. https://doi.org/10.1071/MR03002

Crosse H, Fischer P (1865) Description d'espèces nouvelles de l'Australie méridionale. Journal de Conchyliologie 13: 38–55.

Gonzales C, Gosliner T (2014) Six new species of *Philine* (Opisthobranchia: Philinidae) from the tropical Indo-Pacific. In: Williams GC, Gosliner TM (Eds) The Coral Triangle: The 2011 Hearst Philippine Biodiversity Expedition. California Academy of Sciences, San Francisco, 351–383. https://doi.org/10.5962/bhl.title.154474

Grande C, Templado J, Cervera JL, Zardoya R (2004) Phylogenetic relationships among Opisthobranchia (Mollusca: Gastropoda) based on mitochondrial *cox 1*, *trnV*, and *rrnL* genes. Molecular Phylogenetics and Evolution 33: 378–388. https://doi.org/10.1016/j.ympev.2004.06.008-388

Habe T (1946) Report of the Cephalaspidea Opisthobranchia in Japan. Venus 14: 183–190. [In Japanese]

Habe T (1950) Philinidae in Japan. In: Kuroda T (Ed.) Illustrated catalogue of Japanese shells 8: 48–52. Kyoto, Kairui Bunken Kankokai.

Habe, T (1954) Report on the Mollusca chiefly collected by the S. S. Soyo-Maru of the Imperial Fisheries Experimental Station of the continental shelf bordering Japan during the years 1922–1930. Part 1. Cephalaspidea. Publications of the Seto Marine Biological Laboratory 3: 301–318. [pl. 38] https://doi.org/10.5134/174489

Hamatani I (1961) Notes on veligers of Japanese opisthobranchs (3). Publications of the Seto Marine Biological Laboratory 9: 67–79. https://doi.org/10.5134/174661

Herdman WA (1906) Report to the government of Ceylon on the pearl oyster fisheries of the Gulf of Manaar. The Royal Society, London, 384 pp. [p. 348]

Higo SI, Callomon P, Gotō Y (1999) Catalogue and bibliography of the marine shell bearing Mollusca of Japan: Gastropoda, Bivalvia, Polyplacophora, Scaphopoda. Elle Scientific Publications, Osaka, 749 pp.

Krug PJ, Asif JH, Baeza I, Morley MS, Blom WM, Gosliner TM (2012) Molecular identification of two species of the carnivorous sea slug *Philine*, invaders of the US west coast. Biological Invasions 14: 2447–2459. https://doi.org/10.1007/s10530-012-0242-9

Kumar S, Stecher G, Tamura K (2016) MEGA7: Molecular Evolutionary Genetics Analysis version 70 for bigger datasets. Molecular Biology and Evolution 33: 1870–1874. https://doi.org/10.1093/molbev/msw054

Kuroda T, Habe T (1954) On some Japanese Mollusca described by A. Adams, whose specimens are deposited in the Redpath Museum of Canada (No. 1). Venus 18: 1–16. [pls 1, 2]

Lee C-T (2018) *Philine otukai* 25.50mm. http://leechitse66.blogspot.com.au/2012/10/philine-otukai-2550mm.html [Accessed 6.II.2018]

Lee YC (1998) Thin bubble shells in Taiwan. The Pei-Yo 24: 13–15. [In Chinese]

Lee YC, Wu WL (2005) 作伙去撿螺仔–台灣常見貝類彩色圖誌 [The Taiwan common mollusks in colour]. Forestry Bureau, Council of Agriculture, Taipei, 294 pp. [In Chinese]

Lin G (1997) Fauna Sinica, Phylum Mollusca, Class Gastropoda, Subclass Opisthobranchia, Order Cephalaspidea. Science Press, Beijing, 246 pp. [28 pls.] [In Chinese with English summary]

Lin G (2004) Opisthobranchia. In: Qi Z (Chief Ed.) Seashells of China. China Ocean Press, Beijing, 224–234.

Lischke CE (1872) Diagnosen neuer Meeres-Conchylien von Japan. Malakozoologische Blätter 19: 100–109. [In German]

McArthur AG, Koop BF (1999) Partial 28S rDNA sequences and the antiquity of the hydrothermal vent endemic gastropods. Molecular Phylogenetics and Evolution 13: 255–274. https://doi.org/10.1006/mpev.1999.0645

Miller MA, Pfeiffer W, Schwartz T (2010) Creating the CIPRES Science Gateway for inference of large phylogenetic trees. In IEEE (consortium), Proceedings of the Gateway Computing Environments Workshop (GCE), 14 Nov 2010, New Orleans, 1–8. https://doi.org/10.1109/GCE.2010.5676129

Morton B, Chiu ST (1990) The diet, prey size and consumption of *Philine orientalis* (Opisthobranchia: Philinidae) in Hong Kong. Journal of Molluscan Studies 56: 289–299. https://doi.org/10.1093/mollus/56.2.289

Ohnheiser LT, Malaquias M (2013) Systematic revision of the gastropod family Philinidae (Mollusca: Cephalaspidea) in the north-east Atlantic Ocean with emphasis on the Scandinavian Peninsula. Zoological Journal of the Linnean Society 167: 273–326. https://doi.org/10.1111/zoj.12000

Oskars TR, Bouchet P, Malaquias MAE (2015) A new phylogeny of the Cephalaspidea (Gastropoda: Heterobranchia) based on expanded taxon sampling and gene markers. Molecular Phylogenetics and Evolution 89: 130–150. https://doi.org/10.1016/j.ympev.2015.04.011

Otuka Y (1936) Notes on some shells from southern Taiwan. Venus 6: 155–162. [in Japanese]

Palumbi SR (1996) Nucleic acids II: the polymerase chain reaction. In: Hillis DM, Moritz C, Mable BK (Eds) Molecular Systematics. Sinauer & Associates, Sunderland, Massachusetts, 205–247.

Pattengale ND, Alipour M, Bininda-Emonds ORP, Moret BME, Stamatakis A (2010) How many bootstrap replicates are necessary? Journal of Computational Biology 17: 337–354. https://doi.org/10.1007/978-3-642-02008-7_13

Pilsbry HA (1895) Philinidae. In: Tryon GW, Pilsbry HA (Eds) Manual of conchology; structural and systematic with illustrations of the species. Academy of Natural Sciences of Philadelphia 16: 2–28.

Price RM, Gosliner TM, Valdés Á (2011) Systematics and phylogeny of *Philine* (Gastropoda: Opisthobranchia), with emphasis on the *Philine aperta* species complex. The Veliger 51: 1–58.

Shepelenko M, Brumfeld V, Cohen SR, Klein E, Lubinevsky H, Addadi L, Weiner S (2015) The gizzard plates in the cephalaspidean gastropod *Philine quadripartita*: Analysis of structure and function. Quaternary International 390: 4–14. https://doi.org/10.1016/j.quaint.2015.04.060

Sowerby GB (1855) Thesaurus conchyliorum. Monographs of genera of shells. Sowerby, London, 899 pp. [Vol. 2, p. 601, pl. 125]

Stamatakis A, Hoover P, Rougemont J (2008) A rapid bootstrap algorithm for the RAxML web-servers. Systematic Biology 75: 758–771. https://doi.org/10.1080/10635150802429642

Tanaka Y. 1958. Studies on molluscan larvae (I). Venus 20: 207–219.

Tapparone-Canefri C (1874) Malacologia (Gasteropodi, Acefali e Brachiopodi). Zoologia del Viaggio Intorno al Globo della regia fregata Magenta durante gli anni 1865–68. Stamperia reale di G.B. Paravia e Comp, Torino, 162 pp. [4 pls.] [Explanation and figure, pl. 2] [In Italian] https://doi.org/10.5962/bhl.title.11193

Taylor JD (1982) Diets of sublittoral predatory gastropods of Hong Kong. In: Morton B, Tseng CK (Eds) Proceedings of the First International Marine Biological Workshop. Hong Kong University Press, Hong Kong, 907–920.

Tchang S (1934) Contribution à l'étude de Opistobranchea de la Côte de Tsingtao. Contributions from the Institute of Zoology, National Academy of Peiping 2(2): 1–148. [pls 1–16] [In French]

Thollesson M (1999) Phylogenetic analysis of Euthyneura (Gastropoda) by means of the 16S rRNA gene: use of a 'fast'gene for 'higher-level' phylogenies. Proceedings of the Royal Society of London B: Biological Sciences 266: 75–83. https://doi.org/10.1098/rspb.1999.0606

Thompson JD, Gibson TJ, Plewniak F, Jeanmougin F, Higgins DG (1997) The CLUSTAL X windows interface: flexible strategies for multiple sequence alignment aided by quality analysis tools. Nucleic Acids Research 25: 4876–4882. https://doi.org/10.1093/nar/25.24.4876

Valdés AA (2008) Deep-sea" cephalaspidean" heterobranchs (Gastropoda) from the tropical southwest Pacific. In: Héros V, Cowie RH, Bouchet P (Eds) Tropical Deep-Sea Benthos 25. Mémoires du Muséum national d'Histoire naturelle 196: 587–792.

Wu W-L (2004) List of Taiwan Malacofauna. IV, Gastropoda, Heterogastropoda, Heteropoda, Opisthobranchia and Pulmonata. The Council of Agriculture, Taipei, 160 pp.

Zhang, S. (2008) Order Cephalaspidea. In: Liu JY (Ed.) Checklist of marine biota of China seas. Science Press, Academia Sinica, Beijing, 527–532.

Supplementary material 1

Reconstructed micro-CT scan of C.559479

Authors: Donald J. Colgan, Shane T. Ahyong, Karine Mardon, Ian M. Brereton

Data type: Mpg file

Explanation note: Reconstructed micro-CT scan of C.559479.

Link: https://doi.org/10.3897/zookeys.1060.28809.suppl1

Supplementary material 2

Figure S1. Image from the reconstructed micro-CT scan of C.559479

Authors: Donald J. Colgan, Shane T. Ahyong, Karine Mardon, Ian M. Brereton

Data type: Pdf file

Explanation note: Image from the reconstructed micro-CT scan of C.559479. Dorsal view of the shell of C.559479, with boxed area illustrating irregularly cancellate sculpture.

Link: https://doi.org/10.3897/zookeys.1060.28809.suppl2

Supplementary material 3

Figure S2. Phylogenetic relationships of C.559479 based on maximum likelihood analysis of the D1 28S rRNA dataset

Authors: Donald J. Colgan, Shane T. Ahyong, Karine Mardon, Ian M. Brereton

Data type: Pdf file

Explanation note: Phylogenetic relationships of C.559479 based on maximum likelihood analysis of the D1 28S rRNA dataset. Numbers near nodes refer to bootstrap percentages above 70%. Scale bar indicates 0.01 changes per site. Sequences are identified by accession number and species name or informal designation recorded in GenBank. Accessions with an sp. number designation followed by a space and "TO" with a one or two digit designation refer to sequences from Oskars et al. (2015). Note that that article refers to the undescribed species in alphabetical rather than numerical order so that sp. 4 in GenBank is identified as sp. D in Oskars et al. (2015).

Link: https://doi.org/10.3897/zookeys.1060.28809.suppl3

Supplementary material 4

Figure S3. Phylogenetic relationships of C.559479 based on Maximum Likelihood analysis of the histone H3 dataset.

Authors: Donald J. Colgan, Shane T. Ahyong, Karine Mardon, Ian M. Brereton

Data type: Pdf file

Explanation note: Phylogenetic relationships of C.559479 based on Maximum Likelihood analysis of the histone H3 dataset. Numbers near nodes refer to bootstrap percentages above 70%. The scale bar indicates 0.05 changes per site. Sequences are identified by accession number and species name or informal designation recorded in GenBank. Accessions with a sp. number designation followed by a space and "TO" with a one or two digit designation refer to sequences from Oskars et al. (2015). Note that this article refers to the undescribed species in alphabetical rather than numerical order so that sp. 4 in GenBank is identified as sp. D in Oskars et al. (2015). The sequence indicated by a red square is the Taiwanese specimen with apparent affinity to P. habei (see text).

Link: https://doi.org/10.3897/zookeys.1060.28809.suppl4

ZooKeys 1060: 111–123 (2021)
doi: 10.3897/zookeys.1060.70203
https://zookeys.pensoft.net

RESEARCH ARTICLE

A peer-reviewed open-access journal
ZooKeys
Launched to accelerate biodiversity research

Two new species of the genus *Melixanthus* Suffrian (Coleoptera, Chrysomelidae, Cryptocephalinae) from China

Wen-Yuan Duan[1,2], Feng-Yan Wang[1,2], Hong-Zhang Zhou[1,2]

1 *Key Laboratory of Zoological Systematics and Evolution, Institute of Zoology, Chinese Academy of Sciences, 1 Beichen West Rd., Chaoyang District, Beijing 100101, China* **2** *University of the Chinese Academy of Sciences, 19A Yuquan Rd., Shijingshan District, Beijing 100049, China*

Corresponding author: Hong-Zhang Zhou (zhouhz@ioz.ac.cn)

Academic editor: Astrid Eben | Received 16 June 2021 | Accepted 10 August 2021 | Published 17 September 2021

http://zoobank.org/594190F9-8E0D-4B94-93EE-731612FB209A

Citation: Duan W-Y, Wang F-Y, Zhou H-Z (2021) Two new species of the genus *Melixanthus* Suffrian (Coleoptera, Chrysomelidae, Cryptocephalinae) from China. ZooKeys 1060: 111–123. https://doi.org/10.3897/zookeys.1060.70203

Abstract

Two new species of the genus *Melixanthus* Suffrian, 1854 are described from China: *M. menglaensis* Duan, Wang & Zhou, **sp. nov.** from Yunnan (also in Vietnam, Tonkin) and *M. similibimaculicollis* Duan, Wang & Zhou, **sp. nov.** from Yunnan. Another species, *M. rufiventris* Pic, 1926, is reported for the first time in China. High-quality color images and line drawings of adult habitus, aedeagus, and other important structures are provided for all three species. The types of the new species are deposited in the collection of Institute of Zoology, Chinese Academy of Sciences (IZ-CAS).

Keywords

Cryptocephalini, distributional records, leaf beetles, new species

Introduction

The leaf beetle genus *Melixanthus* Suffrian, 1854 (Chrysomelidae, Cryptocephalini) is mainly distributed in the Oriental region and includes approximately 60 species until now; of these, 11 species are known to occur in China (Gressitt and Kimoto 1961; Tan

et al. 1980; Tan 1988; Tan and Pu 1992; Lopatin 2005; Schöller et al. 2010). This genus was erected very early on as valid genus-level taxon and can be diagnosed by the following characteristics: antennae rather short, usually reaching humeral region of elytra; apical six segments broadened and flatted, about 1.2–2.2 times as long as wide; claws of all legs usually toothed or thickened basally. Not all *Melixanthus* species readily show the character of claws with or without teeth, and at least a few of species are not easily included in or excluded from this genus. This has challenged taxonomists studying this group.

The Chinese fauna of the genus was studied by including in a comprehensive study on the family Chrysomelidae (e.g., Chûjô 1954; Gressitt and Kimoto 1961; Tan et al. 1980; Schöller et al. 2010). Kimoto and Gressitt (1981) studied the chrysomelid fauna of Thailand, Cambodia, Laos, and Vietnam (countries near China), and thus their publication is important in identifying the Chinese species. The most recent and comprehensive study of *Melixanthus*, having excellent species revisions and key to species, was published by Medvedev (2012).

Our present study reports new findings, including the description of two new species of *Melixanthus* from China.

Materials and methods

Dried specimens were relaxed in hot distilled water at 80 ℃ for about 2 h to soften the body and ease dissection. The abdomen was separated with insect pins from the rest of the body, soaked in 10% KOH solution and then in a hot water bath for 15 min to advance the process. After this, specimens were transferred in distilled water to rinse the residual KOH solution off and stop the bleaching process. Afterwards, the aedeagus, spermatheca and rectal sclerites were prepared. The dissected parts were placed into glycerin for observation and measurement with an apochromatic stereomicroscope Zeiss SteREO V12. Color photographs of the adults and genitalia were captured with an Axio Zoom V16 fluorescence stereo zoom microscope and photomontage was performed in Zen 2012 (blue edition) imaging software. Adobe Photoshop CS6 was used in digital post-processing of the color images, and Adobe Illustrator 2020 was used to make the line drawings.

Materials used in this study are from the collection: **IZ-CAS** (Institute of Zoology, Chinese Academy of Sciences, Beijing, China).

Measurements are average values calculated from the values of at least five specimens, or all available specimens in case less than five specimens were available. The following abbreviations are used in the text to indicate the measurements of the specimens:

BL body length (length from the apex of pronotum to the apex of elytra in dorsal view);
BW body width (distance between the humeri, maximal body width);
HL head length (length from occiput to the front apex of mandibles);
HW head width (distance between the outer margin of eyes in frontal view, maximal head width);

PL pronotal length (length from the basal angle to anterior margin, maximal longitudinal length of pronotum);
PW pronotal width (distance of the widest portion of the pronotum);
EL elytral length (length of the maximal elytral length in dorsal view);
AL aedeagus length (length from the apex of aedeagus to the basal margin, maximal aedeagus length);
AW aedeagus width (the maximal width of aedeagus);
SL spermathecal length (length of the maximal spermathecal length, without duct).

Taxonomy

Genus *Melixanthus* Suffrian, 1854

Suffrian 1854: 8; Chapuis 1874: l75; Jacoby 1908: 267; Clavareau 1913: 197; Gressitt 1942: 330 353; Chûjô 1954: 187; Gressitt and Kimoto 1961: 169; Tan et al. 1981: 174; Kimoto and Gressitt 1981: 329; Schöller et al. 2010: 606; Medvedev 2012: 162.

Type species. *Melixanthus intermedius* Suffrian, 1854.

Synonym. *Suffrianus* Weise, 1895: 58. Type species: *Cryptocephalus pumilio* Suffrian, 1854.

Melixanthus menglaensis Duan, Wang & Zhou, sp. nov.

http://zoobank.org/CDAC18DD-5DF4-4115-9CCA-42553FB9E0C2
Figures 1–5

Type locality. China: Yunnan Province: Mengla.

Type material examined. ***Holotype*:** male, **China: Yunnan Province:** Mengla, Menglun, II–IV.1979, coll. unknown (IZ-CAS). ***Paratypes*: China: Yunnan Province:** 4 males, 2 females, same data as holotype (IZ-CAS); 1 female, Xishuangbanna, Gannanba, 14.III.1957, coll. Shuyong Wang (IZ-CAS); 1 female, Xishuangbanna, Gannanba, 21.III.1957, coll. Shuyong Wang (IZ-CAS); 1 female, Cheli, 9. IV.1955, coll. Fengyu Xue (IZ-CAS). **Vietnam: Tonkin:** 4 males, 3 females, III.1937, coll. unknown (IZ-CAS).

Measurements. BL = 3.25–3.60 mm, BW = 2.02–2.24 mm, HL = 0.91 mm, HW = 0.91 mm, PL = 1.08 mm, PW = 2.02 mm, EL = 2.00 mm, AL = 0.87 mm, AW = 0.27 mm, SL = 0.41 mm.

Description. Body (Fig. 3A–D) elongate, almost cylindrical, rounded anteriorly. Head (Fig. 3E) yellow, vertex with a darkish brown M-shaped marking; antennae (Fig. 3F) with basal 5 segments yellowish brown, terminal 6 segments reddish brown; clypeus yellow; labrum yellowish brown; mandibles darkish brown. Pronotum yellow,

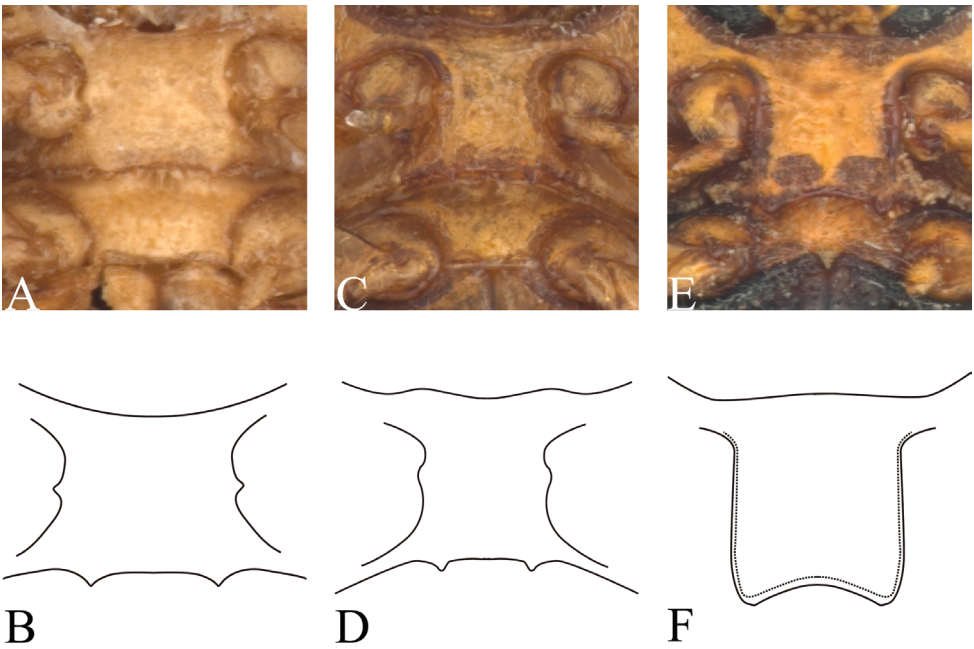

Figure 1. *Melixanthus* prosternum **A, B** *M. menglaensis* Duan, Wang & Zhou, sp. nov. **C, D** *M. similibimaculicollis* Duan, Wang & Zhou, sp. nov. **E, F** *M. bimaculicollis* Baly, 1865.

with two pitchy brown subtriangular markings along anterior margin. Scutellum yellow and margins black. Elytra pitchy brown, with a yellowish-brown band in middle region, covering about 1/2 of whole region; margins pitchy brown. Sometimes entirely yellow, only margins pitchy brown. Ventral surface yellow, metasternum with a rectangular black marking. Legs and pygidium all yellow.

Head (Fig. 3E) densely and coarsely punctate, flattened on midline, longitudinally impressed on frons and vertex. Eyes kidney-shaped, deeply emarginated; antennal insertions a little more widely separated than superior eye-lobes. Clypeus sparsely punctate, strongly arcuate on anterior margin. Antennae (Fig. 3F) with sparsely long hair, short and slightly broad, reaching humeral tubercle; 1st segment clubbed; 2nd oblong, about half as long as 1st; 3rd–5th thin, about equal in length, longer than 2nd; 6 apical segments moderately thickened, about 2.0–2.2 times as long as wide, last segment pointed apically.

Pronotum (Fig. 3A–D) 1.8 times as wide as long, moderately narrowed and rounded anteriorly; surface strongly convex, impunctate and shining. Scutellum triangular, nearly as long as wide, surface smooth, shining.

Elytron (Fig. 3A–D) parallel-sides, apical margin slightly straight, 2.0 times as long as wide, humeri prominent and glabrous. Disc with regular rows of fine punctures, partly confused near apical slope; interspaces without punctures; epipleurae slightly obliquely placed and seen in lateral view.

Ventral side (Fig. 3G) partly clothed with pubescence. Prosternum (Fig. 1A, B) square, anterior margin slightly concave; basal margin nearly straight, and drawn

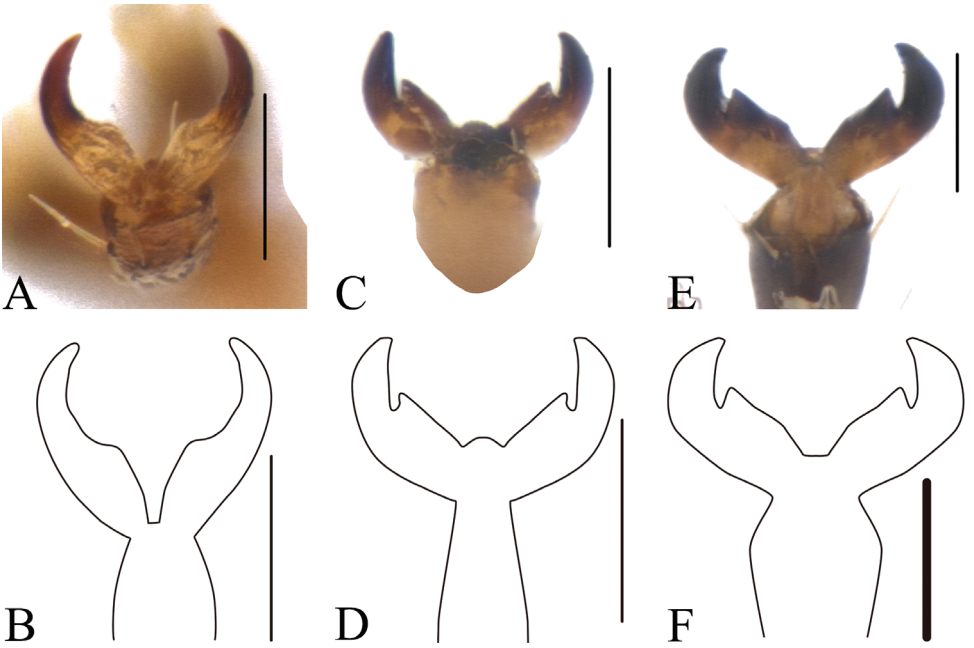

Figure 2. *Melixanthus* claws **A, B** *M. menglaensis* Duan, Wang & Zhou, sp. nov. **C, D** *M. similibimaculicollis* Duan, Wang & Zhou, sp. nov. **E, F** *M. bimaculicollis* Baly, 1865. Scale bars: 0.1 mm.

out into a pair of small denticles. Mesosternum trapeziform, twice as wide as long. Metasternum wrinkled at sutural region and with dense pubescence. Pygidium flat, punctate and pubescent. Claws (Fig. 2A, B) not toothed, thickened basally.

Aedeagus (Figs 4A–C, 5A–C) elongate, about 3.2 times as long as wide, clubbed. Apex of median lobe narrower than middle, acute at apex, slightly curved in lateral view; with several pubescence on each side of apex and upper lateral margins, punctate on ventral side of upper middle part. Median orifice with middle sclerite bending inwards above surface. Upper part of median lobe with a pair of sclerotized prominence, exceeding the median lobe. Inner sac rather narrow, arrow-shaped. Tegmen Y-shaped, weakly sclerotized, almost translucent.

Female. Body more robust than male; **spermatheca** (Figs 4D, 5D) hook-shaped, bent in a right-angle halfway, slightly acute at apex; duct weakly sclerotized, irregularly coiling 9–12 times. **Rectal sclerites** (Fig. 4E) weakly sclerotized, slightly connected between two rectangular sclerites on ventral side.

Distribution. China (Yunnan); Vietnam (Tonkin).

Etymology. The specific epithet is derived from the name (Pinyin) of the type locality, Mengla.

Diagnosis. This species is similar to *M. bimaculicollis* Baly, 1865, but can be distinguished from that species in having finer punctures on the head, a narrower pronotum, an impunctate scutellum, and fine puncture rows on the elytra, whereas *M. bimaculicollis* has the elytra with distinct punctures and a surrounded by dark ring;

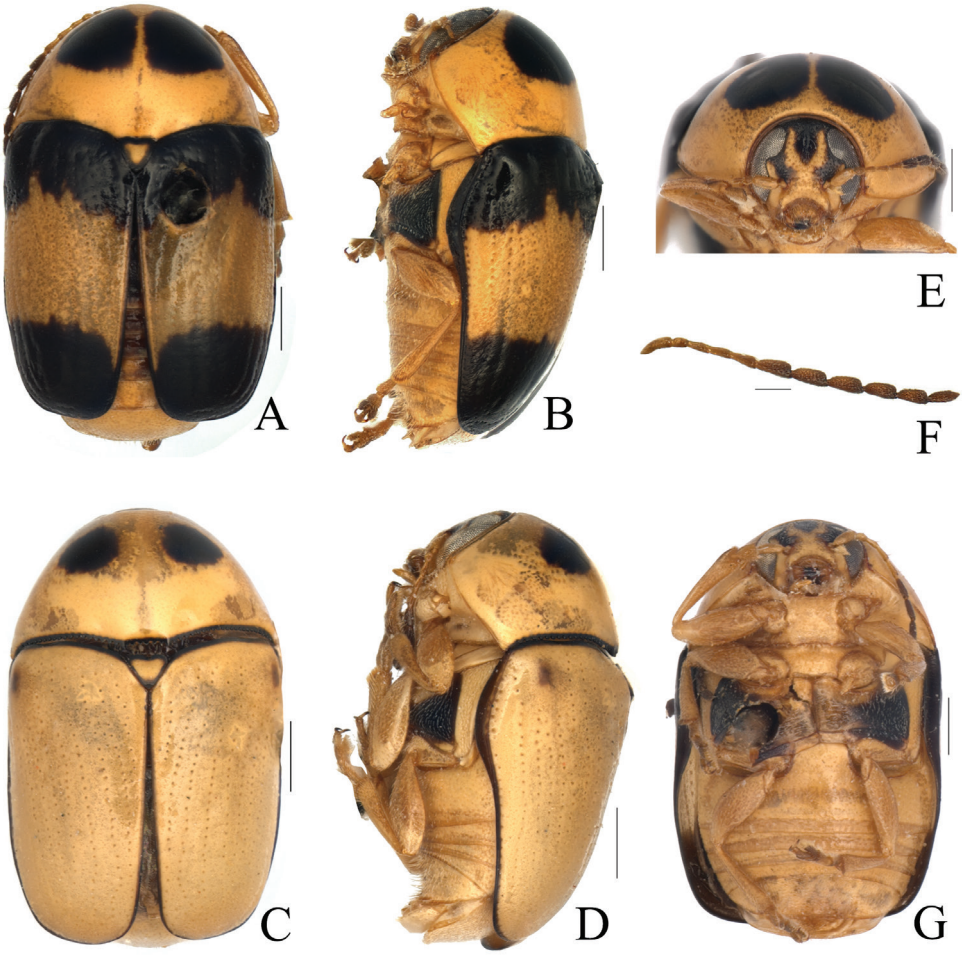

Figure 3. *Melixanthus menglaensis* Duan, Wang & Zhou, sp. nov. **A, C** habitus **B, D** lateral view of habitus **E** head **F** antennae **G** ventral view of habitus. Scale bars: 0.5 mm (**A–E, G**), 0.2 mm (**F**).

its claws are not toothed (Fig. 2A, B) and the basal margin of its prosternum is drawn out into a pair of small, sharp denticles (Fig. 1A, B).

***Melixanthus similibimaculicollis* Duan, Wang & Zhou, sp. nov.**
http://zoobank.org/CF48CD44-29B9-4CCA-BB5F-764FA5F15982
Figures 1, 2, 6, 7

Type locality. China: Yunnan Province: Cheli.

Type material examined. ***Holotype*: male, China: Yunnan Province:** Cheli, 9.III.1957, coll. Fuji Pu (IZ-CAS); ***Paratypes*: China: Yunnan Province:** 1 male,

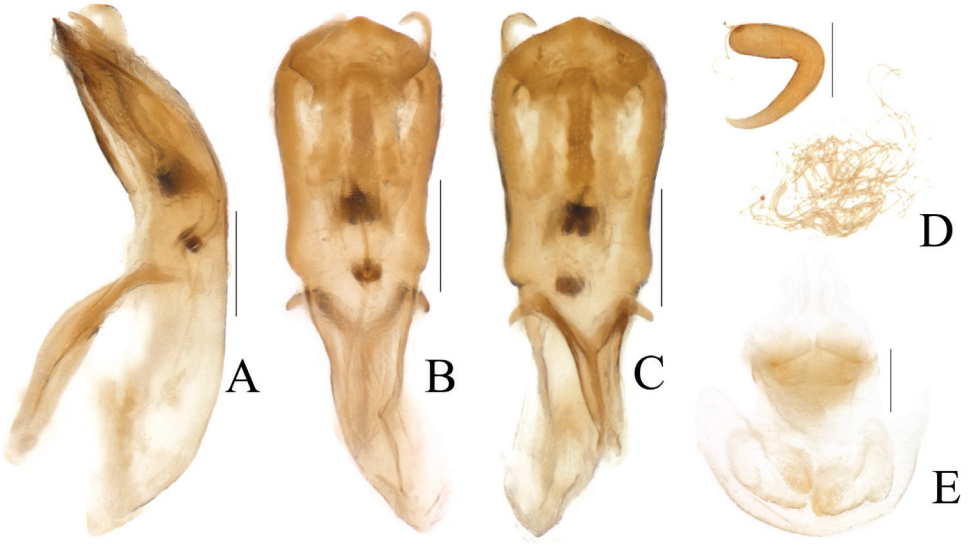

Figure 4. *Melixanthus menglaensis* Duan, Wang & Zhou, sp. nov. **A** lateral view of aedeagus **B** dorsal view of aedeagus **C** ventral view of aedeagus **D** spermatheca **E** female rectal pad. Scale bars: 0.2 mm.

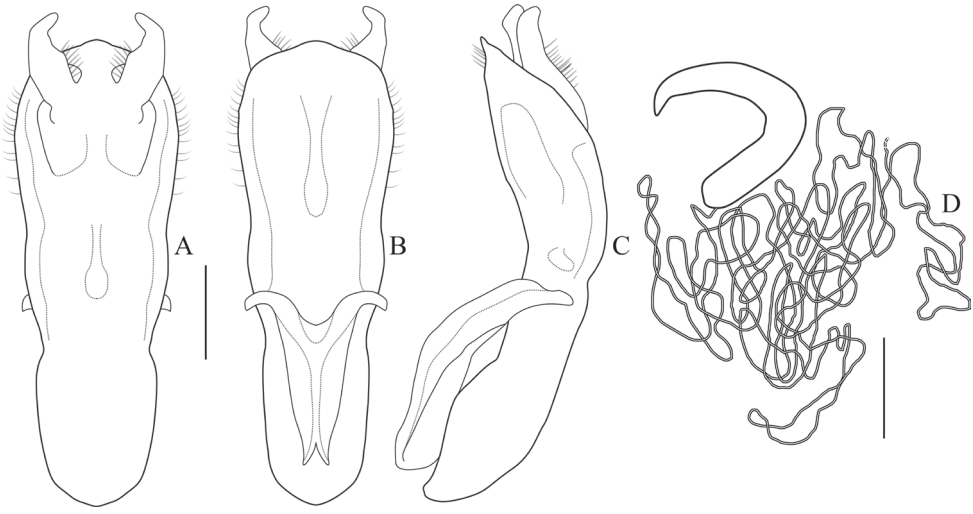

Figure 5. *Melixanthus menglaensis* Duan, Wang & Zhou, sp. nov. **A** dorsal view of aedeagus **B** ventral view of aedeagus **C** lateral view of aedeagus **D** spermatheca. Scale bars: 0.2 mm.

50 km southwest of Mojiang, 30.III.1955, coll. Kryzhanowski (IZ-CAS); 1 female, Longling, 1600 m, 20.V.1955, coll. Kryzhanowski (IZ-CAS).

Measurements. BL = 2.55–2.82 mm, BW = 1.57–1.73 mm, HL = 0.82 mm, HW = 0.85 mm, PL = 0.90 mm, PW = 1.62 mm, EL = 1.81 mm, AL = 0.91 mm, AW = 0.34 mm, SW = 0.39 mm.

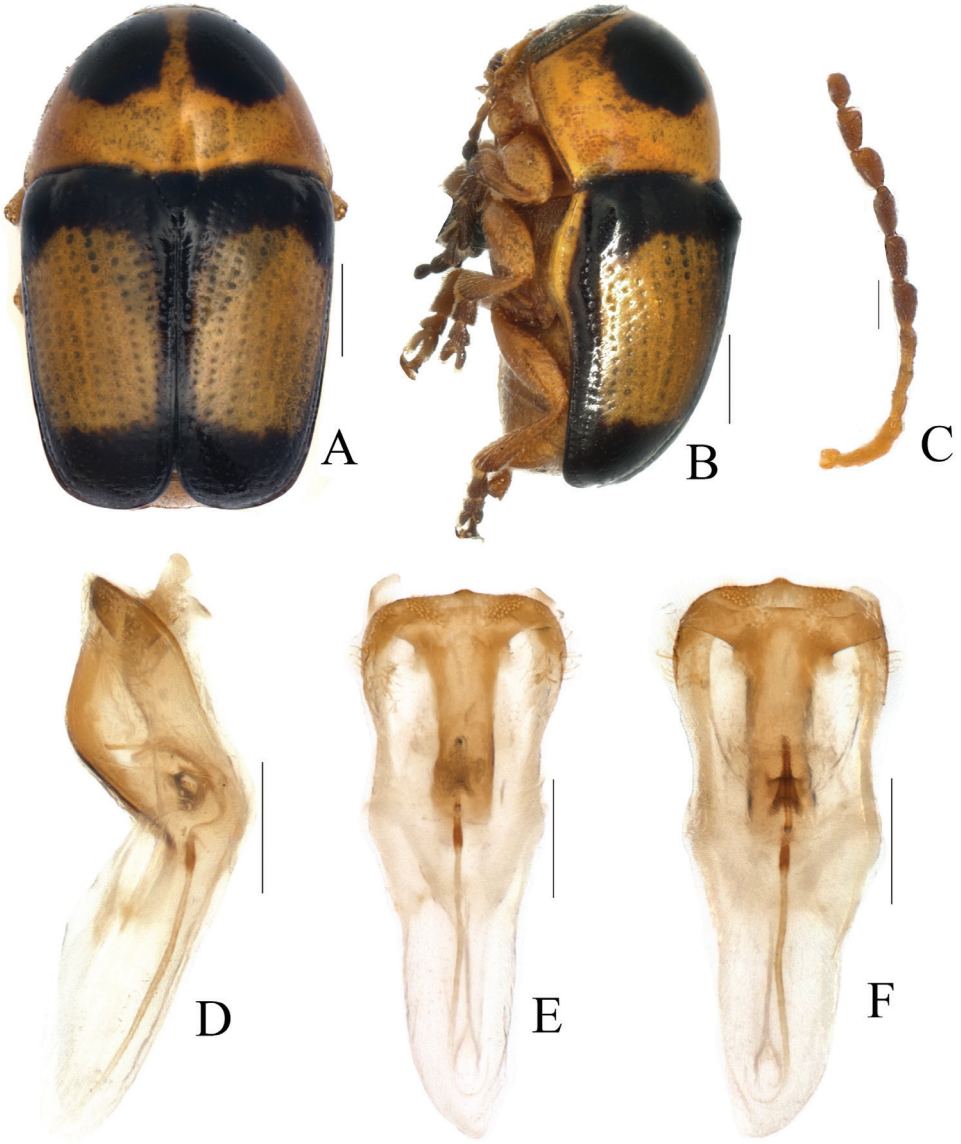

Figure 6. *Melixanthus similibimaculicollis* Duan, Wang & Zhou, sp. nov. **A** habitus **B** lateral view of habitus **C** antennae **D** lateral view of aedeagus **E** ventral view of aedeagus **F** dorsal view of aedeagus. Scale bars: 0.5 mm (**A, B**), 0.2 mm (**C–F**).

Description. Body (Fig. 6A, B) elongate, almost cylindrical, rounded anteriorly. Head yellow, vertex with a darkish brown triangular marking; antennae (Fig. 6C) with basal 5 segments yellowish brown, the rest brown; clypeus yellow; labrum yellowish brown; mandibles reddish brown. Pronotum yellow, and basal margin pitchy brown, forming 2 nearly round pitchy brown markings along anterior margin. Scutellum entirely black. Elytra pitchy black only in basal and apical parts, with a large yellow band

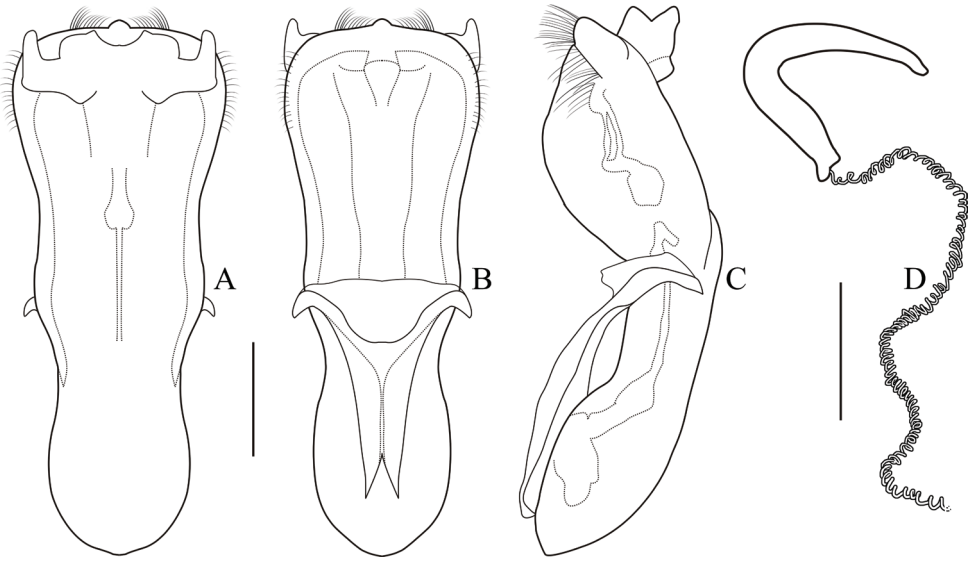

Figure 7. *Melixanthus similibimaculicollis* Duan, Wang & Zhou, sp. nov. **A** dorsal view of aedeagus **B** ventral view of aedeagus **C** lateral view of aedeagus **D** spermatheca. Scale bars: 0.2 mm.

in middle region, covering about 2/3 of whole elytron; sutural and lateral margins also pitchy black. Ventral surface yellowish brown.

Head with sparsely pubescence, without punctures, flattened in midline, and with longitudinal shallow groove on frons. Eyes kidney-shaped, deeply emarginated; antennal insertions about equally separated with superior eye-lobes. Clypeus trapeziform, anterior margin concave, without punctures. Antennae (Fig. 6C) long and slightly thin, reaching 1/3 region of elytra; 1st segment clubbed; 2nd oblong, about 1/2 as long as 1st; 3rd–5th thin, about equal in length, longer than 2nd; 6 apical segments moderately thickened, about 1.7–2.0 times as long as wide, last segment pointed apically.

Pronotum (Fig. 6A, B) 1.8 times as wide as long, moderately narrowed and rounded anteriorly; surface strongly convex, impunctate and shining. Scutellum triangular, nearly as long as wide, surface smooth, shining, apically elevated, observable in lateral view.

Elytra (Fig. 6A, B) with humeri prominent and glabrous, widest slightly behind humerus, feebly truncated at apex. Disc with regular rows of coarse punctures; interspace of rows without any punctures; epipleura slightly obliquely placed and observable in lateral view.

Ventral side smooth, partly clothed with pubescence. Prosternum (Fig. 1C, D) square, anterior margin nearly straight; basal margin slightly concave, and drawn out into a pair of small denticles. Mesosternum trapeziform, 1.5 times as wide as long. Metasternum with coarsely sporadic punctures in sutural region and with sparse pubescence. Pygidium flat, punctate and pubescent. Claws (Fig. 2C, D) distinctly toothed, thickened basally.

Aedeagus (Figs 6D–F, 7A–C) elongate, about 2.7 times as long as wide, clubbed. Anterior margin of median lobe nearly straight, middle part papillary protruding, strongly curved in lateral view; with several pubescence on each side of apex and upper

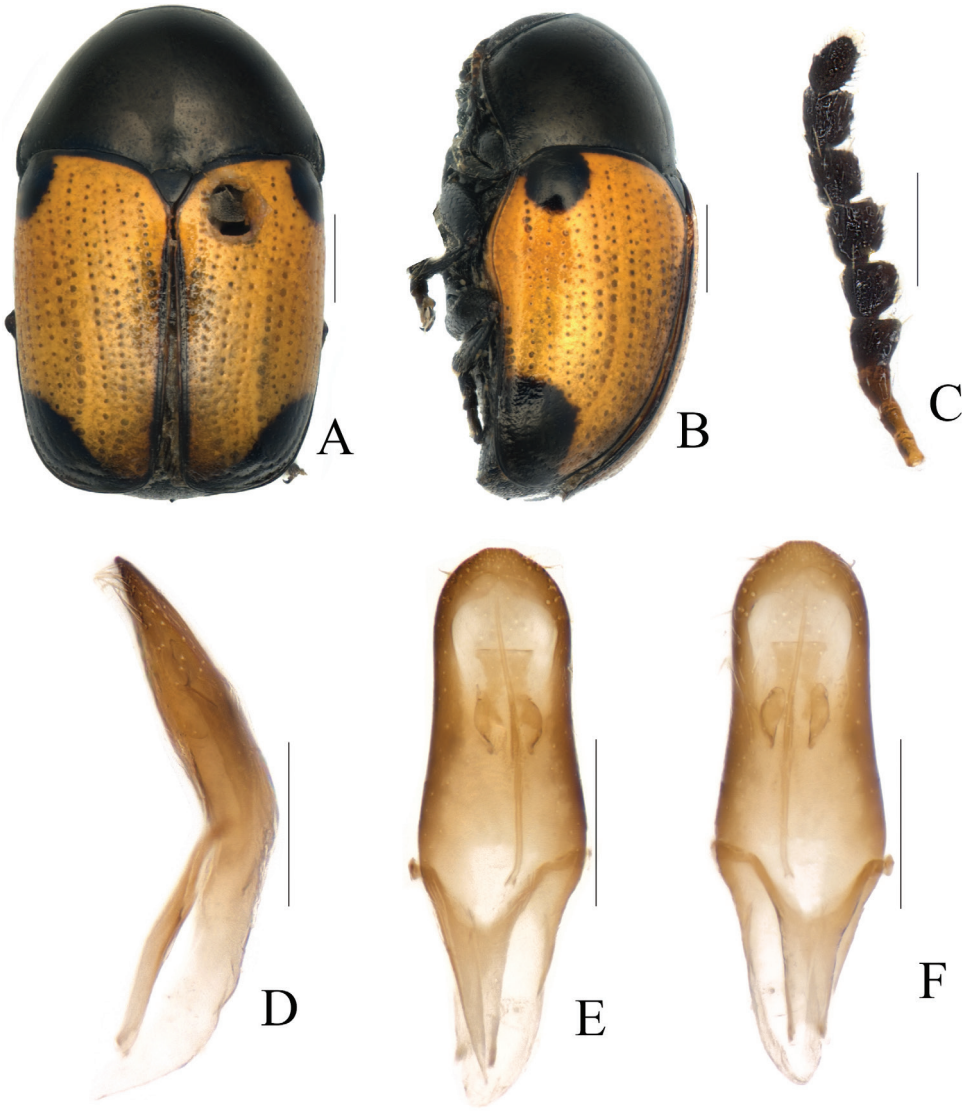

Figure 8. *Melixanthus rufiventris* Pic, 1926 **A** habitus **B** lateral view of habitus **C** antennae **D** lateral view of aedeagus **E** ventral view of aedeagus **F** dorsal view of aedeagus. Scale bars: 0.5 mm (**A, B**), 0.2 mm (**C–E**).

lateral margins, punctate on apex of median lobe. Median orifice with middle sclerite bending inwards above surface. Upper part of median lobe with a pair of sclerotized prominence, exceeding the median lobe. Inner sac rather narrow, arrow-shaped. Tegmen Y-shaped, weakly sclerotized, almost translucent.

Female. Body more robust than male; **spermatheca** (Fig. 7D) hook-shaped, bent at a right-angle halfway, slightly acute at apex. Duct weakly sclerotized, tightly coiled. **Rectal sclerites** absent in specimen studied.

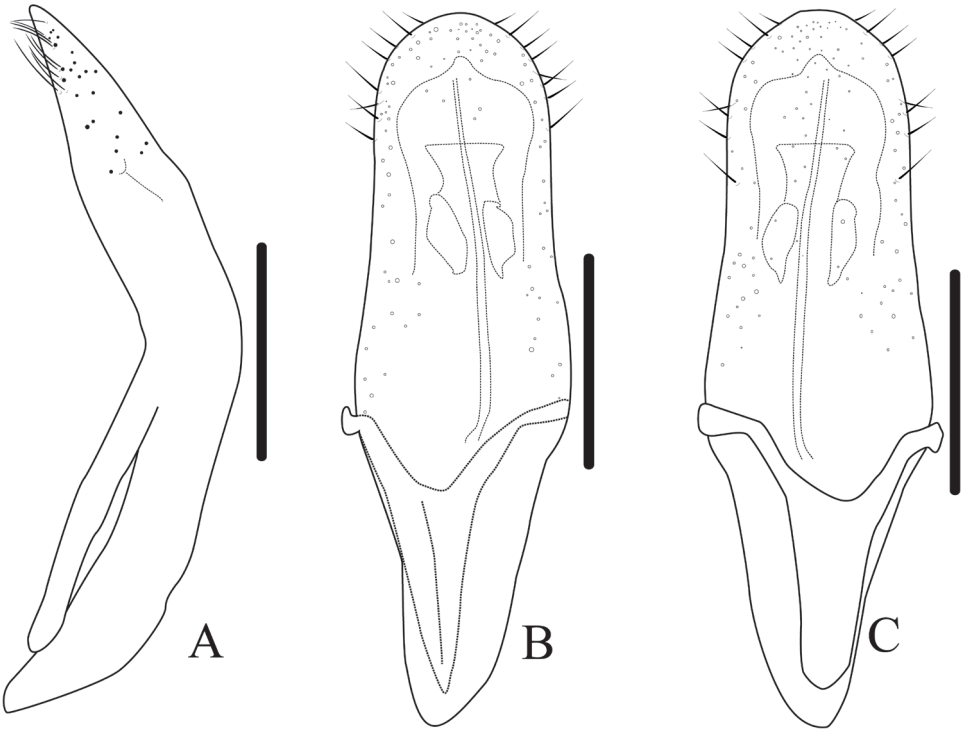

Figure 9. *Melixanthus rufiventris* Pic, 1926 **A** lateral view of aedeagus ventral view of aedeagus **C** dorsal view of aedeagus **D** spermatheca. Scale bars: 0.2 mm.

Distribution. China (Yunnan).

Etymology. The specific epithet is derived from the Latin terms *simili-*, *bi-*, *maculi-* and *collis*, to indicate the new species near to *M. bimaculicollis*.

Diagnosis. The new species is similar to *M. bimaculicollis* Baly, 1865, but can be distinguished from it by the smaller body size; head and scutellum without any punctures; slightly narrower pronotum; elytra with finer punctures, and only basal part punctures surrounded by dark ring; basal margin of prosternum (Fig. 1C, D) drawn out into a pair of small sharp denticles. *Melixanthus similibimaculicollis* is also similar to *M. menglaensis* Duan, Wang & Zhou, sp. nov., but can be distinguished by the following characters: head without punctures; claws toothed (Fig. 2C, D); and body size smaller.

Melixanthus rufiventris Pic, 1926, new country record from China

Figures 8, 9

Pic 1926: 11 (type locality: Tonkin); Kimoto and Gressitt 1981: 333 (Vietnam); Medvedev 2012: 163.

Material examined. China: Hunan province: 3 males, 6 females, Shimen country, Hupingshan town, Wangyue lake, 29.93222°N, 110.7776°E, 248 m, 11.X.2014, coll. Jian Yao (IZ-CAS).

Measurements. BL = 2.65–2.93 mm, BW = 1.64–1.80 mm, HL = 0.75 mm, HW = 0.80 mm, PL = 0.92 mm, PW = 1.73 mm, EL = 1.92 mm, AL = 0.64 mm, AW = 0.20 mm.

Distribution. China (Hunan); Vietnam.

Acknowledgements

We thank the editors and the anonymous reviewers for their valuable suggestions. This study was supported in part by the Ministry of Ecology and Environment, China (no. 2019HJ2096001006) and by the Ministry of Science and Technology of China (2015FY210300). Insect Diversity Observation Network of Sino BON (CAS, China) provided assistances with field investigations. We also want to thank Ms Liang Su (Beijing, China) for her help in preparing some line drawing plates.

References

Baly JS (1865) Phytophaga Malayana. A revision of the phytophagous beetles of the Malay Archipelago, with descriptions of the new species collected by Mr. A.R. Wallace. The Transactions of the Entomological Society of London (Series 3) 4: 1–76. [pls 1–5]

Chapuis F (1874) Famille des Phytophages. In: Lacordaire T, Chapuis F (Eds) Histoire naturelle des Insectes. Genera des coléopteres ou exposé méthodique et critique de tous les genres proposés jusqu'ici dans cet ordre d'insectes. Tome dixieme. Roret, Paris, 1–455.

Chûjô M (1954) A taxonomic study on the Chrysomelidae (Insecta-Coleoptera) from Formosa. Part VII, subfamily Cryptocephalinae. Quarterly Journal of the Taiwan Museum 7: 137–248.

Clavareau H (1913) Coleopterorum Catalogus. Auspiciis et auxilio W. Junk editus a S. Schenkling. Pars 53: Chrysomelidae: 5. Megascelinae, 6. Magalopodinae, 7. Clytrinae, 8. Cryptocephalinae, 9. Chlamydinae, 10. Lamprosominae. Berlin, 278 pp.

Gressitt JL (1942) Plant-beetles from south and west China. III. Clytrinae, Cryptocephalinae and Chlamydinae. Lingnan Science Journal 20: 325–376. [pls 19–22]

Gressitt JL, Kimoto S (1961) The Chrysomelidae (Coleopt.) of China and Korea, part 1. Pacific Insects Monograph 1A: 1–299.

Jacoby M (1908) The Fauna of British India, including Ceylon and Burma. Coleoptera, Chrysomelidae. Vol. 1. Taylor & Francis, London, 534 pp.

Kimoto S, Gressitt JL (1981) Chrysomelidae (Coleoptera) of Thailand, Cambodia, Laos and Vietnam. 2. Clytrinae, Cryptocephalinae and Chlamisinae, Lamprosomatinae and Chrysomelinae. Pacific Insects 23: 329–333.

Lopatin IK (2005) New species of leaf-beetles (Coleoptera, Chrysomelidae) from China. V. Entomologicheskoe Obozrenie 84: 873–880.

Medvedev LN (2012) To the knowledge of Oriental species of *Melixanthus* Suffrian, 1854 (Chrysomelidae: Cryptocephalinae). Entomologische Zeitschrift 122(4): 162–170.

Pic M (1926) Nouveautés diverses. Mélanges Exotico-Entomologiques 47: 1–32.

Schöller M, Löbl L, Lopatin IK (2010) Chrysomelidae: Cryptocephalinae: remaining Cryptocephalini. In Löbl I, Smetana A (Eds). Catalogue of Palaearctic Coleoptera, Vol. 6. Chrysomeloidea. Apollo Books, Stenstrup, 606–617.

Tan JJ (1988) Coleoptera: Eumolpidae. In: Huang FS, Wang PY, Yin WY, Yu PY, Lee TS, Yang CK, Wang XJ (Eds) Insects in Mt. Namjagbarwa region of Xizang. Science Press, Beijing, 309–333.

Tan JJ, Yu PY, Li HX, Wang SY, Jiang SQ (1980) Economic Insect Fauna of China Fasc. 18 Coleoptera: Chrysomeloidea (I). Science Press, Beijing, [xiii +] 213 pp.

Tan JJ, Pu FJ (1992) Two new species of the genus *Melixanthus* Suffrian from Hengduan Mountains, China (Coleoptera: Eumolpidae: Cryptocephalinae). In: Chen SX (Ed.) Insects in Hengduan Mountains region. Vol. 1. Science Press, Beijing, 754–829.

Suffrian E (1854) Verzeichniss der bis jetzt bekannt gewordenen Asiatischen Cryptocephalen. Linnaea Entomologica 9: 1–169.

Weise J (1895) Zwei neue Cryptocephalinen-Gattungen. Deutsche Entomologische Zeitschrift 1895: 57–58. https://doi.org/10.1002/mmnd.48018950112

ZooKeys 1060: 125–153 (2021)
doi: 10.3897/zookeys.1060.62982
https://zookeys.pensoft.net

RESEARCH ARTICLE

A peer-reviewed open-access journal
ZooKeys
Launched to accelerate biodiversity research

Amphibians and reptiles of the Atlantic Forest in Recôncavo Baiano, east Brazil: Cruz das Almas municipality

Arielson S. Protázio[1], Airan S. Protázio[2], Larissa S. Silva[3], Lennise C. Conceição[3], Hugo S. N. Braga[4], Uilton G. Santos[5], André C. Ribeiro[1], Amanda C. Almeida[1], Vívian Gama[1], Marcos V. S. A. Vieira[4], Tiago A. F. Silva[1]

1 *Centro de Ciências Agrárias, Ambientais e Biológicas, Universidade Federal do Recôncavo da Bahia, Rua Rui Barbosa, Centro, 44380-000, Cruz das Almas, Bahia, Brazil* **2** *Departamento de Ensino, Instituto Federal de Educação, Ciência e Tecnologia da Bahia, Rodovia BA 148, Km 04, Vila Esperança, 44900-000, Irecê, Bahia, Brazil* **3** *Programa de Pós-Graduação em Ecologia e Evolução, Universidade Estadual de Feira de Santana, Av. Transnordestina, S/N, Novo Horizonte, 44936-900, Feira de Santana, Bahia, Brazil* **4** *Programa de Pós-Graduação em Zoologia, Universidade Estadual de Santa Cruz, Rodovia Jorge Amado, Km 16, Salobrinho, 45662-900, Ilhéus, Bahia, Brazil* **5** *Programa de Pós-Graduação em Ciência Animal, Universidade Federal da Bahia, Avenida Adhemar de Barros, S/N, Ondina, 40170-110, Salvador, Bahia, Brazil*

Corresponding author: Arielson S. Protázio (neu_ptz@hotmail.com)

Academic editor: Uri García-Vázquez | Received 11 January 2021 | Accepted 20 July 2021 | Published 21 September 2021

http://zoobank.org/7BBA2AD4-3EF3-42A1-8C9D-623FBFB89EDE

Citation: Protázio AS, Protázio AS, Silva LS, Conceição LC, Braga HSN, Santos UG, Ribeiro AC, Almeida AC, Gama V, Vieira MVSA, Silva TAF (2021) Amphibians and reptiles of the Atlantic Forest in Recôncavo Baiano, east Brazil: Cruz das Almas municipality. ZooKeys 1060: 125–153. https://doi.org/10.3897/zookeys.1060.62982

Abstract

A list of amphibian and reptile species that occur in open and forested areas of the Atlantic Forest in the municipality of Cruz das Almas, in the Recôncavo Baiano, eastern Brazil is presented. Field sampling occurred between January 2015 to March 2019, totalling 117 samples distributed in three areas: Parque Florestal Mata de Cazuzinha, Mata da Cascalheira, and Riacho do Machado. A total of 1,848 individuals of 69 species (31 anurans, 14 lizards, 19 snakes, two amphisbaenians, and three testudines) was recorded. Additionally, one individual of *Ophiodes striatus* was found in Mata da Cascalheira after the end of sampling, totalling 15 lizard species and 70 herpetofaunal species. The prevalence of open-area species and the presence of *Phyllopezus lutzae*, *Diploglossus lessonae*, and *Dryadosaura nordestina* in interior forest patches are discussed. Additionally, a new record of the invasive terrapin *Trachemys dorbigni* in the State of Bahia is reported.

Keywords

Amphisbaena, anuran, diversity, lizards, species richness, snakes, testudines

Introduction

The Atlantic Forest is a biome that occupies the entire east of South America and of Brazil and is considered one of the most diverse in species richness and levels of endemism (Mittermeier et al. 2004). Regarding amphibians, ca. 625 species occur in this biome, representing more than 50% of the species recorded in Brazil (Haddad et al. 2013; Rossa-Feres et al. 2017; Segalla et al. 2019), while for reptiles, the richness is ca. 312 species, representing 39.2% of the species that occur in the country (Tozetti et al. 2017; Costa and Bérnils 2018). The high species richness in the Atlantic Forest may be associated with a combination of factors such as latitudinal variation (encompassing tropical and subtropical areas), longitudinal variation (with marked variations in rainfall and humidity), elevational variation and biogeographic history, which have shaped different phyto-physiological units and high environmental heterogeneity (Rossa-Feres et al. 2017), reflecting patterns of richness and diversity within well-defined biogeographic units (Vasconcelos et al. 2014; Moura et al. 2017).

Despite its high richness, Brazil is also a country with high levels of threat to biodiversity. According to the Brazil Red Book of Threatened Species of Fauna (ICMBio 2018), 1,173 species are included in some threat category, including 41 species of amphibians and 80 species of reptiles. For the Atlantic Forest, this scenario is extremely worrying. Considered one of the most threatened hotspots in the world (Mittermeier et al. 2004), the biome has 37 endemic anuran species and 39 reptile species included in the list of threatened species (ICMBio 2018). The main reasons for this high rate are the intense activities related to farming and urban growth, which are responsible for causing major changes in the natural landscape (Rodrigues 2005; Silvano and Segalla 2005; ICMBio 2018). According to data from Rezende et al. (2018), only 28% of the Atlantic Forest maintain its original cover, and these areas represent small, isolated forest fragments in a matrix of pasture, plantation or anthropogenic construction; this scenario can have a catastrophic effect on gene flow and biodiversity maintenance.

The State of Bahia is a state with great richness of herpetofauna species (Hamdan and Lira-da-Silva 2012; Dias and Rocha 2014; Freitas et al. 2019). Although in recent years many studies have been developed to characterise the herpetofauna of this state (see Freitas et al. 2016a, b, 2018; Gondim-Silva et al. 2016; Marques et al. 2016; Mira-Mendes et al. 2018; Leite et al. 2019; Souza-Costa et al. 2020; Rojas-Padilla et al. 2020), the vast majority of these initiatives were limited to investigations in specific regions, especially areas of dense ombrophilous forest in the south and southeast of the state (Argôlo 2004; Camurugi et al. 2010; Dias et al. 2014a; Mira-Mendes et al. 2018; Rojas-Padilla et al. 2020; Souza-Costa et al. 2020), sand dune areas on the northern coast of the state (Tinôco et al. 2007; Dias and Rocha 2014; Gondim-Silva et al. 2016; Marques et al. 2016; Napoli et al. 2017) and high-elevation regions of Chapada Diamantina (northern portion of Serra do Espinhaço) (Leite et al. 2008; Xavier and Napoli 2011; Freitas et al. 2012; Magalhães et al. 2015). Allied to this, many of these studies were carried out within protected areas (Leite et al. 2008; Camurugi et al. 2010; Freitas et al. 2012; Garda et al. 2013; Dias et al. 2014a; Magalhães et al. 2015; Mira-Mendes et al. 2018; Rojas-Padilla et al. 2020), high-

lighting information gaps on the herpetofauna of unprotected areas, making it difficult to identify new areas of ecological relevance.

The Recôncavo Baiano is a region located in the eastern portion of the State of Bahia, corresponding to the portion of land that lies around Todos os Santos Bay (Azevedo 2011). The region has great historical, cultural, and economic importance, standing out for its sugarcane production during the colonial period and, more recently, for its industrial production of petroleum, as well as tobacco and citrus fruits (Sansone 2011). This history of its spatial use was accompanied by intense vegetation suppression and a reduction in original vegetation cover levels. According to data from the Economic-Ecological Zoning of the State of Bahia (Seplan 2015), a management instrument aimed at guiding the use of natural resources, a large part of the Recôncavo Baiano is inserted in the zone called "Tabuleiros Interioranos do Recôncavo" (Interior Trays of the Recôncavo), and only 9.3% of this zone contain the original vegetation cover, although 30% represent a priority area for conservation, revealing alarming levels for biota conservation.

Although a large part of the Recôncavo Baiano is located in the Atlantic Forest, studies characterising the herpetofauna of this region have been conducted almost exclusively in Serra da Jibóia and Serra do Timbó, which represent a set of mountains (elevational range 660–900 m above sea level, respectively) disjoined in the eastern portion of Serra do Espinhaço, in transition with the Caatinga (Juncá 2006; Cruz et al. 2008; Cruz and Napoli 2010; Freitas et al. 2018; Freitas et al. 2019). Furthermore, Freitas (2014) sought to characterise the Atlantic Forest snake fauna of eastern Bahia, including the Recôncavo Baiano; however, despite revealing a high richness of species, his study did not present systematic or standardised searches in the 29 municipalities analysed, which resulted in a sub-sampling in the central portion of the Recôncavo Baiano, including the "Tabuleiros Interioranos".

This panorama reinforces the appeal for increased studies in forested and open areas of eastern Bahia to improve the characterisation of the richness and species composition of the herpetofauna of this portion of the Atlantic Forest. This information is essential to identify and monitor population fluctuations, enabling an accurate diagnosis of the ecosystem's integrity and allowing access to the mechanisms that are involved in generating the region's fauna diversity. In this study, we present a list of amphibian and reptile species that occur in open and forested areas of the municipality of Cruz das Almas, as part of a long-term project that seeks to characterise the herpetofauna of all the municipalities that are part of the Recôncavo Baiano, to minimise differences in the sample efforts along the different regions of the Atlantic Forest and to fill the information gaps regarding the state fauna.

Materials and methods

Study area

The study was conducted in Cruz das Almas municipality, Bahia State, in northeast Brazil (12°40'25"S, 39°06'05"W) (Figure 1). Cruz das Almas is located in the east-

ern portion of Bahia State and inserted in the region of the Recôncavo Baiano, in the Atlantic Forest biome. The region is characterised by original vegetation of Semideciduous Seasonal Forest (Brazão and Araújo 1981); however, it has been almost completely replaced by grazing areas for cattle raising and by plantations. According to the Köppen classification, the climate is tropical monsoon (Am), with an average temperature of 23.9 °C and an annual rainfall of 1,131.2 mm (Silva et al. 2016). Cruz das Almas is located in the area "Tabuleiros Interioranos do Recôncavo" (Interior Trays of the Recôncavo), characterised by a flat and gently undulating top relief, not exceeding 200 m in elevation, in addition to a large amount of micro-basins, which is propitious for agricultural production. Only 5% of the "Tabuleiros Interioranos do Recôncavo" area are inserted in some conservation units, all of them of sustainable use (Seplan 2015).

Field activities were concentrated in three areas of the municipality that presented good conservation status and potential for finding herpetofauna specimens (Figure 2):

(i) Parque Florestal Mata de Cazuzinha (12°39'58"S, 39°06'25"W; elevation 235 m): This is a forest fragment of ca. 20 ha, inserted in an urban matrix. It is considered an area of secondary vegetation, but presents a homogeneous and dense aspect, with predominance of arboreal vegetation of medium and large size. There is no evidence of permanent waterbodies inside the Cazuzinha forest, yet it has a forest structure that enables moisture concentration. Because it is located in an urban environment, the Cazuzinha forest suffers great anthropic pressure associated with hunting, wood removal and waste deposit. The area is intensely frequented by the local population for leisure activities.

(ii) Riacho do Machado (12°40'35.89"S, 39°25'59"W; elevation 226 m): The largest forest patch fragment in Cruz das Almas municipality. It is located between the experimental area of the Empresa Brasileira de Pesquisas Agropecuárias (Brazilian Agricultural Research Corporation) and the campus of the Federal University of Recôncavo da Bahia. This area is inserted in a hillside region and has medium-sized trees. It has a central lake ca. 5 m deep and a stream that names the patch. The homogeneous aspect of the vegetation indicates that the area has not been much accessed for wood removal, probably due to the difficulty of access. Nevertheless, during this study, some actions of burning, cutting and timber extraction were witnessed. Inside the forest, there are regions of "swamps", which are propitious environments for the reproduction of anurans, as well as regions with rocky outcrops.

(iii) Mata da Cascalheira (12°39'29"S, 39°04'48"W; elevation 212 m): Cascalheira forest patch is an area of secondary forest, with predominance of shrubby vegetation and grasses. The forest patch is inserted in a region of hillsides and has a lagoon in the central region, which is ca. 4 m deep and contains large amounts of cattail and macrophytes. Mata da Cascalheira is inserted in the campus of the Federal University of Recôncavo da Bahia, which is a benchmark in agricultural studies. Thus, much of the patch has already been used as pastureland or arable land, with the formation of small puddles during rain events. In addition, it is possible to find

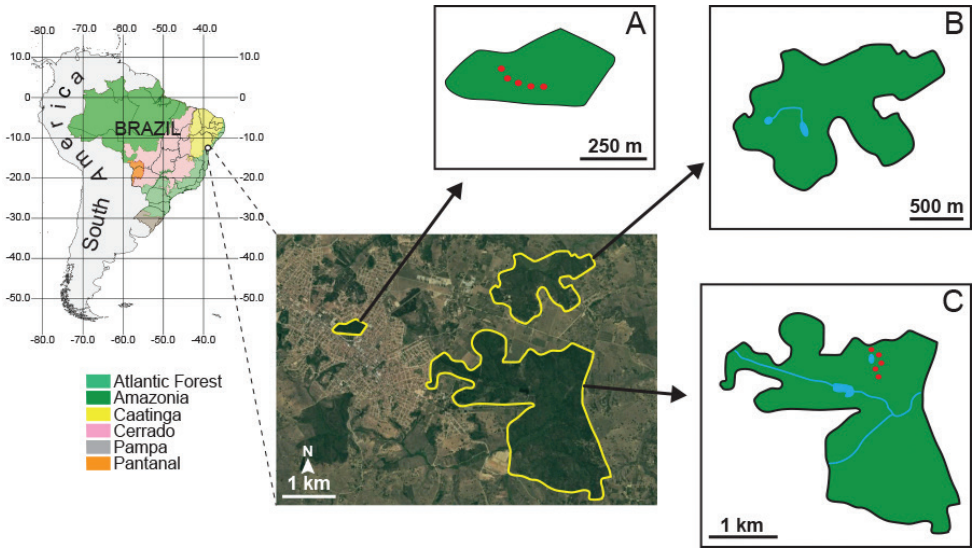

Figure 1. Geographical location of the Cruz das Almas municipality and areas of study **A** Parque Florestal Mata de Cazuzinha **B** Mata da Cascalheira **C** Riacho do Machado. Red dots represent localisation and disposition of the pitfall traps.

some houses near the forest patch, where the residents engage in subsistence farming activity. Some areas of the Mata da Cascalheira were used for the extraction of land and stones for construction.

Data collection

We conducted the field activities from January 2015 to Mach 2019, through non-standard day and night collections in the three different areas, totalling 117 samples. All daytime collections started at 8 am and ended at 5 pm, while night-time collections started at 6 pm and ended at midnight. The collections were performed by at least three and at most eight researchers. To collect the specimens, we used the techniques of visual encountering through random search inside and around the patches, aided by shot guns, and the places investigated were holes, burrows, tree trunks, fallen trunks, the interior of bromeliads, rocks, and all microhabitats conducive to the encounter of individuals in shelter or in activity (Figure 2A–E). For amphibians, we also used the acoustic search to find males in vocalisation activity, concentrating the activities around the waterbodies (Heyer et al. 1994). To enhance the encounter of herpetofauna specimens, we installed five pitfall traps in each area. The traps were arranged in a Y-shape, with four 30-L buckets connected by three 8-m drift fences build with plastic sheets (Figure 2F). The stations were ca. 60 meters apart and remained installed for 32 days in each area; they were inspected daily. The pitfall traps were not efficiently implemented in the Mata da Cascalheira due to the strong human presence, with consequent damage to the buckets, which made it impossible to use

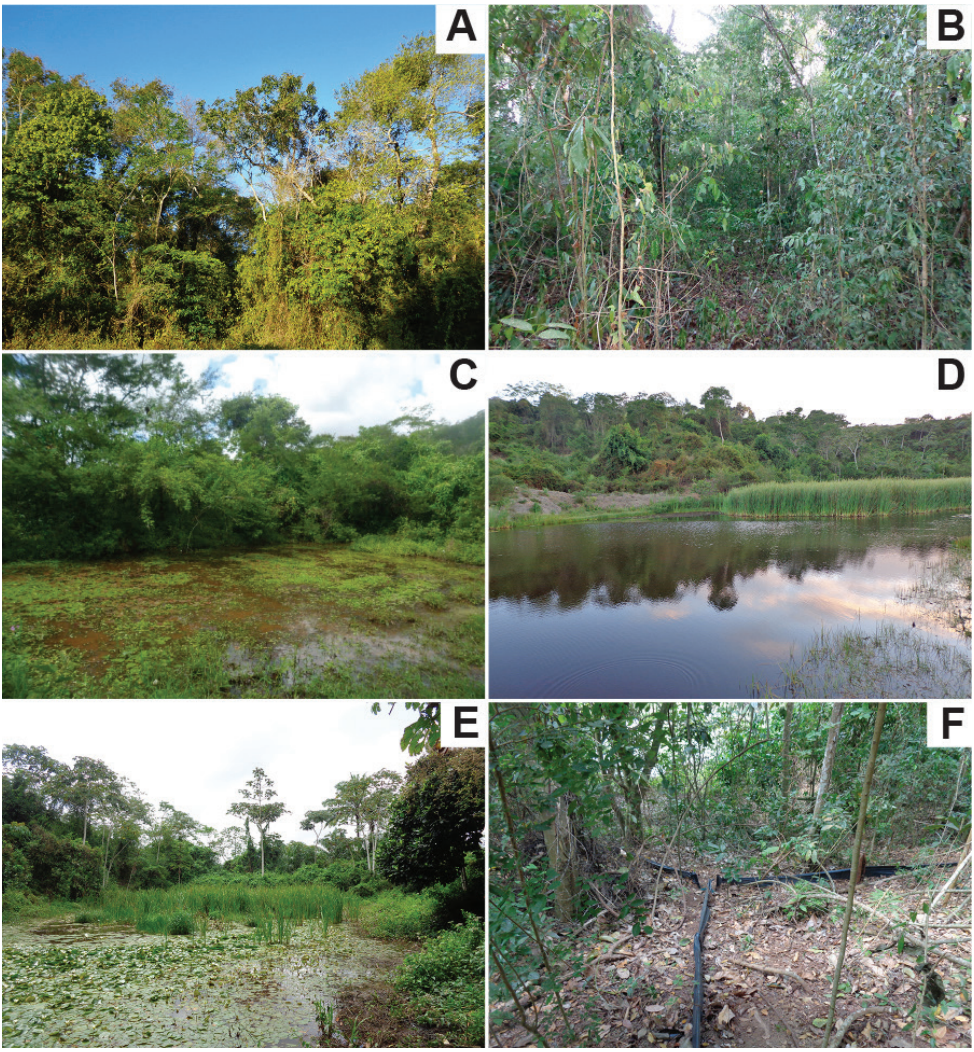

Figure 2. Habitats sampled during the field works **A** view of Mata de Cazuzinha showing tall trees and shrubs **B** inside the Mata de Cazuzinha **C** temporary pond in Mata da Cascalheira **D** lagoon in Mata da Cascalheira **E** temporary pond in the Riacho do Machado **F** pitfall trap in the interior of the forest at Riacho do Machado.

the traps on site. Nevertheless, as we did not seek to perform a comparative analysis between the areas but rather to summarise the species of the herpetofauna found in the region, this scenario did not interfere with our objectives. In addition, we also employed the techniques of occasional encounters and encounters by third parties to better characterise the herpetofauna.

All animals collected were euthanised via intraperitoneal injection of 2% lidocaine, fixed in 10% formaldehyde, preserved in 70% alcohol, and deposited in the Herpeto-

logical Collection of the Universidade Federal do Recôncavo da Bahia (Sisbio Permit 46558-1 and 46558-2; CEUA-UFRB Permit 23007.007559/2016-71). The animals collected had a small fragment of the liver extracted to create a genetic database of the herpetofauna of the Recôncavo Baiano region, providing support for future studies.

Analyses

To evaluate the quality of our sampling effort, we used the data of species richness and abundance of individuals to produce rarefaction curves (1,000 randomisations), using the ESTIMATES 9.1.0 program (Colwell 2013). Since our samples from non-standard samples, we used the individual based curve to standardise our effort, as each sample unit is an individual. Subsequently, the observed richness was compared with the estimated richness from the non-parametric estimators Bootstrap, Chao 2 and Jackknife 1 and 2 (Magurran 2004). As these estimators are sensitive to singletons and doubletons, species with low abundance were inserted in analyses. We built a rarefaction curve for amphibians, a rarefaction curve for lizards, a rarefaction curve for snakes and a rarefaction curve joining all groups (herpetofauna), including amphisbaenians and testudines. In addition, we verified which species are typical of the Atlantic Forest, based on Rossa-Feres et al. (2017) and Tozetti et al. (2017), for amphibians and reptiles, respectively.

Finally, we compared the similarity of the species composition of the amphibian and reptiles of Cruz das Almas with the species composition of other assemblages of the Brazilian Atlantic Forest. We performed an analysis considering only anurans, lizards, and snakes. Data on the composition of anurans from other assemblages were obtained from 32 studies, while data on the composition of lizards and snakes were obtained from 21 studies. For this, we subdivided the Atlantic Forest into four biogeographic sub-regions, based on Silva and Casteleti (2003) to identify regional similarities: (1) north of the São Francisco River, covering the states of Paraíba (PB), Pernambuco (PE), and Rio Grande do Norte (RN) – Mata do Buraquinho (Santana et al. 2008); Macaíba (Magalhães et al. 2013); Boca da Mata (Palmeira and Gonçalves 2015); Serra do Urubu (Roberto et al. 2017); Reserva Biológica (REBIO) Guaribas (Mesquita et al. 2018); (2) south of the São Francisco River, covering the states of Bahia (BA) and Sergipe (SE) – Mata de São João (Couto-Ferreira et al. 2011; Marques et al. 2011); Mata do Junco (Morato et al. 2011); Jequié (Lantyer-Silva et al. 2013); Serra Bonita (Dias et al. 2014a); Conde (Gondim-Silva et al. 2016); Serra da Jibóia (Freitas et al. 2018); Reserva Michelin (Mira-Mendes et al. 2018); Serra do Timbó (Freitas et al. 2019); Serra das Lontras (Rojas-Padilla et al. 2020); Serra Azul and Serra de Mandim (Souza-Costa et al. 2020); (3) southeast Brazil and the Serra do Mar region, covering the states of Espírito Santo (ES), Minas Gerais (MG), São Paulo (SP), and Rio de Janeiro (RJ) – Rio Novo (Feio and Ferreira 2005); Reserva Florestal (RF) de Morro Grande (Dixo and Verdade 2006); Rio Claro (Zina et al. 2007); Estação Ambiental (EA) de Peti (Bertoluci et al. 2009); Ilha de Anchieta (Cicchi et al. 2009); Parque Estadual (PE) Jurupará (Condez et al. 2009); Estação Ecológica (EE)

Juréia-Itatins (Narvaes et al. 2009); Parque Estadual Turístico (PET) do Alto Ribeira (Araujo et al. 2010); Parque Estadual (PE) Carlos Botelho (Forlani et al. 2010); Alto Rio Muriaé (Santana et al. 2010); Estação Ecológica (EE) do Paraíso (Vrcibradic et al. 2011); Serra do Brigadeiro (Moura et al. 2012); Parque Natural Municipal (PNM) de Grumari (Telles et al. 2012); Reserva Ecológica (RE) de Guapiaçu (Almeida-Gomes et al. 2014); São Roque do Canaã (Mônico et al. 2017); and (4) – south Brazil and the Araucaria Forest region, covering the states of Paraná (PR), Santa Cararina (SC) and Rio Grande do Sul (RS) – Rio Grande (Quintela et al. 2006); Parque Estadual (PE) de Itapeva (Colombo et al. 2008); Morretes (Armstrong and Conte 2010); Parque Nacional (PN) das Araucárias (Lucas and Marocco 2011); Parque Natural Municipal (PNM) de Sertão (Zanella et al. 2013). We excluded the species identified at the level of genus and those in which the authors had doubts about the specific epithet. Cluster analysis was performed using the UPGMA algorithm and Jaccard index in the Past 4.05 program (Hammer et al. 2001).

Results

We recorded a total of 1,848 individuals, distributed in 69 species of amphibians and reptiles (31 anurans, 14 lizards, 19 snakes, two amphisbaenians, and three testudines). Additionally, in December 2020, after the end sampling, we found an individual of *Ophiodes striatus* in Mata da Cascalheira, adding a lizard species to the list, totalling 15 lizard species and 70 herpetofauna species. The anurans identified belong to the families Bufonidae (3 spp.), Craugastoridae (1 sp.), Hylidae (13 spp.), Leptodactylidae (11 spp.), Microhylidae (1 sp.) and Phyllomedusidae (2 spp.) (Table 1, Figures 3, 4). The 15 species of lizards belong to the families Dactyloidae (1 sp.), Diploglossidae (2 spp.), Gekkonidae (3 spp.), Gymnophthalmidae (1 sp.), Iguanidae (1 sp.), Mabuyidae (2 spp.), Polychrotidae (1 sp.), Sphaerodactylidae (1 sp.), Teiidae (2 spp.) and Tropiduridae (1 sp.). The 19 snake species belong to the families Boidae (2 spp.), Colubridae (5 spp.), Dipsadidae (9 spp.), Elapidae (1 sp.), Typhlopidae (1 sp.) and Viperidae (1 sp.). The two amphisbaenians species belong to the family Amphisbaenidae (2 spp.), and the testudines belong to the families Chelidae (1 sp.), Emydidae (1 sp.) and Testudinidae (1 sp.) (Table 2, Figures 5–7).

The rarefaction curve approached the asymptote only for amphibians, demonstrating that the sample effort managed to obtain a satisfactory representation of species (Figure 8). However, richness estimators predicted the existence of species not yet added to the list, ranging from one to two species of anurans. For lizards, snakes, and herpetofauna, the rarefaction curves did not reach the asymptote, and the richness estimators added between one and four species, between three and 11 species, and between seven and 21 species, respectively (Table 3). The observation of the species composition of the anurans assemblage from Cruz das Almas revealed the presence of two groups of species: species endemic to the Atlantic Forest (*Rhinella crucifer*, *Pristimantis paulodutrai*, *Boana albomarginata*, *Dendropsophus branneri*, *Dendropsophus elegans*, *Dendropsophus novaisi*, *Phyllomedusa bahiana*, *Scinax auratus*, *Scinax eurydice*) and species

Table 1. Check list of amphibians identified at Cruz das Almas municipality, Bahia State.

Taxon	Species	Abundance
Anura		
Bufonidae	*Rhinella crucifer* (Wied-Neuwied, 1821)	2
	Rhinella granulosa (Spix, 1824)	24
	Rhinella jimi (Stevaux, 2002)	54
Craugastoridae	*Pristimantis paulodutrai* (Bokermann, 1975)	118
Hylidae	*Boana albomarginata* (Spix, 1824)	107
	Boana crepitans (Wied-Neuwied, 1824)	29
	Boana faber (Wied-Neuwied, 1821)	5
	Dendropsophus elegans (Wied-Neuwied, 1824)	229
	Dendropsophus branneri (Cochran, 1948)	84
	Dendropsophus minutus (Peters, 1872)	7
	Dendropsophus novaisi (Bokermann, 1968)	11
	Dendropsophus oliveirai (Bokermann, 1963)	63
	Scinax auratus (Wied-Neuwied, 1821)	46
	Scinax eurydice (Bokermann, 1968)	23
	Scinax pachycrus (Miranda-Ribeiro, 1937)	3
	Scinax x-signatus (Spix, 1824)	60
	Trachycephalus atlas Bokermann, 1966	2
Leptodactylidae	*Leptodactylus fuscus* (Schneider, 1799)	38
	Leptodactylus macrosternum Miranda-Ribeiro, 1926	100
	Leptodactylus mystaceus (Spix, 1824)	16
	Leptodactylus natalensis Lutz, 1930	24
	Leptodactylus vastus Lutz, 1930	24
	Leptodactylus troglodytes Lutz, 1926	54
	Physalaemus albifrons (Spix, 1824)	1
	Physalaemus cuvieri Fitzinger, 1826	106
	Physalaemus kroyeri (Reinhardt & Lütken, 1862)	95
	Pseudopaludicola cf. *mystacalis* (Cope, 1887)	1
	Pseudopaludicola florencei Andrade, Haga, Lyra, Leite, Kwet, Haddad, Toledo & Giaretta, 2018	16
Microhylidae	*Dermatonotus muelleri* (Boettger, 1885)	10
Phyllomedusidae	*Phyllomedusa bahiana* Lutz, 1925	13
	Pithecopus nordestinus (Caramaschi, 2006)	30

distributed in two or more biomes (*Rhinella granulosa*, *Rhinella jimi*, *Boana crepitans*, *Boana faber*, *Dendropsophus minutus*, *Dendropsophus oliveirai*, *Scinax x-signatus*, *Scinax pachycrus*, *Trachycephalus atlas*, *Pithecopus nordestinus*, *Leptodactylus fuscus*, *Leptodactylus macrosternum*, *Leptodactylus mystaceus*, *Leptodactylus natalensis*, *Leptodactylus troglodytes*, *Leptodactylus vastus*, *Physalaemus albifrons*, *Physalaemus cuvieri*, *Physalaemus kroyeri*, *Pseudopaludicola* cf. *mystacalis*, *Pseudopaludicola florencei*, *Dermatonotus muelleri*). For lizards, only *Phyllopezus lutzae* and *Dryadosaura nordestina* are endemic to the Atlantic forest, while for snakes only *Bothrops leucurus* is endemic.

The cluster analysis revealed that the assemblages of anurans, lizards, and snakes from Cruz das Almas formed close groups with those assemblages from northeast Brazil, specifically from north and south of the São Francisco River. This result indicates that there is a faunal similarity between assemblages inserted in the Central Corridor of the Atlantic Forest and the Pernambuco Endemism Centre (Figures 9–11). The anuran assemblage was more similar to the Conde assemblage, whereas the snake assemblage was more similar to the Mata do Buraquinho and REBIO Guaribas assemblages. For lizards, the Cruz das Almas assemblage was more similar to the Serra do Timbó, Serra da Jibóia, Mata de São João, REBIO Guaribas, Mata do Junco, Serra do Urubu, and Mata do Buraquinho assemblages.

Figure 3. Anuran species identified at Cruz das Almas municipality, Bahia State **A** *Rhinella crucifer* **B** *Rhinella granulosa* **C** *Rhinella jimi* **D** *Pristimantis paulodutrai* **E** *Boana albomarginata* **F** *Boana crepitans* **G** *Boana faber* **H** *Dendropsophus branneri* **I** *Dendropsophus elegans* **J** *Dendropsophus minutus* **K** *Dendropsophus novaisi* **L** *Dendropsophus oliveirai* **M** *Scinax auratus* **N** *Scinax eurydice* **O** *Scinax pachycrus*.

Discussion

The anuran species richness identified in Cruz das Almas corresponds to 5% of the anuran richness currently known for the Atlantic Forest (Rossa-Feres et al. 2017) and 2.8% of the anuran richness of Brazil (Segalla et al. 2019). Furthermore, 29% of the

Table 2. Check list of reptiles identified at Cruz das Almas municipality, Bahia State.

Taxon	Species	Abundance
Squamata		
Amphisbaenidae	*Amphisbaena alba* Linnaeus, 1758	14
	Amphisbaena vermicularis Wagler, 1824	5
Lizards		
Dactyloidae	*Norops fuscoauratus* (D'Orbigny, 1837)	9
Diploglossidae	*Diploglossus lessonae* Peracca, 1890	2
	Ophiodes striatus (Spix, 1824)	1
Gekkonidae	*Hemidactylus mabouia* (Moreau de Jonnès, 1818)	144
	Phyllopezus lutzae (Loveridge, 1941)	11
	Phyllopezus pollicaris (Spix, 1825)	50
Gymnophthalmidae	*Dryadosaura nordestina* Rodrigues, Freire, Pellegrino & Sites, 2005	1
Iguanidae	*Iguana iguana* (Linnaeus, 1758)	1
Mabuyidae	*Brasiliscincus heathi* (Schmidt & Inger, 1951)	5
	Psychosaura macrorhyncha (Hoge, 1946)	2
Polychrotidae	*Polychrus acutirostris* Spix, 1825	3
Sphaerodactylidae	*Coleodactylus meridionalis* (Boulenger, 1888)	19
Teiidae	*Ameiva ameiva* (Linnaeus, 1758	35
	Salvator merianae Duméril & Bibron, 1839	4
Tropiduridae	*Tropidurus hispidus* (Spix, 1825)	72
Snakes		
Boidae	*Boa constrictor* Linnaeus, 1758	4
	Epicrates assisi Machado, 1945	5
Colubridae	*Chironius carinatus* (Linnaeus, 1758)	1
	Erythrolamprus miliaris (Linnaeus, 1758)	1
	Erythrolamprus reginae (Linnaeus, 1758)	3
	Leptodeira annulata (Linnaeus, 1758)	1
	Tantilla melanocephala (Linnaeus, 1758)	2
Dipsadidae	*Dipsas neuwiedi* (Ihering, 1911)	3
	Helicops leopardinus (Schlegel, 1837)	1
	Pseudoboa nigra (Duméril, Bibron & Duméril, 1854)	5
	Oxyrhopus petolarius (Linnaeus, 1758)	1
	Oxyrhopus trigeminus Duméril, Bibron & Duméril, 1854	6
	Philodryas olfersii (Lichtenstein, 1823)	7
	Philodryas patagoniensis (Girard, 1858)	1
	Thamnodynastes pallidus (Linnaeus, 1758)	3
	Xenodon merremii (Wagler, 1824)	3
Elapidae	*Micrurus ibiboboca* (Merrem, 1820)	17
Typhlopidae	*Amerotyphlops brongersmianus* (Vanzolini, 1976)	3
Viperidae	*Bothrops leucurus* Wagler, 1824	6
Testudines		
Chelidae	*Phrynops geoffroanus* (Schweigger, 1812)	1
Emydidae	*Trachemys dorbigni* (Duméril & Bibron, 1835)	1
Testudinidae	*Chelonoidis carbonarius* (Spix, 1824)	1

anuran species identified in the Cruz das Almas assemblage are endemic to the Atlantic Forest (Rossa-Feres et al. 2017). The richness of Cruz das Almas anurans, when compared to other assemblages in the Atlantic Forest, revealed a value similar to those from the north and the south of the São Francisco River (Morato et al. 2011, n = 33; Lantyer-Silva et al. 2013, n = 31; Magalhães et al. 2013, n = 34; Palmeira and Gonçalves 2015, n = 32; Mesquita et al. 2018, n = 34) and higher than some assemblages from south and southeast Brazil (Feio and Ferreira 2005, n = 20; Zina et al. 2007, n = 24; Narvaes et al. 2009, n = 20; Zanella et al. 2013, n = 23). However, it was a lower value

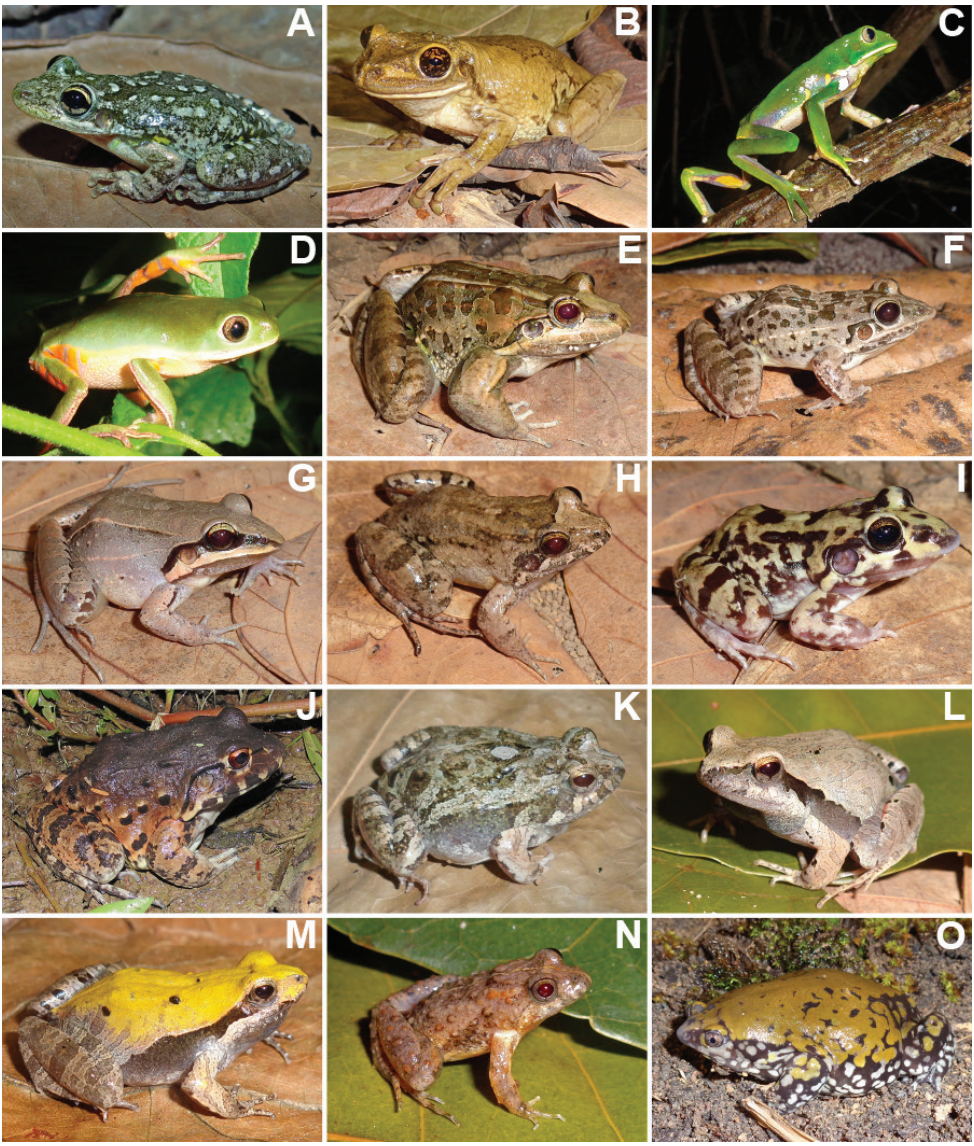

Figure 4. Anuran species identified at Cruz das Almas municipality, Bahia State **A** *Scinax x-signatus* **B** *Trachycephalus atlas* **C** *Phyllomedusa bahiana* **D** *Pithecopus nordestinus* **E** *Leptodactylus macrosternum* **F** *Leptodactylus fuscus* **G** *Leptodactylus mystaceus* **H** *Leptodactylus natalensis* **I** *Leptodactylus troglodytes* **J** *Leptodactylus vastus* **K** *Physalaemus albifrons* **L** *Physalaemus cuvieri* **M** *Physalaemus kroyeri* **N** *Pseudopaludicola florencei* **O** *Dermatonotus muelleri*.

than those from other assemblages from southeast Brazil (Araujo et al. 2010, n = 58; Forlani et al. 2010, n = 64; Moura et al. 2012, n = 57; Almeida-Gomes et al. 2014, n = 70) and from the north of the São Francisco River (Roberto et al. 2017, n = 46). Within Bahia State, the richness of Cruz das Almas revealed a similar value to the as-

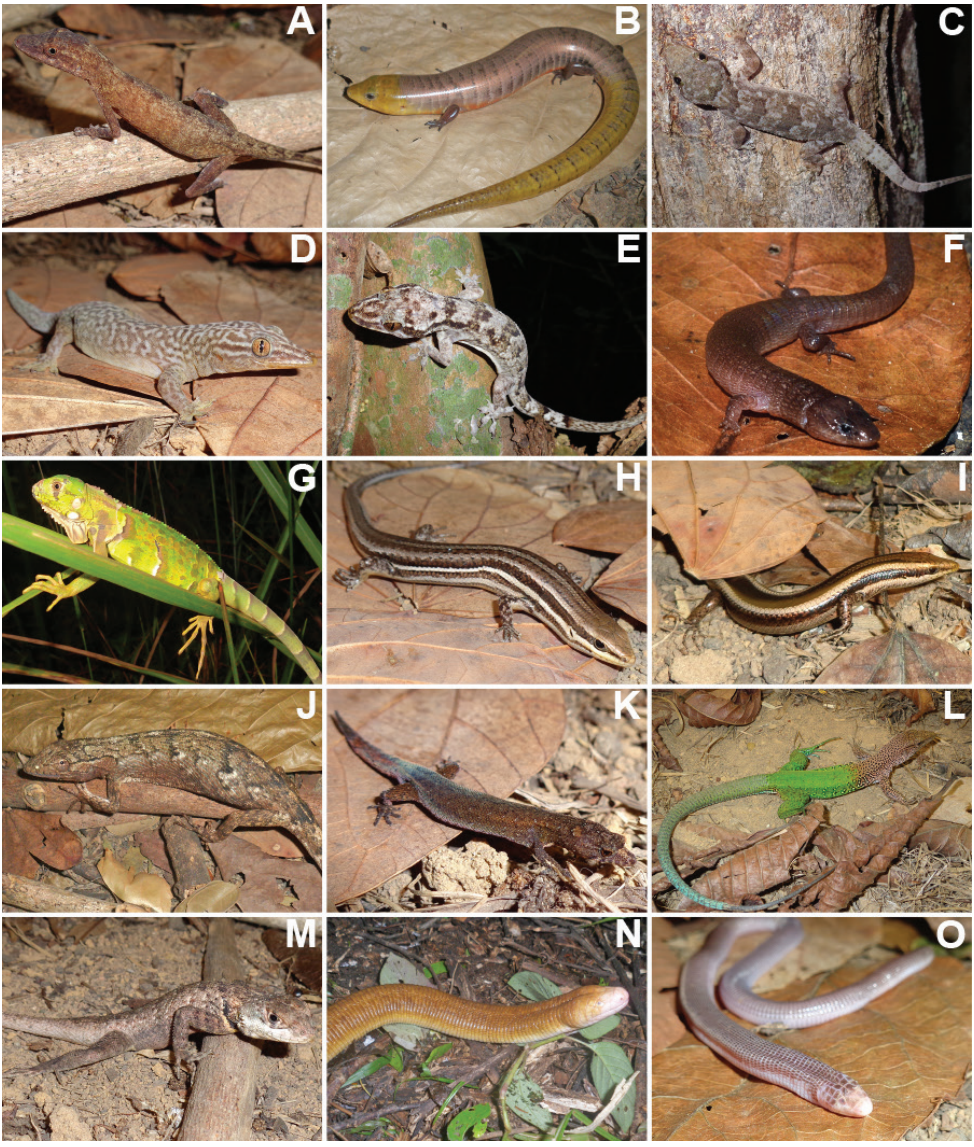

Figure 5. Reptile species identified at Cruz das Almas municipality, Bahia State **A** *Norops fuscoauratus* **B** *Diploglossus lessonae* **C** *Hemidactylus mabouia* **D** *Phyllopezus lutzae* **E** *Phyllopezus pollicaris* **F** *Dryadosaura nordestina* **G** *Iguana iguana* **H** *Brasiliscincus heathi* **I** *Psychosaura macrorhyncha* **J** *Polychrus acutirostris* **K** *Coleodactylus meridionalis* **L** *Ameiva ameiva* **M** *Tropidurus hispidus* **N** *Amphisbaena alba* **O** *Amphisbaena vermicularis*.

semblages from the southeast (Dias et al. 2014b, n = 33–40) and the northern coast (Juncá 2006, n = 25; Bastazini et al. 2007, n = 30; Gondim-Silva et al. 2016, n = 33). Conversely, this value was low when compared with some southern (Dias et al. 2014a, n = 79; Rojas-Padilla et al. 2020, n = 49) and southeast (Mira-Mendes et al. 2018, n = 68) assemblages of the state.

Figure 6. Reptile species identified at Cruz das Almas municipality, Bahia State **A** *Boa constrictor* **B** *Epicrates assisi* **C** *Chironius carinatus* **D** *Erytrolamprus miliaris* **E** *Erytrolamprus reginae* (juvenile) **F** *Leptodeira annulata* **G** *Tantilla melanocephala* **H** *Dipsas neuwiedi* **I** *Pseudoboa nigra* (juvenile) **J** *Pseudoboa nigra* (adult) **K** *Oxyrhopus petolarius* **L** *Oxyrhopus trigeminus* **M** *Philodryas olfersii* **N** *Philodryas patagoniensis* **O** *Thamnodynastes pallidus*.

According to Lantyer-Silva et al. (2013), locations within the Atlantic Forest where the richness of amphibians ranging around 32 species can be considered as having an intermediate richness, which seems to be a common pattern for assemblages of Atlantic Forest-Caatinga ecotones. These assemblages are characterised by

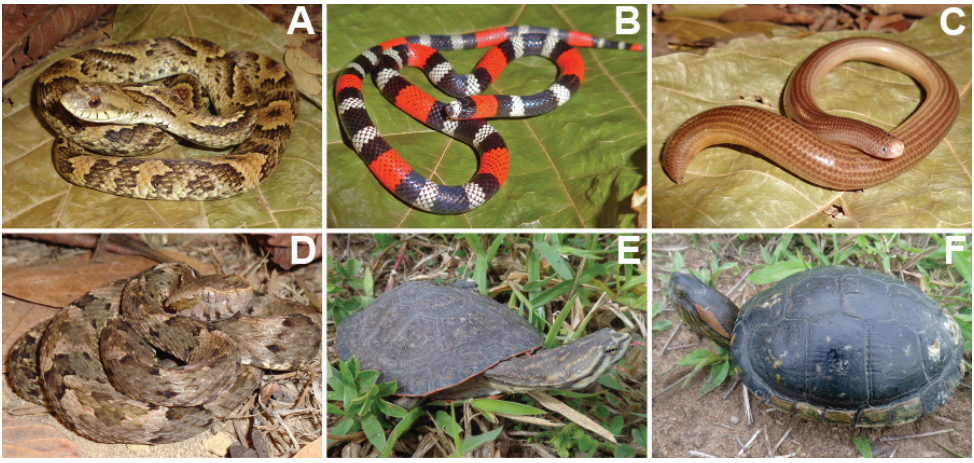

Figure 7. Reptile species identified at Cruz das Almas municipality, Bahia State **A** *Xenodon merremii* **B** *Micrurus ibiboboca* **C** *Amerotyphlops brongersmianus* **D** *Bothrops leucurus* **E** *Phrynops geoffroanus* **F** *Trachemys dorbigni*.

Table 3. Mean and standard deviation of the species richness estimated with different estimators in Cruz das Almas municipality. Herpetofauna represent the combination of amphibians, lizards, snakes, amphisbaenians, and testudines.

	Amphibians	Lizards	Snakes	Herpetofauna
Observed richness	31	15	19	70
Bootstrap	32 ± 0	16 ± 0	22 ± 0	77 ± 0
Chao 2	31 ± 0.62	16 ± 1.79	26 ± 8.06	81 ± 8.05
Jackknife 1	33 ± 1.39	18 ± 1.68	25 ± 2.32	84 ± 3.58
Jackknife 2	31 ± 0	19 ± 0	30 ± 0	91 ± 0
Singletons	2	3	6	14

higher species richness than the Caatinga, as well as a species composition common to both biomes (Lantyer-Silva et al. 2013). Thus, the richness and composition of species of the anurans assemblage from Cruz das Almas leads to a fauna characteristic of transition zones between the Atlantic Forest and Caatinga biomes, even though Cruz das Almas municipality is inserted into the Atlantic Forest biome. This scenario goes against our initial expectations. We expected that the Cruz das Almas assemblage would reveal a greater quantity of endemic species of the Atlantic Forest. However, the species composition was dominated by generalist species, typically associated with open lands. We did not rule out the possibility that the species composition observed in this study is associated with the history of intense land use, the accentuated suppression of vegetation and changes in the natural landscape of Cruz das Almas, which reflected the formation of secondary forest patches, as well as intense open areas destined for pasture and plantation. This remarkable anthropisation may have promoted the selection of species more tolerant to landscape changes, as well as the extinction of species more specialised in forest habitats, causing a reduction in richness (Almeida-Gomes and Rocha 2014). However, studies that seek to verify the variation in species

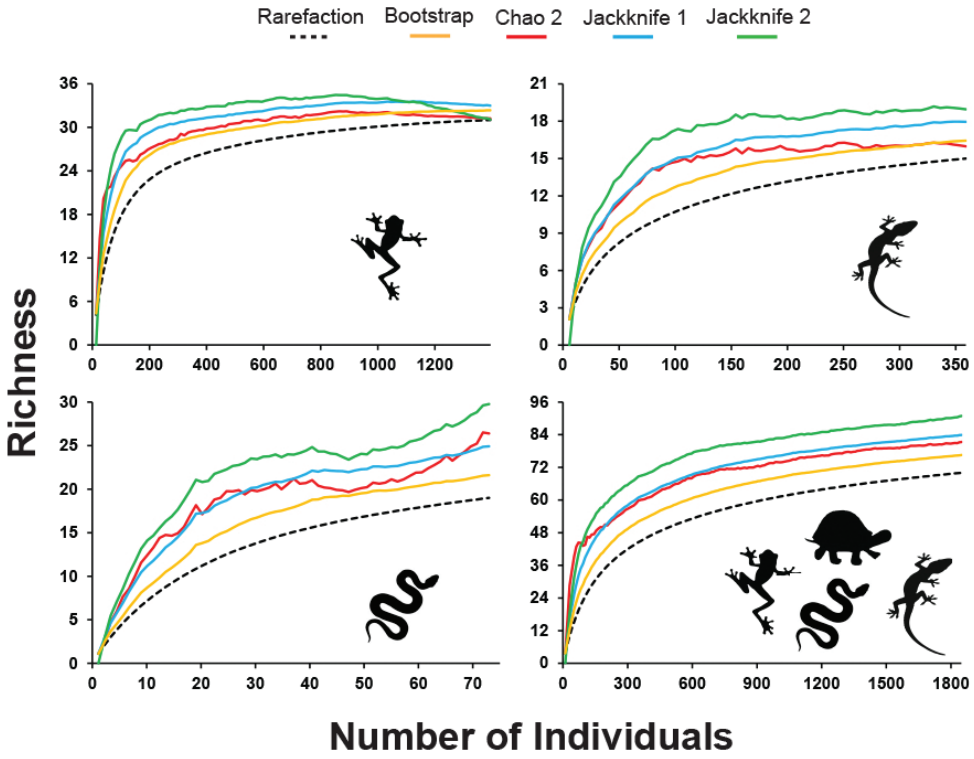

Figure 8. Species rarefaction curves and richness estimators for amphibians, lizards, snakes and herpetofauna collected at Cruz das Almas municipality. Herpetofauna represent the combination of amphibians, lizards, snakes, amphisbaenians, and testudines.

composition between areas with different levels of conservation in this region could better clarify this assumption.

None of the anuran species found in our study revealed an unusual or unexpected record for the region, having been previously reported for the State of Bahia and the Atlantic Forest (Dias et al. 2014a; Gondim-Silva et al. 2016; Freitas et al. 2018; Mira-Mendes et al. 2018; Freitas et al. 2019). Nevertheless, we report a new record of the recently described *Pseudopaludicola florencei* for Bahia State. Besides the locality type (Andaraí, Bahia), the species has been recognised in only two localities (Mutuípe, in the State of Bahia and Nanuque, in the State of Minas Gerais) (Andrade et al. 2018). In Cruz das Almas, *P. florencei* was observed vocalising in small puddles or fillets of water formed after the first rains, always in open areas near Riacho do Machado and Mata da Cascalheira. The species was identified on the basis of morphological and acoustic characteristics, consistent with the original description. Thus, we believe that a more accurate analysis of the advertisement call of other individuals of the genus *Pseudopaludicola* can reveal the presence of the species in other localities of the Atlantic Forest of the east of Bahia.

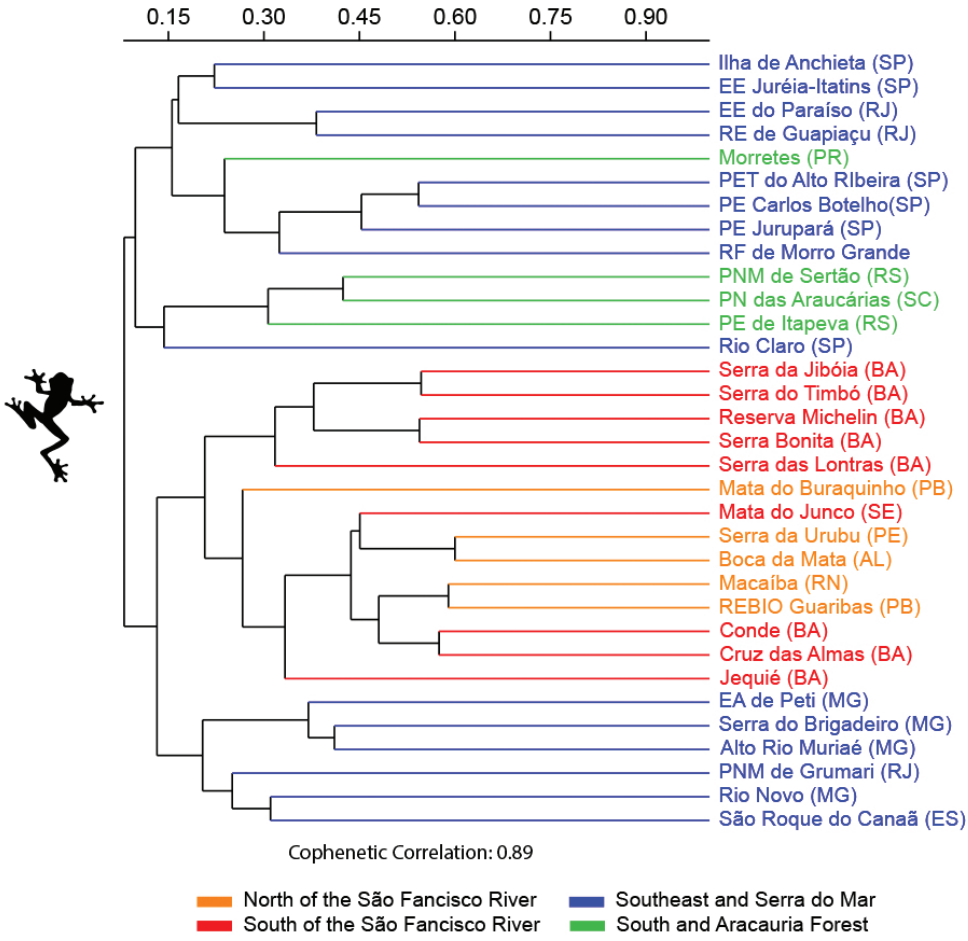

Figure 9. Dendrogram of cluster analysis (Jaccard Indices) of the anuran species composition from 33 localities in Brazilian Atlantic Forest. Abbreviations in Materials and methods.

The Cruz das Almas assemblage presented a low number of typical species from forested areas and prevalence of typical species from open land. This result explains the greater similarity of the Cruz das Almas assemblage with other assemblage from open land and Atlantic Forest-Caatinga ecotones observed in our cluster analysis. Anthropic actions may have shaped the current pattern of the Cruz das Almas assemblage, leading to the reduction of species more specialised to forest habitats. This scenario reveals the need for greater efforts to preserve the remaining forest fragments in the region. Nevertheless, *Pristimantis paulodutrai* was the dominant species in the interior of forest fragments in Mata de Cazuzinha, often found vocalising perched on herbaceous vegetation. Besides *P. paulodutrai*, only *Rhinella jimi*, *Leptodactylus troglodytes*, *Physalaemus cuvieri*, and *Physalaemus kroyeri* were also identified in the Mata de Cazuzinha, but only on the edge, where they used waterbodies formed after the rains. We believe that

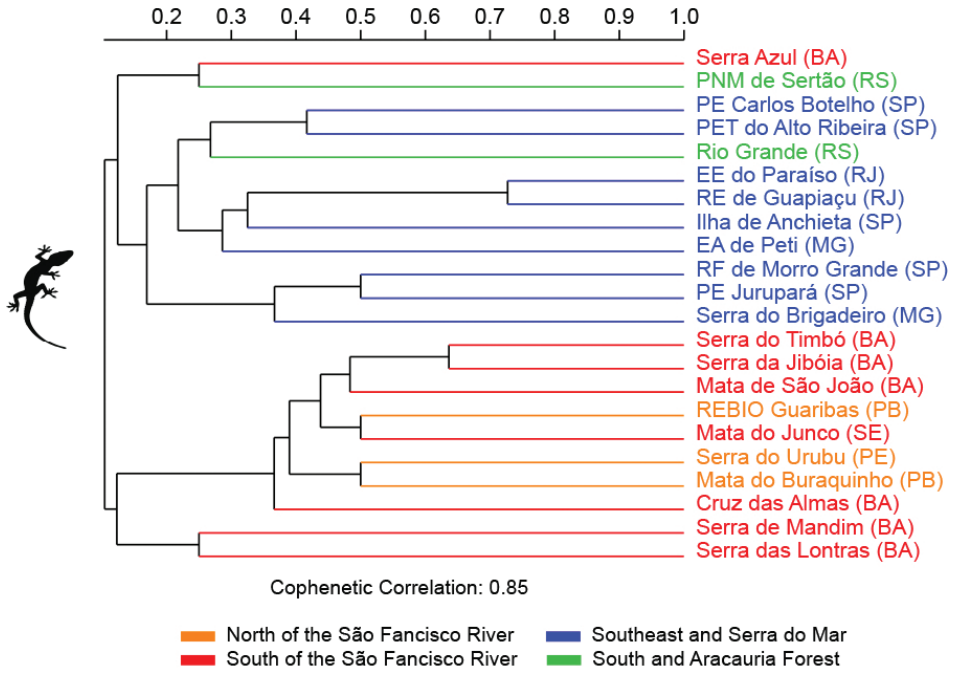

Figure 10. Dendrogram of cluster analysis (Jaccard Indices) of the lizard species composition from 22 localities in Brazilian Atlantic Forest. Abbreviations in Materials and methods.

P. paulodutrai's dominance of the urban forest fragment is due to the absence of waterbodies inside the fragment, which may have limited the permanence of other species.

The reptile species richness of the Cruz das Almas assemblage corresponds to 12.5% of the known reptile richness for the Atlantic Forest (Tozetti et al. 2017) and to 4.9% of the known species richness for Brazil (Costa and Bérnils 2018). Considering the taxa individually, for the Atlantic Forest, the lizards richness corresponds to 17.9%, that of snakes to 10%, that of amphisbaenians to 9.1% and that of testudines to 21.4% (except for *Trachemys dorbigni*) of the biome richness, while for Brazil, the lizard richness corresponds to 5.4%, that of snakes to 4.7%, that of amphibians to 2.8% and that of testudines to 5.5% (Tozetti et al. 2017; Costa and Bérnils 2018). Attempts to compare the richness of reptiles identified in the Cruz das Almas assemblages with the richness of other assemblages of the Atlantic Forest of the Bahia State were hampered due to the lack of systematic inventories involving the different taxonomic categories. We noticed the presence of robust information for snakes, while the information was less common for lizards, evidencing the need for greater efforts to characterise the species of the group in the several phyto-physiognomies of the Atlantic Forest of the State.

For the lizards, our results revealed the presence of species previously recorded for Bahia State and the Atlantic Forest (Couto-Ferreira et al. 2011; Hamdan and Lira-da-Silva 2012; Freitas 2014). However, a comparison of the assemblage richness of Cruz das Almas lizards with that of other assemblages from the Atlantic Forest revealed a

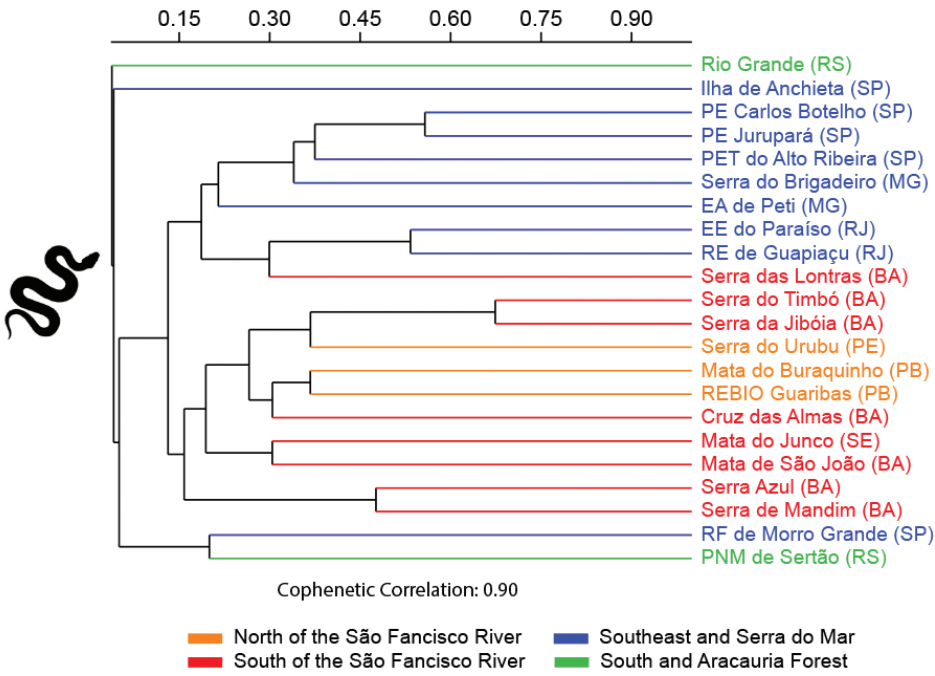

Figure 11. Dendrogram of cluster analysis (Jaccard Indices) of the snake species composition from 22 localities in Brazilian Atlantic Forest. Abbreviations in Materials and methods.

value similar to that of assemblages in the north and south of the São Francisco River (Santana et al. 2008, *n* = 13; Roberto et al. 2017, *n* = 16), while the value was higher in relation to several assemblages in the south and southeast of Brazil (Dixo and Verdade 2006, *n* = 5; Quintela et al. 2006, *n* = 8; Bertoluci et al. 2009, *n* = 5; Forlani et al. 2010, *n* = 10; Moura et al. 2012, *n* = 9; Almeida-Gomes et al. 2014, *n* = 10) and lower in relation to one assemblage north of the São Francisco River (Mesquita et al. 2018, *n* = 20). Observing the richness of only the assemblages within the State of Bahia, the richness found in the present study was inferior to the richness of lizards from the northern coast (Couto-Ferreira et al. 2011, *n* = 23), Serra da Jibóia (Freitas et al. 2018, *n* = 19), and Serra do Timbó (Freitas et al. 2019, *n* = 19). However, the richness of Cruz das Almas lizards was higher than that recorded for nine sand dunes of the southern and northern coast of Bahia (Dias and Rocha 2014, *n* = 4–11), mountainous forests in southern Bahia (Rojas-Padilla et al. 2020, *n* = 7), fragments of ombrophilous forest of southeast Bahia (Dias et al. 2014b, *n* = 3 or 4), and the semideciduous seasonal forest of southeast Bahia (Souza-Costa et al. 2020, *n* = 6). Although the richness estimators revealed that there are lizard species that have not yet been sampled in the Cruz das Almas assemblage, their values were low, indicating that there may be few species. Additionally, the dissimilarity between the Cruz das Almas lizard assemblage and other assemblages from the Brazilian northeast, in particular those that formed the largest group, may be associated with the absence of some species, such

as *Ameivula ocellifera*, *Enyalius bibronii*, *Enyalius catenatus*, *Gymnodactylus darwinii*, *Kentropyx calcarata*, *Polychrus marmoratus*, and *Tropidurus semitaeniatus*. These species are frequently found in inventory studies (see Roberto et al. 2017; Freitas et al. 2018; Mesquita et al. 2018), and their absence in the Cruz das Almas assemblage may have led to the pattern observed in our cluster.

Analysis of the species composition revealed two endemic species of the Atlantic Forest (*Phyllopezus lutzae* and *Dryadosaura nordestina*), which corresponds to 14.9% of the lizard fauna recorded in the study (Tozetti et al. 2017). The presence of *P. lutzae*, *Diploglossus lessonae*, and *D. nordestina* can be considered unusual records for Cruz das Almas. *Phyllopezus lutzae* has the type locality Salvador, the capital of the Bahia State (Loveridge 1941), and since its description, the species has been reported for areas of Atlantic Forest in northeastern Brazil, often associated with restinga environments and using bromeliads as microhabitat (Vrcibradic et al. 2000; Albuquerque et al. 2019). In Cruz das Almas, the species was found inside the forests, using bromeliads and tree trunks, in syntopia with the congener *Phyllopezus pollicaris*. In addition, the species was also found on the edge of the forest patches, on the trunks of trees that had epiphytic bromeliads and isolated in pasture matrices. This record represents the distribution of the species outside the restinga environment, with insertion in interior forest patches, and highlights the need for efforts directed at expanding information on the spatial distribution and behaviour of the species.

The lizard *Diploglossus lessonae* can be found in areas of Atlantic Forest and Caatinga in northeast Brazil (Vanzolini et al. 1980). Although the presence of this species is well documented north of the São Francisco River, reports for Bahia are limited to the municipalities of Feira de Santana, Miguel Calmon and Santo Amaro (see Caldas et al. 2016), with the last report in 2009 (ca. 12 years ago). It is possible that the scarcity of information on *D. lessonae* records for the Bahia State is associated with the secretive habit and burrowing behaviour of the species (Vitt 1985), requiring greater field effort. In Cruz das Almas, *D. lessonae* was found in habitat with slightly compacted soil and higher density of leaf litter, which is perhaps a characteristic of the essential habitat for the presence of the species. Finally, *Dryadosaura nordestina* is a species distributed in an area of Atlantic Forest of the Brazilian northeast. Although the occurrence of the species is well documented (Garda et al. 2014), information on populations in the State of Bahia is still scarce, and the species was included in the list of threatened fauna of the State of Bahia, in the vulnerable category (Sema 2017). A single individual from *D. nordestina* was found in Cruz das Almas, accessed through a pitfall trap in Mata de Cazuzinha. These data are different from the data of Lion et al. (2016), who pointed out *D. nordestina* as the most abundant species in small forest patches in the Rio Grande do Norte State. We believe that the increase in sample effort in more interior forest patches in eastern Bahia may reveal new records of occurrence of *Phyllopezus lutzae*, *D. lessonae*, and *D. nordestina*. Nevertheless, the encounter of *D. lessonae* and *D. nordestina* in the urban forest fragment highlights the importance of the preservation of the forest enclaves to maintain populations of these species.

For snakes, none of the species found in our study represents a new finding, as they are species that were previously registered in the State of Bahia and for the Atlantic Forest (Argôlo 2004; Hamdan and Lira-da-Silva 2012; Freitas 2014; Marques et al. 2016). Furthermore, *Bothrops leucurus* was the only species with a distribution endemic to the Atlantic Forest. A comparison of the richness of Cruz das Almas snakes with other assemblages of the Atlantic Forest revealed a similar value with several assemblages from north and south of the São Francisco River (Santana et al. 2008, n = 18; Marques et al. 2011, n = 15; Morato et al. 2011, n = 15) and south (Quintela et al. 2006, n = 16) and southeast Brazil (Araujo et al. 2010, n = 22; Vrcibradic et al. 2011, n = 19; Almeida-Gomes et al. 2012, n = 24). However, the richness value was lower than that observed in some snake assemblages in southeast Brazil (Condez et al. 2009, n = 46; Forlani et al. 2010, n = 48; Moura et al. 2012, n = 29) and north of the São Francisco River (Mesquita et al. 2018, n = 42). Within Bahia State, the snake richness of Cruz das Almas was lower than that registered on the northern coast (Marques et al. 2016, n = 50), Serra da Jibóia (Freitas et al. 2018, n = 37) and the southern and southeastern forests (Argôlo 2004, n = 61; Rojas-Padilla et al. 2020, n = 41) of the State. Moreover, the richness of snakes was greater than that obtained by Dias et al. (2014b) for four localities between the municipalities of Almadina, Floresta Azul, Ilhéus in southeast Bahia (5–8 species), and by Dias and Rocha (2014), who investigated the composition of snakes in nine localities of the sand dunes of Bahia (0–4 species). Nevertheless, the richness of Cruz das Almas snake species was similar to that obtained by Souza-Costa et al. (2020) for fragments of semideciduous seasonal forest in the Serras de Mandim and Azul in southwestern Bahia (13–18 species).

We believe that the difference in snake species richness between the assemblages of the Bahia State may be more associated with the sample design involved in the data collection than necessarily with a biological effect arising from the locality and study area. Dias et al. (2014b) performed a rapid inventory for data collection (12 days), which may have made it impossible to find seasonal or less abundant species, while Dias and Rocha (2014) only performed monitoring in restinga areas, not including other phyto-physiognomies, which may have reduced the sampling power only for species frequenting sand dunes. Similarly, the studies that showed high richness covered extensive areas, encompassing several municipalities and including different phyto-physiognomies (Argôlo 2004; Marques et al. 2016; Freitas et al. 2018). Thus, considering the existence of a directly proportional relationship between area vs. richness (Magurran 2004), it is possible that the size of the study area explains the variation in richness between studies and makes comparisons difficult.

Although we found a species richness similar to that presented by Souza-Costa et al. (2020), we noticed a difference in the composition of snake species, with the Cruz das Almas assemblage being dominated by species with a habit of living in open environments or being generalists in the use of habitat (Argôlo 2004), while there was a depletion of species more specialised to forested environments, typically of the genera *Corallus*, *Clelia*, *Dipsas*, and *Imantodes* and with previous records in the Serra da Jibóia (Freitas et al. 2018) and Serra do Timbó (Freitas et al. 2019), ca. 46 and 80 km from Cruz das Almas, respectively, and which we expected to be found in the studied area.

The lack of more specialised species in forest environments may help explain why the Cruz das Almas snake assemblage was more similar to the Mata do Buraquinho and REBIO Guaribas assemblages. The former is inserted in an Atlantic Open Forest ecosystem and is characterised by being a less dense forest with opened canopy (Marques et al. 2021). The latter is inserted in an ecosystem of Stational Semidecidual Forest and "tabuleiros", a type of vegetation of savanna similar to the Cerrado (Mesquita et al. 2018). Thus, these assemblages are subject to the dominance of species adapted to live in more open lands. As for the anurans, we believe that the absence of snakes specialised to forested environments that were expected to be found in the Cruz das Almas assemblage is an effect of anthropisation and habitat alteration, with the accentuated reduction and transformation of forested environments into cultivable areas and housing.

Finally, in this study, we report a new record of the water tiger *Trachemys dorbigni* for the Bahia State. The species is distributed throughout southern South America, in the countries of Argentina, Uruguay and Brazil, especially in the States of Rio Grande do Sul and Santa Catarina (Uetz et al. 2019). However, it is considered introduced into the Atlantic Forest (Tozetti et al. 2017) and has already been registered in the municipality of Salvador, capital of the Bahia State (Ecoa 2013). In Cruz das Almas, *T. dorbigni* was found wandering in a pasture area, with the presence of some sprawling residences. Thus, we do not rule out the possibility that the individual was being raised as a pet. Recent data have shown that Brazil has an intense reptile trade, which was enhanced by online shopping (Alves et al. 2019). In addition, the Recôncavo Baiano has a strong local trade of reptiles, with snakes being the main group traded (Macedo 2018). For Sy (2015) breeding reptiles as pets can promote the entry of exotic animals into ecosystems, and this is an extremely harmful phenomenon for native biota. Although we have no evidence that the presence of *T. dorbigni* in the studied assemblages comes from the trade of wild animals, we warn about the growth of the activity in the Recôncavo Baiano and the potential environmental damage that this entails, especially for ecosystems that are already heavily impacted.

The two amphisbaenian species identified in our study are common and frequently recorded in the Atlantic Forest inventories from the Brazilian northeast (Couto-Ferreira et al. 2011; Freitas et al. 2018; Mesquita et al. 2018). Despite the fossorial habit of the group, the number of species recorded in our study was similar to that recorded in other studies in the Atlantic Forest (Santana et al. 2008; Roberto et al. 2017; Rojas-Padilla et al. 2020). Perhaps the long-term fieldwork and the use of different methods of data collection have been important to record these organisms. Finally, the present study shows new data about the species composition of the herpetofauna in the Atlantic Forest of the east of Bahia, which helps to fill the information gap about the herpetofauna in unprotected areas. We highlight the prevalence of generalist species, typically associated with open lands and the presence of the threatened lizard *Dryadosaura nordestina*, as well as the invasive turtle *Trachemys dorbigni* in forest patches. This information can be helpful for characterising the fauna of this region and the factors involved in determining the composition of amphibian and reptile species in other assemblages in the Atlantic Forest of northeast Brazil.

Acknowledgements

We thank Joanna K. G. Oliveira, Diego S. Macedo, Ubiraci R. Carmo Júnior, and Lucas S. Nascimento for their valuable contributions in field work. We thank the ICMbio for collection license. We thank Daniel O. Mesquita and an anonymous reviewer for comments and suggestions that improved this article.

References

Albuquerque PRA, Morais MSR, Moura PTS, Santos WNS, Costa RMT, Delfim FR, Pontes BES (2019) *Phyllopezus lutzae* (Loveridge, 1941) (Squamata, Phyllodactylidae): new records from the Brazilian state of Paraíba. Check List 15: 49–53. https://doi.org/10.15560/15.1.49

Almeida-Gomes M, Siqueira CC, Borges-Junior VNT, Vrcibradic D, Fusinatto LA, Rocha CFD (2014) Herpetofauna of the Reserva Ecológica de Guapiaçu (REGUA) and its surrounding areas, in the state of Rio de Janeiro, Brazil. Biota Neotropica 14: 1–15. https://doi.org/10.1590/1676-0603007813

Almeida-Gomes M, Rocha CFD (2014) Landscape connectivity may explain anuran species distribution in an Atlantic forest fragmented area. Landscape Ecology 29: 29–40. https://doi.org/10.1007/s10980-013-9898-5

Alves RRN, Monielly B, Araújo C, Policarpo IS, Pereira HM, Borges AKM, Vieira WLS, Vasconcellos A (2019) Keeping reptiles as pets in Brazil: ethnozoological and conservation aspects. Journal for Nature Conservation 49: 9–21. https://doi.org/10.1016/j.jnc.2019.02.002

Andrade FS, Haga IA, Lyra ML, Leite FSF, Kwet A, Haddad CFB, Toledo LF, Giaretta AA (2018) A new species of *Pseudopaludicola* Miranda-Ribeiro (Anura: Leptodactylidae: Leiuperinae) from eastern Brazil, with novel data on the advertisement call of *Pseudopaludicola falcipes* (Hensel). Zootaxa 4433: 71–100. https://doi.org/10.11646/zootaxa.4433.1.4

Araujo CO, Condez TH, Bovo RP, Centeno FC, Luiz AM (201) Amphibians and reptiles of the Parque Estadual Turístico do Alto Ribeira (PETAR), SP: an Atlantic Forest remnant of Southeastern Brazil. Biota Neotropica 10: 257–274. https://doi.org/10.1590/S1676-06032010000400031

Argôlo AJS (2004) As serpentes dos Cacauais do Sudeste da Bahia. Editus, Ilhéus.

Armstrong CG, Conte CE (2010) Taxocenose de anuros (Amphibia: Anura) em uma área de Floresta Ombrófila Densa no Sul do Brasil. Biota Neotropica 10: 39–46. https://doi.org/10.1590/S1676-06032010000100003

Azevedo PO (2011) Recôncavo: território, urbanização e arquitetura. In: Caroso, C, Tavares F, Pereira C (Eds) Baía de Todos os Santos: aspectos humanos. EDUFBA, Salvador, 205–252.

Bastazini CV, Munduruca JFV, Rocha PLB, Napoli MF (2007) Which environmental variables better explain changes in anuran community composition? a case study in the restinga of Mata de São João, Bahia, Brazil. Herpetologica 63: 459–471. https://doi.org/10.1655/0018-0831(2007)63[459:WEVBEC]2.0.CO;2

Bertoluci J, Canelas MAS, Eisemberg CC, Palmuti CFS, Montingelli GG (2009) Herpetofauna da Estação Ambiental de Peti, um fragmento de Mata Atlântica do estado de Minas Gerais, sudeste do Brasil. Biota Neotropica 9: 147–155. https://doi.org/10.1590/S1676-06032009000100017

Brazão JEM, Araújo AP (1981) Vegetação. As regiões fitoecológicas, sua natureza e seus recursos econômicos. Estudo fitogeográfico. In: Brasil (Ed.) Folha SD.24 Salvador. Geologia, Geomorfologia, Pedologia, Vegetação, Uso Potencial da Terra. Ministério das Minas e Energia. Projeto RADAMBRASIL, Rio de Janeiro.

Caldas FLS, Santana DO, Faria RG, Bocchiglieri A, Mesquita DO (2016) *Diploglossus lessonae* Peracca, 1890 (Squamata: Anguidae): new records from northeast Brazil and notes on distribution. Check List 12: 1–5. https://doi.org/10.15560/12.5.1982

Camurugi F, Lima TM, Mercês EA, Juncá FA (2010) Anurans of the Reserva Ecológica da Michelin, municipality of Igrapiúna, State of Bahia, Brazil. Biota Neotropica 10: 305–312. https://doi.org/10.1590/S1676-06032010000200032

Cicchi PJP, Serafim H, Sena MA, Centeno FC, Jim J (2009) Herpetofauna em uma área de Floresta Atlântica na Ilha Anchieta, município de Ubatuba, sudeste do Brasil. Biota Neotropica 9: 201–212. https://doi.org/10.1590/S1676-06032009000200019

Colombo P, Kindel A, Vinciprova G, Krause L (2008) Composição e ameaças à conservação dos anfíbios anuros do Parque Estadual de Itapeva, município de Torres, Rio Grande do Sul, Brasil. Biota Neotropica 8: 229–240. https://doi.org/10.1590/S1676-06032008000300020

Colwell RK (2013) EstimateS: statistical estimation of species richness and shared species from samples. http://viceroy.eeb.uconn.edu/estimates/ [last accessed 1 August 2021]

Condez TH, Sawaya RJ, Dixo M (2009) Herpetofauna dos remanescentes de Mata Atlântica da região de Tapiraí e Piedade SP, sudeste do Brasil. Biota Neotropica 9: 157–185. https://doi.org/10.1590/S1676-06032009000100018

Costa HC, Bérnils RS (2018) Répteis do Brasil e suas Unidades Federativas: lista de espécies. Herpetologia Brasileira 8: 11–57.

Couto-Ferreira D, Tinôco MS, Oliveira MLT, Browne-Ribeiro HC, Fazolato CP, Silva RM, Barreto GS, Dias MA (2011) Restinga lizards (Reptilia: Squamata) at the Imbassaí Preserve on the northern coast of Bahia, Brazil. Journal of Threatened Taxa 3: 1990–2000. https://doi.org/10.11609/JoTT.o2800.1990-2000

Cruz CAG, Napoli MF (2010) A new species of smooth horned frog, genus *Proceratophrys* Miranda-Ribeiro (Amphibia: Anura: Cycloramphidae), from the Atlantic rainforest of Eastern Bahia, Brazil. Zootaxa 2660: 57–67. https://doi.org/10.11646/zootaxa.2660.1.5

Cruz CAG, Napoli MF, Fonseca PM (2008) A new species of *Phasmahyla* Cruz, 1990 (Anura: Hylidae) from the State of Bahia, Brazil. South American Journal of Herpetology 3: 187–195. https://doi.org/10.2994/1808-9798-3.3.187

Dias EJR, Rocha CFD (2014) Habitat structural effect on squamata fauna of the restinga ecosystem in Northeastern Brazil. Anais da Acadêmica Brassileira de Ciência 86: 359–371. https://doi.org/10.1590/0001-3765201420130006

Dias IR, Medeiros TT, Nova MFV, Solé M (2014a) Amphibians of Serra Bonita, southern Bahia: a new hotpoint within Brazil's Atlantic Forest hotspot. Zookeys 449: 105–130. https://doi.org/10.3897/zookeys.449.7494

Dias IR, Mira-Mendes CV, Solé M (2014b) Rapid inventory of herpetofauna at the APA (Environmental Protection Area) of the Lagoa Encantada and Rio Almada, Southern Bahia, Brazil. Herpetology Notes 7: 627–637.

Dixo M, Verdade VK (2006) Herpetofauna de serrapilheira da Reserva Florestal de Morro Grande, Cotia (SP). Biota Neotropica 6: 1–20. https://doi.org/10.1590/S1676-06032006000200009

Duellman WE, Trueb L (1994) Biology of Amphibians. Johns Hopkins University Press, Baltimore.

Ecoa (2013) Animais e plantas do Parque Metropolitano de Pituaçu: lista de espécies. Centro de Ecologia e Conservação Animal.

Feio RN, Ferreira PL (2005) Anfíbios de dois fragmentos de Mata Atlântica no município de Rio Novo, Minas Gerais. Revista Brasileira de Zoociências 7: 121–128.

Forlani MC, Bernardo PH, Haddad CFB, Zaher H (2010) Herpetofauna do Parque Estadual Carlos Botelho, São Paulo, Brasil. Biota Neotropica 10: 265–309. https://doi.org/10.1590/S1676-06032010000300028

Freitas MA (2014) Squamate reptiles of the Atlantic Forest of northern Bahia, Brazil. Check List 10: 1020–1030. https://doi.org/10.15560/10.5.1020

Freitas MA, Abegg AD, Dias IR, Moraes EPF (2018) Herpetofauna from Serra da Jibóia, an Atlantic Rainforest remnant in the state of Bahia, northeastern Brazil. Herpetology Notes 11: 59–72.

Freitas MA, Colli GR, Entiauspe-Neto OM, Trinchão L, Araújo D, Lima TO, França DPF, Gaiga R, Dias P (2016a) Snakes of Cerrado localities in western Bahia, Brazil. Check List 12: 1–10.

Freitas MA, Entiauspe-Neto OM, Lima TO, Silva-Neto JS, Araújo D, Silva JMS (2016b) Snakes of Juazeiro, Bahia, middle of São Francisco River, Brazil. Boletim do Museu Biológico Mello Leitão 38: 331–345.

Freitas MA, Silva TFS, Fonseca PM, Hamdan B, Filadelfo T, Abegg AD (2019) Herpetofauna of Serra do Timbó, an Atlantic Forest remnant in Bahia State, northeastern Brazil. Herpetology Notes 12: 245–260.

Freitas MA, Veríssimo D, Uhlig V (2012) Squamate reptiles of the central Chapada Diamantina, with a focus on the municipality of Mucugê, state of Bahia, Brazil. Check List 8: 16–22. https://doi.org/10.15560/8.1.016

Garda AA, Costa TB, Santos-Silva CR, Mesquita DO, Faria RG, Conceição BM, Silva IRS, Ferreira AS, Rocha SM, Palmeira CNS, Rodrigues R, Ferrari SF, Torquato S (2013) Herpetofauna of protected areas in the Caatinga In: Raso da Catarina Ecological Station (Bahia, Brazil). Check List 9: 405–414. https://doi.org/10.15560/9.2.405

Garda AA, Medeiros PHS, Lion MB, Brito MRM, Vieira GHC, Mesquita DO (2014) Autoecology of *Dryadosaura nordestina* (Squamata: Gymnophthalmidae) from Atlantic forest fragments in Northeastern Brazil. Zoologia 31: 418–425. https://doi.org/10.1590/S1984-46702014000500002

Gondim-Silva FAT, Andrade ARS, Abreu RO, Nascimento JS, Corrêa GP, Menezes L, Trevisan CC, Camargo SS, Napoli MF (2016) Composition and diversity of anurans in the Restinga of the Conde municipality, Northern coast of the state of Bahia, Northeastern Brazil. Biota Neotropica 16: 1–16. https://doi.org/10.1590/1676-0611-BN-2016-0157

Haddad CFB, Toledo LF, Prado CPA, Loebmann D, Gasparini JL, Sazima I (2013) Guia de Anfíbios da Mata Atlântica: diversidade e biologia. Anolisbooks, São Paulo.

Hamdan B, Lira-da-Silva RM (2012) The snakes of Bahia state, northeastern Brazil: species richness, composition and biogeographical notes. Salamandra 48: 31–50.

Heyer WR, Donnelly MA, McDiarmid RW, Hayek LC, Foster MS (1994) Measuring and monitoring biological diversity: standard methods for amphibians. Smithsonian Institution Press, Washington.

ICMBio (2018) Livro Vermelho da Fauna Brasileira Ameaçada de Extinção. Volume 1. ICMBio, Brasília.

Juncá FA (2006) Diversidade e uso de hábitat por anfíbios anuros em duas localidades de Mata Atlântica, no norte do estado da Bahia. Biota Neotropica 6: 1–17. https://doi.org/10.1590/S1676-06032006000200018

Lantyer-Silva ASF, Siqueira-Júnior S, Zina J (2013) Checklist of amphibians in a transitional area between the Caatinga and the Atlantic Forest, central-southern Bahia, Brazil. Check List 9: 725–732. https://doi.org/10.15560/9.4.725

Leite AK, Oliveira MLT, Dias MA, Tinôco MS (2019) Species composition and richness of the herpetofauna of the semiarid environment of Nordestina, in northeastern Bahia, Brazil. Biotemas 32: 63–78. https://doi.org/10.5007/2175-7925.2019v32n4p63

Leite FSF, Eterovick PC, Juncá FA (2008) Status do conhecimento, endemismo e conservação de anfíbios anuros da Cadeia do Espinhaço, Brasil. Megadiversidade 4: 158–176.

Lion MB, Garda AA, Santana DJ, Fonseca CR (2016) The conservation value of small fragments for Atlantic Forest reptiles. Biotropica 48: 265–275. https://doi.org/10.1111/btp.12277

Loveridge A (1941) *Bogertia lutzae* - a new genus and species of gecko from Bahia, Brazil. Proceedings of the Biological Society of Washington 54: 195–196.

Lucas EM, Marocco JC (2011) Anurofauna (Amphibia, Anura) em um remanescente de Floresta Ombrófila Mista no Estado de Santa Catarina, Sul do Brasil. Biota Neotropica 11: 377–384. https://doi.org/10.1590/S1676-06032011000100035

Macedo DS (2018) Etno-herpetologia no recôncavo baiano: perspectivas e consequências da criação de répteis. Monography. Universidade Federal do Recôncavo da Bahia, Cruz das Almas.

Magalhães FM, Laranjeiras DO, Costa TB, Juncá FA, Mesquita DO, Röhr DL, Silva WP, Vieira GHC, Garda AA (2015) Herpetofauna of protected areas in the Caatinga IV: Chapada Diamantina National Park, Bahia, Brazil. Herpetology Notes 8: 243–261.

Magalhães FM, Dantas AKBP, Brito MRM, Medeiros PHS, Oliveira AF, Pereira TCSO, Queiroz MHC, Santana DJ, Silva WP, Garda AA (2013) Anurans from an Atlantic Forest-Caatinga ecotone in Rio Grande do Norte State, Brazil. Herpetology Notes 6: 1–10.

Magurran AE (2004) Measuring Biological Diversity. Blackwell, Oxford.

Marques MCM, Trindade W, Bohn A, Grelle CEV (2021) The Atlantic Forest: an introduction to the megadiverse forest of South America. In: Marques MCM, Grelle CEV (Eds) The Atlantic Forest: history, biodiversity, threats and opportunities of the mega-diverse forest. Springer, Cham, 3–22.

Marques R, Mebert K, Fonseca E, Rödder D, Solé M, Tinôco MS (2016) Composition and natural history notes of the coastal snake assemblage from Northern Bahia, Brazil. Zookeys 611: 93–142. https://doi.org/10.3897/zookeys.611.9529

Marques R, Tinôco MS, Couto-Ferreira D, Fazolato CP, Browne-Ribeiro HC, Travassos MLO, Dias MA, Mota JVL (2011) Reserva Imbassaí Restinga: inventory of snakes on the northern coast of Bahia, Brazil. Journal of Threatened Taxa 3: 2184–2191. https://doi.org/10.11609/JoTT.o2812.2184-91

Mesquita DO, Alves BCF, Pedro CKB, Laranjeiras DO, Caldas FLS, Pedrosa IMMC, Rodrigues, JB, Drummond LO, Cavalcanti LBQ, Wachlevski M, Nogueira-Costa P, França RC, França FGR (2018) Herpetofauna in two habitat types (tabuleiros and Stational Semidecidual Forest) in the Reserva Biológica Guaribas, northeastern Brazil. Herpetology Notes 11: 455–474.

Mira-Mendes CV, Ruas DS, Oliveira RM, Castro IM, Dias IR, Baumgarten JE, Juncá FA, Solé M (2018) Amphibians of the Reserva Ecológica Michelin: a high diversity site in the lowland Atlantic Forest of southern Bahia, Brazil. Zookeys 753: 1–21. https://doi.org/10.3897/zookeys.753.21438

Mittermeier RA, Gil PR, Hoffmann M, Pilgrim J, Brooks T, Mittermeier CG, Lamoreux J, Fonseca GAB (2004) Hotspots revisited. CEMEX, Mexico City.

Mônico AT, Clemente-Carvalho RBG, Lopes SR, Peloso PLV (2017) Anfíbios anuros de brejos e lagoas de São Roque do Canaã, Espírito Santo, Sudeste do Brasil. Papéis Avulsos de Zoologia 57: 197–206. https://doi.org/10.11606/0031-1049.2017.57.16

Morato SAA, Lima AMX, Staut DCP, Faria RG, Souza-Alves JP, Gouveia SF, Scupino MRC, Gomes R, Silva MJ (2011) Amphibians and Reptiles of the Refúgio de Vida Silvestre Mata do Junco, municipality of Capela, state of Sergipe, northeastern Brazil. Check List 7: 756–762. https://doi.org/10.15560/11015

Moura MR, Argôlo AJS, Costa HC (2017) Historical and contemporary correlates of snake biogeographical subregions in the Atlantic Forest hotspot. Journal of Biogeography 44: 640–650. https://doi.org/10.1111/jbi.12900

Moura MR, Motta AP, Fernandes VD, Feio RN (2012) Herpetofauna da Serra do Brigadeiro, um remanescente de Mata Atlântica em Minas Gerais, Sudeste do Brasil. Biota Neotropica 12: 209–235. https://doi.org/10.1590/S1676-06032012000100017

Napoli MF, Silva LM, Abreu RO (2017) Anfíbios. In: Nunes JMC, Matos MRB (Eds) Litoral Norte da Bahia: caracterização ambiental, biodiversidade e conservação. EDUFBA, Salvador, 357–392.

Narvaes P, Bertoluci J, Rodrigues MT (2009) Composição, uso de hábitat e estações reprodutivas das espécies de anuros da floresta de restinga da Estação Ecológica Juréia-Itatins, sudeste do Brasil. Biota Neotropica 9: 117–123. https://doi.org/10.1590/S1676-06032009000200011

Palmeira CNS, Gonçalves U (2015) Anurofauna de uma localidade na Mata atlântica setentrional, Alagoas, Brasil. Boletim do Museu de Biologia Mello Leitão 37: 141–163.

Quintela FM, Loebmann D, Gianuca NM (2006) Répteis continentais do município de Rio Grande, Rio Grande do Sul, Brasil. Biociências 14: 180–188.

Rezende CL, Scarano FR, Assad ED, Joly CA, Metzger JP, Strassburg BBN, Tabarelli M, Fonseca GA, Mittermeier RA (2018) From hotspot to hopespot: an opportunity for the brazilian Atlantic Forest. Perspectives in Ecology and Conservation 16: 208–214. https://doi.org/10.1016/j.pecon.2018.10.002

Roberto IJ, Oliveira CR, Araújo-Filho JA, Oliveira HF, Ávila RW (2017) The herpetofauna of the Serra do Urubu mountain range: a key biodiversity area for conservation in the brazilian Atlantic Forest. Papéis Avulsos de Zoologia 57: 347–373. https://doi.org/10.11606/0031-1049.2017.57.27

Rocha CFD, Hatano FH, Vrcibradic D, Van Sluys M (2008) Frog species richness, composition and β-diversity in coastal Brazilian restinga habitats. Brazilian Journal of Biology 68: 101–107. https://doi.org/10.1590/S1519-69842008000100014

Rodrigues MT (1996) Lizards, snakes, and amphisbaenians from the Quaternary sand dunes of the middle Rio Sao Francisco, Bahia, Brazil. Journal of Herpetology 30: 513–523. https://doi.org/10.2307/1565694

Rodrigues MT (2005) Conservação dos répteis brasileiros: os desafios para um país megadiverso. Megadiversidade 1: 87–94.

Rojas-Padilla O, Menezes VQ, Dias IR, Argôlo AJS, Solé M, Orrico VGD (2020) Amphibians and reptiles of Parque Nacional da Serra das Lontras: an important center of endemism within the Atlantic Forest in southern Bahia, Brazil. Zookeys 1002: 159–185. https://doi.org/10.3897/zookeys.1002.53988

Rossa-Feres DC, Garey MV, Caramaschi U, Napoli MF, Nomura F, Bispo AA, Brasileiro CA, Thomé MTC, Sawaya RJ, Conte CE, Cruz CAG, Nascimento LB, Gasparini JL, Almeida AP, Haddad CFB (2017) Anfíbios da Mata Atlântica: Lista de espécies, histórico dos estudos, biologia e conservação. In: Monteiro-Filho ELA, Conte CE (Eds) Revisões em Zoologia: Mata Atlântica. Editora UFPR, Curitiba, 237–314.

Sansone L (2011) Um contraponto baiano de açúcar e petróleo: mercadorias globais, identidades globais? In: Caroso C, Tavares F, Pereira C (Eds) Baía de Todos os Santos: aspectos humanos. EDUFBA, Salvador, 351–375.

Santana DJ, São Pedro VA, Hote PS, Roberti HM, Sant'Anna AC, Figueiredo-de-Andrade CA, Feio RN (2010) Anurans in the region of the High Muriaé River, state of Minas Gerais, Brazil. Herpetology Notes 3: 1–10.

Santana GG, Vieira WLS, Pereira-Filho GA, Delfim FR, Lima YCC, Vieira KS (2008) Herpetofauna em um fragmento de Floresta Atlântica no Estado da Paraíba. Biotemas 21: 75–84. https://doi.org/10.5007/2175-7925.2008v21n1p75

Segalla MV, Caramaschi U, Cruz CAG, Garcia PCA, Grant T, Haddad CFB, Santana DJ, Toledo LF, Langone JA (2019) Lista de espécies brasileiras. Herpetologia Brasileira 8: 65–96.

Sema (2017) Lista Oficial das Espécies da Fauna Ameaçadas de Extinção do Estado da Bahia. Portaria SEMA n° 37.

Seplan (2015) Zoneamento Ecológico-Econômico do Estado da Bahia. Secretaria do Planejamento, Salvador.

Silva JMC, Casteleti CHM (2003) Status of the biodiversity of the Atlantic Forest of Brazil. In: Galindo-Leal C, Câmara IG (Eds) The Atlantic forest of South America: biodiversity status, threats, and outlook. CABS and Island Press, Washington, 43–59.

Silva TSM, Coelho-Filho MA, Coelho EF (2016) Boletim meteorológico da estação convencional de Cruz das Almas, BA: variabilidade e tendências climáticas. Embrapa Mandioca e Fruticultura, Cruz das Almas.

Silvano DL, Segalla MV (2005) Conservação de anfíbios no Brasil. Megadiversidade 1: 79–86.

Souza-Costa CA, Mira-Mendes CV, Dias IR, Silva KB, Argôlo AJS, Solé M (2020) Squamate reptiles from seasonal semi-deciduous forest remnants in southwestern Bahia, Brazil. Bonn Zoological Bulletin 69: 85–94.

Sy EY (2015) Checklist of exotic species in the Philippine pet trade, II. Reptiles. Journal of Nature Studies 14: 66–93.

Telles FBS, Menezes VA, Maia-Carneiro T, Dorigo TA, Winck GR, Rocha CFD (2012) Anurans from the "Restinga" of Parque Natural Municipal de Grumari, state of Rio de Janeiro, southeastern Brazil. Check List 8: 1267–1273. https://doi.org/10.15560/8.6.1267

Tinôco MS, Browne-Ribeiro HC, Souza-Alves JP (2007) Snake communities and Atlantic Forest conservation in Brazil. Solitaire 18: 8–9.

Tozetti AM, Sawaya RJ, Molina FB, Bérnils RS, Barbo FE, Leite JCM, Borges-Martins M, Recoder RS, Teixeira-Junior M, Argôlo AJS, Morato SAA, Rodrigues MT (2017) Répteis. In: Monteiro-Filho ELA, Conte CE (Eds) Revisões em Zoologia: Mata Atlântica. Editora UFPR, Curitiba, 315–364.

Uetz P, Freed P, Hošek J (2019) The Reptile Database. http://www.reptile-database.org/ [last acessed 1 August 2021]

Valdujo PH, Recoder RS, Vasconcellos MM, Portella AS (2009) Amphibia, Anura, São Desidério, western Bahia uplands, northeastern Brazil. Check List 5: 903–911. https://doi.org/10.15560/5.4.903

Vanzolini PE, Ramos-Costa AMM, Vitt LJ (1980) Répteis das Caatingas. Academia Brasileira de Ciências, Rio de Janeiro.

Vasconcelos TS, Prado VHM, Silva FR, Haddad CFB (2014) Biogeographic distribution patterns and their correlates in the diverse frog fauna of the Atlantic Forest hotspot. PLoS ONE 9: 1–9. https://doi.org/10.1371/journal.pone.0104130

Vitt LJ (1985) On the biology of the little known anguid lizard, *Diploglossus lessonae* in Northeast Brazil. Papéis Avulsos de Zoologia 36: 69–76.

Vrcibradic D, Hatano FH, Rocha CFD, Sluys MVS (2000) Geographic distribution. *Bogertia lutzae*. Herpetologial Review 31: 112.

Vrcibradic D, Rocha CFD, Kiefer MC, Hatano FH, Fontes AF, Almeida-Gomes M, Siqueira CC, Pontes JAL, Borges-Junior VNT, Gil LO, Klaion T, Rubião ECN, Van Sluys M (2011) Herpetofauna, Estação Ecológica Estadual do Paraíso, state of Rio de Janeiro, southeastern Brazil. Check List 7: 745–749. https://doi.org/10.15560/11013

Xavier AL, Napoli MF (2011) Contribution of environmental variables to anuran community structure in the Caatinga Domain of Brazil. Phyllomedusa 10: 45–64.

Zanella N, Paula A, Guaragni SA, Machado LS (2013) Herpetofauna do Parque Natural Municipal de Sertão, Rio Grande do Sul, Brasil. Biota Neotropica 13: 290–298. https://doi.org/10.1590/S1676-06032013000400026

Zina J, Ennser J, Pinheiro SCP, Haddad CFB, Toledo LF (2007) Taxocenose de anuros de uma mata semidecídua do interior do Estado de São Paulo e comparações com outras taxocenoses do Estado, sudeste do Brasil. Biota Neotropica 7: 49–57. https://doi.org/10.1590/S1676-06032007000200005

ZooKeys 1060: 155–169 (2021)
doi: 10.3897/zookeys.1060.67216
https://zookeys.pensoft.net

SHORT COMMUNICATION

A peer-reviewed open-access journal
ZooKeys
Launched to accelerate biodiversity research

A new cockroach (Blattodea, Corydiidae) with pectinate antennae from mid-Cretaceous Burmese amber

Guanyu Chen[1], Lifang Xiao[1], Junhui Liang[2], Chungkun Shih[1,3], Dong Ren[1]

1 *College of Life Sciences and Academy for Multidisciplinary Studies, Capital Normal University, 105 Xisanhuanbeilu, Haidian District, Beijing 100048, China* **2** *Tianjin Natural History Museum, 31 Youyi Road, Hexi District, Tianjin, 300203, China* **3** *Department of Paleobiology, National Museum of Natural History, Smithsonian Institution, Washington, DC, 20013–7012, USA*

Corresponding author: Dong Ren (rendong@mail.cnu.edu.cn)

Academic editor: Fred Legendre | Received 11 April 2021 | Accepted 24 August 2021 | Published 24 September 2021

http://zoobank.org/FF74D1EF-11A4-4D51-919F-0DB6CF7E25C3

Citation: Chen GY, Xiao LF, Liang JH, Shih CK, Ren D (2021) A new cockroach (Blattodea, Corydiidae) with pectinate antennae from mid-Cretaceous Burmese amber. ZooKeys 1060: 155–169. https://doi.org/10.3897/zookeys.1060.67216

Abstract

A new species of fossil cockroach, *Fragosublatta pectinata* **gen. et sp. nov.**, is described from mid-Cretaceous Burmese amber. The new species is assigned to the family Corydiidae based on the following combination of characters: pronotum with tubercles, tegmina obovate with smallish anal region and spinules on the antero-ventral margin of the front femur (type C1). The new species is the second reported cockroach with ramified antennae. This finding broadens the diversity of Blattodea in mid-Cretaceous Burmese amber and provides further evidence of convergent evolution for antennal structures among different insect lineages.

Keywords

Convergent evolution, Myanmar, new genus, new species, pectinate antenna, sexual dimorphism, systematic palaeoentomology

Introduction

Blattodea is an order of insects consisting of cockroaches and termites (Inward et al. 2007; Zhao et al. 2019). Up to date, about 5000 extant cockroach species and 1500 fossil species have been documented (Liang et al. 2019; Li et al. 2020).

Diverse insects have been documented from the mid-Cretaceous Burmese (Myanmar) amber recently (Ross 2020, 2021). An ecosystem with a humid climate in the mid-Cretaceous enriched the diversity of cockroach species (Liang et al. 2019). Up to now, 11 families, 28 genera and 36 species of cockroaches in Burmese amber have been documented as shown in Table 1 (Ross 2021). However, only two extinct species of Corydiidae have been reported in Burmese amber so far. The specimens in Burmese amber give us an opportunity to better understand the morphological characters of ancient insects.

Antennae of insects harbor the functions of smell, taste and other senses (Schneider 1964). Some insects have evolved ramified antennae, ranging from forms that are pectinate or bipectinate to plumose (Gao et al. 2016). As documented in the fossil record, 26 insect species in six orders, mostly males, have preserved ramified antennae, e.g., *Atefia rasnitsyni* (Hymenoptera), *Palaeopsilotreta burmanica* (Trichoptera), *Vitimopsyche pectinella* (Mecoptera), *Ol xiai* (Blattodea), *Oligopsychopsis penniformis* (Neuroptera), *Cerophytum albertalleni* (Coleoptera), as summarized in Table 2. Nevertheless, cockroaches with ramified antennae are very rare, with only one reported species (*Ol xiai*, male) in Olidae having bipectinate antennae (Vršanský and Wang 2017).

Herein, we describe a new genus and species, *Fragosublatta pectinata* gen. et sp. nov., assigned to Corydiidae. This new finding broadens the diversity of Blattodea in mid-Cretaceous Burmese amber, clarifies the varieties of their antennal morphology, and suggests a potential sexual dimorphism for these cockroaches.

Material and methods

The type specimen was collected from deposits in the Hukawng Valley of Kachin in northern Myanmar, approximately 100 km southwest of the village of Tanai. The age of Myanmar amber is documented as 98.79±0.62 Mya, in the mid-Cretaceous (Grimaldi and Ross 2017). Myanmar amber pieces have preserved abundant specimens of plants, insects and other invertebrates. The latest comprehensive list of insect taxa from Myanmar amber comprises 28 orders, 421 families, 975 genera and 1383 species (Ross 2020, 2021). The type specimen is housed in the Key Laboratory of Insect Evolution and Environmental Changes, College of Life Sciences and Academy for Multidisciplinary Studies, Capital Normal University, Beijing, China (CNUB; Dong Ren, Curator).

The new specimen was examined and photographed using a Leica M205C dissecting microscope with a Leica DFC450 digital camera system. The detailed and enlarged photos were taken by using a Nikon SMZ 25 microscope with a Nikon DS-Ri 2 digital camera system. Cool white transmitted light from microscope's LED illuminators passed through the specimen from the top, and cool white light, emitted from double optical fibers, irradiated the specimen from two sides simultaneously. Line drawings were prepared by using Adobe Illustrator CC and Adobe Photoshop CS5 graphics software.

Morphological terminology largely follows Roth (2003); venational terms follow Snodgrass (1935), with further interpretations by Smart (1951) and Li and Wang (2017) as a frame of reference.

Table 1. Records of cockroaches described in Burmese amber.

Family	Species	Reference
Blattulidae	*Huablattula hui*	Qiu et al. 2019a
	Huablattula jiewenae	Qiu et al. 2019a
Mesoblattinidae	*Spinaeblattina myanmarensis*	Hinkelman 2019
	Mesoblatta maxi	Hinkelman and Vršanská 2020
Raphidiomimidae	*Raphidiomimula burmitica*	Grimaldi and Ross 2004
Liberiblattinidae	*Spongistoma angusta*	Sendi et al. 2020a
	Stavba babkaeva	Vršanský et al. 2019
	Stavba vrsanskyi	Chen et al. 2020
	Stavba jarzembowskii	Li et al. 2020
Olidae	*Ol xiai*	Vršanský and Wang 2017
Alienopteridae	*Vzrkadlenie miso*	Sendi et al. 2020a
	Formicamendax vršanskýi	Hinkelman 2020
	Teyia branislav	Vršanský et al. 2018a
	Teyia huangi	Vršanský et al. 2018a.
	Meilia jinghanae	Vršanský et al. 2018a
	Caputoraptor vidit	Vršanský et al. 2018a
	Alienopterix ocularis	Vršanský et al. 2018a
	Alienopterix smidovae	Vršanský et al. 2021
	Alienopterix mlynskyi	Vršanský et al. 2021
	Nadveruzenie postava	Vršanský et al. 2021
Umenocoleidae	*Jantaropterix ellenbergeri*	Mlynský et al. 2019
	Cratovitisma bechlyi	Podstrelená and Sendi 2018
	Perspicuus pilosus	Koubová and Mlynský 2020
	Perspicuus vršanský	Koubová and Mlynský 2020
	Antophiloblatta hispida	Sendi et al. 2020a
Blattidae	*Cretaperiplaneta kaonashi*	Qiu et al. 2020
	Balatronis cretacea	Šmídová and Lei 2017
	Bubosa poinari	Šmídová. 2020
	Spinka fussa	Vršanský et al. 2018b
Corydiidae	*Nodosigalea burmanica*	Li and Huang 2018
	Magniocula apiculata	Qiu et al. 2019b
Nocticolidae	*Mulleriblattina bowangi*	Sendi et al. 2020b
	Crenocticola svadba	Sendi et al. 2020b
	Crenocticola burmanica	Li and Huang 2019
Manipulatoridae	*Manipulator modificaputis*	Vršanský and Bechly 2015
Incertae sedis	*Cercoula brachyptera*	Li and Huang 2021

Systematic palaeoentomology

Order Blattodea Brunner von Wattenwyl, 1882
Family Corydiidae Saussure & Zehntner, 1893

Genus *Fragosublatta* Chen, Shih & Ren, gen. nov.
http://zoobank.org/97CB1AFA-A97C-4A12-AA36-CD3070D3F840

Diagnosis. (male only). Sc field narrow (about a third of the width of the R region) with Sc short and branched. CuA almost straight with comb-like branches. CuP sharply curved. The first and the second hind tarsomeres with no plantulae but with spines. Cercus monoliform.

Etymology. *Fragosublatta* is a combination of *fragosus* (Latin for fractured), referring to the fractured pronotum, and the generic name of *Blatta*. Gender is feminine.

Remarks. The new species is assigned to the family Corydiidae based on these characters: pronotum with tubercles, tegmina obovate with smallish anal region and spinules on the antero-ventral margin of the front femur (type C1). The new genus is differentiated from other extinct genera mainly by the forewing and legs: CuA with comb-like branches and the first and the second hind tarsomeres apparently lacking plantulae but with spines. Besides, the subgenital plate of the new species is almost symmetrical, which is similar to *Nodosigalea burmanica* (Li & Huang, 2018), but the new species has comb-like CuA branches to justify the erection of a new genus.

Fragosublatta pectinata **Chen, Shih & Ren, sp. nov.**
http://zoobank.org/0576681A-20FA-46D6-8ED9-6003EA0F69DB
Figs 1–4

Type material. ***Holotype*****:** CNU-BLA-MA2015001, a male specimen. The specimen was preserved in amber at an angle. Most of the insect body parts are preserved, but major parts of the head and all left tibiae and tarsi are missing. The pronotum and the left forewing are fractured.

Locality and horizon. Hukawng Valley, Kachin State, northern Myanmar; lowermost Cenomanian, mid-Cretaceous.

Diagnosis. As for the genus due to monotype.

Description. Medium-sized brown cockroach, body narrow and flattened, overall body length 8.21 mm/width 2.97 mm (Fig. 1A, B). Major parts of head not preserved. Eyes and labial palps invisible. Mandibles with two sharp teeth preserved (Fig. 3A). Only four maxillary palps preserved (total length 1.02 mm), with terminal palpomere oval in shape. Sensilla on palps dense and small, < 0.01 mm wide. Both antennae detached from head and missing some antennomeres (Fig. 2A, B); antennae with 19 and 40 antennomeres respectively; length of antennae slightly shorter than forewing length; both antennae with comb-like extensions at end of each flagellomere. Basal flagellomeres simple, thick and short, medial 20 successive flagellomeres pectinate and apical 13 flagellomeres simple (Fig. 3). Longest comb-like extension of pectinate flagellomeres 0.19 mm. Antennomeres roundish to cylindrical with widest base of 0.13 mm. Pronotum (length 2.15 mm/width 1.84 mm, as preserved) with dense tubercles, nearly vaulted (Fig. 1C), partly sclerotized and melanized, anterior margin covered with obvious hairs. Scutellum distinct, long and wide (ca 0.75/ca1.18 mm).

Forewing obovate, overlapping each other and completely covering abdomen. Left forewing overlapping right forewing. Right forewing 7.7 mm long, anterior margin arched, apex rounded (Fig. 2C). Right forewing costa 2.13 mm long. Sc field narrow, slightly curved, dichotomized with two veins not meeting margin, occupying about one third of forewing length. R regularly branched. M with only two branches. CuA almost straight, posterior-most veins comb-like, up to nine veins preserved. CuP

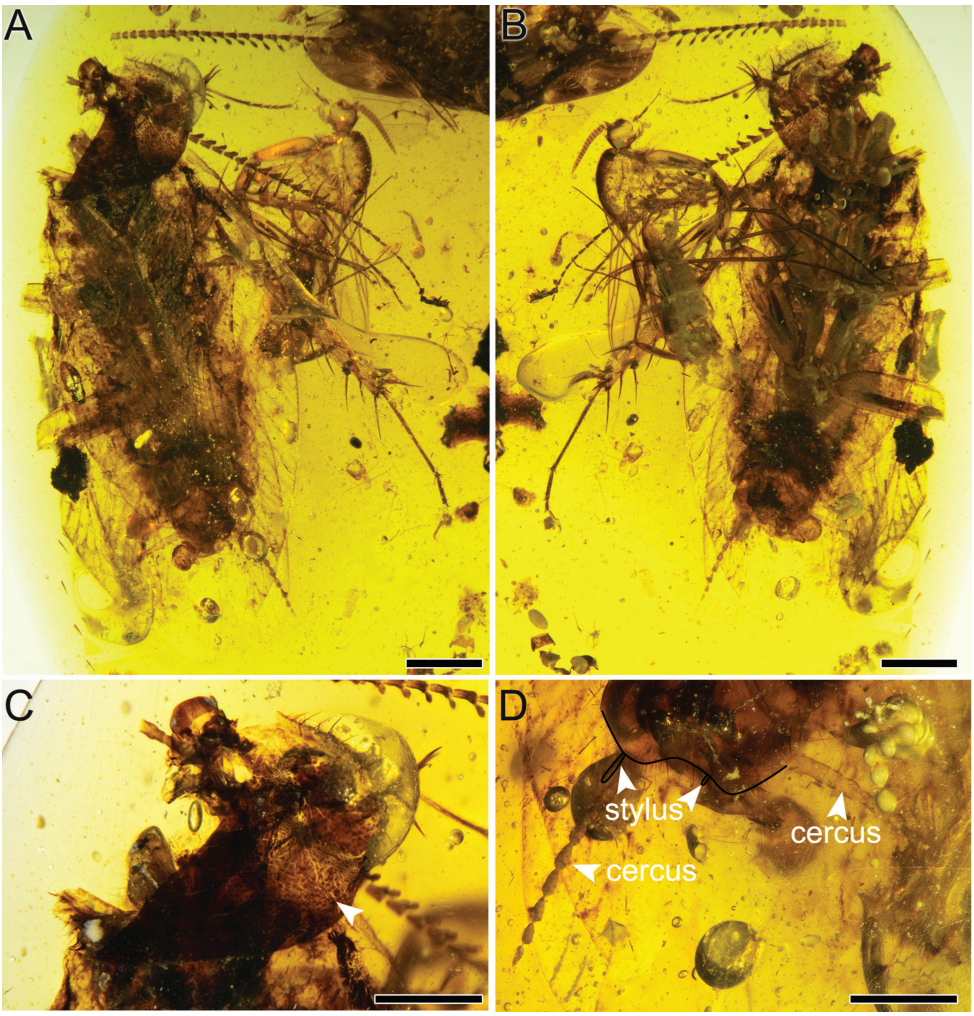

Figure 1. Holotype of *Fragosublatta pectinata* gen. et sp. nov. CNU-BLA-MA2015001 **A** photograph of habitus in dorsal view **B** photograph of habitus in ventral view **C** photograph of the pronotum, with arrowhead indicating the tubercles **D** photograph of the moniliform cercus and asymmetrical stylus. Scale bars: 1.0 mm (**A, B**), 0.2 mm (**C, D**).

sharply curved. Most of clavus area sclerotized, anal area obviously smallish, with seven veins. Left forewing 7.37 mm long, damaged basally. R with six visible branches. M with only two branches preserved. CuA richly branched with distinct intercalary veins. CuP simple, probably with only two and relatively straight A veins. Hind wing membranous, transparent. R branched, with 6–7 visible veins, reaching wing margin.

From fore legs to hind legs gradually stronger. Fore coxa short and wide (length 0.76 mm/width 0.37 mm). Femur with carination, 1.15 mm long and 0.28 mm wide, antero-ventral margin of fore femur with even spinules (type C1 according to Roth 2003), terminal spine 0.36 mm long, slightly curved (Fig. 4A). Tibia (length 0.73 mm/

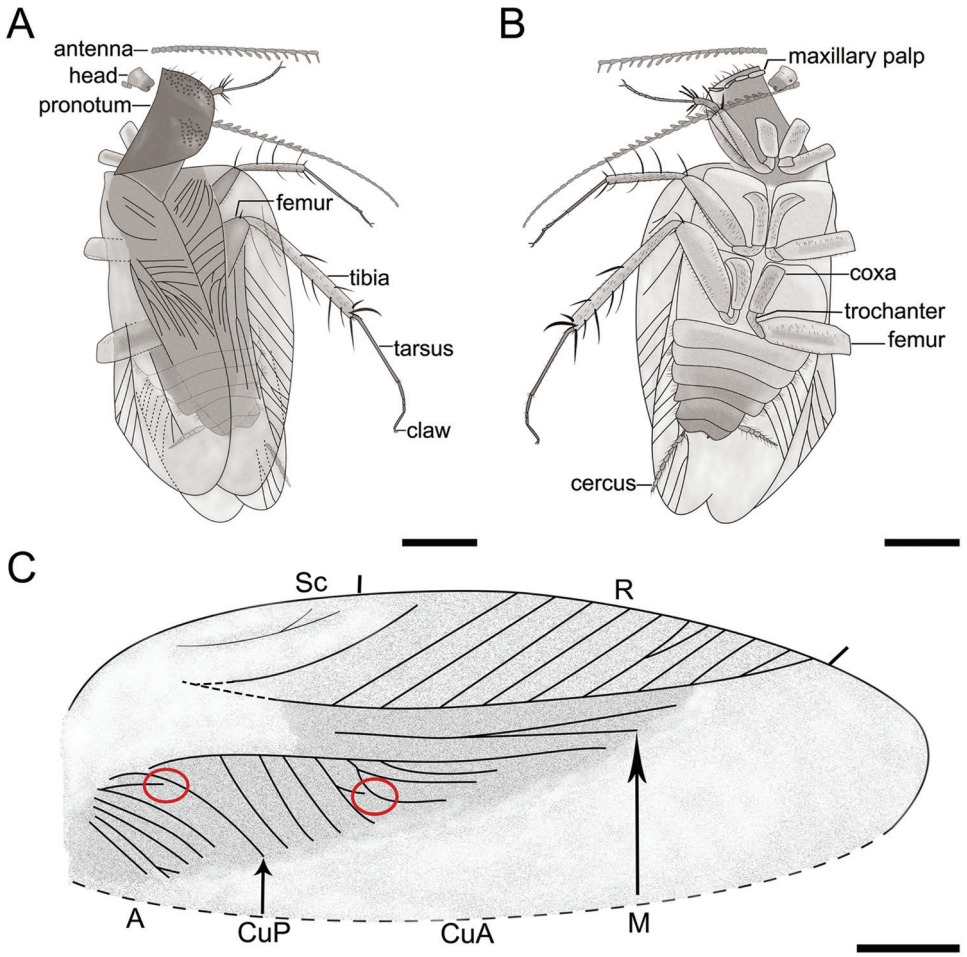

Figure 2. Holotype of *Fragosublatta pectinata* gen. et sp. nov. CNU-BLA-MA2015001 **A** line drawing in dorsal view **B** line drawing in ventral view **C** line drawing of the right forewing, with circles indicating the incomplete veins. Scale bars: 1.0 mm (**A, B**), 0.5 mm, (**C**).

width 0.17 mm) typical in Corydiidae, with long spines, most of spines with serrations (Fig. 4B). Tarsi five-segmented (length 0.76/0.18/0.14/0.13/0.23 mm), with a total of 1.44 mm long and 0.04 mm wide. Claw symmetrical (Fig. 4A), strong, 0.18 mm long, arolium absent. Mid coxa with carination, 1.04 mm long and 0.2 mm wide. Trochanter comparatively longer (length 0.39 mm). Femur 1.87 mm long and 0.44 mm wide with two rows of spinules. Terminal spine not curved distinctly, 0.48 mm long (Fig. 4C). Tibia approximately as long as femur, 1.51 mm long and 0.17 mm wide, with seven spines. Tarsi 2.03 mm long and 0.05 mm wide, first tarsomere longest (length 0.68 mm), terminal tarsomere with symmetrical claws (length 0.13 mm). Hind coxa 1.2 mm long with obvious carination, narrowing from top to bottom. Hind trochanter 0.4 mm long and 0.6 mm wide. Femur strong (length 2.03 mm/width

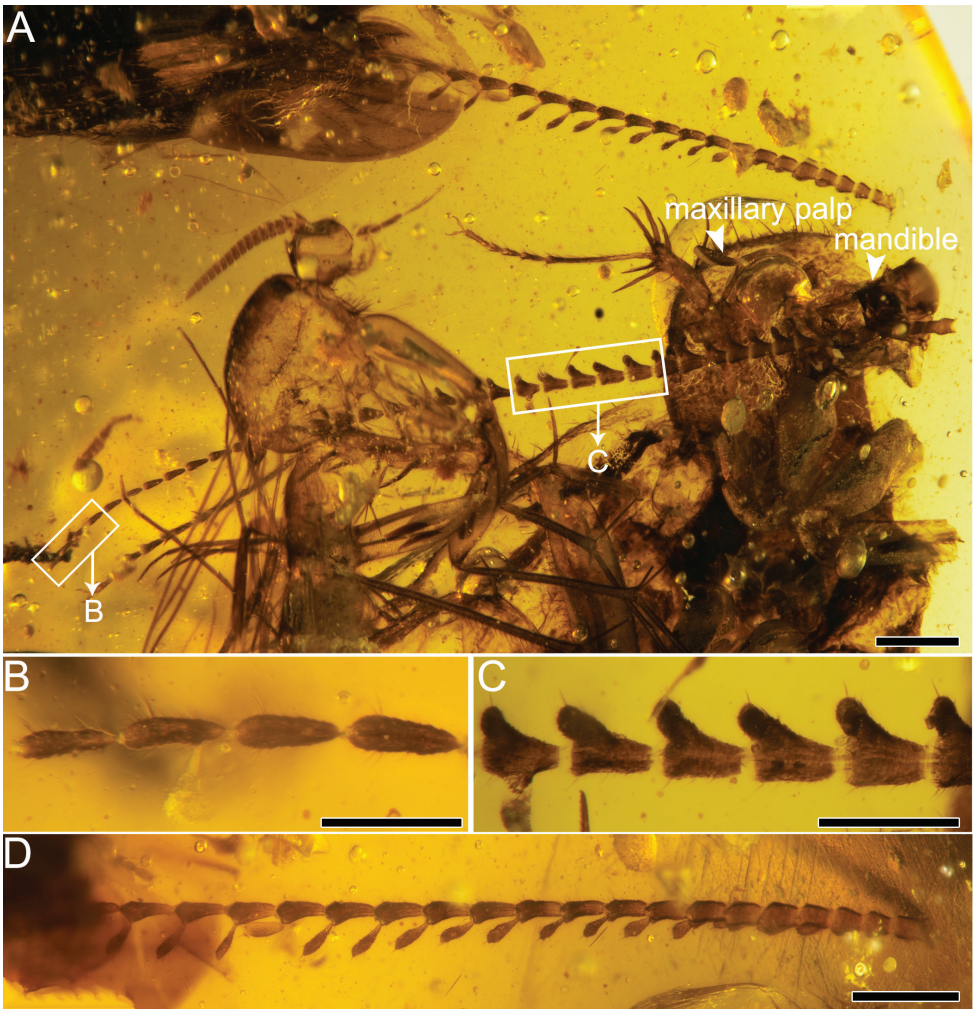

Figure 3. Holotype of *Fragosublatta pectinata* gen. et sp. nov. CNU-BLA-MA2015001 **A** photograph of the two antennae, with arrowheads indicating the maxillary palp and the mandible **B** the apical section of the longer antenna **C** the medial section of the longer antenna **D** photograph of the shorter antenna. Scale bars: 0.5 mm (**A**), 0.1 mm (**B, C**), 0.25 mm (**D**).

0.60 mm) with terminal spine 0.29 mm long (Fig. 4C). Tibia longer (length 3.08 mm/ width 0.28 mm) with at least 10 spurs. Tarsi five-segmented (tarsomeres 1–5 lengths 0.82–0.39–0.37–0.36–0.41 mm) but narrow (width 0.07 mm). Plantulae present at four proximal tarsomeres in fore and mid tarsi, which also exist in third and fourth tarsomeres of hind leg. First and second hind tarsomeres apparently have spines, but lack plantulae (Fig. 4A, D, E). Six sternites visible on abdomen, with sparse chaetae. Cercus moniliform, completely preserved with up to 0.23 mm long sensilla chaetica, divided into eight cercomeres on left (ca 1.51 mm) and nine on right (ca 1.73 mm), basally thicker and apically narrower (Fig. 1D). Hind margin of subgenital plate con-

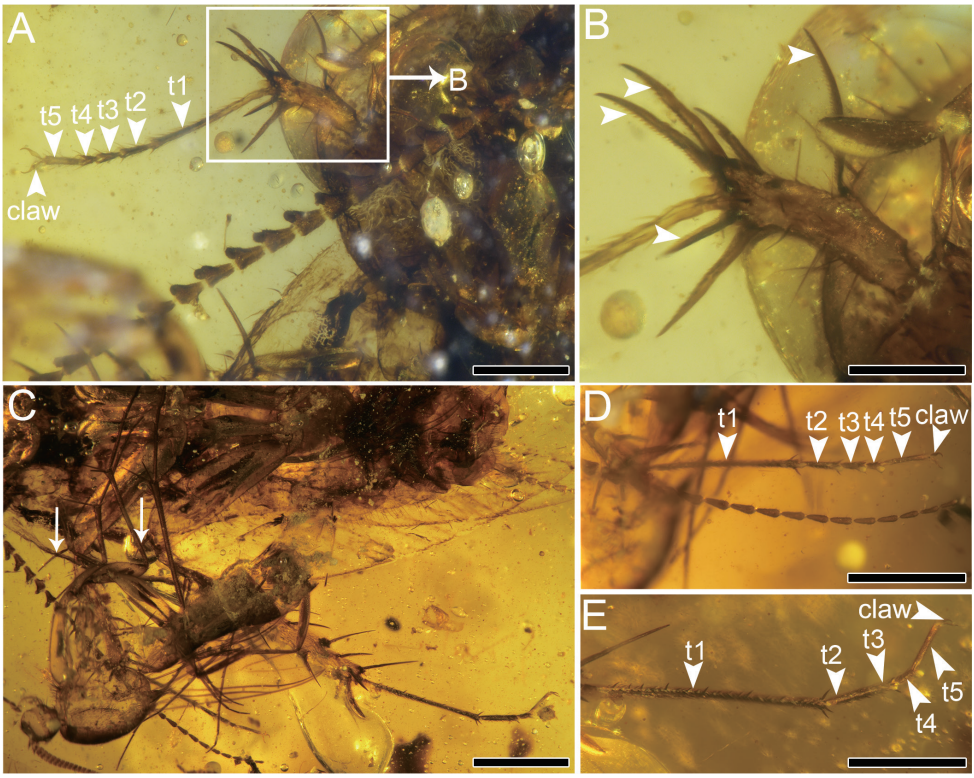

Figure 4. Holotype of *Fragosublatta pectinata* gen. et sp. nov. CNU-BLA-MA2015001 **A** photograph of the foreleg **B** details of the foretibia spurs, with arrowheads indicating the serration **C** photograph of the midleg and hind leg, with arrowheads indicating the terminal spines **D** photograph of the midtarsus **E** photograph of the hind tarsus. Scale bars: 0.5 mm (**A, C**), 0.25 mm (**B, D, E**).

vex, setose, with a wide concave incision medially. Styli asymmetrical, left stylus longer (length 0.35 mm) than right stylus (0.16 mm long). Both styli unsegmented.

Etymology. The name *pectinata* is derived from the Latin word of *pectinatus* referring to the pectinate antennae.

Remarks. The antennae are detached from the head of *Fragosublatta pectinata* gen. et sp. nov., but the basal antennomeres of both antennae are close to the head (Fig. 3A). As shown in Figs 1B and 2B, the length of the left antennae, as preserved, is slightly shorter than the forewing length, which is consistent with the length ratios of the antennae/forewing for many documented fossil cockroaches (Liang et al. 2019). Therefore, we have high confidence that these two antennae belong to *Fragosublatta pectinata* gen. et sp. nov. based on these observations. Besides, there are two syninclusions in this amber piece, including a Mycetophiloidea Diptera and a Hemiptera 'Homoptera' (suspected) close to the hind legs of the new species. Due to poor preservation, we cannot identify the detailed taxonomic classification for these two syninclusions.

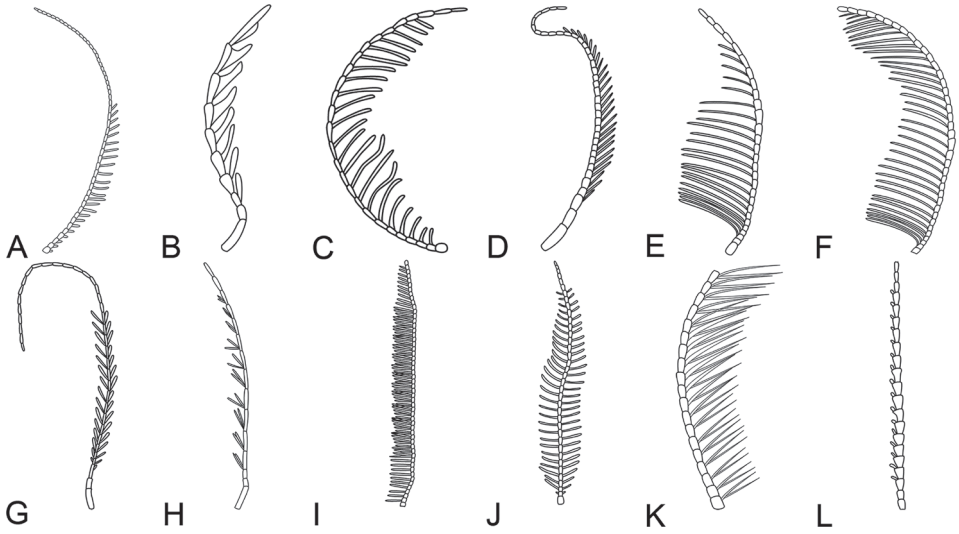

Figure 5. Line drawings of ramified antennae from insects of different orders **A** the pectinate antenna of Mecoptera (*Vitimopsyche pectinella*) **B** the pectinate antenna of Coleoptera (*Cerophytum albertalleni*) **C** the pectinate antenna of Neuroptera (*Cretodilar burmanus*) **D** the pectinate antenna of Hymenoptera (*Jibaissodes peichenae*) **E** the plumose antenna of Hymenoptera (*Jibaissodes bellus*) **F** the flabellate antenna of Hymenoptera (*Atefia rasnitsyni*) **G** the bipectinate antenna of Trichoptera (*Bipectinata orientalis*) **H** the bipectinate antenna of Trichoptera (*Palaeopsilotreta burmanica*) **I** the bipectinate antenna of Trichoptera (*Cathayamodus fournieri*) **J** the bipectinate antenna of Neuroptera (*Cretogramma engeli*) **K** the bipectinate antenna of Blattodea (*Ol xiai*) **L** The pectinate antenna of Blattodea (*Fragosublatta pectinata* gen. et sp. nov.).

Discussion

The new genus and species, *Fragosublatta pectinata* gen. et sp. nov., displays distinctive comb-like extensions of pectinate antennae. This antennal modification of comb-like extensions also occurs among Cretaceous fossils of other insect orders, such as Trichoptera, Mecoptera, Hymenoptera, Coleoptera and Neuroptera (Table 2, Fig. 5). Nevertheless, there are some differences in the number and the length of comb-like extensions of pectinate or bipectinate flagellomeres. Other than the fossil insect orders mentioned above, pectinate or bipectinate antennae are known in extant insect orders, for example, Diptera (Keroplatidae, Ditomyiidae), Lepidoptera (Lymantridae, Saturniidae, etc.) and Megaloptera (Corydalidae) (Ševčík 2000; Tegoni et al. 2004; Liu and Yang 2006; Symonds et al. 2011; Ševčík et al. 2015). This new finding of pectinate antennae for a cockroach in the mid-Cretaceous, in conjunction with the other 26 fossil insects in six orders (Table 2), provides further evidence to support structural convergent evolution for ramified antennae among different insect lineages. The most direct effect of the ramified antennal structure to enhance insect sensing is the overall expansion of the antenna surface area and the corresponding increase in the number of receptors (Gao et al. 2016). Since there are only two reported male cockroaches with pectinate or

Table 2. Ramified antennal types of different insect orders in the Cretaceous.

Order	Antennal type	Family	Species	Locality	Reference
Mecoptera	pectinate	Mesopsychidae	*Vitimopsyche pectinella*	China	Gao et al. 2016
	pectinate	Mesopsychidae	*Vitimopsyche kozlovi*	China	Ren et al. 2009
Trichoptera	bipectinate	Calamoceratidae	*Bipectinata orientalis*	Myanmar	Wichard et al. 2020
	bipectinate	Odontoceridae	*Palaeopsilotreta cretacea*	Myanmar	Wichard et al. 2020
	bipectinate	Odontoceridae	*Palaeopsilotreta burmanica*	Myanmar	Wichard et al. 2020
	bipectinate	Odontoceridae	*Palaeopsilotreta xiai*	Myanmar	Wichard et al. 2020
	bipectinate	Incertae sedis	*Cathayamodus fournier*i	China	Gao et al. 2016
Hymenoptera	pectinate	Megalodontesidae	*Jibaissodes peichenae*	China	Wang et al. 2019
	plumose	Megalodontesidae	*Jibaissodes bellus*	China	Gao et al. 2016
	flabellate	Incertae sedis	*Atefia rasnitsyni*	Brazil	Krogmann et al. 2013
Coleoptera	pectinate	Cerophytidae	*Cerophytum albertalleni*	Myanmar	Yu et al. 2019
	pectinate	Brachypsectridae	*Vetubrachypsectra burmitica*	Myanmar	Qu et al. 2019
	pectinate	Lycidae	*Prototrichalus sepronai*	Myanmar	Molino-Olmedo et al. 2020
	pectinate	Cantharidae	*Burmomiles willerslevorum*	Myanmar	Fanti et al. 2018
	pectinate	Cantharidae	*Sanaungulus curtipennis*	Myanmar	Fanti et al. 2018
	pectinate	Cantharidae	*Sanaungulus ghitaenoerbyae*	Myanmar	Fanti et al. 2018
Neuroptera	bipectinate	Incertae sedis	*Oligopsychopsis penniformis*	Myanmar	Chang et al. 2017
	bipectinate	Kalligrammatidae	*Burmogramma liui*	Myanmar	Liu et al. 2018
	bipectinate	Kalligrammatidae	*Burmopsychops labandeirai*	Myanmar	Liu et al. 2018
	bipectinate	Kalligrammatidae	*Cretogramma engeli*	Myanmar	Liu et al. 2018
	bipectinate	Kalligrammatidae	*Oligopsychopsis grandis*	Myanmar	Liu et al. 2018
	pectinate	Dilaridae	*Cretanallachius magnificus*	Myanmar	Huang et al. 2015
	pectinate	Dilaridae	*Cretadilar olei*	Myanmar	Makarkin 2016
	pectinate	Dilaridae	*Burmopsychops groehni*	Myanmar	Makarkin 2016
	pectinate	Dilaridae	*Cretodilar burmanus*	Myanmar	Liu et al. 2016
Blattodea	bipectinate	Olidae	*Ol xiai*	Myanmar	Vršanský and Wang 2017

bipectinate antennae, potential sexual dimorphism for mid-Cretaceous cockroaches is suggested, pending future reports of more examples and conspecific females.

The fore tibia spurs of the new species have serrations on their inner surface, which is special among cockroaches (Fig. 4B). To our best knowledge, only *Nodosigalea burmanica* (Corydiidae) possesses similar serrations in Burmese amber (Li and Huang 2018). Besides, the tarsal plantulae in fore and mid legs are usually considered as adhesive devices allowing the cockroach to perch or forage on leaves, while the tarsal spines on hind legs are supposed to help the cockroach with rapid movement (Bell et al. 2007).

In addition, the venation and cercus of the new species are also interesting. In the right forewing, there are two incomplete CuA and A (Fig. 2C). This character has been reported in the Raphidiomimidae (Liang et al. 2009). It is likely that this phenomenon was due to the fusion of veins. The basal part of cercus for this new species is cylindrical while the terminal part is moniliform. The function or derivation of this structure of the cercus are unknown, pending future research with new fossil specimens.

Conclusions

This study documents and reports a new species of cockroach, *Fragosublatta pectinata* gen. et sp. nov., assigned to the Corydiidae. The pectinate antennae of this new species

have been compared to 26 other ramified antennal structures in six orders of insects in the Cretaceous. This finding enriches the diversity of morphological characters of cockroaches and suggests that some extinct representatives of this family might have had sexual dimorphism in their antennae. Furthermore, diversified structures of ramified antennae in different orders of fossil insects during the Cretaceous provide further evidence supporting the convergent evolution of antennal structures among different insect lineages.

Acknowledgements

We thank the Editorial Board of ZooKeys and express our gratitude to Dr Fred Legendre, Dr André Nel, Dr Christopher Glasby and Lucia Šmídová for critical and valuable reviews of the manuscript. D.R. was supported by grants from the National Natural Science Foundation of China (No. 31730087 and 32020103006). The authors declare no competing interests.

References

Bell WJ, Nalepa CA, Roth LM (2007) Cockroaches: Ecology, Behavior, and Natural History. Johns Hopkins University Press, Baltimore, 230 pp.

Chang Y, Fang H, Shih CK, Ren D, Wang YJ (2017) Reevaluation of the subfamily Cretanallachiinae Makarkin, 2017 (Insecta: Neuroptera) from Upper Cretaceous Myanmar amber. Cretaceous Research 84: 533–539. https://doi.org/10.1016/j.cretres.2017.10.028

Chen T, Xu CP, Chen L (2020) A new cockroach (Insecta: Blattaria: Liberiblattinidae) from mid-Cretaceous Burmese amber. Acta Palaeontologica Sinica 59(1): 64–69. https://doi.org/10.19800/j.cnki.aps.2020.01.08

Fanti F, Damgaard AL, Ellenberger S (2018) Two new genera of Cantharidae from Burmese amber of the Hukawng Valley (Insecta, Coleoptera). Cretaceous Research 86: 170–177. https://doi.org/10.1016/j.cretres.2018.02.015

Gao TP, Shih CK, Labandeira CC, Santiago-Blay JA, Yao YZ, Ren D (2016) Convergent evolution of ramified antennae in insect lineages from the Early Cretaceous of northeastern China. Proceedings of the Royal Society B: Biological Sciences 283: e20161448. https://doi.org/10.1098/rspb.2016.1448

Grimaldi DA, Ross AJ (2004) *Raphidiomimula*, an enigmatic new cockroach in cretaceous amber from Myanmar (Burma) (Insecta: Blattodea: Raphidiomimidae). Journal of Systematic Palaeontology 2(2): 101–104. https://doi.org/10.1017/S1477201904001142.

Grimaldi DA, Ross AJ (2017) Extraordinary Lagerstätten in amber, with particular reference to the Cretaceous of Burma. In: Fraser NC, Sues HD (Eds) Terrestrial Conservation Lagerstätten: Windows into the Evolution of Life on Land. Dunedin Press, Edinburgh, 287–342.

Hinkelman J (2019) *Spinaeblattina myanmarensis* gen. et sp. nov. and *Blattoothecichnus argenteus* ichnogen. et ichno sp. nov. (both Mesoblattinidae) from mid-Cretaceous Myanmar amber. Cretaceous Research 99: 229–239. https://doi.org/10.1016/j.cretres.2019.02.026

Hinkelman J, Vršanská L (2020) A Myanmar amber cockroach with protruding feces contains pollen and a rich microcenosis. The Science of Nature 107(13): 1–19. https://doi.org/10.1007/s00114-020-1669-y

Hinkelman J (2020) Earliest behavioral mimicry and possible food begging in a Mesozoic alienopterid pollinator. Biologia 75: 83–92. https://doi.org/10.2478/s11756-019-00278-z

Huang DY, Azar D, Cai CY, Garrouste R, Nel A (2015) The first Mesozoic pleasing lacewing (Neuroptera: Dilaridae). Cretaceous Research 56: 274–277. http://dx.doi.org/10.1016/j.cretres.2015.06.001

Inward D, Beccalon G, Eggleton P (2007) Death of an order: a comprehensive molecular phylogenetic study confirms that termites are eusocial cockroaches. Biology Letters 3(3): 331–335. https://doi.org/10.1098/rsbl.2007.0102

Koubová I, Mlynský T (2020) Two new mid-Cretaceous dictyopterans (Umenocoleidae: Vitisminae) from northern Myanmar exemplify taphonomic bias. Amba Projekty 10(1): 1–16.

Krogmann L, Engel MS, Bechly G, Nel A (2013) Lower Cretaceous origin of long-distance mate finding behaviour in Hymenoptera (Insecta), Journal of Systematic Palaeontology 11(1): 83–89. http://doi.org/10.1080/14772019.2012.693954

Li JX, Zhao XD, Gao YP, Wang B, Xiao CX (2020) Cockroach *Stavba jarzembowskii* sp. nov. (Blattaria: Liberiblattindae) from mid-Cretaceous Burmese amber. Cretaceous Research 115: e104531. https://doi.org/10.1016/j.cretres.2020.104531

Li XR, Wang ZQ (2017) Updating the knowledge of assassin bug cockroaches (Blattodea: Blaberidae: Paranauphoeta Brunner von Wattenwyl): Species from China and taxonomic changes. Entomological Science 20: 302–317. http://doi.org/10.1111/ens.12258.

Li XR, Huang DY (2018) A new Cretaceous cockroach with heterogeneous tarsi preserved in Burmese amber (Dictyoptera, Blattodea, Corydiidae). Cretaceous Research 92: 12–17. https://doi.org/10.1016/j.cretres.2020.104383

Li XR, Huang DY (2019) A new mid-Cretaceous cockroach of stem Nocticolidae and re-estimating the age of Corydioidea (Dictyoptera: Blattodea). Cretaceous Research 106: e104202. https://doi.org/10.1016/j.cretres.2019.104202

Li XR, Huang DY (2021) A brachypterous cockroach (Dictyoptera: Blattaria: Blattoidea) and its potential relevance to the palaeoenvironment of mid-Cretaceous Myanmar amber locality. Cretaceous Research 120: e104730. http://doi.org/10.1016/j.cretres.2020.104730.

Liang JH, Vršanský P, Ren D, Shih CK (2009) A new Jurassic carnivorous cockroach (Insecta, Blattaria, Raphidiomimidae) from the Inner Mongolia in China. Zootaxa 1974: 17–30.

Liang JH, Shih CK, Ren D (2019) Blattaria – Cockroaches. Chapter 7. In: Ren D, Shih CK, Gao T, Yao Y, Wang Y (Eds) Rhythms of Insect Evolution: Evidence from the Jurassic and Cretaceous in Northern China. John Wiley & Sons Ltd, 91–112. https://doi.org/10.1002/9781119427957.ch7

Ren D, Shih CK, Gao TP, Wang YJ, Yao YZ (2019) Rhythms of Insect Evolution: Evidence from the Jurassic and Cretaceous of Northern China Wiley-Blackwell, New York, 710 pp. https://doi.org/10.1002/9781119427957

Liu Q, Lu XM, Zhang QQ, Chen J, Zheng XT, Zhang WW, Liu XY, Wang B (2018) High niche diversity in Mesozoic pollinating lacewings. Nature Communications 9: e3793. https://doi.org/10.1038/s41467-018-06120-5

Liu X, Yang D (2006) Revision of the fishfly genus Ctenochauliodes van der Weele (Megaloptera, Corydalidae). Zoologica Scripta 35: 473–490. https://doi.org/10.1111/j.1463-6409.2006.00240.x

Liu XY, Aspock H, Winterton S, Zhang WW, Aspock U (2016) Phylogeny of pleasing lacewings (Neuroptera: Dilaridae) with a revised generic classification and description of a new subfamily. Systematic Entomology 42: 448–471. https://doi.org/10.1111/syen.12225

Makarkin VN (2016) New taxa of unusual Dilaridae (Neuroptera) with siphonate mouthparts from the mid-Cretaceous Burmese amber. Cretaceous Research 74: 11–22. http://dx.doi.org/10.1016/j.cretres.2016.12.019

Mlynský T, Wu H, Koubová I (2019) Dominant Burmite cockroach *Jantaropterix ellenbergeri* sp. n. might laid isolated eggs together. Palaeontographica Abteilung A 314(1–3): 69–79. https://doi.org/10.1127/pala/2019/0091

Molino-Olmedo F, Ferreira VS, Branham MA, Ivie MA (2020) The description of *Prototrichalus* gen. nov. and three new species from Burmese amber supports a mid-Cretaceous origin of the Metriorrhynchini (Coleoptera, Lycidae). Cretaceous Research 111: e104452. https://doi.org/10.1016/j.cretres.2020.104452

Podstrelená L, Sendi H (2018) *Cratovitisma* Bechly, 2007 (Blattaria:Umenocoleidae) recorded in Lebanese and Myanmar ambers. Palaeozoology-Stratigraphy 310(3–6): 121–129. https://doi.org/10.1127/pala/2018/0076

Qiu L, Wang ZQ, Che YL (2019a) First record of Blattulidae from mid-Cretaceous Burmese amber (Insecta: Dictyoptera). Cretaceous Research 99: 281–290. https://doi.org/10.1016/j.cretres.2019.03.011

Qiu L, Wang ZQ, Che YL (2019b) A new corydiid cockroach with large holoptic eyes in Upper Cretaceous Burmese amber (Blattodea: Corydiidae: Euthyrrhaphinae). Cretaceous Research 96: 179–183. https://doi.org/10.1016/j.cretres.2018.12.018

Qiu L, Liu YC, Wang ZQ, Che YL (2020) The first blattid cockroach (Dictyoptera: Blattodea) in Cretaceous amber and the reconsideration of purported Blattidae. Cretaceous Research 109: e104359. https://doi.org/10.1016/j.cretres.2019.104359

Qu TQ, Yin ZW, Huang DY, Cai CY (2019) First Mesozoic brachypsectrid beetles in mid-Cretaceous amber from northern Myanmar (Coleoptera: Elateroidea: Brachypsectridae). Cretaceous Research 106: e104190. https://doi.org/10.1016/j.cretres.2019.07.020

Rehn JWH (1951) Classification of the Blattaria as indicated by their wings (Orthoptera). Memoirs of the American Entomological Society 14: 1–134.

Ren D, Labandeira CC, Santiago-Blay JA, Rasnitsyn A, Shih CK, Bashkuev A, Logan MAV, Hotton CL, Dilcher D (2009) A Probable Pollination Mode Before Angiosperms: Eurasian, Long-Proboscid Scorpionflies. Science 326(5954): 840–847. https://doi.org/10.1126/science.1178338

Ross AJ (2012) Testing decreasing variabililty of cockroach forewings through time using four Recent species: *Blattella germanica*, *Polyphaga aegyptiaca*, *Shelfordella lateralis* and *Blaberus craniifer*, with implications for the study of fossil cockroach forewings. Insect Science 19: 129–142. https://doi.org/10.1111/j.1744-7917.2011.01465.x

Ross AJ (2020) Supplement to the Burmese (Myanmar) amber checklist and bibliography. Palaeoentomology 3(1): 103–118. https://doi.org/10.11646/palaeoentomology.3.1.14

Ross AJ (2021) Supplement to the Burmese (Myanmar) amber checklist and bibliography. Palaeoentomology 4(1): 57–76. https://doi.org/10.11646/palaeoentomology.4.1.11.

Roth LM (2003) Systematics and phylogeny of cockroaches (Dictyoptera: Blattaria). Oriental Insects 37: 1–186. http://doi.org/10.1080/003-5316.2003.10417344.

Schneider D (1964) Insect antennae. Annual. Review of Entomology 9: 103–122. https://doi.org/10.1146/annurev.en.09.010164.000535

Sendi H, Hinkelman J, Vršanská L, Kúdelová T, Kúdela M, Zuber M, Kamp T, Vršanský P (2020a) Roach nectarivory, gymnosperm and earliest flower pollination evidence from Cretaceous ambers. Biologia 75: 1613–1630. https://doi.org/10.2478/s11756-019-00412-x

Sendi H, Vršanský P, Podstrelená L, Hinkelman J, Kúdelová T, Kúdela M, Vidlička L, Ren XJ, Quicke DLJ (2020b) Nocticolid cockroaches are the only known dinosaur age cave survivors. Gondwana Research 82: 288–298. https://doi.org/10.1016/j.gr.2020.01.002

Ševčík J (2000) A new species of *Symmerus* from Laos (Diptera: Ditomyiidae). Entomological Problems 31(2): 181–182.

Ševčík J, Mantic M, Blagoderov V (2015) Two new genera of Keroplatidae (Diptera), with an updated key to the World genera of Keroplatini. Zoobank 55(1): 387–399.

Smart J (1951) The wing-venation of the American cockroach Periplaneta americana Linn. (Insecta: Blattidae). Proceedings of the Zoological Society of London 121: 501–509. https://doi.org/10.1111/j.1096-3642.1951.tb00750.x

Šmídová L, Lei XJ (2017) The earliest amber-recorded type cockroach family was aposematic (Blattaria: Blattidae). Cretaceous Research 72: 189–199. http://dx.doi.org/10.1016/j.cretres.2017.01.008

Šmídová L (2020) Cryptic bark cockroach (Blattinae: *Bubosa poinari* gen. et sp. nov.) from mid-Cretaceous amber of northern Myanmar. Cretaceous Research 109: 104383. https://doi.org/10.1016/j.cretres.2020.104383

Snodgrass RE (1935) Principles of Insect Morphology. McGraw-Hill Book Company, New York and London, 667 pp.

Symonds MRE, Johnson TL, Elgar MA (2011) Pheromone production, male abundance, body size, and the evolution of elaborate antennae in moths. Ecology and Evolution 2(1): 227–246. https://doi.org/10.1002/ece3.81

Tegoni M, Campanacci V, Cambillau C (2004) Structural aspects of sexual attraction and chemical communication in insects. Trends in Biochemical Sciences 29(5): 257–263. https://doi.org/10.1016/j.tibs.2004.03.003

Vršanský P, Vidlička L, Barna P, Bugdaeva E, Markevich V (2013) Paleocene origin of the cockroach families Blaberidae and Corydiidae: Evidence from Amur River region of Russia. Zootaxa 3635: 117–126. https://doi.org/10.11646/zootaxa.3635.2.2

Vršanský P, Bechly G (2015) New predatory cockroaches (Insecta: Blattaria: Manipulatoridae fam.n.) from the Upper Cretaceous Myanmar amber. Geologica Carpathica 66(2): 133–138. https://doi.org/10.1515/geoca-2015–0015

Vršanský P, Wang B (2017) A new cockroach, with bipectinate antennae, (Blattaria: Olidae fam. nov.) further highlights the differences between the Burmite and other faunas. Biologia 72(11): 1327–1333. http://doi.org/10.1515/biolog-2017–0144

Vršanský P, Bechly G, Zhang QQ, Jarzembowski EA, Mlynský T, Šmídová L, Barna P, Kúdela M, Aristov D, Bigalk S, Krogmann L, Li LQ, Zhang Q, Zhang HC, Ellenberger S, Müller P, Gröhn C, Xia FY, Ueda K, Vďačný P, Valaška D, Vršanská L, Wang B (2018a) Batesian insect-insect mimicry-related explosive radiation of ancient alienopterid cockroaches. Biologia 73: 987–1006. https://doi.org/10.2478/s11756-018-0117-3

Vršanský P, Šmídová L, Sendi H, Barna P, Müller P, Ellenberger S, Wu H, Ren XY, Lei XJ, Azar D, Šurka J, Su T, Deng WYD, Shen XH, Lv J, Bao T, Bechly G (2018b) Parasitic cockroaches indicate complex states of earliest proved ants. Biologia 74: 65–89. https://doi.org/10.2478/s11756-018-0146-y.

Vršanský P, Vršanská L, Beňo M, Bao T, Lei XJ, Ren XJ, Wu H, Šmídová L, Bechly G, Jun L, Yeo M, Jarzembowski E (2019) Pathogenic DWV infection symptoms in a Cretaceous cockroach. Palaeontographica Abteilung A 314(1–3): 1–10. https://doi.org/10.1127/pala/2019/0084

Vršanský P, Sendi H, Hinkelman J, Hain M (2021) *Alienopterix* Mlynský et al., 2018 complex in North Myanmar amber supports Umenocoleoidea/ae status. Biologia 76: 2207–2224. https://doi.org/10.1007/s11756-021-00689-x

Wang YM, Wang M, Shih CK, Rasnitsyn AP, Yao J, Ren D, Gao TP (2019) A new sawfly of Megalodontesidae (Insecta, Hymenoptera, Pamphilioidea) with pectinate antennae from the Early Cretaceous of China. ZooKeys 893: 115–123. http://doi.org/10.3897/zookeys.893.38512

Wichard W, Espeland M, Muller P, Wang B (2020) New species of caddisflies with bipectinate antennae from Cretaceous Burmese amber (Insecta, Trichoptera: Odontoceratidae, Calamoceratidae). European Journal of Taxonomy 653: 1–17. https://doi.org/10.5852/ejt.2020.653

Yu YL, Slipinski A, Lawrence JF, Yan E, Ren D, Pang H (2019) Reconciling past and present: Mesozoic fossil record and a new phylogeny of the family Cerophytidae (Coleoptera: Elateroidea). Cretaceous Research 99: 51–70. https://doi.org/10.1016/j.cretres.2019.02.024

Zhao ZP, Yin XC, Shih CK, Gao TP, Ren D (2019) Termite colonies from mid-Cretaceous Myanmar demonstrate their early eusocial lifestyle in damp wood. National Science Review 7(2): 381–390. https://doi.org/10.1093/nsr/nwz141

ZooKeys 1060: 171–182 (2021)
doi: 10.3897/zookeys.1060.71652
https://zookeys.pensoft.net

RESEARCH ARTICLE

A peer-reviewed open-access journal
ZooKeys
Launched to accelerate biodiversity research

A parasitic insect on a parasitic plant: a new species of the genus *Formicoccus* Takahashi (Hemiptera, Coccomorpha, Pseudococcidae) from Ishigaki Island, Japan

Hirotaka Tanaka[1,2], Kenji Suetsugu[3], Satoshi Kamitani[4]

1 *Faculty of Agriculture, Ehime University, Tarumi 3-5-7, Matsuyama, Ehime 790-8566, Japan* **2** *The Kyushu University Museum, Hakozaki 6-10-1, Higashi-ku, Fukuoka, 812-8581, Japan* **3** *Department of Biology, Graduate School of Science, Kobe University, 1-1 Rokkodai, Nada-ku, Kobe, 657-8501, Japan* **4** *Entomological Laboratory, Faculty of Agriculture, Kyushu University, Motooka 744, Fukuoka, 819-0395, Japan*

Corresponding author: Hirotaka Tanaka (coccoidea@gmail.com)

Academic editor: Roger Blackman | Received 15 July 2021 | Accepted 1 August 2021 | Published 24 September 2021

http://zoobank.org/D90713AA-340C-4A64-BB89-35A45218A592

Citation: Tanaka H, Suetsugu K, Kamitani S (2021) A parasitic insect on a parasitic plant: a new species of the genus *Formicoccus* Takahashi (Hemiptera, Coccomorpha, Pseudococcidae) from Ishigaki Island, Japan. ZooKeys 1060: 171–182. https://doi.org/10.3897/zookeys.1060.71652

Abstract

A new species of the genus *Formicoccus* Takahashi (Hemiptera, Coccomorpha, Pseudococcidae) collected from the holoparasitic plant *Balanophora fungosa* J. R. & G. Forst (Balanophoraceae), on Ishigaki Island, Japan, is described as *Formicoccus yoshinoi* Tanaka, **sp. nov.** based on the morphology of adult females. This species is similar to *F. formicarius* (1900) and *F. erythrinae* Williams, 2004, but differs from them by having fewer than six cerarii, and only one type of ventral oral collar tubular duct distributed on the medial area of the posterior abdominal segments. Keys to the Oriental species of the genus *Formicoccus* are provided.

Keywords

Description, fungus root, mealybug, morphology, Nansei-shoto, taxonomy

Introduction

Mealybugs of the family Pseudococcidae (Hemiptera), are the second largest group of the infraorder Coccomorpha (García Morales et al. 2021). Adult females in this family are soft-bodied insects, commonly coated in white powdery wax with lateral wax filaments or have a waxy felted covering (Williams 2004). Members of the Coccomorpha, including mealybugs, are plant parasites, most of which suck sap from phloem tissue, and many are important crop pests (García Morales et al. 2021). Generally, mealybug species have been investigated from biological, agricultural, and economic perspectives.

To date, 78 species of mealybugs in 32 genera have been recorded in Japan (García Morales et al. 2021), many of which are important agricultural and horticultural pests (Kawai 1972, 1980, 2003) and have been relatively well-characterized taxonomically. However, there have been comparatively few taxonomic studies and faunal surveys of non-pest mealybug species, and it is believed that many species remain undescribed and unrecorded in Japan (Kawai 1980). In particular, faunal surveys of mealybugs that feed on certain minor and unique plant species groups, e.g., parasitic plants, ferns, grasses, and bamboos have not been well-studied in Japan, especially hypogeal species, thus many more mealybug species are likely to be present on these understudied host plants.

During a botanical survey led by the second author (KS) in the southwestern islands of Japan (the Ryukyu Islands), on Ishigaki Island, a unique undescribed species was found belonging to the genus *Formicoccus* (Pseudococcidae) parasitising a Japanese fungus root, *Balanophora fungosa* J. R. & G. Forst (Balanophoraceae), which is one of the non-photosynthetic and holoparasitic plants in Japan. The present study describes and illustrates the species as new to science based on the morphology of adult females. Keys to the Oriental species of *Formicoccus* are provided.

Materials and methods

The specimens described in the present study were collected on 14 December 2019 from *Balanophora fungosa* on Ishigaki Island, Japan, by Mr. Keiya Yoshino. The slide-mounting method used followed the method described by Tanaka (2014). The morphology of the slide-mounted specimens was observed using a phase-contrast light microscope (BH2-PH; Olympus Corporation, Tokyo, Japan). The terminology and descriptive format used in the present study follow Williams (2004) and Tanaka and Kamitani (2021). The descriptions are based on multiple specimens, each character measurement is specified for the holotype, followed by the range of measurements for all type specimens in parentheses, if different. The type specimens of the species described below were deposited in the Ehime University Museum, Matsuyama, Japan (**EUMJ**) and the Entomological Laboratory, Faculty of Agriculture, Kyushu University, Fukuoka, Japan (**ELKU**). In the lists of material examined below, the collection data are listed as they appear on the slide labels, with "/" indicating the end of each line.

Taxonomy

***Formicoccus* Takahashi, 1928: 253**

Type species. *Formicoccus cinnamomi* Takahashi, original designation.

Key to adult females of *Formicoccus* species in the Oriental region

(adapted and modified from Takahashi 1930, 1940; Tang 1992; Williams 2004)

1	Antennae with 9 segments	***F. schimae* Takahashi, 1929**
–	Antennae with 6–8 segments	**2**
2	Cerarii numbering 17–18 pairs	**3**
–	Cerarii numbering 16 or fewer pairs	**4**
3	Anal ring with 6 setae	**6**
–	Anal ring with 8 or more setae	**7**
4	Cerarii numbering fewer than 6 pairs; only one type of ventral oral collar tubular duct present	***F. yoshinoi* Tanaka, sp. nov.**
–	Cerarii numbering 14–16 pairs; 2 types of ventral oral collar tubular ducts present	**5**
5	Penultimate cerarii (C17) with ca. 9–12 conical setae; several dorsal setae associated with 2 or 3 trilocular pores	***F. tripurensis* Williams, 2004, in part**
–	Penultimate cerarii (C17) with 2–8 conical setae; dorsal setae not associated with trilocular pores	***F. robustus* (Ezzat & McConnell, 1956), in part**
6	Circulus absent	***F. lingnani* (Ferris, 1954)**
–	Circulus present	**9**
7	Circulus absent	***F. dispersus* Williams, 2004**
–	Circulus present	**8**
8	Anal ring with more than 10 setae	***F. cinnamomi* Takahashi, 1928**
–	Anal ring with fewer than 10 setae	***F. polysperes* Williams, 2004, in part**
9	Dorsal surface of each anal lobe moderately to heavily sclerotised	**10**
–	Dorsal surface of each anal lobe membranous, except for possible weak sclerotisation around some setal collars only	**13**
10	Many dorsal setae conical, those on midline of abdomen associated with trilocular pores forming dorsal cerarii	***F. monicola* (Green, 1922)**
–	Dorsal setae not conical, each one short, slender, and stiff, or elongate and flagellate, not forming dorsal cerarii on midline of abdomen	**11**
11	Dorsal setae short and stiff, 15–25 μm long	**12**
–	Dorsal setae long and flagellate, mostly 55–75 μm long	***F. matileae* Williams, 2004**
12	Anal lobe cerarii (C18) with 4 conical setae. Penultimate cerarii (C17) with 7 conical setae	***F. burckhardti* Williams, 2004**
–	Anal lobe cerarii (C18) with 6 conical setae. Penultimate cerarii (C17) with 4 or 5 conical setae	***F. bambusicola* (Takahashi, 1930)**

13 All cerarii containing short, conical setae **17**
– Either all cerarii with many long, conical, or flagellate setae forming tufts, or some cerarii on head and thorax containing paired flagellate setae..... **14**
14 Abdominal cerarii with short and conical setae only. Cerarii on head and thorax with long paired flagellate setae. Oral collar tubular ducts on venter absent from thorax. Abdominal segments not strongly lobed laterally..... ..... ***F. acerneus*** **Williams, 2004**
– All cerarii each with many elongate cerarian setae, either conical or flagellate, forming tufts, cerarian setae often extending onto venter even in teneral specimens. Oral collar tubular ducts on venter present on thorax. Abdominal segments usually strongly lobed laterally **15**
15 Multilocular disc pores present on ventral abdominal margins. Most dorsal setae on head and thorax long, each 50–100 μm long..... **16**
– Multilocular disc pores absent from ventral abdominal margins. Most dorsal setae on head and thorax short, each 25–40 μm long..... ..... ***F. formicarii*** **(Green, 1922)**
16 Most cerarian setae conical although elongate, sometimes with flagellate tips. Hind femur without translucent pores..... ***F. simplicior*** **(Green, 1922)**
– All cerarian setae elongate and flagellate. Hind femur with translucent pores ..... ***F. formicarius*** **(Newstead, 1900)**
17 Anal lobe cerarii (C18) each mostly with 2 conical cerarian setae..... **18**
– Anal lobe cerarii (C18) each mostly with more than 2 conical cerarian setae **20**
18 Penultimate cerarii (C17) each with 2 conical cerarian setae **19**
– Penultimate cerarii (C17) each mostly with more than 2 conical cerarian setae..... ***F. erythrinae*** **Williams, 2004**
19 Conical cerarian setae on anal lobe cerarii (C18) with flagellate tips. Dorsal setae mostly longer than anal ring length..... ..... ***F. macarangae*** **(Takahashi, 1940)**
– Conical cerarian setae on anal lobe cerarii (C18) without flagellate tips. Dorsal setae mostly shorter than anal ring length.... ***F. sibolangiticus*** **Williams, 2004**
20 Ventral oral collar tubular ducts present anterior to abdomen, on head only or head and thorax..... **24**
– Ventral oral collar tubular ducts absent from head and thorax, confined to abdomen..... **21**
21 Cerarii on head not clearly separated; boundaries of cerarii on head not clear ..... ***F. citricola*** **(Tang, 1992)**
– Cerarii on head mostly clearly separated; boundaries of cerarii on head clear **22**
22 Ventral setae thick, stout and curved, including anal lobe bar setae, cisanal and obanal setae..... ***F. tripurensis*** **Williams, 2004, in part**
– Ventral setae slender and flagellate, including anal lobe bar setae, cisanal and obanal setae **23**

23 Hind coxae noticeably wider and larger than anterior coxae. Multilocular disc pores on venter absent from abdominal segment IV. Most cerarii on head and thorax with slender cerarian setae..... ***F. cameronensis*** **(Takahashi, 1951)**

– Hind coxae same shape as anterior coxae, only slightly larger. Multilocular disc pores on venter present on abdominal segment IV. Most cerarii on head and thorax with conical cerarian setae..... ***F. robustus*** **(Ezzat & McConnell, 1956), in part**

24 Most dorsal setae short and weakly knobbed, except for conspicuously long flagellate setae on abdominal segment VIII on either side of anal ring..... ***F. latens*** **Williams, 2004**

– Dorsal setae all short and pointed. Setae situated on either side of anal ring little if any longer than other dorsal setae..... **25**

25 Most dorsal setae anterior to abdominal segment VIII short and thick, 6.0–10.0 μm long; base of most setae ca. as wide as a trilocular pore and often wider. Ventral oral collar tubular ducts absent from opposite ocular cerarii (C3) and from margins of mesothorax and metathorax..... ***F. polysperes*** **Williams, 2004, in part**

– Most dorsal setae anterior to abdominal segment VIII short and slender, 10–17 μm long; base of most setae narrower than a trilocular pore. Ventral oral collar tubular ducts present opposite ocular cerarii (C3) and on margins of mesothorax and metathorax..... ***F. mangiferacola*** **Williams, 2004**

Formicoccus yoshinoi **Tanaka, sp. nov.**

http://zoobank.org/16C9E917-1BDE-45BA-A3B7-0F59D8F631F5

Figures 1–3

Japanese common name: Tsuchitorimochi-Konakaigaramushi

Type material. ***Holotype*****:** Adult ♀, Japan / Okinawa prefecture **/** Ishigaki Is., Sakieda / 24.445794°N / 124.079765°E / on *Balanophora* / *fungosa* / 14.xii.2019 / coll. K. Yoshino; mounted singly (ELKU). ***Paratypes*****:** 2 adult ♀♀, same data as for holotype, mounted singly (1 EUMJ, 1 ELKU). 4 adult ♀♀, Japan / Okinawa prefecture / Ishigaki Is., Kabira / 24.451620°N / 124.159781°E /on *Balanophora* / *fungosa* / 14. xii.2019 / coll. K. Yoshino; mounted singly (2 EUMJ, 2 ELKU)

Diagnosis. Slide-mounted adult female mostly oval. Anal lobes with well-developed and narrow anal lobe bar. Antenna mostly with seven segments and many flagellate setae. Legs relatively short and stout, but well developed. Hind legs with numerous translucent pores present on both dorsal and ventral surfaces of coxae. Circulus present between ventral abdominal segments III and IV. Ostioles present. Anal ring situated ca. half length from apex of abdomen or end of posterior abdominal segments, bearing 6 setae. Cerarii numbering fewer than 6 pairs; all cerarii situated on posterior abdominal segments. Dorsal setae slender, relatively long and flagellate, densely present and covering almost entire body surface. Dosal trilocular pores evenly distributed. Oral

Figure 1. Live individuals of *Formicoccus yoshinoi* Tanaka, sp. nov. feeding on the underground part of the host plant, *Balanophora fungosa*.

rim ducts and oral collar tubular ducts absent on dorsum. Discoidal pores sparsely distributed on both body surface. Multilocular disc pores mostly present in medial area of ventral abdominal segments VI–IX. One size of oral collar tubular ducts present on venter, forming an irregular submarginal band on posterior abdominal segments and forming transverse rows on medial area of abdominal segments VI–IX.

Description (n = 7). Live adult female feeding on the underground part of host plant (Figs 1, 2) and secreting white powdery wax on all body surfaces (Figs 1, 2). Body shape of mature adult female mostly hemispherical in shape (Fig. 2).

Slide-mounted adult female mostly oval, 2.4 (2.4–3.2) mm long and 1.6 (1.6–2.9) mm wide; derm membranous; segmentation relatively well-developed. Anal lobes distinct but not prominent, dorsal and ventral surfaces of each lobe with weakly sclerotised area, ventral surface with long apical seta, 192–194 (178–194) μm long and with well-developed and narrow anal lobe bar; anal lobe bar fairly conspicuous, but occasionally fainted and rarely difficult to see. Antenna 368–372 (322–407) μm long, with 7 (7–8) segments and many flagellate setae; subapical segment with one fleshy seta and apical segment with 4 (3–4) fleshy setae. Legs relatively short and stout, but well-developed, with many flagellate setae; hind trochanter + femur 319–332 (300–356) μm long, hind tibia + tarsus 243–250 (239–278) μm long; claw 38–43 (38–46) μm long.

Figure 2. Live mature adult females of *Formicoccus yoshinoi* Tanaka, sp. nov.

Ratio of lengths of hind tibia + tarsus: trochanter + femur 0.73–0.78 (0.73–0.82); ratio of lengths of hind tibia to tarsus 1.87–2.07 (1.60–2.13). Paired tarsal digitules present, subequal in length to the minutely knobbed claw digitules. Hind legs with numerous translucent pores present on both dorsal and ventral surface of coxae. Labium ca. 280 (220–285) μm long, slightly longer than clypeus. Circulus present between abdominal segments III and IV, 85 (50–100) μm long and 215 (140–235) μm wide. Ostioles present, each with inner edges of lips not sclerotised; anterior ostioles each with a total for both lips of 106–118 (46–118) trilocular pores and 19–21 (16–25) setae; each posterior ostiole with a total for both lips of 105–118 (64–122) trilocular pores and 18–23 (16–24) setae. Anal ring 108 (90–108) μm wide, situated ca. half the length from apex of abdomen to end of posterior abdominal segments, with two rows of cells, bearing six setae (Fig. 3. AR); each seta 83–110 (83–118) μm long. Cerarii numbering 5 (3–6) pairs, all cerarii situated on posterior abdominal segments. Anal lobe cerarii (C18) each situated on sclerotised cuticle, containing 2 (1–4) conical setae, each seta 15–20 (15–28) μm long and ca. 4–6 μm wide at base; 12–16 (11–20) auxiliary setae and a concentration of trilocular pores. Penultimate cerarii (C17) each situated on weakly sclerotised cuticle, containing 2–4 (1–6) conical setae and many auxiliary setae. Cerarii situated further forward generally each with 0–4 conical setae and at least one cerarii contain more than three conical setae and many auxiliary setae.

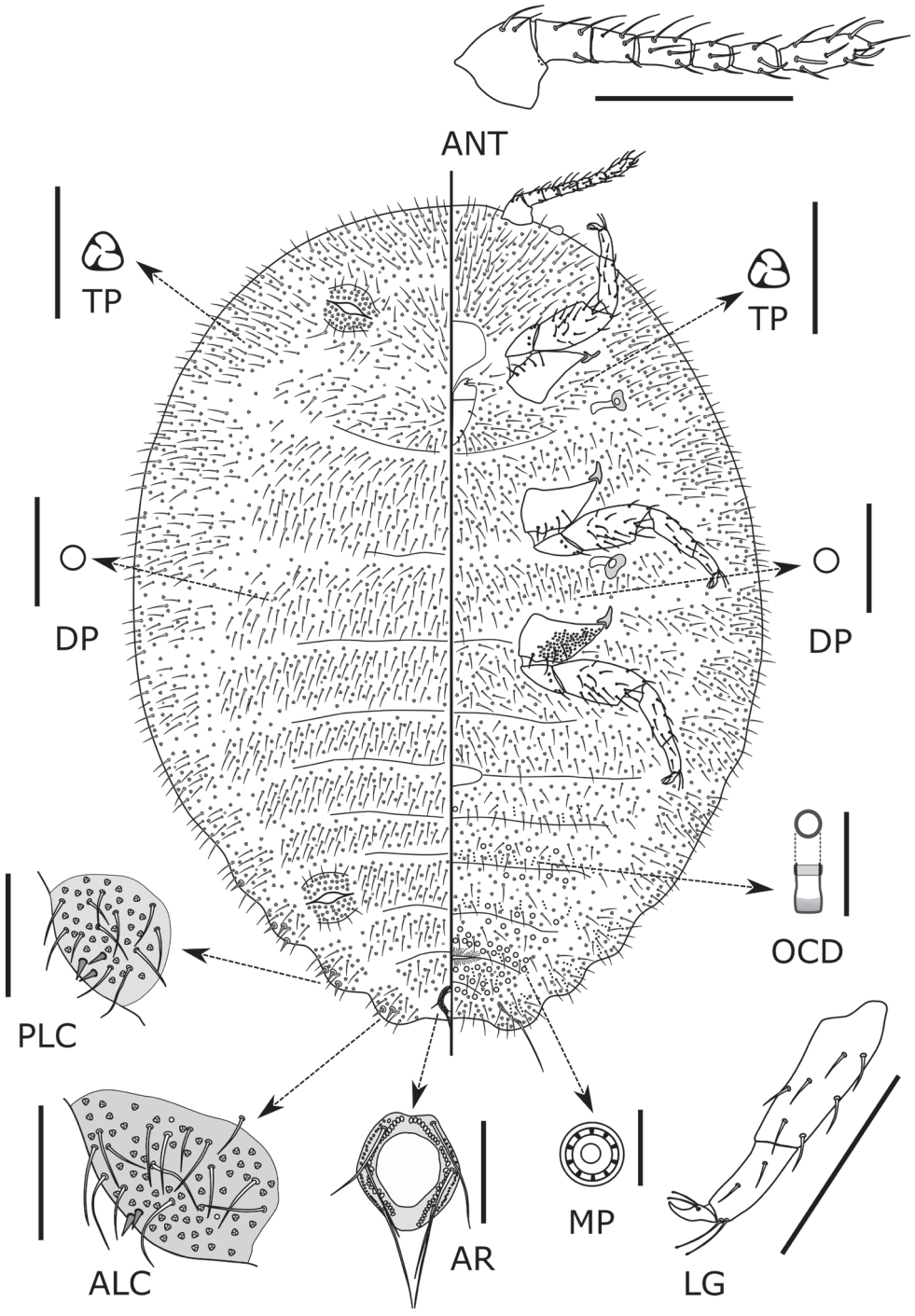

Figure 3. *Formicoccus yoshinoi* Tanaka**,** sp. nov., adult female. Abbreviations: **ALC**, anal lobe cerarius (C18); **ANT**, antenna; **AR**, anal ring; **DP**, discoidal pore; **LG**, hind tibia. tarsus and claw; **MP**, multilocular pore; **OCD**, oral collar duct; **PLC**, penultimate cerarius (C17); **TP**, trilocular pore. Scale bars: 200 μm for **ANT** and **LG**; 100 μm for **ALC**, **AR**, and **PLC**; 10 μm for other details.

Dorsum. Setae slender, relatively long and flagellate, each 21–68 (14–68) μm long, longest setae present on medial area of posterior abdominal segments, densely present and covering almost entire body surface. Trilocular pores ca. 3–4 μm wide, evenly distributed. Oral rim ducts and oral collar tubular ducts absent. Discoidal pores slightly smaller than trilocular pores, sparsely distributed on body surface.

Venter. Ventral derm with slender flagellate setae, each 31–123 (15–123) μm long, longest on medial area of posterior abdominal segments. Multilocular disc pores, each 7–9 (6–9) μm wide, mostly present in medial area of abdominal segments VI–IX. Trilocular pores ca. 3–4 μm wide, evenly distributed. Oral rim ducts absent. Oral collar tubular ducts present, of one size, each with outer ductule 2–4 μm in diameter (slightly smaller than that of a trilocular pore) forming an irregular submarginal band on posterior abdominal segments and forming transverse rows on medial area of abdominal segments VI–IX. Discoidal pores slightly smaller than trilocular pores, sparsely present on body surface.

Host plants. *Balanophora fungosa* (Balanophoraceae).

Biology. *Balanophora fungosa* is characterized by unusual mushroom-shaped inflorescences that emerge above the ground and warty tubers that are attached to their host plants (Hansen 1972). Specimens of *Formicoccus yoshinoi* were found in aggregations on the tuber of this species. Given that (i) no other plants associated with *F. yoshinoi* Tanaka, sp. nov. were found during the survey and (ii) *B. fungosa* individuals infected by *F. yoshinoi* Tanaka, sp. nov. were found at two independent sites, this species might be a specialist on *Balanophora* species. It is worth investigating whether the species feeds on other plant species.

Remarks. In his taxonomic revision of the genus *Formicoccus* Takahashi, 1928, in Southern Asia, Williams (2004) emphasised the following morphological character states as defining morphological features of the genus: the presence of 18 pairs of cerarii, the presence of anal lobe bars on the ventral side of the anal lobe, and the presence of more than two cerarian setae on at least some abdominal cerarii. However, there are exceptions in the first two-character states, with a species with fewer than 17 pairs of cerarii (*F. tripurensis*) and a species with an uncertain presence of anal lobe bars (*F. lingnani*) were included in the genus. The species described in this study also does not have 18 pairs of cerarii, and the species' anal lobe bars are quite fainted and often difficult to see in a few specimens.

Danzig and Gavrilov-Zimin (2015) rejected the use of anal lobe bar as a generic character state of the genus *Formicoccus*. They regarded that the presence or absence of the anal lobe bar fell into individual variations and instead used the presence of more than six setae in the anal ring as a critical generic character state of the genus. According to their opinion, the species described in this study are not *Formicoccus*. However, the debate on the definition of the genus *Formicoccus* is still ongoing, and no consensus has been reached yet.

Zhang and Wu (2017) regarded the number of anal ring setae as having no generic significance. Based on their studies, the anal ring typically bears six basic setae, and when more setae are present, the extra setae are usually slender and short, and vary in their positions. They placed some species with anal lobe bars (*F. citricola* and *F. sinensis*

(Borchsenius, 1962)) in the genus *Formicoccus*. It is clear that a more detailed study is required to better understand the importance of such morphological character states, particularly using a combination of molecular and morphological characters. Under these circumstances, we tentatively included the species described in this study into the genus *Formicoccus*.

Formicoccus yoshinoi Tanaka, sp. nov. is similar to *F. formicarius* (Newstead, 1900) in having: (i) long flagellate dorsal setae; (ii) relatively short and stout legs; (iii) only one type of ventral oral collar tubular duct; and (iv) a round body shape, but differs from this species as follows (characters of *F. formicarius* are given in parentheses): (i) having fewer than six cerarii with 0–6 conical cerarian setae (with 18 pairs of cerarii with long and stout flagellate setae); and (ii) having a transverse row of ventral oral collar tubular ducts on the medial area of posterior abdominal segments (lacking ventral oral collar tubular ducts on medial area of abdominal segments). The species is also similar to *F. erythrinae* Williams, 2004, in having: (i) long flagellate dorsal setae; (ii) relatively short legs; and (iii) round body shape, but differs from the latter species as follows (characters of *F. erythrinae* are given in parentheses): (i) having fewer than six cerarii (having 18 cerarii); and (ii) having only one type of ventral oral collar tubular duct (with two types of ventral oral collar tubular ducts).

Etymology. Named after the collector of type series, an independent researcher of plants in Ishigaki Is., Mr. Keiya Yoshino.

Acknowledgements

The authors are grateful to Dr. Takumasa Kondo, Corporación Colombiana de Investigación Agropecuaria (AGROSAVIA), Colombia, for reviewing this manuscript. We also thank an independent researcher, Mr. Keiya Yoshino, for help with field study and photography. We would like to thank Editage (www.editage.com) for English language editing.

References

Borchsenius NS (1962) Notes on the Coccoidea of China. 11. New genera and species of mealybugs fam. Pseudococcidae (Homoptera, Coccoidea). Trudy Zoologicheskogo Instituta Akademiya Nauk SSSR. Leningrad 30: 221–244.

Danzig EM, Gavrilov-Zimin IA (2015) Palaearctic mealybugs (Homoptera: Coccinea: Pseudococcidae). Part 2: Subfamily Pseudococcinae. Russian Academy of Sciences, Zoological Institute, St. Petersburg, 619 pp.

Ezzat YM, McConnell HS (1956) A classification of the mealybug tribe Planococcini (Pseudococcidae: Homoptera). Bulletin of the Maryland Agriculture Experiment Station A-e84: 1–108.

Ferris GF (1954) Report upon scale insects collected in China (Homoptera: Coccoidea). Part V. (Contribution No. 89). Microentomology 19: 51–66.

García Morales M, Denno BD, Miller DR, Miller GL, Ben-Dov Y, Hardy NB (2021) ScaleNet: a literature-based model of scale insect biology and systematics. Database. http://scalenet.info

Green EE (1922) The Coccidae of Ceylon, Part V. Dulau & Co. London, 345–472. https://doi.org/10.5962/bhl.title.8551

Hansen B (1972) The genus *Balanophora* J.R. and G. Forster. A taxonomic monograph. Dansk Botanisk Arkiv 28: 1–188.

Kawai S (1972) [Diagnostic notes and biology of the coccid-species occurring on cultivated or wild trees and shrubs in Japan (Homoptera: Coccoidea).] Bulletin of the Tokyo-To Agricultural Experiment Station 6: 1–54. [in Japanese]

Kawai S (1980) Scale Insects of Japan in Colors. Zenkoku Nôson Kyôiku Kyôkai, Tokyo, 455 pp. [in Japanese]

Kawai S (2003) Kaigaramushi [Coccoidea]. In: Umeya K, Okada T (Eds) Agricultural Insect Pests in Japan. Zenkoku Nôson Kyôiku Kyôkai, Tokyo, 1203 pp. [in Japanese]

Newstead R (1900) Observations on Coccidae (No. 18). Entomologist's Monthly Magazine 36: 247–251.

Takahashi R (1928) Coccidae of Formosa (2). Transactions of the Natural History Society of Formosa 18: 253–261.

Takahashi R (1929) Observations on the Coccidae of Formosa – 1. Report, Government Research Institute, Department of Agriculture, Formosa 40: 1–82.

Takahashi R (1930) Observations on the Coccidae of Formosa, Part II. Report Department of Agriculture Government Research Institute, Formosa 43: 1–45.

Takahashi R (1940) Some Coccidae from Formosa and Japan (Homoptera), V. Mushi, Fukuoka Entomological Society 13: 18–28.

Takahashi R (1951) Some mealybugs (Pseudococcidae, Homoptera) from the Malay Peninsula. Indian Journal of Entomology 12(1950–1): 1–22.

Tanaka H (2014) [How to make slide-mounted specimens of scale insects, a method of a Japanese coccidologist]. Shokubutsu Boeki 68: 483–488. [in Japanese]

Tanaka H, Kamitani S (2021) Two new species of Coccomorpha (Hemiptera: Sternorrhyncha) collected from Japanese silver grass, *Miscanthus sinensis* (Poaceae) in Okinawa Island, Japan. Zootaxa 4941: 569–579. https://doi.org/10.11646/zootaxa.4941.4.6

Tang FT (1992) [The Pseudococcidae of China.] Chinese Agricultural Science Technology Press Beijing, 768 pp. [in Chinese]

Williams DJ (2004) Mealybugs of Southern Asia. Natural History Museum, Southdene SDN. BHD, Kuala Lumpur, 896 pp.

Zhang JT, Wu SA (2017) A study of the genus *Paraputo* Laing, 1929 of China, with description of two new species (Hemiptera, Sternorrhyncha, Coccomorpha). ZooKeys 709: 57–70. https://doi.org/10.3897/zookeys.709.15161

ZooKeys 1060: 183–192 (2021)
doi: 10.3897/zookeys.1060.67904
https://zookeys.pensoft.net

COMMENTARY

A peer-reviewed open-access journal
ZooKeys
Launched to accelerate biodiversity research

A solution to the enigma of the type locality of *Telmatobius halli* Noble, 1938 (Anura, Telmatobiidae), a frog lost for 86 years

Claudio Correa[1]

1 *Laboratorio de Sistemática y Conservación de Herpetozoos, Departamento de Zoología, Facultad de Ciencias Naturales y Oceanográficas, Universidad de Concepción, Barrio Universitario S/N, Concepción, Chile*

Corresponding author: Claudio Correa (ccorreaq@udec.cl)

Academic editor: Angelica Crottini | Received 26 April 2021 | Accepted 29 July 2021 | Published 24 September 2021

http://zoobank.org/95CE80C0-C741-421E-B105-DE67A7D0CB43

Citation: Correa C (2021) A solution to the enigma of the type locality of *Telmatobius halli* Noble, 1938 (Anura, Telmatobiidae), a frog lost for 86 years. ZooKeys 1060: 183–192. https://doi.org/10.3897/zookeys.1060.67904

Abstract

For 80 years, there were no sightings of the Andean frog, *Telmatobius halli*, due to the ambiguity with which its type locality was described ("warm spring near Ollagüe", northern Chile). The type specimens were collected during the International High Altitude Expedition to Chile (IHAEC) in 1935 and were subsequently described in 1938. In 2018 and 2020, two studies independently reported the rediscovery of the species, but they reached different conclusions about its identity and geographic distribution. In fact, the populations identified as *T. halli* in those studies are more phylogenetically related to other species than to each other, so they clearly do not belong to the same taxon. Although the study of 2020 is more in line with the geographic information of the description, it does not consider some bibliographic details and the transport limitations of the IHAEC. Here, based on a detailed analysis of the chronicles of the IHAEC and other bibliographic sources, I first refute the proposals of the 2018 and 2020 studies and then provide a possible solution. The combined information from the chronicles indicates that the type locality of *T. halli* is found at the sources of the Loa River, a different place from those identified in the two previous studies. By also incorporating geographic information of the time, I conclude that its true type locality is Miño, an abandoned mining camp located near the origin of the Loa River, where currently no populations of the genus have been described.

Keywords

Hall's water frog, International High Altitude Expedition to Chile, Loa River, Miño, northern Chile, Ollagüe

Telmatobius is one of the most representative and diversified genera of the highlands of the central Andes (Barrionuevo 2017). It currently comprises 63 species that are distributed in Ecuador, Perú, Bolivia, Chile and Argentina, mainly above 2000 m elevation (~ 1–30°S; Frost 2021). The distribution of the genus in Chile is restricted to the high Andean area of the extreme northeast of the country, where there are nine species, seven of them endemic (Correa 2019). The richness of the genus in Chile reached a maximum of 10 species with the description of *T. chusmisensis* Formas, Cuevas & Nuñez, 2006 (Formas et al. 2006), but since that date a series of taxonomic and systematic studies have better defined its diversity, phylogenetic relationships and geographic distribution in the country (Sáez et al. 2014; Victoriano et al. 2015; Fibla et al. 2017, 2018; Cuevas et al. 2020). Two of these studies, Fibla et al. (2018) and Cuevas et al. (2020), independently claimed to have clarified the location of the type locality and the identity of *T. halli* Noble, 1938, a species that had not been sighted for 80 years despite the efforts to find it (Formas et al. 2003, 2005; IUCN 2015).

Telmatobius halli was described by Noble (1938) based on five adult females, one sexually immature female, and six larvae collected by Frank Gregory Hall during the International High Altitude Expedition to Chile (IHAEC) in 1935. The difficulty in locating the species was due to the vagueness with which Noble (1938) described the type locality: "Warm spring near Ollague, Chile, 10,000 ft. altitude, June, 25, 1935" (the correct spelling of the town is Ollagüe, which is at an elevation of 3705 m, 12,155.5 feet, according to Cuevas et al. 2020). Several populations of *Telmatobius* have been discovered near Ollagüe in the 21st century (Fig. 1). Populations located immediately to the north were described as new species, *T. philippii* Cuevas & Formas, 2002 (Cuevas and Formas 2002) and *T. fronteriensis* Benavides, Ortiz & Formas, 2002 (Benavides et al. 2002). Then Formas et al. (2003), based on a morphological reanalysis of some type specimens, showed that *T. halli* is a good species compared to these new taxa. On the other hand, populations on the salt flats of Carcote and Ascotán, located south of Ollagüe (Fig. 1), were initially named as *Telmatobius* sp. (e.g., Sáez et al. 2014), but were later identified as *Telmatobius* cf. *philippii* (Lobos et al. 2018) or *T. halli*, in the case of the population of Aguas Calientes of the Carcote salt flat (Cuevas et al. 2020; see below).

Fibla et al. (2018) and Cuevas et al. (2020) used different approaches to solve the riddle of *T. halli*, although both reviewed key bibliographic sources of the IHAEC and compared the morphology of specimens of the type series with live individuals from candidate populations. Fibla et al. (2018) also performed a morphometric analysis of adults and molecular phylogenetic analyses, where all the species and some populations from north and south of Ollagüe were included. Two specimens from the type series were included in the morphometric analysis, but none was included in the phylogenetic analyses (probably due to the impossibility of obtaining DNA from them). Cuevas et al. (2020) redescribed the species using morphological characters of adults and larvae from their own candidate population, Aguas Calientes, which were compared with type specimens. Despite the soundness of their integrative approaches, Fibla et al. (2018) and Cuevas et al. (2020) arrived at different conclusions because they focused

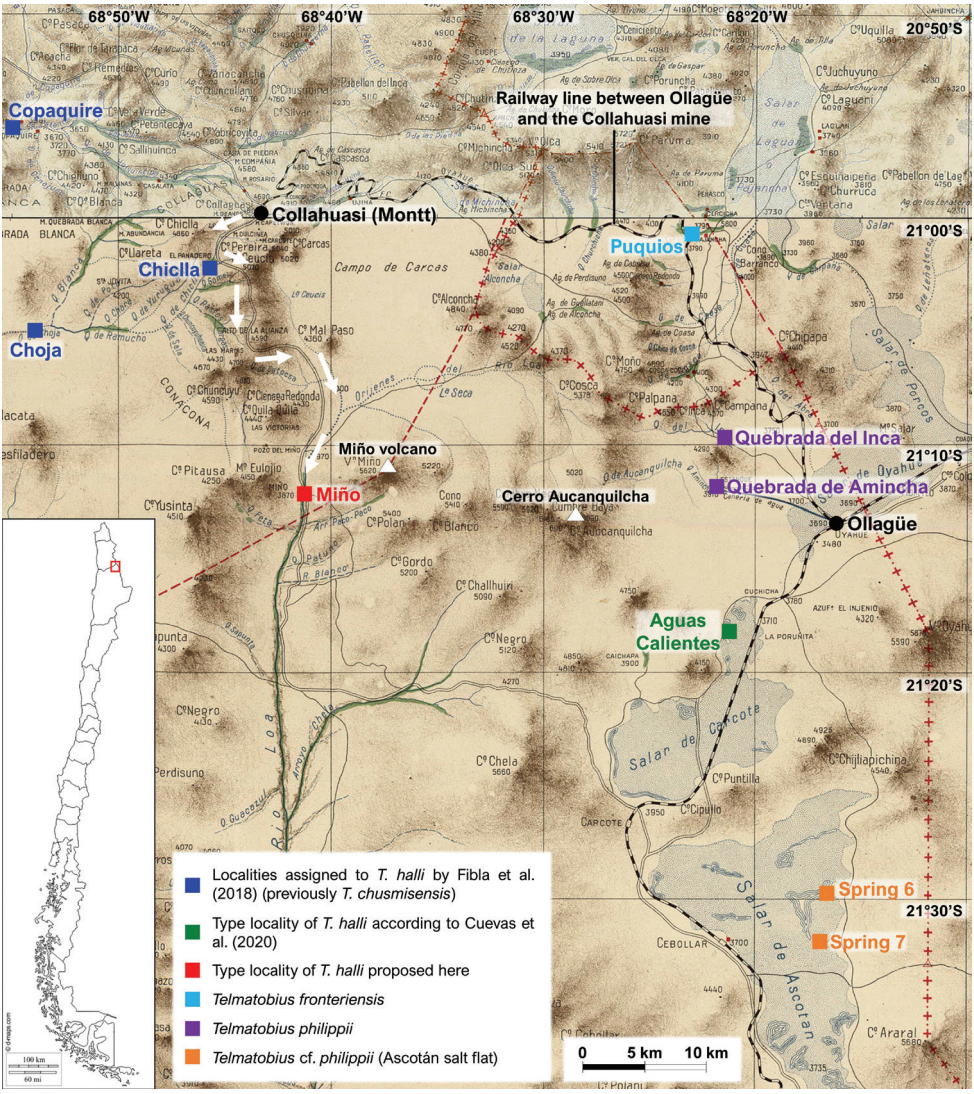

Figure 1. Upper area of the Loa River and surroundings, showing the location of populations recently assigned to *Telmatobius halli*, its type locality according to this study and other *Telmatobius* populations near Ollagüe. The railway line that connected Ollagüe with the Collahuasi mine (to the Montt station) and the dirt road that connected the Collahuasi mine and Chicla with Miño (white arrows) are indicated. Note that the road continues from Miño to the Carcote salt flat. The background map was constructed by joining two maps published by the Comisión Chilena de Límites in 1912.

on candidate populations located in different zones (Fig. 1). In fact, the populations identified as *T. halli* in both studies are more related to other species than to each other (they even belong to different species groups) according to the most complete phylogenetic studies of Chilean species, in which type material of *T. halli* was not included (Sáez et al. 2014; Fibla et al. 2018). Consequently, there are currently two incompat-

ible hypotheses about the identity and location of *T. halli*, which in both cases would be threatened by its very restricted distribution range.

The proposal of Cuevas et al. (2020) fits better with the little information given in the description (Noble 1938), since according to these authors *T. halli* inhabits the hot spring "Aguas Calientes" (21°17'44.4"S, 68°20'08.7"W, 3717 m), located in the northwest margin of the Carcote salt flat, 12 km southwest (straight line) of Ollagüe (Fig. 1). Although compelling, a careful examination of the chronicles of the IHAEC (Keys 1936a, 1936b; Keys et al. 1938; Dill 1979, 1980) shows that the solution of Cuevas et al. (2020) is highly unlikely and that it does not consider important background information contained in some of them. This information also allows me to rule out the proposal of Fibla et al. (2018) (see below).

Here I propose a solution to the enigma of the type locality of *T. halli* based on the descriptions of the activities of the IHAEC provided by two of its members, David Bruce Dill and Ancel Keys, historical maps and other bibliographic sources. To understand this new proposal, it is necessary to review in detail the information used by Fibla et al. (2018) and Cuevas et al. (2020).

Fibla et al. (2018) present the dates and altitudes of the places visited by the IHAEC (in their Table 1; see Keys 1936a, 1936b and Keys et al. 1938); then they summarize the itinerary of the expedition and mention a visit on a "free" Sunday to a "recreational area for the miners, located about 915 m a.s.l. lower than the mining area (at about 4000 m a.s.l.)." Referring to that visit, they transcribe a passage from Dill (1979), which describes the place and the circumstances in which Frank G. Hall collected the specimens that were used to describe the species. Considering these data, the dates of the expedition's stay in the Collahuasi mine and the difficulty of movement at that time, Fibla et al. (2018) conclude that the populations of the Choja-Chijlla and Copaquire ravines, located near the mine, would correspond to *T. halli* (Fig. 1; throughout the text, Fibla et al. 2018 mention Choja-Chijlla together, but on their map they show them separately; here I located these two localities according to their map and I used the most common way of writing the second place, Chiclla). These populations were previously considered as *T. chusmisensis* in the molecular phylogenetic study of Sáez et al. (2014).

At this point, it is necessary to transcribe a more extensive fragment of the chronicle of the IHAEC of Dill (1979): "In 10 days [referring to the stay in Ollagüe], we were ready to move on to Montt [a train station very close to the Collahuasi mine] at 16,400 feet, the highest point reached by any standard gauge railroad. The rich underground copper mine was on standby at the time, manned only by a mine manager and a small maintenance crew. Within another 10-day period we had completed our observations and enjoyed another Sunday trip [Dill describes a previous one during the stay in Ollagüe], this time down 3,000 feet to a recreation area built for the mine staff. A concrete swimming pool filled with spring water was the major attraction. Greg [Frank Gregory Hall] searched the area for animal life and captured a frog that he preserved and eventually sent to the National Museum where it proved to be a new species. Appropriately it was named *Telmatobius halli*. By this time it was late June and our train returned to Ollagüe." Cuevas et al. (2020) provide a longer and modified version of

this citation; I transcribed it literally, but inserted some clarifications in square brackets and added the last statement.

There are several elements in the preceding text that are important to understand fully the problem of the type locality of *T. halli*. First, the Sunday trip, an event described by Keys (1936b) and Dill (1979, 1980). This recreational trip, in which apparently all the members of the expedition participated, was made during their stay in Collahuasi (June 13 to 25) and should have taken place on June 23, as Fibla et al. (2018) inferred. Second, the altitude. Dill (1979) explicitly indicates that they descended 3000 feet (mentioned also by Dill 1980, see below), which means that on that trip they reached an altitude of 12,440 feet according to the height reported for Collahuasi (Montt) (4700 m, 15,440 feet; Keys 1936a, 1936b; Keys et al. 1938). Third, the concrete swimming pool filled with spring water. A very important detail is that Dill (1980) mentions that it was a "warm" spring (see below). And fourth, the train. The expedition moved from Chuquicamata to Ollagüe, and from there to Collahuasi (and from there back to Ollagüe), in four outfitted train cars, as Keys (1936a, 1936b) describe and show in photos.

Cuevas et al. (2020) also transcribe another text that mentions the same Sunday trip (Dill 1980): "The twelve days at Montt found us all busy except on Sunday when the resident engineers, Messrs. Packard and Bell, took us down about 3,000 ft to a concrete swimming pool fed by a warm spring, the origin of Rio Loa, where we enjoyed a swim. This had been a recreation spot for the mine staff. There was enough water running from the spring to support a flourishing green oasis. Hall, the naturalist, collected some specimens which he preserved and transported back to his laboratory. One specimen proved to be a new species of frog, which authorities at the National Museum appropriately named *Telmatobius halli*. On June 25, our cars were pulled back to Ollagüe where they remained until our mission was completed in mid-July." Again, Cuevas et al. (2020) provide a modified version of this citation, but I transcribed it literally and added the last statement. Here there are two additional details that are crucial to the argument that follows: the pool was at "the origin of Rio Loa" and the spring supported a "flourishing green oasis".

Taking into account these elements, I will first discard the proposals of Fibla et al. (2018) and Cuevas et al. (2020) and then present a third account describing the finding of amphibians during the IHAEC that supports my own proposal.

The proposal of Fibla et al. (2018) rests strongly on the existence of known populations of *Telmatobius* near Collahuasi mine to the west, until then identified as *T. chusmisensis* (Sáez et al. 2014), and the difficulties of movement at the time of the IHAEC. Although this last argument is convincing, the coordinates that they provide (for Choja-Chiclla together and Copaquire separately; Fig. 1) are about 20–25 km from the mine, following the shortest route through the ravines, which can hardly be considered "near the camp" as the authors mention. In addition, they recognize that they did not find any pool with warm water like the one described in the chronicles, although they report the temperature of the water in Copaquire, which is warmer than that of another nearby stream, Chiclla. Nevertheless, the strongest argument to rule out the Fibla et al. (2018) hypothesis is that according to Dill (1980) (see quote

above) the place where the pool was located is "the origin of Río Loa". The same location had already been pinpointed by Keys (1936b) ("the source of the Rio Loa"), who also specified the altitude, 12,000 feet. Although the Choja-Chiclla and Copaquire ravines belong to the Loa River basin (Niemeyer and Cereceda 1984), they are formed by intermittent water systems that vanish into the plain where the Llamara salt flat is located, north of the Loa River. It is highly unlikely that the members of the expedition confused the streams located west of the mine with those that give rise to the Loa River, located south of the mine, considering that they had maps of the area (e.g., the ones shown in Keys 1936a and 1936b).

As mentioned above, the working hypothesis of Cuevas et al. (2020) is more congruent with the data associated with the description of *T. halli*, specifically the presence of a *Telmatobius* population in a warm (thermal as also they point out) spring near Ollagüe (Fig. 1). Additionally, the authors show a photograph of a pool that is roughly at the altitude of the site described by Dill (1979, 1980) and Keys (1936b) (see above), which could have been built on top of a previous one. This pool is surrounded by vegetation, which is consistent with the flourishing green oasis described by Dill (1980). Despite these similarities, the location of this site also does not correspond to the origin or source of the Loa River, as specified by Dill (1980) and Keys (1936b), since the Carcote salt flat is located in an endorheic basin that is not hydrographically connected with the tributaries of the Loa River (Niemeyer and Cereceda 1984).

There is another problem with the hypothesis of Cuevas et al. (2020): the logistics of the trip. The expedition arrived in Collahuasi from Ollagüe by train. Therefore, to travel to Ollagüe they would have had to take a train back (a journey of 91 km, Titus 1909) and then travel by another means of transport from Ollagüe to the Carcote salt flat (a journey of around 13 additional km, following the shortest route) (Fig. 1). Considering the conditions of that time, this would have been a fairly long journey in time and distance, without considering the costs and difficulties of moving a train (even assuming that they could move the train at any time, which is unlikely). In addition, the Sunday trip took place in the last days of their stay in Collahuasi, so it seems unlikely that they traveled to Ollagüe for a recreational trip, returned to Collahuasi and then almost immediately returned to Ollagüe (a detail that none of the chroniclers mention).

Although these last explanations respond to common sense, they are still only reasonable guesses about the movements of the expedition. Below I transcribe and translate literally a third account that is at the end of the section "Life in Collahuasi (4,700 meters)" from a chronicle of the IHAEC written in Spanish by Keys (1936a). This source, which was not consulted by Fibla et al. (2018), but is cited by Cuevas et al. (2020), clears up any doubts that could arise from my previous arguments: "Below Collahuasi, we examined the sources of the Loa River, the only one that reaches the sea in an area that spans 10° latitude. The water rises in a series of springs at a height of 3,700 meters, at the base of the Miño volcano (5,820 meters) and partly at the foot of Cerro Aucanquilcha. The fact that these sources are uniformly at the same level for a distance of several miles indicates the existence of horizontal stratification. Sedimentary formations of the Cretaceous sur-

face a few hundred meters above the source line. Some of the springs are hot, but at this point the water is pure; some 50 kilometers below, salty springs begin to enter its waters, whose salt content is constantly increasing. We found many toads and tadpoles in the temperate ponds. The gorge of the Loa River begins a short distance from its sources; its roughness reminds us that the mountains and hills of this region owe their smoothness to the exceptionally small amount of water for erosion." I think that this narration, which integrates several of the elements mentioned above (origin of the Loa River, an altitude of around 12,000 feet and springs of warm water), complements well the description of the Sunday trip. More importantly, it mentions the discovery of adult amphibians and larvae in that place. Although it does not explicitly mention that it was part of the Sunday trip, the concrete swimming pool or that G. Hall collected the amphibians, it is unlikely to be a different trip than the one described in the other two accounts transcribed above, since the activities of the IHAEC had another objective and there was probably not much time for recreation. In addition, part of the differences among the stories can be attributed to the fact that they were written by different members of the IHAEC.

A review of maps from the beginning of the 20th century (Titus 1909; Oficina de Mensura de Tierras 1910; Comisión Chilena de Límites 1912; Richard Mayer 1917) and other sources allowed me to find a place called Miño, which is located at the source of the Loa River, at the base of the Miño volcano, and which has some characteristics compatible with the three narrations (Fig. 1). According to Riso Patrón (1924), (the settlement of) Miño is located at 3870 m (12,697 feet) and a road that connects Chiclla (near Collahuasi) with the Carcote and Ascotán salt flats passes through there (Fig. 1). Berenguer and Cáceres (2008) describe the ruins of this place, which they qualify as relatively large, indicating that it probably served as a post and mining camp from at least the 18th century to the late 19th century. There are currently at least three sets of ruins that can be clearly seen on Google Earth (satellite image of December 22, 2018; accessed on September 10, 2020), scattered around two waterways, in an area with abundant vegetation (21°11'49"S, 68°39'58"W, 3900 m, 12,795 feet). Although the satellite image do not show signs of the pool where the members of the IHAEC would have swum that Sunday, I propose that Miño is the true type locality of *T. halli*. There are no described populations of *Telmatobius* at this location, but about 180 km downstream, following the course of the Loa River, is the only known population of *T. dankoi* Formas, Northland, Capetillo, Nuñez, Cuevas & Brieva, 1999 (Formas et al. 1999).

A final comment. It is likely that we will never know why the type locality of *T. halli* was described so ambiguously and with an incorrect altitude (near Ollagüe at 10,000 feet), which has prevented this species from being found for 86 years. Considering this insurmountable limitation, it must be recognized that Fibla et al. (2018) and Cuevas et al. (2020) advanced in the right direction to solve the enigma, resorting to bibliographic sources, but paradoxically their conclusions imply that there are currently several populations of *Telmatobius* with the same name, which clearly do not correspond to the same species according to molecular phylogenetic studies (Sáez et al. 2014; Fibla et al. 2018). Therefore, the solution to this new conundrum requires intensive field work in and around Miño to try to locate the population originally described as *T. halli*.

Acknowledgements

I am deeply grateful to Francisco Rivera for the stimulating exchange of information, material, and ideas during this investigation, which helped me define and refine the proposal presented here. I am also grateful for the crucial help of Diego Baldo, who provided me with a copy of one of the key references for this study (Keys 1936a), and Javiera Cisternas and Patricio Saldivia, who got me a copy of the book chapter of Dill (1980). I also appreciate the help of Jesús Morales to develop the map. Finally, I want to thank Isabel Jara and Ian Thomson for answering my questions during this investigation and Felipe Durán and Sergio Araya for their comments on a preliminary version of this work. I dedicate this study to my father, Osvaldo Miguel del Carmen Correa Correa, who died on December 3, 2020 due to complications from Covid-19 during the review of the first version of this manuscript (submitted to another journal on September 15, 2020).

References

Barrionuevo JS (2017) Frogs at the summits: phylogeny of the Andean frogs of the genus *Telmatobius* (Anura, Telmatobiidae) based on phenotypic characters. Cladistics 33(1): 41–68. https://doi.org/10.1111/cla.12158

Benavides E, Ortiz JC, Formas JR (2002) A new species of *Telmatobius* (Anura, Leptodactylidae) from northern Chile. Herpetologica 58(2): 210–220. https://doi.org/10.1655/0018–0831(2002)058[0210:ANSOTA]2.0.CO;2

Berenguer J, Cáceres I (2008) El Qhapaq Ñan en Chile. Tramo 2: Miño – Lasana, Región de Antofagasta. Informe presentado al Programa Qhapaq Ñan-Chile, Consejo de Monumentos Nacionales, Tagua Tagua Consultores, Santiago, 79 pp. Unpublished. https://doi.org/10.13140/RG.2.1.3931.4007

Comisión Chilena de Límites (1912) Mapas de la Rejión Andina (1906–1912). Comisión Chilena de Límites, Santiago.

Correa C (2019) Nueva lista comentada de los anfibios de Chile (Amphibia, Anura). Boletín Chileno de Herpetología 6: 1–14.

Cuevas CC, Formas JR (2002) *Telmatobius philippii*, una nueva especie de rana acuática de Ollagüe, norte de Chile (Leptodactylidae). Revista Chilena de Historia Natural 75(1): 245–258. https://doi.org/10.4067/S0716-078X2002000100022

Cuevas CC, Formas JR, Alvarado-Rybak M, Peñafiel-Ricaurte A, Azat C (2020) Rediscovery of the enigmatic Andean frog *Telmatobius halli* Noble (Anura: Telmatobiidae), re-description of the tadpole and comments on new adult's characters, type locality and conservation status. Zootaxa 4834(2): 195–206. https://doi.org/10.11646/zootaxa.4834.2.2

Dill DB (1979) Case history of a physiologist: F.G. Hall. The Physiologist 22: 8–21.

Dill DB (1980) Ten men on a mountain. In: Horvath SM, Yousef MK (Eds) Environmental Physiology: Aging, Heat and Altitude. Elsevier, North Holland Inc., New York, 453–466.

Fibla P, Sáez PA, Salinas H, Araya C, Sallaberry M, Méndez MA (2017) The taxonomic status of two *Telmatobius* frog species (Anura: Telmatobiidae) from the western Andean

slopes of northernmost Chile. Zootaxa 4250(4): 301–314. https://doi.org/10.11646/zootaxa.4250.4.1

Fibla P, Salinas H, Lobos G, Del Pozo T, Fabres A, Méndez MA (2018) Where is the enigmatic *Telmatobius halli* Noble 1938? Rediscovery and clarification of a frog species not seen for 80 years. Zootaxa 4527(1): 61–74. https://doi.org/10.11646/zootaxa.4250.4.1

Formas JR, Benavides E, Cuevas C (2003) A new species of *Telmatobius* (Anura: Leptodactylidae) from Río Vilama, northern Chile, and the redescription of *T. halli* Noble. Herpetologica 59(2): 253–270. https://doi.org/10.1655/0018-0831(2003)059[0253:ANSOTA]2.0.CO;2

Formas JR, Cuevas CC, Nuñez JJ (2006) A new species of *Telmatobius* (Anura: Leptodactylidae) from northern Chile. Herpetologica 62(2): 173–183. https://doi.org/10.1655/05-08.1

Formas JR, Northland I, Capetillo J, Nuñez JJ, Cuevas CC, Brieva LM (1999) *Telmatobius dankoi*, una nueva especie de rana acuática del norte de Chile (Leptodactylidae). Revista Chilena de Historia Natural 72(3): 427–445. https://doi.org/10.4067/S0716-078X2002000100022

Formas JR, Veloso A, Ortiz JC (2005) Sinopsis de los *Telmatobius* de Chile. Monografías de Herpetología 7: 103–114.

Frost DR (2021) Amphibian Species of the World: an Online Reference. Version 6.1. Electronic Database accessible at https://amphibiansoftheworld.amnh.org/index.php. American Museum of Natural History, New York, USA. https://doi.org/10.5531/db.vz.0001

IUCN [IUCN SSC Amphibian Specialist Group] (2015) *Telmatobius halli*. The IUCN Red List of Threatened Species, 2015: e.T21582A79809691. https://doi.org/10.2305/IUCN.UK.2015-4.RLTS.T21582A79809691.en

Keys A (1936a) La vida en las grandes alturas. La expedición internacional de 1935 a Chile. Revista Geográfica Americana 3(35): 79–98.

Keys A (1936b) The physiology of life at high altitudes. The international high altitude expedition to Chile, 1935. The Scientific Monthly 43(4): 289–312. https://www.jstor.org/stable/16163

Keys A, Matthews BHC, Forbes WH, McFarland RA (1938) Individual variations in ability to acclimatize to high altitude. Proceedings of the Royal Society of London B 126(842): 1–24. https://doi.org/10.1098/rspb.1938.0043

Lobos G, Rebolledo N, Sandoval M, Canales C, Perez-Quezada JF (2018) Temporal Gap Between Knowledge and Conservation Needs in High Andean Anurans: The Case of the Ascotán Salt Flat Frog in Chile (Anura: Telmatobiidae: *Telmatobius*). South American Journal of Herpetology 13(1): 33–43. https://doi.org/10.2994/SAJH-D-16-00062.1

Niemeyer H, Cereceda P (1984) Hidrografía. Geografía de Chile. Tomo VIII. Instituto Geográfico Militar, Santiago, 320 pp.

Noble GK (1938) A new species of the frog of the genus *Telmatobius* from Chile. American Museum Novitates 973: 1–3.

Oficina de Mensura de Tierras (1910) Atlas de Chile. Ejecutado por orden de S. E. el Presidente de la República Excmo. Señor don Pedro Montt. Imprenta y Litografía Universo, Santiago.

Richard Mayer (1917) Commercial map of Northern Chili, Bolivia & southern Peru. Richard Mayer, New York.

Riso Patrón L (1924) Diccionario Jeográfico de Chile. Imprenta Universitaria, Santiago, xxiv, 958 pp.

Sáez PA, Fibla P, Correa C, Sallaberry M, Salinas H, Veloso A, Mella J, Iturra P, Méndez MA (2014) A new endemic lineage of the Andean frog genus *Telmatobius* (Anura, Telmatobiidae) from the western slopes of the central Andes. Zoological Journal of the Linnean Society 171(4): 769–782. https://doi.org/10.1111/zoj.12152

Titus A (1909) Apuntes para una monografía de los Ferrocarriles Particulares de Chile (Continuación). Anales del Instituto de Injenieros de Chile 9(8): 337–361.

Victoriano PF, Muñoz-Mendoza C, Sáez PA, Salinas HF, Muñoz-Ramírez C, Sallaberry M, Fibla P, Méndez MA (2015) Evolution and Conservation on Top of the World: Phylogeography of the Marbled Water Frog (*Telmatobius marmoratus* Species Complex; Anura, Telmatobiidae) in Protected Areas of Chile. Journal of Heredity 106(S1): 546–559. https://doi.org/10.1093/jhered/esv039